Geophysical Investigation of Sedimentary Basin Development: Viking Graben, North Sea.

Fragiskos A Zervos

Ph.D.

University of Edinburgh

1986

DECLARATION

This thesis has been composed solely by myself. The work presented is entirely my own except where clearly indicated or acknowledged otherwise.

Fragiskos A Zervos

To my parents

and Pauline

ACKNOWLEDGEMENTS

To acknowledge everyone who has helped me over the years would mean publishing another thesis and I don't think it would "sell", so I will begin to thank those immediate to me and enclose many thanks to everyone in BGS for giving me a warm and friendly environment in which to work.

I would like my gratitude to be acknowledged to the following:

To Roger Scrutton, my supervisor, for all his guidance and for having endured me over the years with all my "queries", and for making me feel so much at home in the very beginning.

To Bob McQuillin for primarily allowing me such a splendid opportunity to work in BGS. Bob you don't know how really privileged I feel to have been able to use all the facilities available and for you to have had faith in knowing that it would pay off.

To Derek Reay for being there over the years not only as a colleague but as a much respected friend. Endlessly being there, listening to all my naggings and ups and downs. A friendship which I shall never forget! Thanks a lot Derek.

To Geoff Day for his father-like support over the years and for his help in correcting this manuscript. I hope it didn't keep you up too many nights Geoff.

To Dr R Hipkin for allowing me access to 3-D gravity programmes and for giving me important advice in gravity modelling.

To Linda Nisbet for her patience, for always smiling and for helping me put my first paper from scrawl into type.

To Elaine Bates and Jane McKenzie for being able to decipher my scrawl and eventually typing my thesis.

To MESRP and Hydrocarbons for giving me constant advice, data facilities, and for putting up with me hanging around their offices.

Again I wish my thanks to be deeply felt towards all those in BGS and I feel so privileged at having had such a chance in my life to work with you. I will always have strong and pleasant memories of my stay.

To my girlfriend Pauline Stuart for babysitting and tolerating me for two happy years and for her constant advice in trying to help me make my dreams come true. Pauline - thanks a lot.

Last but not least, I wish to thank the two people who have had not only to bear their son's burden, but have travelled with me in spirit through my seemingly endless journey to my final goal, my parents, Sophia and Antonis. The people who have shown me the path...

ABSTRACT

The purpose of this study is to investigate the structure of the Viking Graben and adjacent areas using geophysical and geological techniques. The results thus obtained are used to construct a model for the development of the sedimentary basins of the northern North Sea since the beginning of the Mesozoic era.

The regional consideration of the gravity field of the northern North Sea basin revealed the presence of a mass excess beneath the low density sediments. This high amplitude, long wave length anomaly is explained by thinning of the crust. Predictions obtained from the gravity data confirm the crustal structure derived so far from seismic experiments. "Normal" porosity-depth curves were constructed for three different sedimentary rock types in order to backstrip and decompact the sediments. Montmorillonite to illite transformation is proposed to be the main cause of the few undercompacted sedimentary sequences observed. Using well data the subsidence of the basement was calculated by backstripping and decompacting the sediments. By comparing the observed subsidence paths with those predicted by a simple stretching mechanism, a model is proposed to account for the geophysical development of the northern North Sea since Top-Permian times. Finally very close agreement is shown between the present crustal thickness values estimated from the modelling of wells and the values derived from the investigation of the gravity field.

CONTENTS

CHAPTER 1

GEOLOGICAL HISTORY, SUBSIDENCE MECHANISMS, OBJECTIVES AND DATA

CHAPTER 2

INVESTIGATION OF THE GRAVITY FIELD

CHAPTER 3

POROSITIES AND OVERPRESSURE

CHAPTER 1

GEOLOGICAL HISTORY, SUBSIDENCE MECHANISMS, OBJECTIVES AND DATA

Introduction

The objective of this work is the geophysical investigation of the tectonic development of the Viking Graben and adjacent sedimentary basins in the northern North Sea. A digression from the main theme is made in order to follow up some interesting aspects of overpressuring in the sedimentary infill of the graben.

This chapter forms an introduction to the rest of the thesis. Section one outlines the geological history of the North Sea and section two is the summary of similar work done in the area. The North Sea is typical of many epicontinental basins and in section three the various mechanisms proposed to account for their formation are discussed. Finally, in section four the techniques, the type of data and the sources of the computer programs used in this study are briefly outlined.

In Chapter 2 the present day crustal thickness is obtained using seismic control for the upper crust and gravity modelling for the deep crustal structure. Thinning of the crust is probably the main cause for the development of the sedimentary basins.

In Chapter 3 the "normal" porosity-depth relation for different sedimentary rock types is calculated using well-log information from 28 wells and mechanisms are sugested for the cause of the few non "normally" compacted (overpressured) sequences observed. This porosity study is considered to be fundamental to the main project in order to obtain the subsidence of the basement by removing the loading effects of the sediments and correcting for compaction.

In Chapter 4 the subsidence of the water filled basement is calculated and quantitatively examined since Top Permian times by studying 25 wells along six seismic profiles across the Viking Graben.

Finally, in Chapter 5 a model for the formation of the northern North Sea basin is proposed by comparing the observed subsidence paths with those predicted by theoretical models of basin formation.

1.1 The Structural Framework and the Geological History of the North Sea Area

The North Sea basin is located on the northwest European Continental margin. The main structural elements of the North Sea, shown in Fig. 1.1 are the N-S trending Viking and Central Grabens which run through the centre of the basin, and the smaller Witchground Graben which leads into the Moray Firth basin.

Extensive papers describing the geology of the North Sea occur in volumes edited by Woodland (1975), Hardman (1980), Illing and Hobson (1981) and Glennie (1984). Individual papers reviewing the North Sea have been published by P. Ziegler (1975a, 1975b, 1977, 1978, 1981), W. Ziegler (1975), Kent (1975), Selley (1976), Watson and Swanson (1975).

The following structural development draws extensively on these sources and is shown as an isometric block diagram in Fig. 1.2.

1.1.1 Pre-Permian

The area now occupied by the North Sea once lay at the boundary between the Laurentian plate to the northwest and the Baltic to the southeast.

The Pre-Permian story of the North Sea was dominated by the alternative separation and compression of these plates. During separation, sediments were deposited in troughs along the plate boundaries; during compression the sediments were folded and metamorphased.

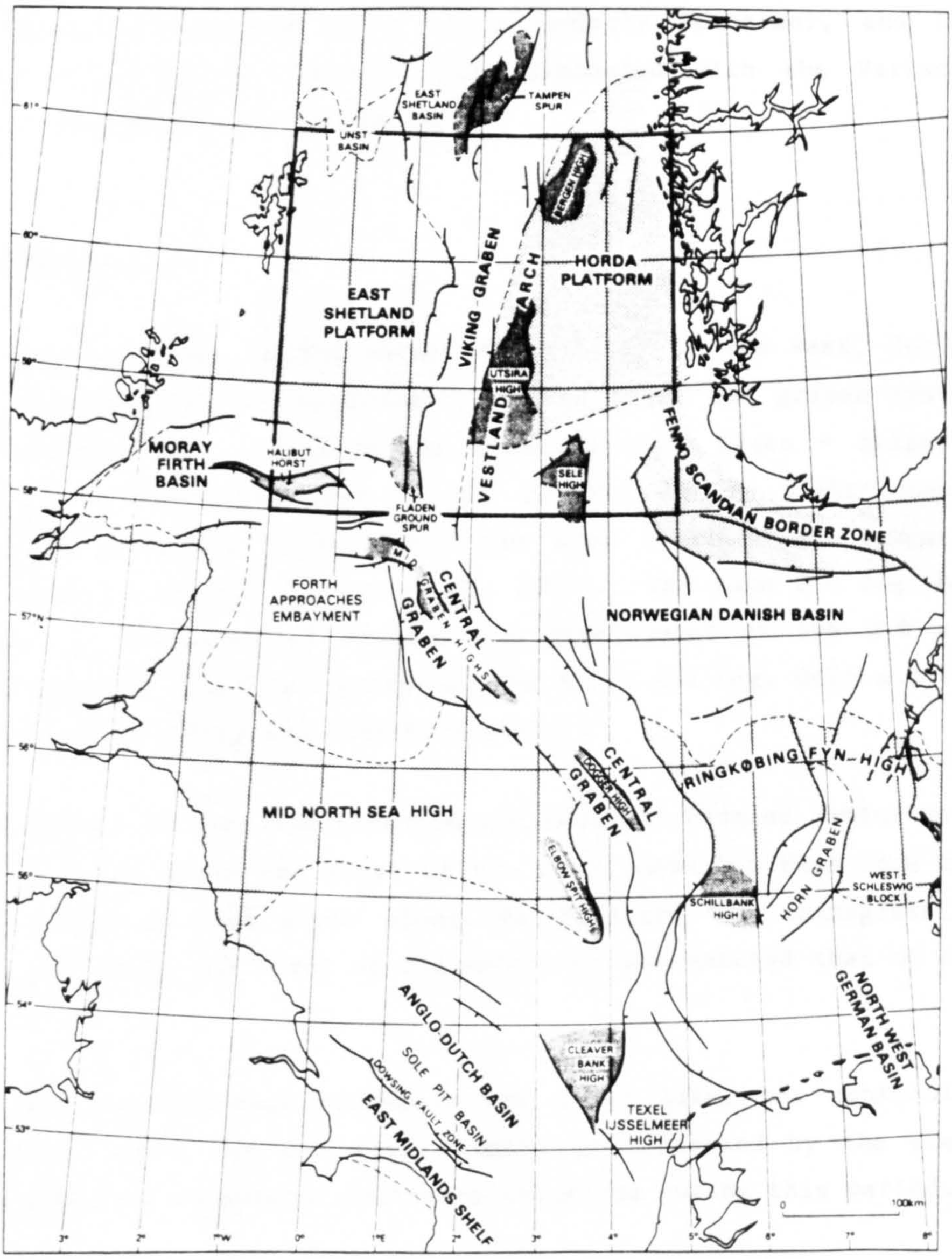

Fig. 1.1. *Major structural units in the North Sea, after Day et al (1981), with the area of interest enclosed by heavy line.*

There are two major Pre-Permian cycles of sedimentation and orogenesis. One began in the Late Precambrian and culminated in the Caledonian orogeny (Late Silurian-Early Devonian), and the second began in the Devonian and culminated with the Variscan orogeny in the Late Carboniferous.

1.1.2 Permian

The early collapse of the Variscan Highlands in the west, during early Permian and the development of the horst and graben system that was possibly allied to the creation of a proto - Atlantic fracture system, gave rise to E-W tension and to right-lateral extension movements in the North Sea area (Glennie and Boegner, 1981) and in Germany (Drong et al, 1982). The same E-W regional tension is suspected of causing the development of the N-S and NW-SE oriented fracture systems of the North Sea (eg. Oslo and the Horn Grabens, Viking and Central Grabens).

The surfaces of both the northern and southern Permian basins were probably well below the level of the open ocean, so that once the water began to flow south along the fracture the transgression continued until the level of the Zechstein Sea matched that of the ocean.

Although the Zechstein sediments are water lain, the continuing prevalence of a hot and arid climate is witnessed by the great thicknesses of evaporitic sediments deposited during this period.

1.1.3 Triassic

During Early Triassic times regional extension resulted in the initiation of the main N-S trending graben system, cross cutting the Permian basins and the Mid North Sea High. Early Triassic alluvial fan and fluvial deposits are overlain by Late Triassic

lacustrine and sabkha facies. By the end of the Triassic the grabens were almost completely infilled, with sediment thicknesses reaching 3-4km in the Viking and Horn grabens (Ziegler, 1981).

1.1.4 Jurassic

The Jurassic was a period of active faulting in response to continued crustal extension. Differential fault-controlled subsidence, contemporaneous with sedimentation, had a marked influence on stratigraphic thicknesses and facies, especially during the Late Jurassic. Of faults moving during the Jurassic, many can be assigned to older structural trends.

1.1.5 Cretaceous

The Cretaceous spans the change from the tectonically-controlled sedimentation of the Early Cretaceous, with its extensive areas of land, to the much quieter fully marine conditions associated with regional subsidence centred over the axial graben system, which characterises the Late Cretaceous. In some areas the movements were largely along pre-existing lines of faulting (eg. Moray Firth Basin), but in the Viking Graben new faults were also initiated, particularly outside the original margins of the trough, which had the effect of broadening the depositional basin.

1.1.6 Tertiary to Recent

Cenozoic subsidence was dominated by a broad synclinal down-warp, in contrast of the Mesozoic, which was dominated by major faulting and rifting. A minor tensional event though which occurred during the Early Paleocene, resulted in reactivation of some faults.

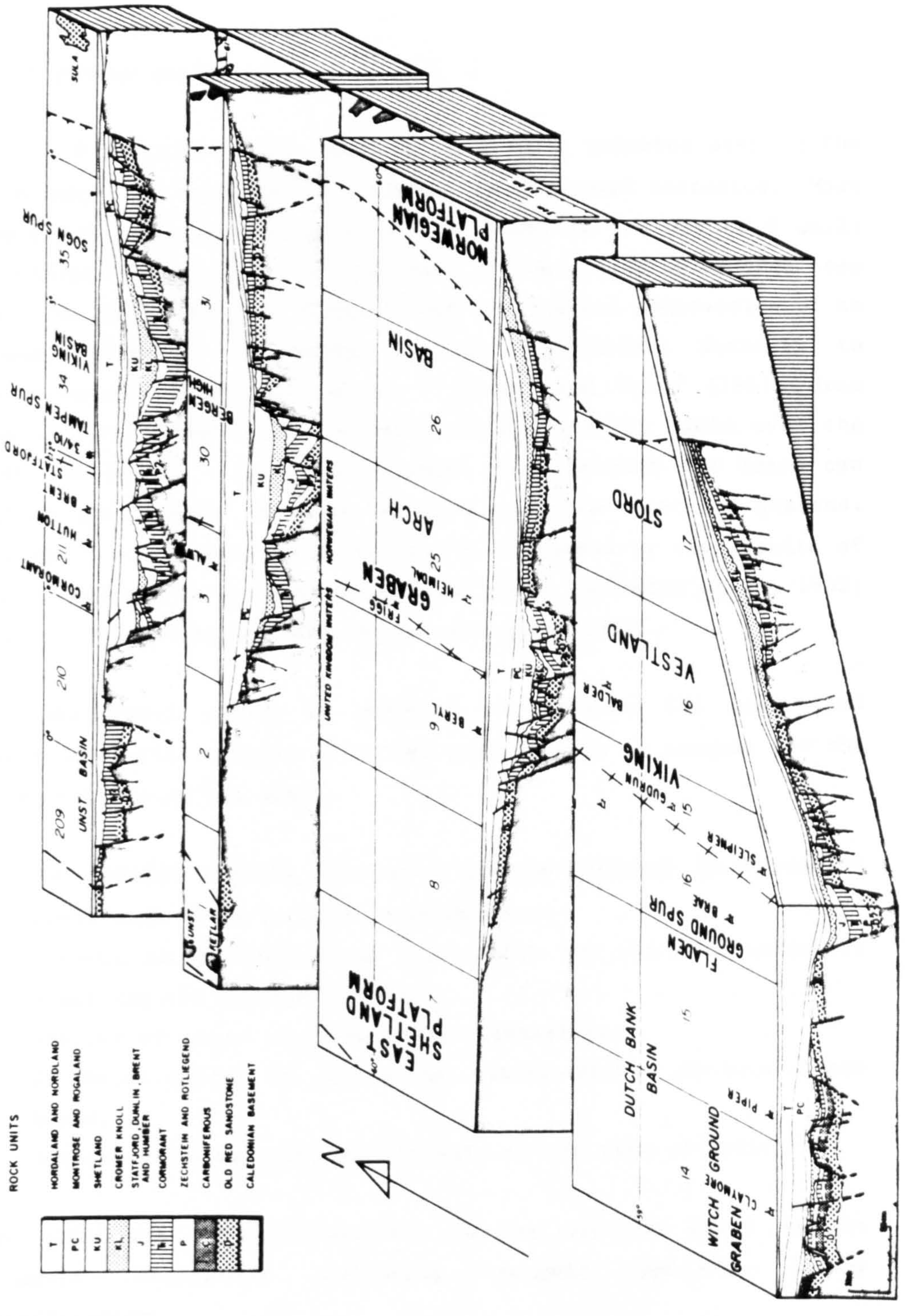

Fig. 1.2. *Isometric block diagram of the Northern North Sea illustrating the differing structural development of the Unst Basin, the Viking Graben, the Stord Basin and Witch Ground Graben. (After Glennie, 1984).*

1.2 Previous Work

Clark (1973) first noted that the subsidence patterns seen in the North Sea could be related to Mesozoic extensional tectonics. More recently Sclater and Christie (1980), based on a study of 8 wells and seismic data, suggested that most of the steady subsidence seen since the mid-Cretaceous results from the thermal contraction of an already thinned lithosphere due to the Middle Jurassic to mid-Cretaceous stretching event. Donato and Tully (1981) drew similar conclusions from the study of the gravity field over the North Sea basin. A zone of thinned crust beneath the basin can explain the absence of large negative anomalies over the grabens. Thinned crust beneath the North Sea is confirmed by the results of seismic refraction surveys across the basin (Collette et al, 1965; Solli, 1976; Christie, 1982; Barton and Wood, 1984).

Thus any model which is proposed to explain the geological evolution of the northern North Sea must be able to account for the major features of the basin:

1) The initial rifting subsidence phases followed by a passive subsidence which is still continuing.
2) Thinned crust beneath the basin with the thickest sediments overlying the maximum thinning.
3) Absence of large negative gravity anomalies.
4) No major uplift at any stage either within or around the basin.
5) Absence or minor volcanic activity at the time of uplifting.

Each model and its applicability to the northern North Sea is discussed separately following roughly Bally's (1980) classification.

1.3 Models for the Evolution of Sedimentary Basins

1.3.1 Gravity loading

Subsidence due to sediment loading is based on local Airy isostasy, Dietz (1963). A more sophisticated approach is to treat the lithosphere as a thin elastic plate and investigate its flexure in response to the sediment loading by elastic beam theory. Walkott (1972) used this technique to show the growth of a sedimentary lens at a continental margin, with particular relevance to deltas such as that of the Niger.

According to Bott (1980), Turcotte (1980) subsidence due solely to this mechanism cannot reasonably exceed two to three times the initial water depth and thus may not apply to very thick sequences of shallow water deposits.

This model cannot explain the absence of large negative gravity anomalies in the Viking Graben, where the observed gravity values are greater than -10mGals, because replacement of the crust by less dense sediments would produce a negative gravity anomaly.

Watts and Ryan (1976) also showed that neither local nor flexural loading can explain the substantial thicknesses of shallow water sediments typically observed on the shelves of passive margins as in our case.

A "driving force" other than sediment loading is needed. Here the importance of the sediment loading effect is to increase the amount of subsidence caused by a factor of between about two and three, depending on the mean sediment density, Bott (1980).

Thus, sediment loading appears to be a contributory factor in most subsidence cases, although it appears to be the primary cause only where great sediment volumes are deposited in initially deep water.

1.3.2 Thermal hypothesis

Isostatic subsidence can be caused by cooling of the previously heated lithosphere and the associated increase in density. The basic thermal hypothesis of Hsü (1965) has been theoretically developed in an elegant way by Sleep (1971, 1973). He proposed a model, where as the temperature of the crust and lithosphere are raised by some means, the crust is uplifted and thinned due to surface erosion. Later, cooling would cause subsidence of such an attenuated crust. However, the amounts of uplift and surface erosion required to explain the origin of the North Sea basin (ie, in excess of 5km) is not evident to produce the space for the Cretaceous and Tertiary infill.

1.3.3 Diapiric intrusion

Subsidence is caused by cracking of the continental lithosphere in response to tensional stresses allowing intrusion of ultrabasic dikes and/or diapirs, Royden et al (1980).

An initial subsidence resulting from the increased density of the crust is followed by an exponential thermal subsidence. Such a subsidence is observed in the oceans. However, there is little evidence of dyke swarms in the North Sea basin, Leckie (1982), and it is unlikely that dyke injection can occur at depths where the lithosphere behaves as viscous fluid (Sclater et al, 1980).

1.3.4 The metamorphism hypothesis

Isostatic subsidence can be caused by a density increase of lower crustal or lithospheric rocks due to gabbro-eclogite phase changes or else metamorphism. Falvey (1974), later modified by Middleton (1980), also favours metamorphism of the lower crust during basin

formation. An initial subsidence occurs due to thermal metamorphism of the lower crust from greenschist to amphibolite facies in response to heating, with an increase in density of between 150 and 200kg/m^3. This causes a slight thinning of the crust which to some extent counters the thermal uplift. As the continental lithosphere cools, subsidence below the initial level occurs because of the denser and slightly thinner crust.

According to Bott (1980) an extreme example of an increase in density of 200kg/m^3 affecting 15km of lower crust gives crustal thinning of about 1km. The maximum sediment thickness is then between about 3 and 4km. Hence this version of the thermal hypothesis also fails to account for the great sediment thicknesses (up to 10km) observed in the North Sea basin. A similar difficulty faces the intrusion model.

Haxby et al (1976) suggest that hot mantle diapirs intruding into the lithosphere could result in the thermal metamorphism of the lower crust from gabbro to eclogite. No thermal dome is produced at the surface since the less dense diapir is balanced by the formation of dense eclogite. As the diapir cools the basin subsides to a depth below its original level due to the excess weight of the eclogite body. However, experimental evidence (Ringwood and Green, 1966) indicates that the gabbro-eclogite transformation would occur with a drop in temperature or an increase in pressure, not with just an increase in temperature as suggested by Haxby et al (1976). Although the sediments would be compensated by the dense eclogite body this model does not account for the initial faulting event or the presence of thinned crust beneath the North Sea basin. It has also been difficult to demonstrate that such a process as phase changes has occurred on a large scale in nature, Sleep et al (1980).

The effect of transformation of metastable phases to denser stable phases at lower crustal conditions on passive margins has been discussed by Neugebauer and Spohn (1978).

If for some reason this gabbro-eclogite phase migrates upwards, subsidence occurs in response to sediment loading. This was the idea that Collette (1968) invoked to explain the subsidence and crustal thinning observed from refraction studies in the North Sea basin, Collette et al (1965). The crust is thinned as more dense eclogite breaks free from the overlying crust and disappears into the mantle. O'Connell and Wasserberg (1967) worked on the general behaviour of such a model. According to Artyushkov et al (1980) such a process is implausible, because a mixture of bodies of usual crustal and mantle composition will always remain lighter than mantle matter and, consequently, can not sink into it.

If the Moho corresponds to the gabbro-eclogite phase change subsidence will occur due to a drop in temperature, however, heat flow measurements over subsiding basins indicate a higher than normal heat flux eg. Pannonian Basin, Sclater et al (1980).

Bullard and Griggs (1961) demonstrate that if the Moho were a phase boundary it could not be the same boundary beneath the oceans and the continents. The gabbro-eclogite transition takes place over a broad temperature and pressure range, Ringwood and Green (1966), which is not compatible with the seismic evidence for the sharp discontinuity, Wood and Barton (1983).

Mareschal et al (1982) used heat flow, seismic and gravity data to determine the nature of the crust-mantle boundary, but due to the low correlation coefficient between pressure and temperature they were unable to give strong support to the idea that the Moho corresponds to a phase change.

The rate of subsidence in the North Sea basin decreases rather than increases with age, thus ruling out any mechanism of long term subsidence involving Moho migration, Sclater and Christie (1980).

1.3.5 Lower crustal creep

A stress-based hypothesis which may account for subsidence at passive margins appeals to thinning of the continental crust near the margin by progressive creep of ductile middle and lower crustal material towards the suboceanic upper mantle, Bott (1971, 1973).

The flow is driven by the release of gravitational energy as the continent-ocean crustal transition becomes progressively more gradational. The hypothesis depends on the ability of the lower and middle continental crust to flow significantly by steady state creep, while the overlying elastic layer subsides by elastic flexure or by normal faulting.

Bott and Dean (1972) showed that passive margins are associated with a differential stress system as a result of unequal topographic loading across the margins and associated upthrust of the low density continental crust in isostatic equilibrium with the oceanic region.

The additional loading and compensatory upthrust on the continental side effectively squeezes the continental crust, causing horizontal deviatonic tension peaks in the middle of the crust, decreasing to zero at the surface and at Moho.

Kusznir and Bott (1977) have shown that if the lower crust is treated as viscoelastic, then stress differences in the upper elastic layer will be increased. According to this hypothesis, the crustal thinning will cause isostatic subsidence of the shelf and possibly slope, which will be accentuated by the sediment load.

Vetter and Meissner (1979) modified Bott's concepts and divided the lithosphere into an upper brittle layer and a lower layer in which high temperature creep occurs. In their view - and in contrast to

Bott - these authors feel that the viscosity of the middle crust is too high to permit creep.

This model can only explain sedimentation and subsidence within the graben and cannot account for the broad subsidence seen during the Late Cretaceous and Tertiary in the North Sea basin, and fails to explain the absence of high negative anomalies as a result of thinning of the crust.

Beaumont (1979) states that it is difficult to decide among competing rheologies (Elastic, Elastic-Perfectly plastic, Visco elastic and Lower Crustal Creep) or various combinations of these properties.

1.3.6 Stretching

Both the space problem and the thermal subsidence can be resolved if the basin is produced by stretching the continental crust over a broad region. Many authors, for example, Artemjev and Artyushkov (1971), Voight (1974), Lowell et al (1975) and Morton and Black (1974), have invoked stretching to account for normal faulting and crustal thinning observed in rifted regions. McKenzie (1978) examined the consequences of stretching the lithosphere during basin formation. Rapid extension results in the attenuation of both the crust and the lithosphere, allowing the passive upwelling of hot asthenosphere. Provided that the crust is thicker than 20km there is an initial fault controlled subsidence due to replacement of light crust by dense asthenosphere. When the faulting ceases the thermal anomaly decays by conduction and a further slow subsidence occurs. The simple stretching model of McKenzie (1978) assumes stretching occurs instantaneously.

This assumption of instantaneous stretching will not lead to significant error if the duration of the stretching is less than 40my (Jarvis and McKenzie, 1980) as it was assumed for the initial

extensional event during the Top Permian in the North Sea basin where the observed stretching factor is approximately 1.15, see section 5.4.7.

Royden and Keen (1980) modified the simple stretching model of McKenzie (1978) to allow for differential extension in the upper and lower lithosphere. The upper lithosphere extends by a factor δ and the lower independently by a factor β. This model is difficult to test since β is unknown and cannot be estimated except from the subsidence.

Keen et al (1981a) developed the simple stretching model to allow for segregation of basaltic melt from the asthenosphere. Although this model can account for the major features observed in the development of the North Sea the volume of volcanic rocks is small and this model is considerably more applicable to the continent-ocean transition, Beaumont et al (1982).

A model which allows for stretching over a period of time will give a closer approximation to the observed evolution of the North Sea, because the main extensional event lasted from Mid-Jurassic to Aptian times, approximately 60my. Such a model has been developed by Jarvis and McKenzie (1980), and predicts as a function of β, both the initial subsidence and the thermal one, where β is the increase in surface area. The subsidence and sediment fill are compensated by the thinned crust, thus the gravity anomalies are small.

Both the simple stretching model (McKenzie, 1978) and the finite duration of stretching model (Jarvis and McKenzie, 1980) are discussed in more detail and applied in Chapter 5.

1.4 Area of Study, Data Type and Computer Programs

The area of study is the northern North Sea between latitude 58.00-61.00N and longitude 1.00W-5.00E shown in Fig 1.1. As a result of intensive oil exploration within the above area, much gravity, well and seismic data has now become available for study.

Six detailed published seismic profiles across the Viking Graben, reaching the basement, were used to calculate the gravity effect of the sediments and consequently the regional gravity variation which was assumed to be caused by the thinning of the crust. For the gravity study, 58 wells were used to derive the density variation of the sediments and a Bouguer anomaly map was compiled for the whole area using data from four different sources.

The subsidence pattern of the basement is obtained by backstripping the sediments and allowing for decompaction of 25 wells situated along the gravity-seismic profiles. The subsidence was later corrected taking into account the depth of deposition. This paleodepth information was obtained from well reports based on micropaleontological studies.

The sediments were decompacted along three "normal" porosity ("normal" compaction) curves which were constructed by using data from 28 wells. Not all the wells were found to be "normally" compacted, therefore 14 from the above 28 wells were studied in detail to establish the extent and the cause (if possible) of the undercompacted sedimentary sequences.

In all, more than 100 commercial wells were used in the different aspects of this study from both UK and Norwegian sectors of the northern North Sea. However, there are problems inherent in well data. Since all wells are drilled on structures suitable for the discovery of oil or gas, generally over structural highs, the succession will be incomplete or condensed and hence, atypical. Through working in the British Geological Survey I had easy access

to all the released wells drilled in the UK, therefore wells with the most complete geological section have been chosen, where possible, in an attempt to reduce these problems. The detailed descriptions and locations of the different data sets mentioned above, will be given in individual chapters.

No computer programs were originally developed for this study. They were mainly supplied by Universities and other Institutions and they had to be converted in order to be usable in BGS computers. The list of computer programs is as follows:

1. A 2-D gravity modelling program (MAGRAV) supplied by Marine Geophysics Unit of BGS (section 2.4).
2. A 3-D gravity modelling program (section 2.5) supplied by Dr R Hipkin (Department of Geophysics, Edinburgh University).
3. A 3-D isometric projection program (SURFACE 2) supplied by NERC Computing Services (section 2.4.2).
4. A program to backstrip and decompact the sediments assuming local isostatic compensation (sections 4.2 and 4.4).
5. A program to apply the instantaneous and finite period extension models (section 5.2). The two latter programs were supplied by Dr P Barton (Department of Geophysics, Cambridge University).

In order to quantify the development of the basin a detailed study of the crustal thickness is needed. This is successfully done by gravity modelling and described in the next chapter.

CHAPTER 2

INVESTIGATION OF THE GRAVITY FIELD

Introduction

Bouguer anomaly gravity values over the northern North Sea are generally higher than -10mGal despite the fact that there are up to 9km of low density sediments within the grabens. Collette et al (1965) first suggested that this isostatic equilibrium was achieved by thinning of the crust since Permian times. Subsequent refraction experiments in the Viking (Solli, 1976), Witchground/ Buchan (Christie and Sclater, 1980) and Central Grabens (Wood and Barton, 1983) have confirmed this picture of crustal thinning beneath the grabens. Donato and Tully (1981) analysed nine regional gravity profiles and predicted a maximum thinning of about 10km beneath both the Viking and Central Grabens. They calculated only 5km thinning beneath the Outer Moray Firth Basin (Witchground/Buchan grabens) whilst Dimitropoulos and Donato (1981) predicted no significant thinning beneath the Inner Moray Firth basin where a large negative gravity anomaly is situated.

This chapter presents the results of a study of the Moho topography based on an investigation of the gravity field of the northern North Sea. Gravity data from the Norwegian sector was combined with published BGS data in the UK sector to compile a Bouguer gravity anomaly map of the whole northern North Sea. Recent seismic reflection and refraction data have also provided greater control for the gravity models than was available for previous studies (eg. Donato and Tully, 1981).

2.1 Data Sources and Reliability

The Bouguer anomaly gravity map was compiled from four data sets which are described below. Their distribution is shown in Fig 2.1, with the map area enclosed by a heavy line.

Gravity surveys:

(i) Maps of the British Geological Survey (BGS) 1:250 000 Bouguer anomaly gravity map series. Each map covers an area of 2° longitude by 1° latitude and is contoured at an interval of 2mGal. Most surveys were run on a N-S, E-W rectangular grid, with average line spacing of 12km by 7km respectively. Analysis of the cross-over values at line intersections reveals the internal consistency of the surveys. The absolute accuracy was established by linking readings into harbour bases connected to stations in the National Gravity Reference Net 1973 (NGRN 73). Internal accuracy is estimated to be 1-2mGal for recent surveys but variations between lines of up to 4mGal exist in older surveys, when navigation accuracy was lower and meter platforms were less stable (Tully and Donato, 1985). Apart from the rectangular grid, a number of BGS lines run across the Viking Graben into the Norwegian sector were used as a framework to which all other surveys in this sector were referred. The calculated anomalies on these lines were estimated to be accurate to within 2mGal.

(ii) A survey carried out by the Federal Institute of Geosciences and Natural Resources (FIGNR), Hannover, in 1974. Data cover an area from the Shetland Islands to the Norwegian coast, between 60°N and 62°N. Plaumann (1979) discusses the results of the marine gravity measurements. Discrepancies with BGS data are probably due to two breakdowns of the gravimeter, platform vibration on the two grid tie-lines, and a large (12mGal) non-linear drift, all of which reduced the accuracy of this survey. As a result approximately 25% of the FIGNR data was discarded because misties with BGS data exceeded 3mGal and no consistent offset could be applied.

(iii) A survey, mainly in the Norwegian sector, carried out by Western Geophysical for Statoil who kindly made the results available.

(iv) A survey conducted jointly by the US Army Topographic Command and the Geographical Survey of Norway (NGO) in 1970. Approximately 40% of the data was discarded because misties with other data sets were greater than 3mGal.

Gravity anomalies in all the surveys are calculated using the International Gravity Formula of the Geodetic Reference System 1967 (IGF 67) and referred to the International Gravity Standardisation Net of 1971 (IGSN 71). The NGO survey was originally tied to the European Calibration System 1962 and the anomalies were calculated using the 1930 International Gravity Formula. A correction of -7.5mGal was applied to convert the data to the IGF 67 (average +7.2mGal over the area) and to refer it to the IGSN 71 (average -14.7mGal) (Hospers and Finnstrom, 1984)

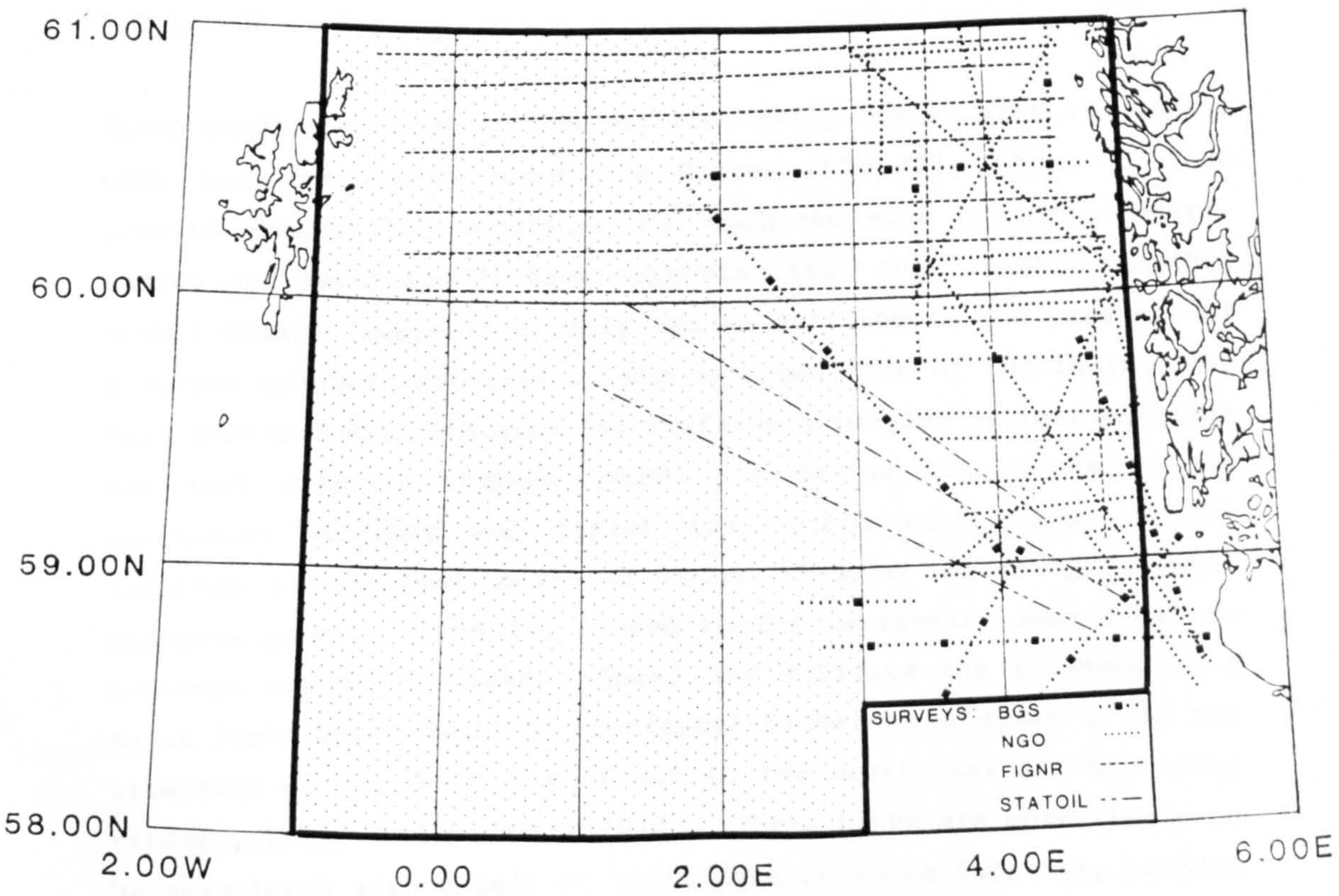

Fig. 2.1 Data sources used in the compilation of the Bouguer anomaly map. Shaded area covers published Bouguer anomaly maps by BGS.

2.2 General Discussion of the Main Gravity Anomalies

The most striking feature of the Bouguer anomaly map (Fig 2.2) is the absence of a large negative anomaly corresponding to the position of the major North Sea graben system. Anomalies mostly range between -5 and +20mGal, clearly indicating some form of isostatic compensation to be present beneath the sedimentary basins.

The following simple interpretation of the major anomalies refers to features numbered on Fig 2.2. The faults indicated are based on the tectonic maps of the North Sea (Hamar, 1979; Day et al, 1981) and outline the main graben features.

2.2.1 UK sector

Steep gradients occur in the Western Viking Graben area associated with boundary faults along the Graben (1), (2), (3). A broad gravity anomaly (2) occurs on the upthrown side of these faults. Donato and Tully (1982) have suggested that this anomaly together with a related magnetic anomaly can be ascribed to the presence of a buried granite batholith on the upthrown side of the fault. The East Shetland Platform area (4) exhibits a complex pattern of highs and lows with no obvious trend. A narrow low occurs to the north-east of Unst and Fetlar (5), which corresponds to the location of the Unst Basin of Permo-Triassic and younger rocks. Elongate gravity highs (6) extend to the north-east away from the southern end of Shetland. These may indicate the presence of a major fault which could be considered either as a splay or as the extension of the Great Glen Fault to the north-east (Flinn, 1961; Pitcher, 1969; Bott & Watts, 1970). These highs are more likely to be associated with a belt of basic igneous rocks (possibly bounded by a major fault) such as is seen on land (McQuillan & Brooks, 1967). Towards the southern edge of the East Shetland Platform a deep gravity low (7) correlates with an area of thickened sediments

assumed to be of Permo-Triassic and/or Devonian age beneath a Tertiary cover. The Inner Moray Firth Basin is bounded to the north by the Caithness Ridge which appears on the map as a narrow east-west trending gravity high (8). The Halibut Horst, a buried Devonian ridge to the east of the Inner Moray Firth, can be seen as a positive anomaly (9).

2.2.2 Norwegian sector

Along the coast a gravity gradient (10) clearly indicates the presence of major faults which mark the western boundary of the Norwegian Continental Platform. Two distinctive gravity highs (11, 12) occur on the upthrown side of these faults. Hospers and Finnstrom (1984) have calculated maximum source depths of 5-10km for these anomalies, on the basis of half-width estimates for buried spheres and horizontal cylinders. This would seem to be too deep to be reconciled with the known basement depth of 1 to 2km (Hamar et al, 1980) which suggests that they are not due to sharp basement topography. Alternatively, it is quite possible that the elongate gravity ridge reflects basement lithology, which in this case would mean the presence of rocks of relatively high density within the basement. Both features (11), (12) have associated magnetic anomalies with the contours showing much more irregularity than in the surrounding areas (Hospers & Rathore, 1984), and could be due to the presence of basic igneous rocks within the basement as suggested by Hospers and Finnstrom (1984). Another indication supporting this suggestion is the fact that Late Carboniferous to Jurassic igneous rocks are known to occur nearby on land (Faerseth et al, 1976). An area of high gravity anomalies (13) on the eastern side of the Viking Graben corresponds to the Utsira High. The extension of the Vestland Arch from the Utsira High to the north is clearly displayed as a series of north-south contours (14) along the eastern edge of the Viking Graben. An area of broad gravity lows within the Horda Platform (15) indicates the presence

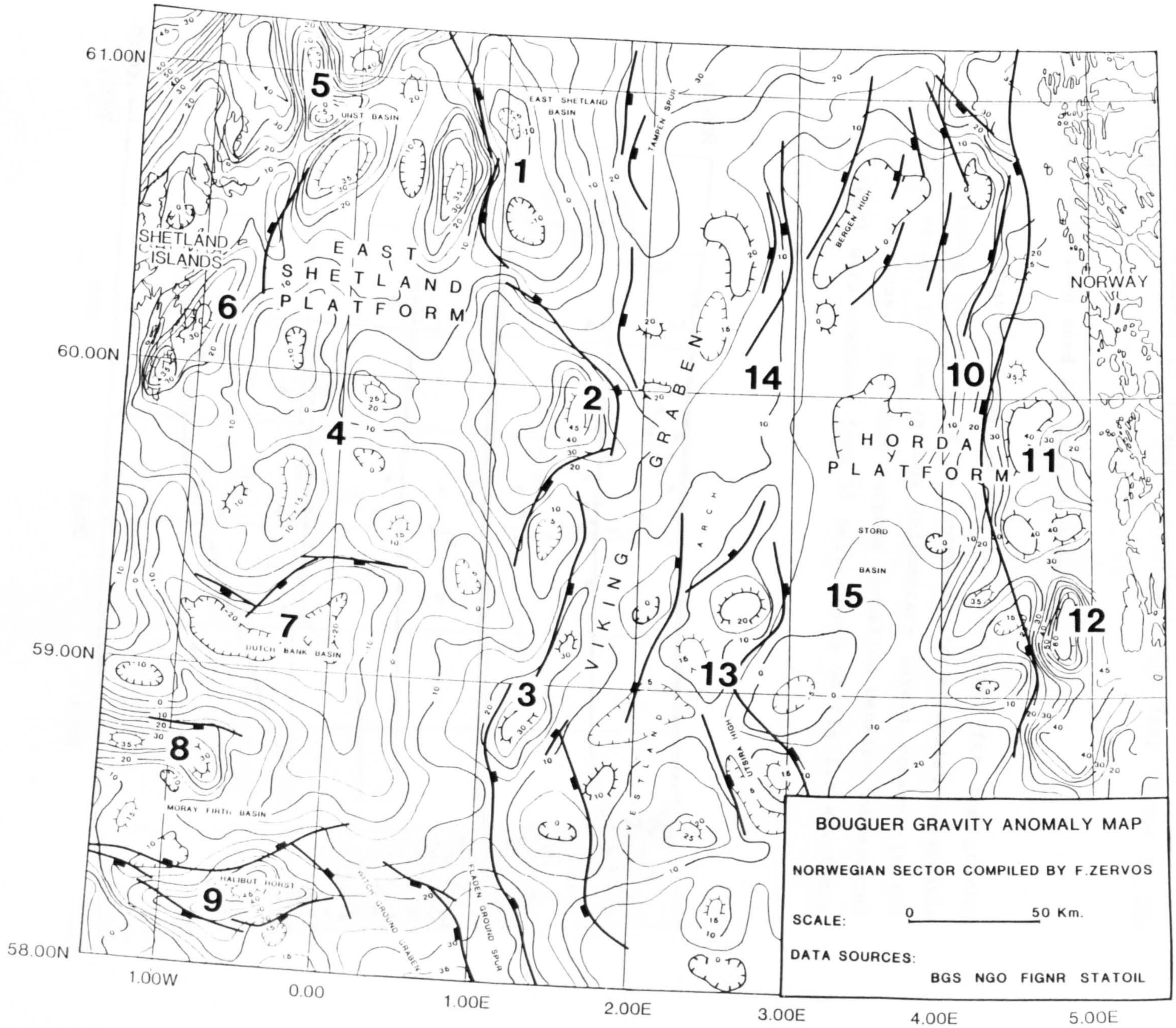

Fig. 2.2 *Bouguer anomaly map of the northern North Sea. Gravity anomalies are calculated using the IGF 1967 and referred to the IGSN 1971 and a density of 2.67g/cc was used for the Bouguer corrections.*

of the N-S elongated Stord Basin. This is a large sedimentary basin of Triassic to Jurassic age, about 4km deep (Hamar et al, 1980).

2.3 Densities used for Gravity Modelling

Before any gravity anomalies can be calculated for the gravity backstripping exercise, it is necessary to establish reasonable density values for the various sedimentary layers present in the seismic sections. For this purpose Formation Density Compensated logs (FDC) were examined from 58 wells shown on Fig 2.3 and Table 2.1.

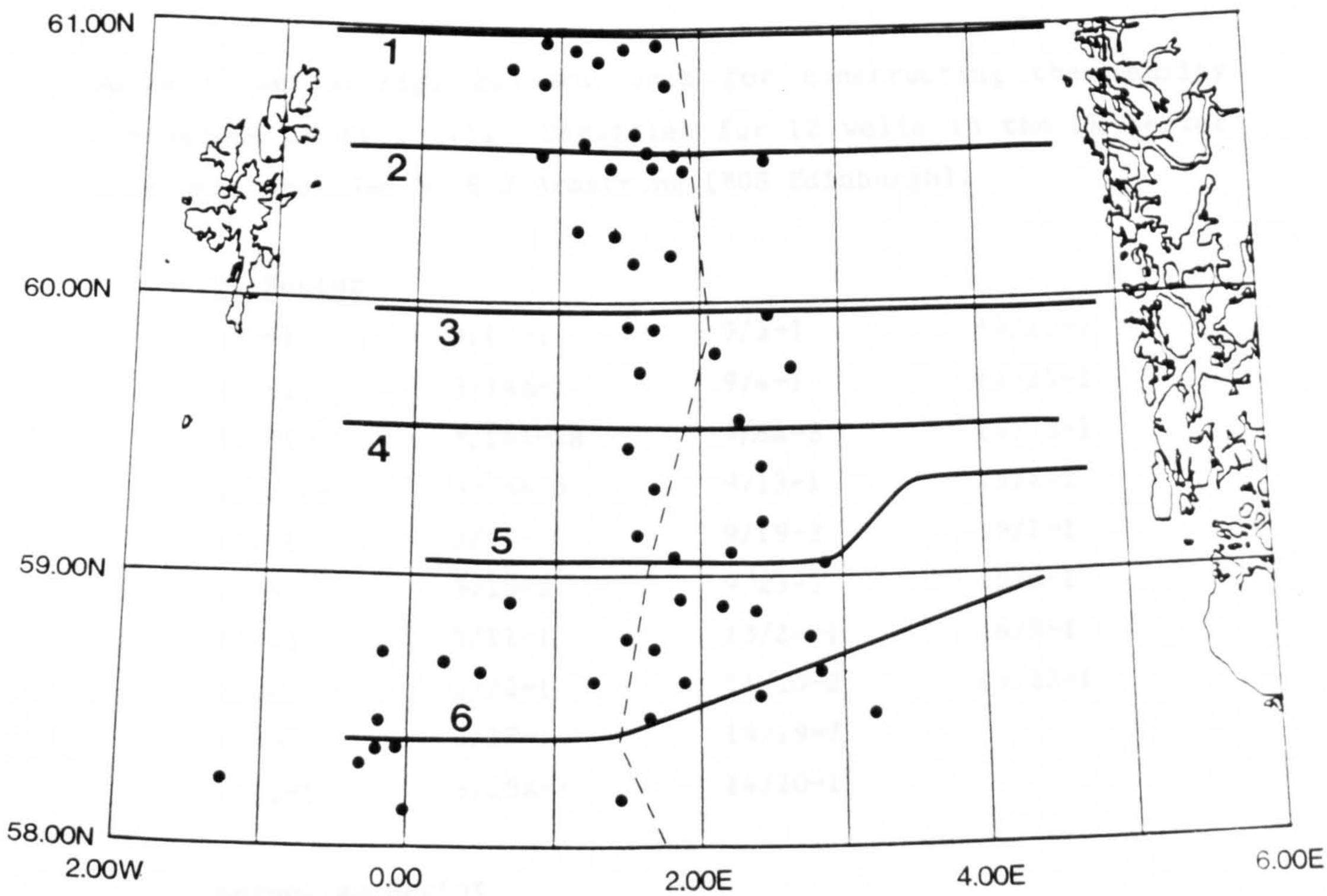

Fig. 2.3 *Gravity-seismic profiles and wells used for deriving densities (58 in all). The wells are listed in Table 2.1.*

Density values were averaged every 50ft down the well and a mean density was chosen for individual stratigraphic units marked on the seismic profiles. Obviously the FDC logs were usually run only over limited sections within each well and not all stratigraphic units were present in all wells. Nevertheless, by using 58 wells an adequate number of observations was obtained.

The following stratigraphic units were considered: Eocene to Recent, Paleocene, Upper Cretaceous, Lower Cretaceous, Jurassic, Triassic, Permian-Carboniferous-Devonian. The histogram of densities for the above units and the densities chosen for gravity modelling are shown in Fig 2.4. Some units showed large variation

Table 2.1

Wells shown in Fig. 2.3 and used for constructing the density histograms of Fig. 2.4. Densities for 12 wells in the UK sector have been provided by E J Armstrong (BGS Edinburgh).

UK Sector			
2/4-1	3/12-1	9/3-1	14/20-2
2/5-1	3/14A-1	9/4-1	14/24-1
2/5-10	3/14A-2B	9/8A-8	14/25-1
2/15-2A	3/14A-3	9/13-1	15/4-1
3/1-1	3/15-1	9/19-2	15/7-1
3/2-1	3/15-3	9/23-1	15/8-1
3/3-3	3/21-1	13/24-1	16/8-1
3/4-1	3/22-1	14/10-2	16/23-1
3/4-7	3/23-1	14/19-7	
3/11-1	3/25A-2	14/20-1	

Norwegian Sector			
15/3-1	16/2-1	24/9-1	25/8-2
15/3-9	16/3-2	25/1-1	25/10-2
15/6-2	16/5-1	25/2-4	25/11-1
15/6-4	16/6-1	25/2-6	25/12-1
16/1-2	17/4-1	25/4-1	30/5-1

in density, associated with lithological changes and the considerable variation in the depth of burial, eg. depth of Devonian varied from 2 to 5km.

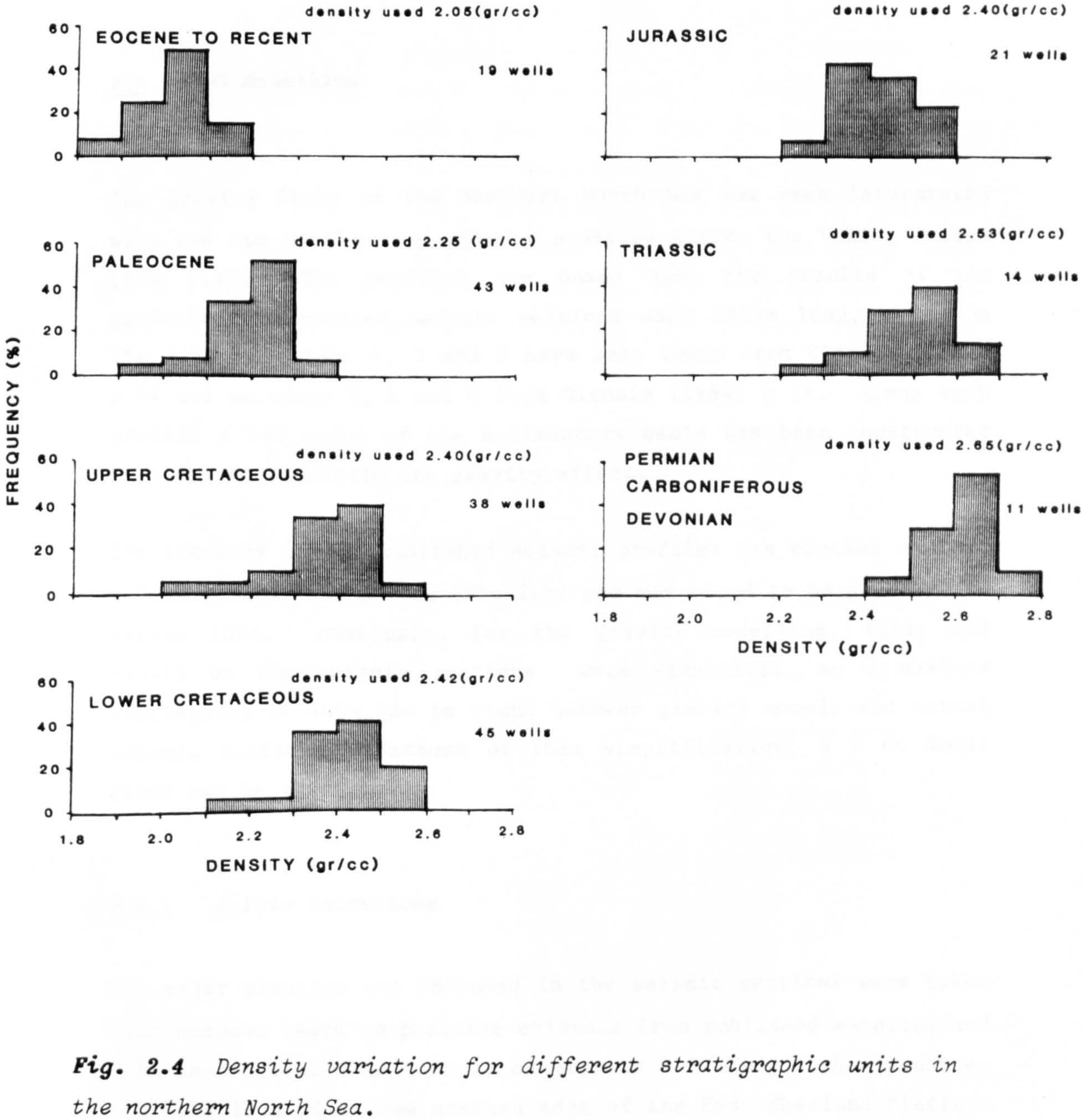

Fig. 2.4 *Density variation for different stratigraphic units in the northern North Sea.*

Salt was encountered on profile 5 (Fig 2.5) buried beneath Triassic sediment at a depth of approximately 6km. This was known to be a local structure and as such it was replaced in the model by a Permo-Triassic layer of density 2.6g/cc (rather than using salt density of 2.1-2.4g/cc), (Parasnis, 1979). Densities of 2.72g/cc and 2.62g/cc were assumed for the basement and granites respectively.

2.4 2-D Modelling

The gravity field of the northern North Sea has been interpreted with the aid of six long gravity profiles across the Viking Graben (Fig 2.3). The profiles are based upon the results of six published interpreted seismic sections each 285km long, shown on Fig 2.5. Sections 1, 3 and 5 have been taken from Ziegler (1982) p 54 and sections 2, 4 and 6 from Glennie (1984) p 36. Along each profile a 2-D model of the sedimentary basin has been constructed in order to backstrip its gravity effect.

The accuracy of the published seismic profiles was checked against released wells along them (Fig 2.5) and was found to be accurate to within 100m. Obviously, for the gravity modelling, folds and faults on the seismic sections were simplified, so a maximum discrepancy of 400m can be found between gravity models and actual seismic sections. Because of this simplification, a 2 to 3mGal error can be introduced.

2.4.1 Acidic intrusions

Two major granites not included in the seismic sections were taken into account based on positive evidence from published material and well inspection. The granite on profile 3 (Viking Graben granite, Fig 2.5) located at the eastern edge of the East Shetland Platform

at about 60°N 1°E, was proposed by Donato and Tully (1982) and is associated with a pronounced magnetic anomaly of approximately 300nT amplitude and a negative gravity residual anomaly of approximately 30mGal. It can be modelled as a cylinder of radius 20km with its base at 10km depth.

The second granite (Utsira High granite) appears on profiles 5 and 6 (Fig 2.5), having an elongated shape of about 80 x 40km, associated with a negative gravity residual anomaly of approximately 37mGal and a broad magnetic anomaly of 100nT. Further evidence for this granite comes from the released wells shown in Fig 2.6, of which four reached granitic basement and three encountered unspecified igneous/metamorphic basement of possible granitic composition. A 2-D gravity model of the Utsira High granite gives the base at 10km depth. The granite may extend deeper than this but the gravity effect of this was found to be insignificant.

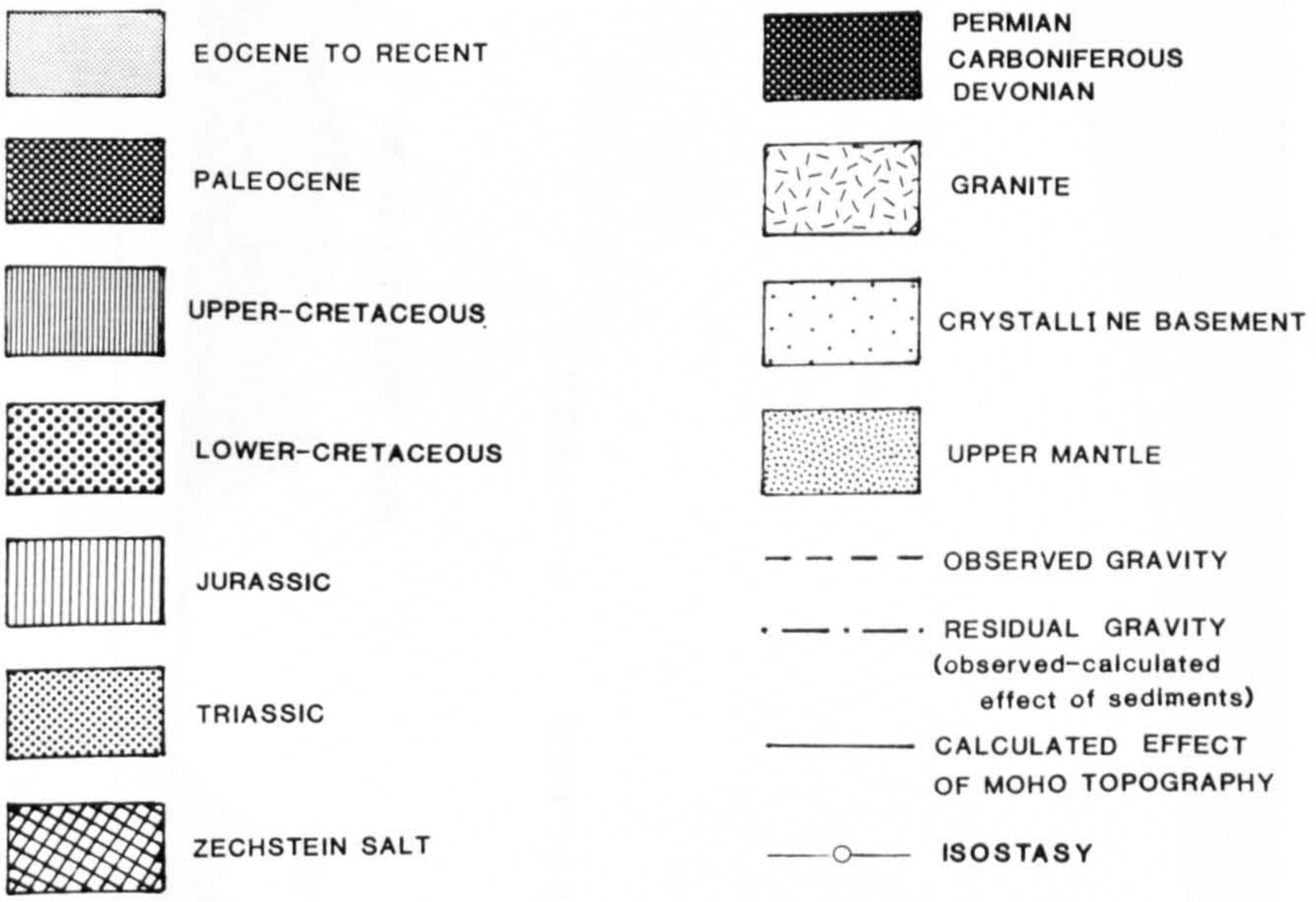

Fig. 2.5 *The following 6 pages illustrate the gravity-seismic profiles across Northern North Sea. The wells shown were used for stratigraphic control and for the basement subsidence modelling (section 5.2). Key for the following profiles (above).*

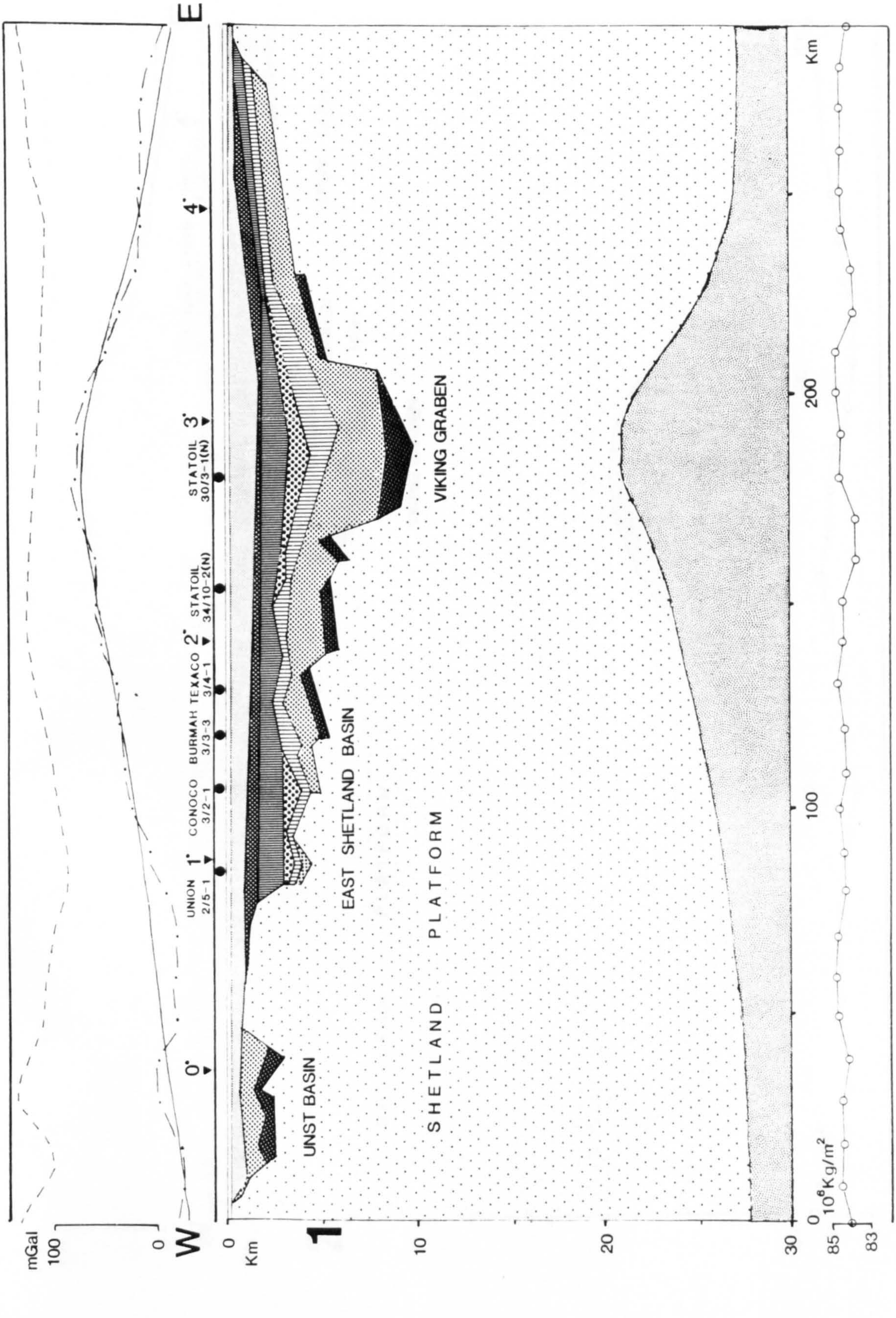
E
4°
3°
2°
1°
0°
W
UNION 2/5-1
CONOCO 3/2-1
BURMAH 3/3-3
TEXACO 3/4-1
STATOIL 34/10-2(N)
STATOIL 30/3-1(N)
VIKING GRABEN
EAST SHETLAND BASIN
SHETLAND PLATFORM
UNST BASIN
mGal
100
0
Km
0
10
20
30
1
Km
200
100
0
10^6Kg/m^2
85
83

Fig. 2.5 *(cont.)*

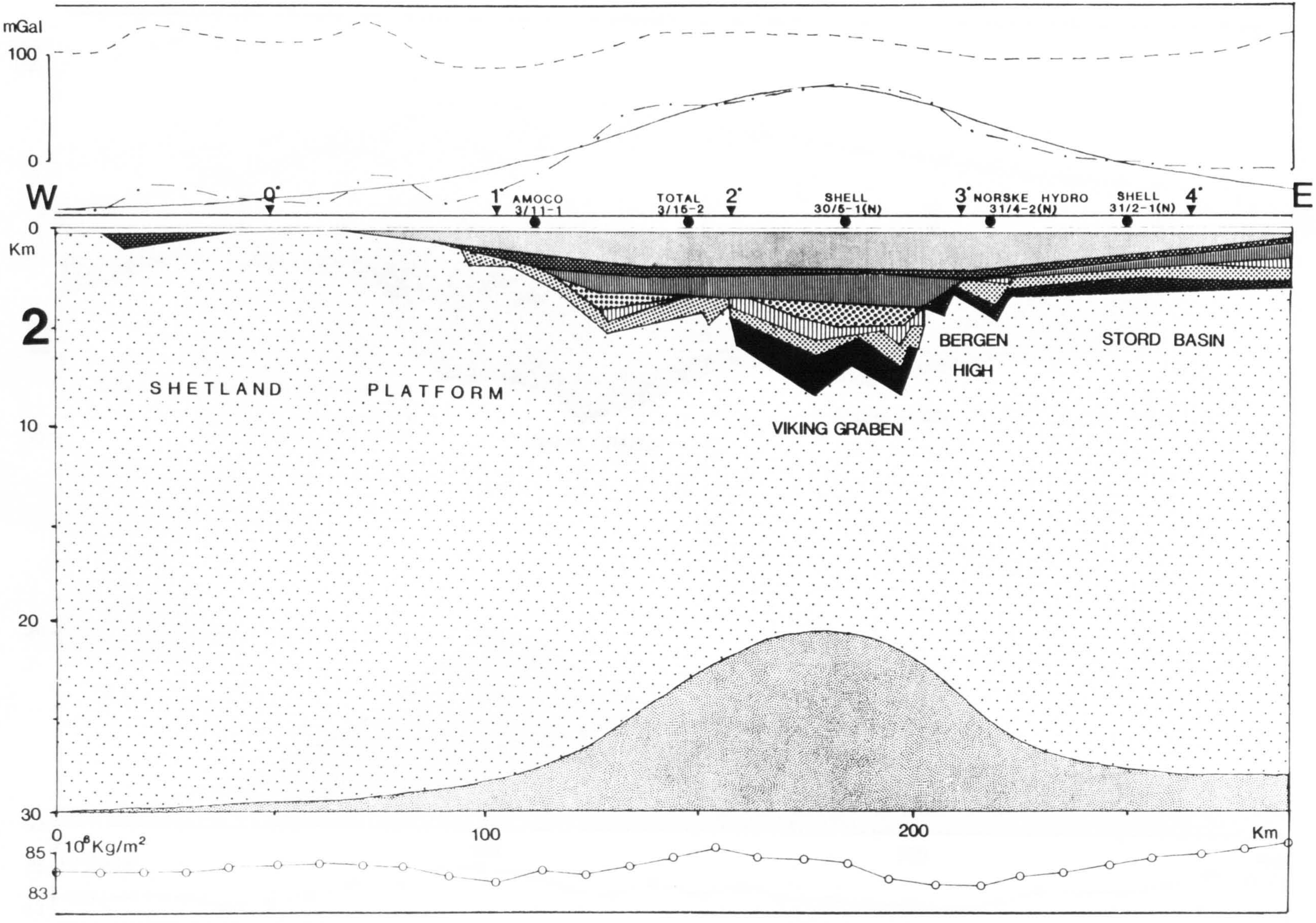
mGal
100
0
W
0°
1°
AMOCO 3/11-1
TOTAL 3/16-2
2°
SHELL 30/6-1(N)
3°
NORSKE HYDRO 31/4-2(N)
SHELL 31/2-1(N)
4°
E
0
Km
2
10
20
30
SHETLAND PLATFORM
VIKING GRABEN
BERGEN HIGH
STORD BASIN
0
100
200
Km
10⁶ Kg/m²
85
83

Fig. 2.5 (cont.)

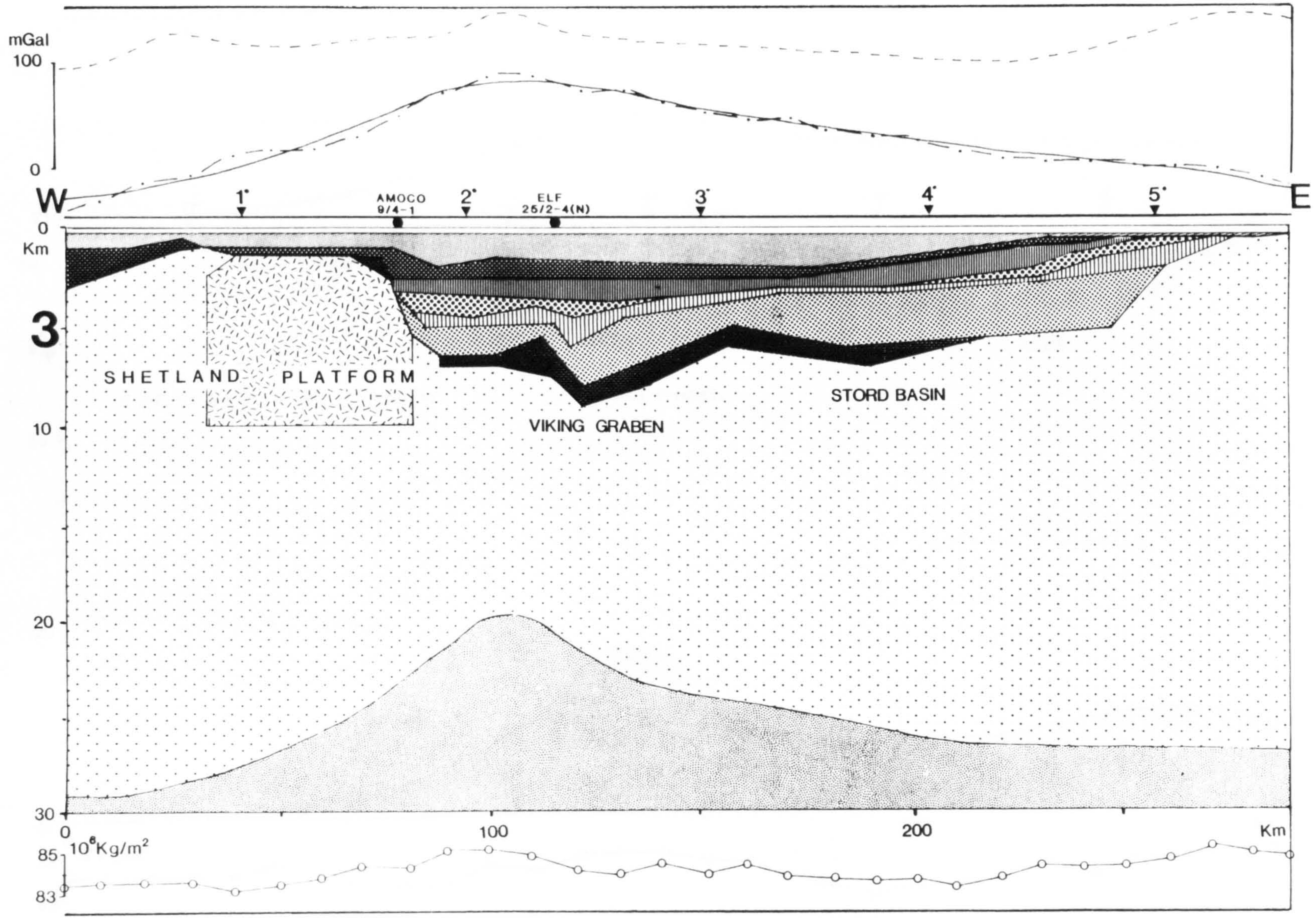
mGal
100
0
W
1°
AMOCO
9/4-1
2°
ELF
25/2-4(N)
3°
4°
5°
E
0
Km
3
SHETLAND PLATFORM
VIKING GRABEN
STORD BASIN
10
20
30
0
100
200
Km
85
10⁶Kg/m²
83

Fig. 2.5 (cont.)

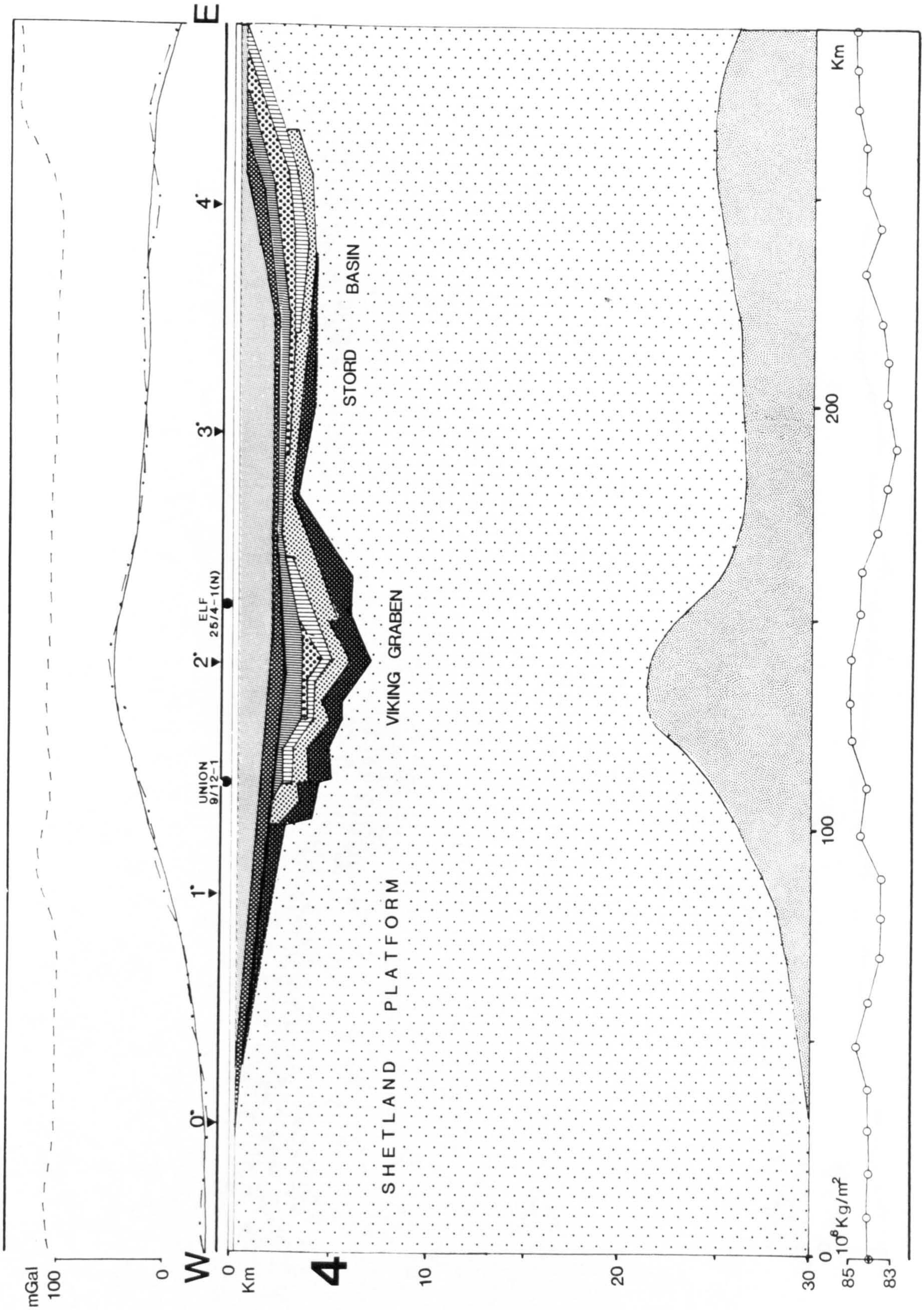
E
4°
3°
2°
ELF
26/4-1(N)
1°
UNION
9/12-1
0°
W
BASIN
STORD
VIKING GRABEN
SHETLAND PLATFORM
Km
200
100
0
mGal
100
0
Km
10
20
30
10^6 Kg/m²
85
83

Fig. 2.5 *(cont.)*

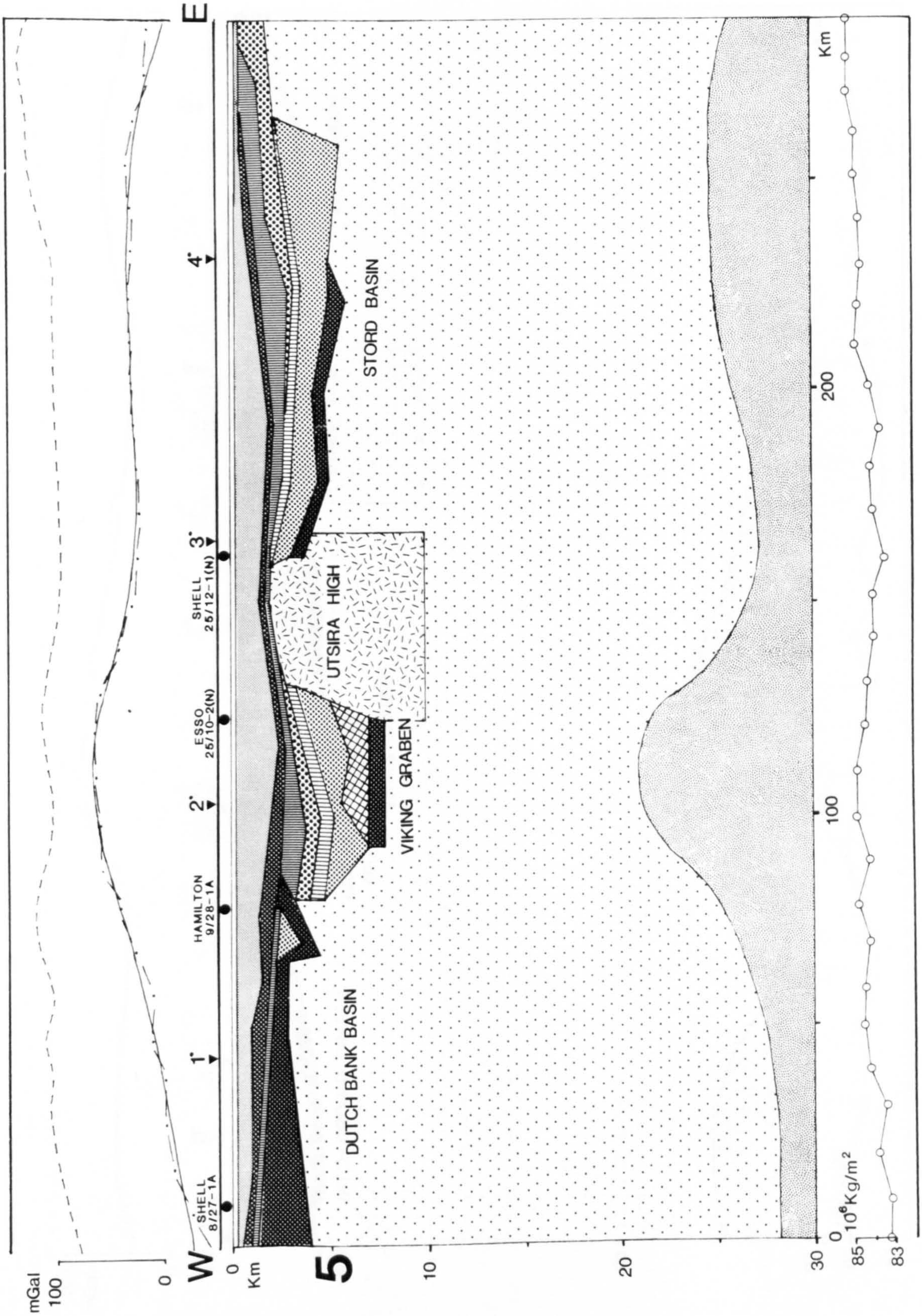
E
4°
3°
2°
1°
SHELL 25/12-1(N)
ESSO 25/10-2(N)
HAMILTON 9/28-1A
SHELL 8/27-1A
W
STORD BASIN
UTSIRA HIGH
VIKING GRABEN
DUTCH BANK BASIN
Km
0
5
10
20
30
mGal
100
0
Km
200
100
0
10^6Kg/m^2
85
83

Fig. 2.5 *(cont.)*

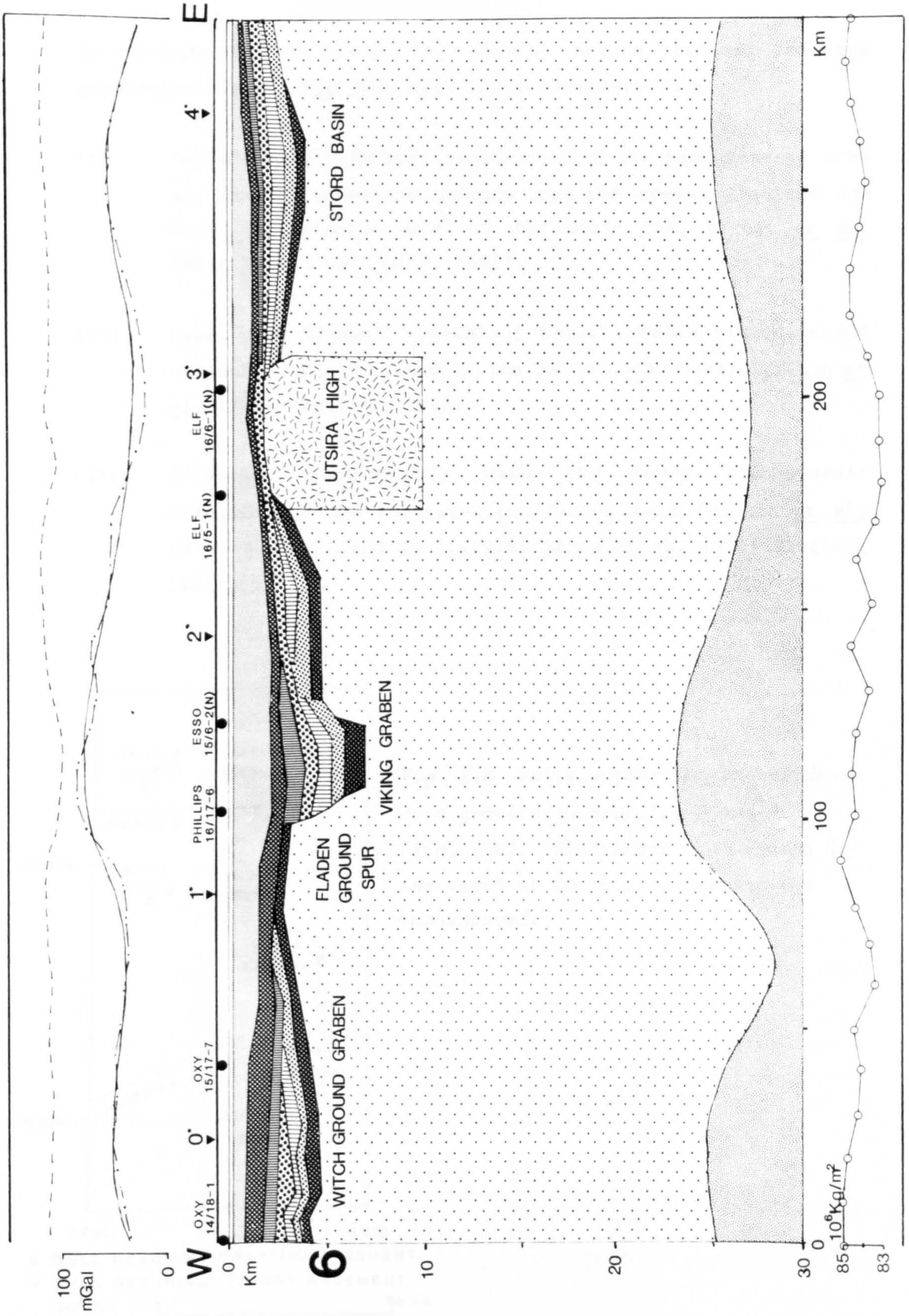
E
4°
3°
2°
1°
0°
W
STORD BASIN
UTSIRA HIGH
FLADEN GROUND SPUR
VIKING GRABEN
WITCH GROUND GRABEN
ELF 16/6-1(N)
ELF 16/5-1(N)
PHILLIPS 16/17-6
ESSO 15/6-2(N)
OXY 15/17-7
OXY 14/18-1
Km
200
100
0
10
20
30
100 mGal
0
10^6 Kg/m²
85
83

Fig. 2.5 *(cont.)*

No estimate of the age of the granite can be obtained from the geophysical data. Possible ages to be considered are:

(i) Devonian; late Caledonian plutons of the same general area as the Aberdeenshire gabbros and the coeval granites now known to underlie parts of the North Sea, (Frost et al, 1981; Donato and Tully, 1982).

(ii) Late Carboniferous - Permian; early permian plutonism and volcanism is widespread at the NW European Shelf, (Dixon et al, 1981; Ziegler, 1981).

(iii) Jurassic; contemporary with the major mid-Jurassic volcanism of the Forties-Witch Ground area (Howitt et al, 1975; Woodhall and Knox, 1979; Dixon et al, 1981; Ziegler, 1981).

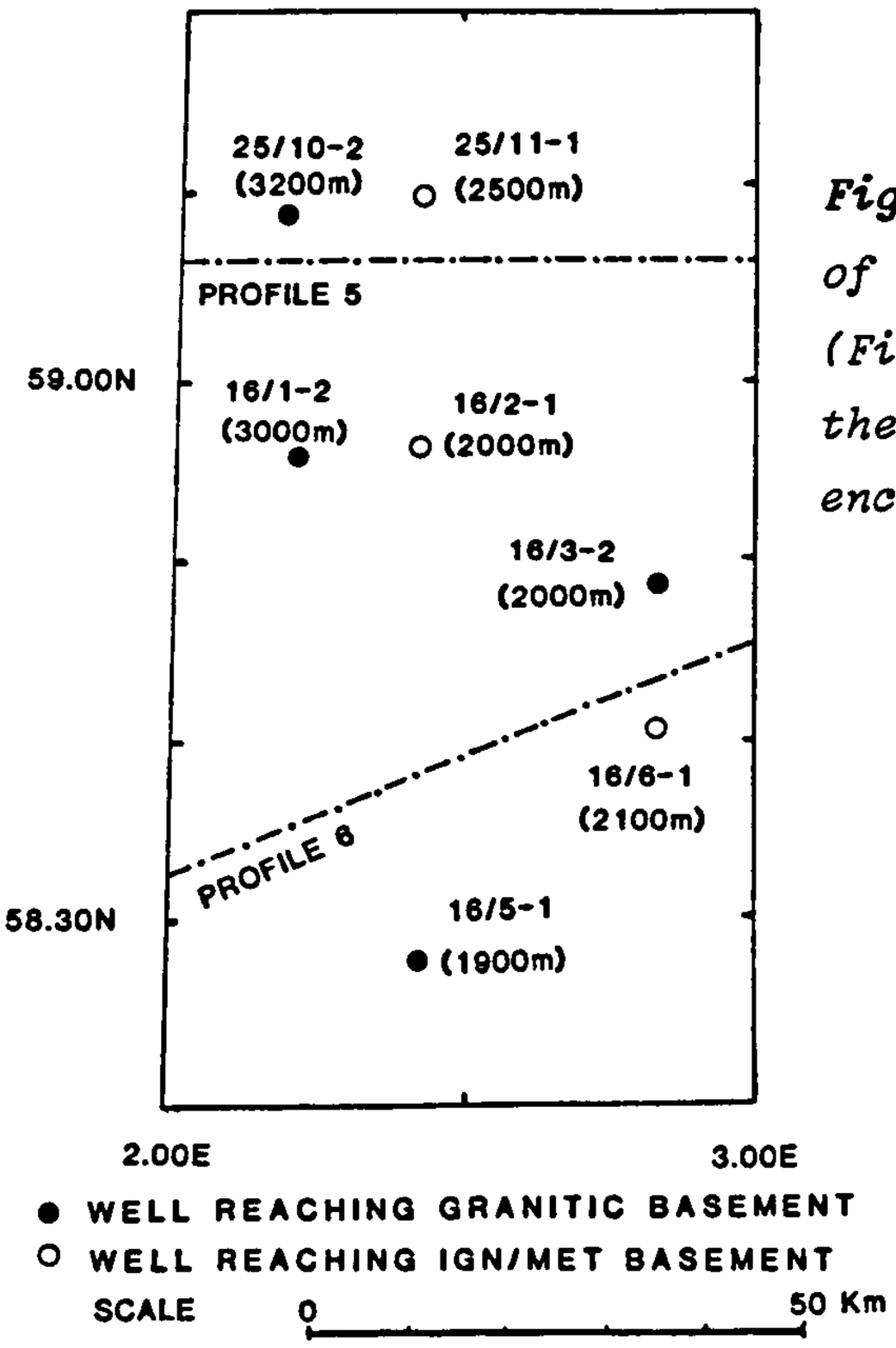

Fig. 2.6 Wells supporting the evidence of a granite on profiles 5 and 6 (Fig. 2.5). The number in brackets is the depth at which the basement was encountered.

It seems most likely, however, particularly on consideration of the stratigraphic history apparently demonstrated by the published profiles (Fig 2.5), that the Utsira High granite is similar to the numerous Caledonian granites observed onshore.

2.4.2 Interpretation of the residual anomaly

A large discrepancy was found between observed gravity anomalies and those calculated for the attraction of the sediments in all six profiles in the Viking Graben area, although on the flanks a rough agreement was achieved. By subtracting the effect of the sediments from the observed gravity values, a positive residual anomaly is produced having an amplitude of approximately 100mGal and a long wavelength of at least 100km across the Viking Graben (Fig 2.5). The residual anomaly can be explained in terms of a thinning of the crust beneath the Stord Basin, Witch Ground and Viking Grabens. Attempts were made to match the residual gravity with the calculated gravity effect obtained by varying the Moho topography.

A density of 3.35g/cc was used for the upper mantle and in this case the density of the crust was assumed to be 2.85g/cc instead of 2.72g/cc when the effect of the sediments was calculated, to take into account a density increase with depth.

The maximum thinning of the crust of about 20km was calculated beneath the Viking Graben, excluding the sediment thickness and assuming an initial crustal thickness of 30km. Similar conclusions have been drawn by Donato and Tully (1981) investigating the thickness of the crust using gravity data from the UK sector of the North Sea.

A contour map of Moho depth (Fig 2.7) was constructed from the 2-D seismic-gravity models (Fig 2.5) and this is shown as an isometric projection in (Fig 2.8).

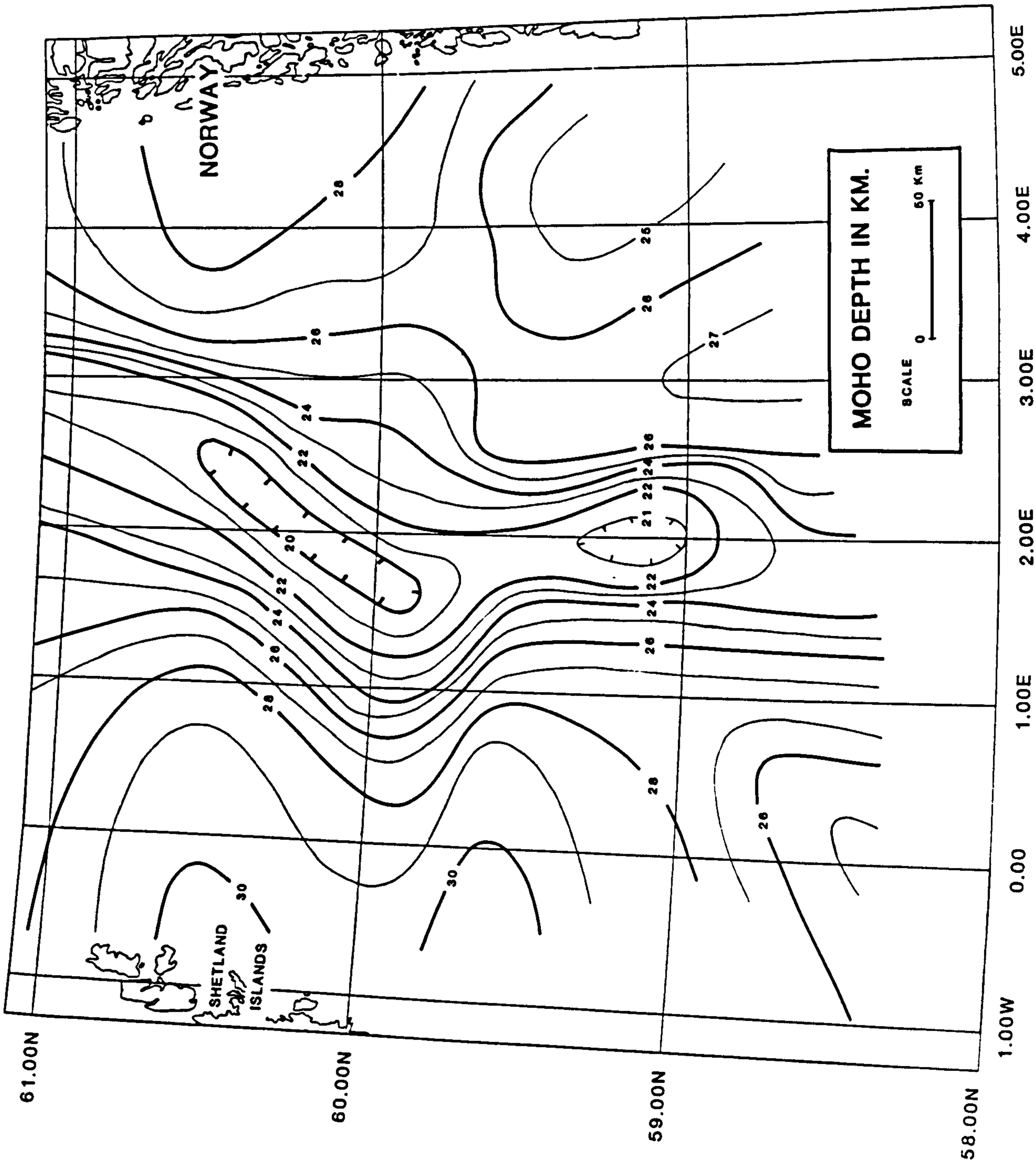

Fig. 2.7 Moho topography constructed from 2-D gravity-seismic models (Fig. 2.5).

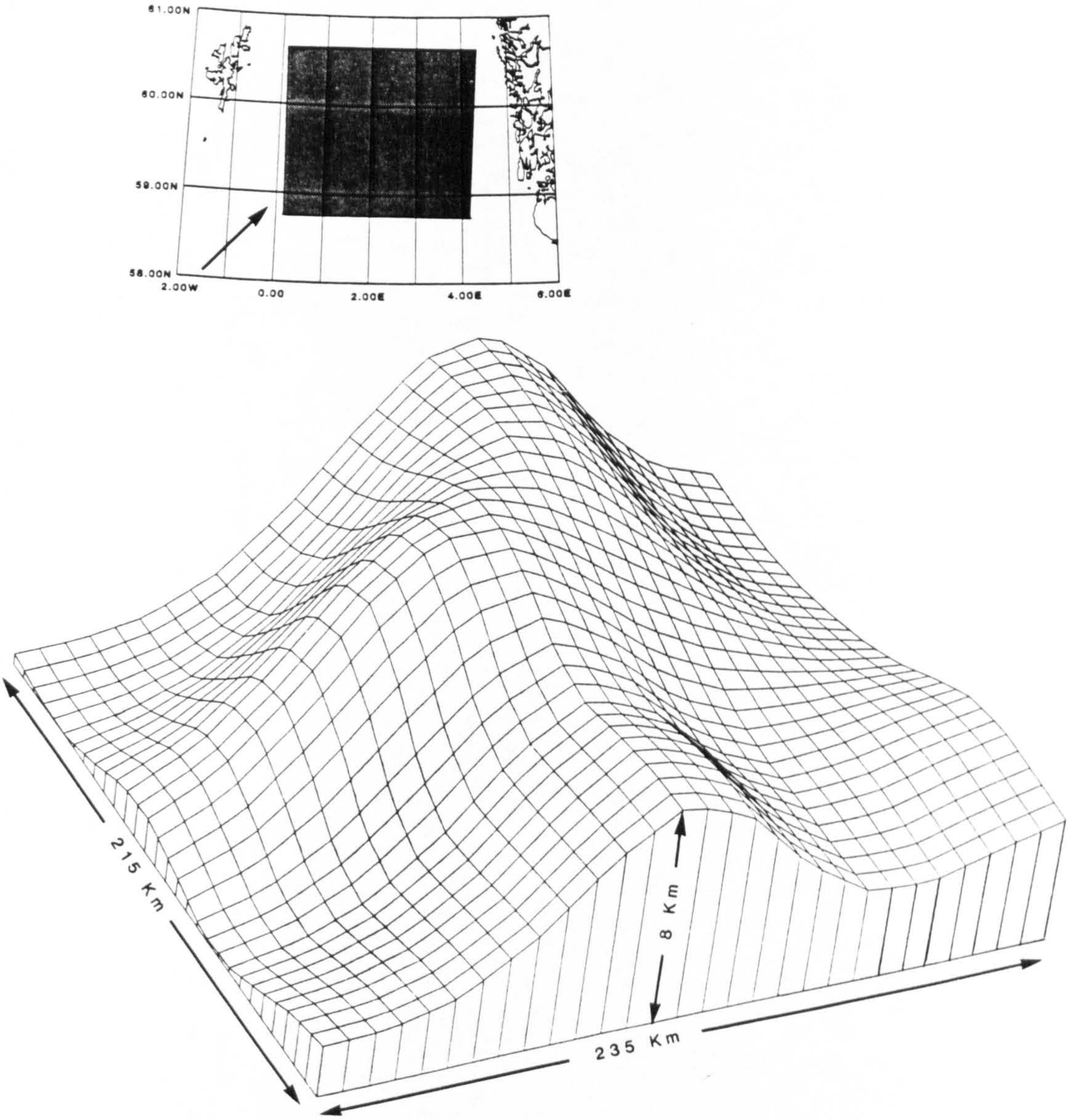

Fig. 2.8 *Isometric projection of Moho topography constructed from Fig. 2.7. The base of the diagram lies 30km below sea level. The vertical scale is greatly exaggerated with the maximum relief being approximately 10km. The location of the study area is shown in the top figure with the arrow pointing in the direction of viewing from an elevation of 35°.*

2.5 3-D Modelling

The 2-D gravity modelling assumes infinite extension of the cross-sections along strike. This is approximately the case especially for the Upper Cretaceous and Tertiary sediments, but it is obvious that the shape of the profiles changes in detail along the length of the basin. Three-dimensional modelling represents a more rigorous approach and has been used to check the results of the 2-D model. Unfortunately, there is insufficient published data available, particularly in the Norwegian sector, to enable the construction of isopach maps over the whole area.

The regional Bouguer anomaly gravity map (Fig 2.9) was compiled from the residual gravity values of the six gravity-seismic profiles (Fig 2.5). This map is considered to reflect the gravity effect of the Moho topography through its long wavelength anomalies. A more accurate model of the Moho could be obtained if any remaining short wavelengths, due to shallow structures, were eliminated mathematically. This was in effect done by digitising the regional map (Fig 2.9) on a 10km grid and applying a Gaussian filter in the X and Y directions. The filtered map was then used to construct a 3-D model of the Moho, assuming a crust/mantle density contrast of 0.5g/cc and a crustal thickness of 30km on either side of the graben. The results from the 3-D model (Fig 2.10) are very similar to those obtained in the 2-D model. The Moho contours follow the same trend and the maximum local discrepancy between models is about 2km. It is therefore concluded that 2-D modelling is sufficiently accurate for the degree of detail required here.

2.6 Lateral Density Variations within the Crust

Refraction profiles shot across the Viking (Solli, 1976) and Witchground/Buchan (Christie, 1982) grabens show crustal thinning beneath the grabens but reveal no information about lateral heterogeneity within the crust. Barton and Wood (1984), following

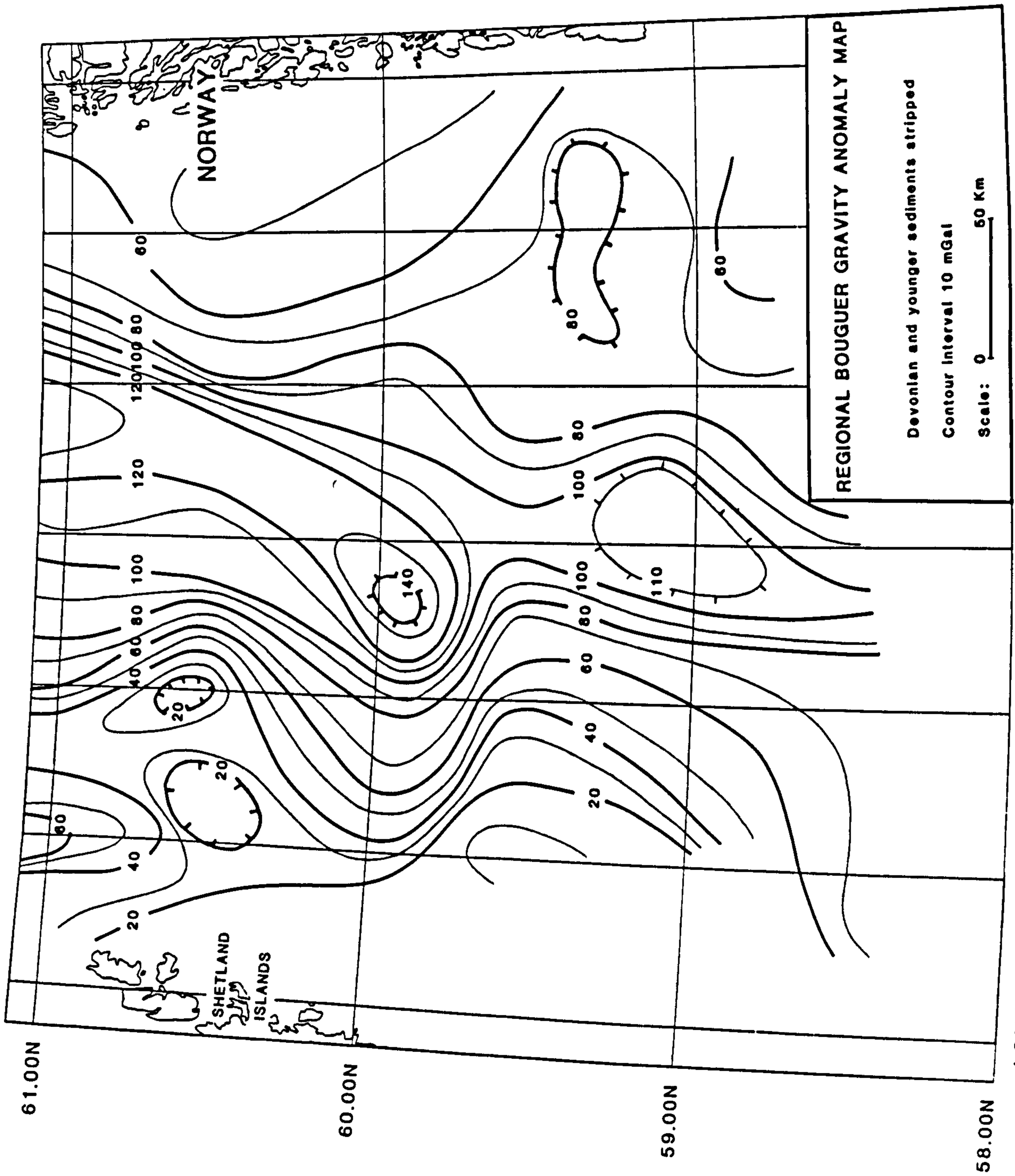

Fig. 2.9 Regional Bouguer anomaly map contoured from the residual gravity values of the gravity-seismic profiles (Fig. 2.5).

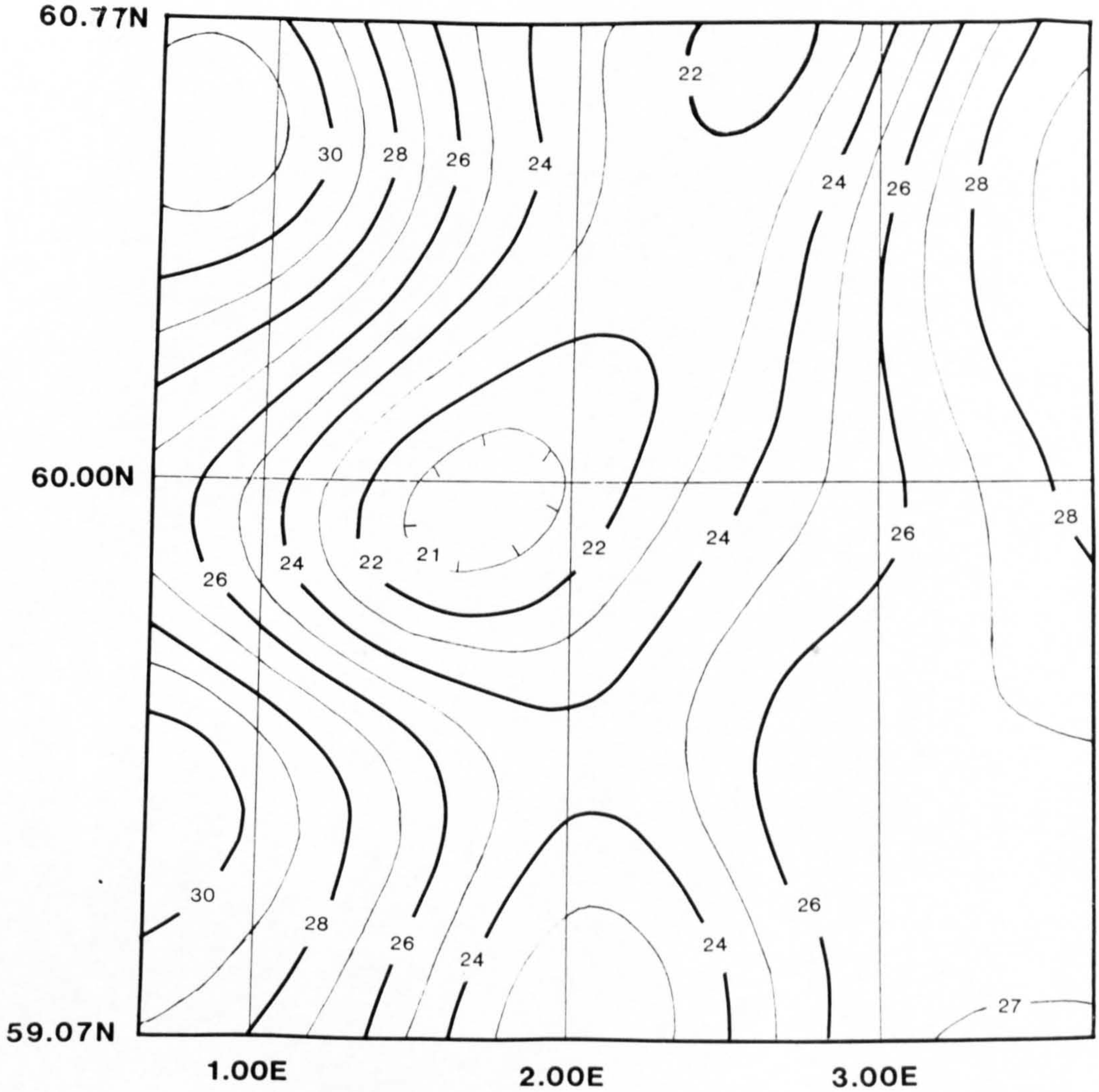

MOHO DEPTH IN KM.

(Three dimensional modelling)

SCALE

0 50 Km.

Fig. 2.10 *Moho topography in 3-D constructed from the filtered version of the regional Bouguer gravity anomaly map (Fig. 2.9).*

the method of Cassell (1982), modelled a laterally varying structure beneath their Central Graben refraction profile and their results represent the best constructed seismic model so far obtained for the crustal structure of the North Sea. They have modelled a high velocity anomaly within the lower crust just to the west of the Central Graben. Converting seismic velocities to suitable densities, using the range of values possible within the scatter of points shown on a velocity-density plot of Ludwig et al (1970), the gravity anomaly created was found to be less than 16mGal. The introduction of such an anomaly beneath the Viking Graben would introduce an error of only 1 or 2km in the modelled depth of the Moho topography. For upper crustal bodies to produce a significant contribution to the positive regional gravity anomaly, requires them to have unrealistic dimensions and densities. All the available evidence indicates therefore that crustal thinning is responsible for the observed regional gravity anomaly.

2.7 Initial Crustal Thickness

The estimates of crustal thickness on the margins of the basin have an important effect on the amount of crustal thinning required by the model to fit the regional gravity high. Refraction experiments indicate that crustal thickness may reach 35km beneath both Scotland (Bamford et al, 1978) and Norway (Cassell et al, 1982). In this study it is more appropriate to consider the results of refraction studies at the margin of the northern North Sea sedimentary basin which show Moho depths of 29-32km west of the Central Graben (Barton and Wood, 1984; Sclater and Christie, 1980), 30-32km on the East Shetland Platform (Sclater and Christie, 1980) and 27-28km on the south-east margin of the Viking Graben falling to 30km at the Norwegian coast (Barton and Wood, 1984; Cassell et al, 1982). The value of 30km chosen for the gravity modelling is a rough mean of these values and is considered to be a realistic value for the thickness of the crust beneath the Viking Graben prior to Permo-Triassic rifting (see also section 5.2).

2.8 Density Contrast

The density contrast at the crust-mantle boundary is fundamental in determining the magnitude of the calculated anomaly. Reference may be made once again to the refraction experiments (Solli, 1976; Sclater and Christie, 1980; Barton and Wood, 1984) which clearly identified a Moho refractor with velocities of 8.3, 8.16 and 8.1km.s^{-1} respectively. The lower crustal velocities obtained by Solli (1976) and Sclater and Christie (1980) were poorly constrained and more credence is given to the range of 6.6-7.0km.s^{-1} given by Barton and Wood (1984) for the lower crust laterally adjacent to the upwelling of the mantle beneath the crust. The above velocities were converted to densities using the velocity density plot by Ludwig et al (1970) and giving a density value of 3.35±0.03g/cc for the upper mantle and a mean value of 2.85±0.1g/cc for the lower crust. The chosen density contrast of 0.5g/cc corresponds to the middle of this range, but this uncertainty could lead to slightly different results. It also has to be pointed out that Moho depth determinations greater than 30km are associated with crustal velocities that would give rise to a crust/mantle density contrast slightly lower than 0.5g/cc. A combination of a crustal thickness of 32km and density contrast of 0.45g/cc yields virtually identical results to the ones described in this chapter.

2.9 Isostasy

Each gravity profile on Fig 6 includes a quasi-isostatic vertical mass summation down to 30km depth. The isostasy curves vary around a mean value of 84Gg/m^2, representing a 30km thick crust of mean density 2.8g/cc. The short wavelength variation of these curves around a mean value indicates a reasonable isostatic compensation of each profile. There is a slight tendency however for the isostasy curve to follow roughly the Moho topography, which can easily be caused by a slight inaccuracy in the estimation of density contrast between lower crust and mantle.

2.10 Discussion and Conclusions

The sediments were stripped off the sedimentary basin leaving a regional gravity anomaly. The peak of the anomaly is located in the area of the thickest sedimentary section with its wavelength increasing but amplitude decreasing from north to south. The magnitude and wavelengths are similar to those for gravity anomalies observed over the ancient intercontinental rifts (Ramberg, 1972; Chase and Gilmer, 1973; Ocola and Meyer, 1973; Blundell, 1978). The regional anomaly is explained in terms of thinning of the crust beneath the Stord Basin, Witch Ground and Viking Grabens. These results closely agree with predictions obtained from gravity data for this area (Donato and Tully, 1981).

The refraction data of Christie and Sclater (1980) and of Wood and Barton (1983) have provided some confirmation of a similar picture below the Witch Ground and Central Grabens respectively. The profile of Christie and Sclater (1980) crosses the western ends of profiles 3 to 6 giving a discrepancy of 2km for the first intersection (profile 3) and less than 1km for the rest. Their seismic study was combined with independent well subsidence data to show that the crustal structure and basement subsidence patterns are both compatible with a simple uniform extensional mechanism over 60Myrs for the post-Paleozoic evolution of the North Sea. A detailed account of this work was given by Barton and Wood (1984) and Barton and Matthews (1984) where no major lateral density variations, seen as variations in velocity, were detected within the crust. The refraction profile was later used to label the Moho depth below the Central Graben in a normal incidence deep reflection profile coincident with the refraction one (Barton *et al*, 1984). Profile 1 almost coincides with part of Solli's refraction profile (Ziegler, 1982) which yields similar results. On profiles 1 and 2 a short wavelength discrepancy of 18mGal maximum can be observed between residual and calculated gravity from Moho topography at the East Shetlands Platform area. This is

due to either basic igneous rocks such as are seen on the Shetland Islands (McQuillan and Brooks, 1967) or small-scale lateral density variations within the pre-Permian basement. Close to the Norwegian coast, however, the Moho depth is found to be approximately 28km coinciding with the value given by Ramberg et al (1977), deepening rapidly towards the mainland.

Any possibility of large scale lateral density variations within the crust, causing the regional anomaly is incompatible with the present geological knowledge of the area. It can be concluded, therefore, that the large amplitude, long wavelength regional positive anomaly is due almost entirely to the effects of crustal thinning with possible lateral density variations not affecting the Moho topography by more than 2km.

The Moho topography in the gravity profiles seems, in the first order, to reflect the shape of the sedimentary basin. The isostasy curves suggest that basement subsidence and sediment loading have been largely accommodated by local Airy-type isostatic equilibration (eg. Barton and Wood (1984) for the Central Graben) rather than by flexure as described by Donato and Tully (1981).

For comparison with the 2-D approach of the Moho topography, a 3-D model was constructed showing that the contours follow the same trend as in the 2-D case with a maximum local discrepancy of about 2km between the two models. Relief in the Moho is more pronounced in the 3-D model but the crustal thinning is still at a maximum under the graben. The 2-D approach is adequate in this case because the Tertiary basin which accounts for greater than 60% of the total sediment gravity effect is approximately 2-D with length/width ratio >4/1.

The gravity interpretation is of course non-unique and a number of different models can be made to fit the regional positive anomaly. They all however retain a similar maximum crustal thinning and

width of the thinning beneath the Viking Graben with the main variation the steepness of the Moho topography towards this maximum. Refraction evidence from Solli (1976), Christie and Sclater (1980), Wood and Barton (1983) and deep reflection interpretation, Barton et al (1984), Brewer et al (1983), Brewer and Smythe (1984), Hall et al (1984) in the North Sea and surrounding seas suggests that the Moho has a rather smooth swell shape rather than a diapiric structure, even though the latter is numerically agreeable with the data. The model illustrated was chosen because of its compatibility with the refraction data and the present geological knowledge of the northern North Sea area.

The quantitative estimation of the crustal thickness is the first step in the investigation of the Viking Graben geophysical development. The next step will be the basement subsidence modelling and crustal thickness estimation of backstripped and decompacted wells. To be able to do this though, it is essential to know the porosity-depth relationship of the sediments. This is in fact dealt with in the next Chapter, where the "normal" porosities from well-log investigation, for the three dominant lithologies in the northern North Sea, are established and mechanisms are suggested for the cause of the few non "normally" compacted sequences observed.

CHAPTER 3

POROSITIES AND OVEPRESSURE

Introduction

In order to study the geological history of the Viking Graben from well-log information, a porosity-depth investigation is a fundamental pre-requisite to backstripping and decompacting the sediments (see sections 4.2 and 4.4). Porosities from 28 wells were calculated in order to establish "normal" porosity trends and abnormally high porosities, which are interpreted in terms of "normal" and abnormally high pressures respectively.

Formation pressure at any depth is considered "normal" when it is approximately equal to the hydrostatic head of water at the same depth. Formations with pressures higher than hydrostatic are encountered worldwide in formation ranging in age from the Cenozoic era (Pleistocene age) to as old as the Paleozoic era (Cambrian age) at varying depths (Dickinson, 1953; Reynolds, 1970; Magara, 1975a; Fertl, 1976 and others). Formation pressures up to twice the hydrostatic have been observed in overpressured Tertiary, Cretaceous and Jurassic formations in the North Sea basin, (Byrd, 1975; Selley, 1978; Sclater and Christie, 1980; Goff, 1983). Similarly, in this study a number of cases of abnormally undercompacted (overpressured) sequences were encountered. These in themselves, are of interest in understanding the infill history of a subsiding basin since they supposedly reflect rapid sedimentation periods, (eg. Hubbert and Rubey, 1959; Rochow, 1967; Bredehoeft and Hanshaw, 1968; Magara, 1971; Fertl and Timko, 1972; and Smith, 1973). It was therefore decided to find out if the rapid sedimentation is a justified cause for under compaction in the northern North Sea.

Furthermore, such a study is considered very important because the problems associated with overpressure are of direct concern to all phases of oil exploration and development; geophysics, drilling, geological and petroleum engineering. Knowledge of the pressure distribution in a given area frequently minimizes the problems.

Therefore, some questions about overpressure arise and need to be answered:

1. What is its lateral distribution; is it a widespread phenomenon at the northern North Sea?

2. Is it encountered at a certain depth or certain stratigraphic units?

3. Is it created by a single cause or by a combination of causes?

A brief description is given of the porosity well-logs, their limitations and the method used in this study in order to calculate porosities for the three dominant lithologies of the northern North Sea; sandstones, siltstones and shales. "Normal" porosity depth curves are deduced for the above "clean" lithologies (free of hydrocarbons) along which the wells were decompacted and sedimentation rates were computed for all the age determinations available in the Composite log, as in section 4.2. Finally the mechanisms causing abnormal pressure worldwide are discussed and a mechanism is proposed to account for the overpressured cases observed in the northern North Sea.

3.1 Porosity Definition

Primary porosity

Primary porosity, usually granular, is the porosity developed by the original sedimentation process by which the rock was created.

all practical purposes, porosity is the non-solid part of the rock filled with fluids.

Secondary porosity

Secondary porosity is created by a process other than primary cementation and compaction of the sediments. An example of secondary porosity is the dissolving of limestone or dolomite by ground water, a process which creates vugs and caverns. Fracturing, dolomitization and subsequent chemical changes also create secondary porosity. In most cases, secondary porosity results in a much higher permeability than primary granular porosity.

Effective porosity

Effective porosity is the porosity available to free fluids excluding unconnected porosity and space occupied by bound water and disseminated shale. This type of porosity is closely related to permeability.

In general, porosities tend to be lower in the deeper and older rocks. This decrease in porosity is due primarily to overburden and cementation.

Shales follow very much the same porosity/depth trend as sandstones except that porosities are normally lower in shales. For example, in a recent mud the porosity measures about 50%. It decreases exponentially with depth until normal porosities are less than 10%, at about 3000m depth. This is typical of Tertiary shales, with older shales being considerably more compacted and thus lower in porosity. Shales are essentially plastic and therefore compress more easily than sands. These basic trends of porosity versus depth are not really noticeable in carbonates, which usually however tend to be pseudo-plastic and compress considerably more than sands.

In this study we do not distinguish between primary, secondary or effective porosity; we refer to the **TOTAL POROSITY** (primary + secondary) observed in "clean" formations.

3.2 Total Porosity From Well-Logs

In this section a brief description is given of the three well-logs (Sonic, Formation Density, Neutron) used by the oil industry to evaluate porosities. The following draws extensively on Schlumberger (1969) and Dresser Atlas (1974) where the above logs and their limitations are fully documented.

3.2.1 Sonic log

Basically with the use of multiple transmitters and receivers, the sonic logging tool measures the minimum time that it takes for an acoustic pulse to travel through the rock complex. This interval distance varies from tool to tool, but is most typically two feet along the borehole wall. The total time that it takes for the acoustic pulse to travel in the rock complex is proportional to (1) the amount of fluid in the pore space times the time that it would take to travel through that fluid and (2) the amount of rock matrix times the time that it would take to travel through the rock matrix. Thus an equation can be written:

$$\Delta t = f\Delta t_{fl} + (1-f)\Delta t_{ma}$$

Therefore the porosity can be calculated directly as follows:

$$f = \frac{\Delta t - \Delta t_{ma}}{\Delta t_{fl} - \Delta t_{ma}}$$

Limitations of Sonic log

This porosity tool is most effective where the formation being measured is consolidated and compacted. In this case gas normally has little effect, but where rocks are unconsolidated or not compacted, travel time is readily influenced by formation fluids, whether it be water, gas or oil.

Because this tool measures the first acoustic pulse arriving at the receiver, that pulse normally circumvents any fracture or vugular porosity. Hence the sonic log normally does not measure secondary porosity. Accordingly the porosity calculations which one makes with the sonic tool are, quite typically, the minimum porosity in that interval. The optimum porosity range for this tool is between 5 and 20 percent. Below this, excellent matrix transit time values are necessary (see equation above), and above this, the tool is adversely affected by shaliness and under-compaction.

3.2.2 Compensated Formation Density log (FDC)

The density log is a sidewall pad device which has a source of gamma rays and two receivers. The gamma ray flux at the receivers is a function of Compton scattering which, in turn, is a function of the electron density in the rock matrix. Here again, it is necessary to indirectly determine the parameter sought, which is the density. The electron density is simply related to the element (bulk) density only if the number of protons is equal to the number of neutrons. When this is not true, corrections must be made. This is why, what the tool actually measures is apparent density.

The bulk density of the formation is equal to the density of the fluid times the percentage of that fluid, plus the density of the rock matrix times the percentage of that matrix. In other words:

$$\rho_b = f\rho_{fl} + (1 - f)\rho_{ma}$$

Therefore the porosity is given by:

$$f = \frac{\rho_b - \rho_{ma}}{\rho_{fl} - \rho_{ma}}$$

Just as with the sonic tool, in order to convert the density measurements to porosity, we need to assume a rock matrix and fluid density.

Limitations of FDC log

There are some limitations to the borehole density tool, one of these being the fact that the tool is a padded sidewall tool and sees less than 25% of the borehole wall. Laboratory results have shown that when the log goes through a gas zone this porosity measurement is optimistic. In carbonate sequences where vugular and fracture porosities are an important component of total porosity and permeability of the system, the density tool often gives a pessimistic porosity. The density tool is most effective where porosity is heterogeneous and ranges between 10 and 35 percent.

3.2.3 Neutron Porosity logs

Neutron tools are typically of two types: the first has a single source and single receiver, and is a sidewall system. The receiver, in this case, measures epithermal neutrons from the source. The second and more common type has one source and two receivers. These two receivers measure thermal neutrons, and it is a compensated system for borehole rugosity and diameter. In either case, the principle is basically the same. What the detectors measure is the neutron flux at a particular energy level. Accordingly, they measure how much the formation has slowed the high energy neutrons from the source.

The high energy neutrons from the source are slowed by collision with the nuclei of the various elements in the formation. The elements that have an atomic mass closest to that of the neutrons

tend to slow the neutrons more than do elements that have fairly large atomic mass. Therefore, hydrogen, having about the same atomic mass as the neutrons, tends to slow neutrons more readily than other elements. What the neutron porosity tool predominantly measures is the hydrogen ion content in the formation.

The standard calibration for neutron porosity tools is in the limestone sequence at the API pits in Houston. Hence, many neutron porosity logs are given in limestone units. However, correction curves are available for sandstone and dolomite.

Limitations of Neutron Porosity logs

Since the neutron porosity tools measure the amount of hydrogen in the formation, where hydrogen exists in a chemically bound sate, the neutron porosity tool will give an anomalously high porosity. This will occur in shales and gypsum. One hundred percent gypsym with zero effective porosity will show a porosity on the neutron log of 50 percent. Similar values can be measured on shales and shaley sandstones. Hence, a little shale in the formation can adversely affect the true porosity reading with the neutron tool.

Since most of the stratigraphic units in the northern North Sea are shales or siltstones, where the neutron tool gives particularly anomalous readings, it was decided not to use it for porosity estimation in this work.

3.3 Porosity Estimation

In order to estimate the porosity in pure limestone stratigraphic sections, the standard Schlumberger (1969) techniques were applied using the sonic-log. Unfortunately no porosity log interpretation charts are available for shales, because shales have no effective porosity, so the same technique could not be applied. Instead a Density (FDC) - Sonic crossplot was used to evaluate shale, shaley sands and sandstone porosity. The method is fully described in the following section.

3.3.1 FDC - Sonic crossplot

The reasons for using this particular crossplot are:

1. Both logs (FDC, Sonic) are more often run than any other log, for seismic interpretation purposes.

2. Sandstone, shaley sand and shale porosities can all easily be evaluated from the same graph.

3. For sandstone in particular, the crossplot method gives more accurate porosity values (within 5%) than the individual logs.

4. Both logs detect overpressured sections.

Porosity and the percentage of shale may be determined graphically if the assumption is made that the laminated and disseminated shale exhibit the same physical properties as the nearest massive shale in the section which is located using the Gamma Ray log. The method is similar to that employed by the petrographer in developing a triangular plot of the fractions in a three component sample, for instance sand, silt, and clay. In this case the triangle will not be equilateral, but the vertices will represent 100% water (100% porosity), 100% shale, and 100% sand, Fig. 3.1.

To develop the triangle, a rectangular co-ordinate system is established with the bulk density values on the vertical axis decreasing upward and acoustic travel time on the horizontal axis increasing to the right.

The point of the 100% sand vertex is located by a density value of 2.65g/cc (quartz density) and a travel time of 55.5μsec/ft (average travel time in cemented sandstones). The 100% water point (100% porosity) is also located from established values for ρ_w=1.0g/cc and Δt for water = 198 μsec/ft. The shale point is positioned by plotting the density and travel time determined for the nearest

massive shale. The method is based on the assumption that the nearby massive shale (located by the Gamma Ray log) and the laminated or disseminated shale have the same physical properties.

Since the 100% shale point determines the shear of the triangle grid, each part of the log containing shale of different properties may require the construction of a new triangle. As an average 5 to 6 different triangles were used per well. Note that lines are drawn parallel to the base of the triangle at uniform intervals to indicate porosity values from 0-100%. Lines drawn parallel to the side opposite the 100% shale vertex indicate uniform shale percentages. Both logs (Sonic FDC) were digitized every 100ft.

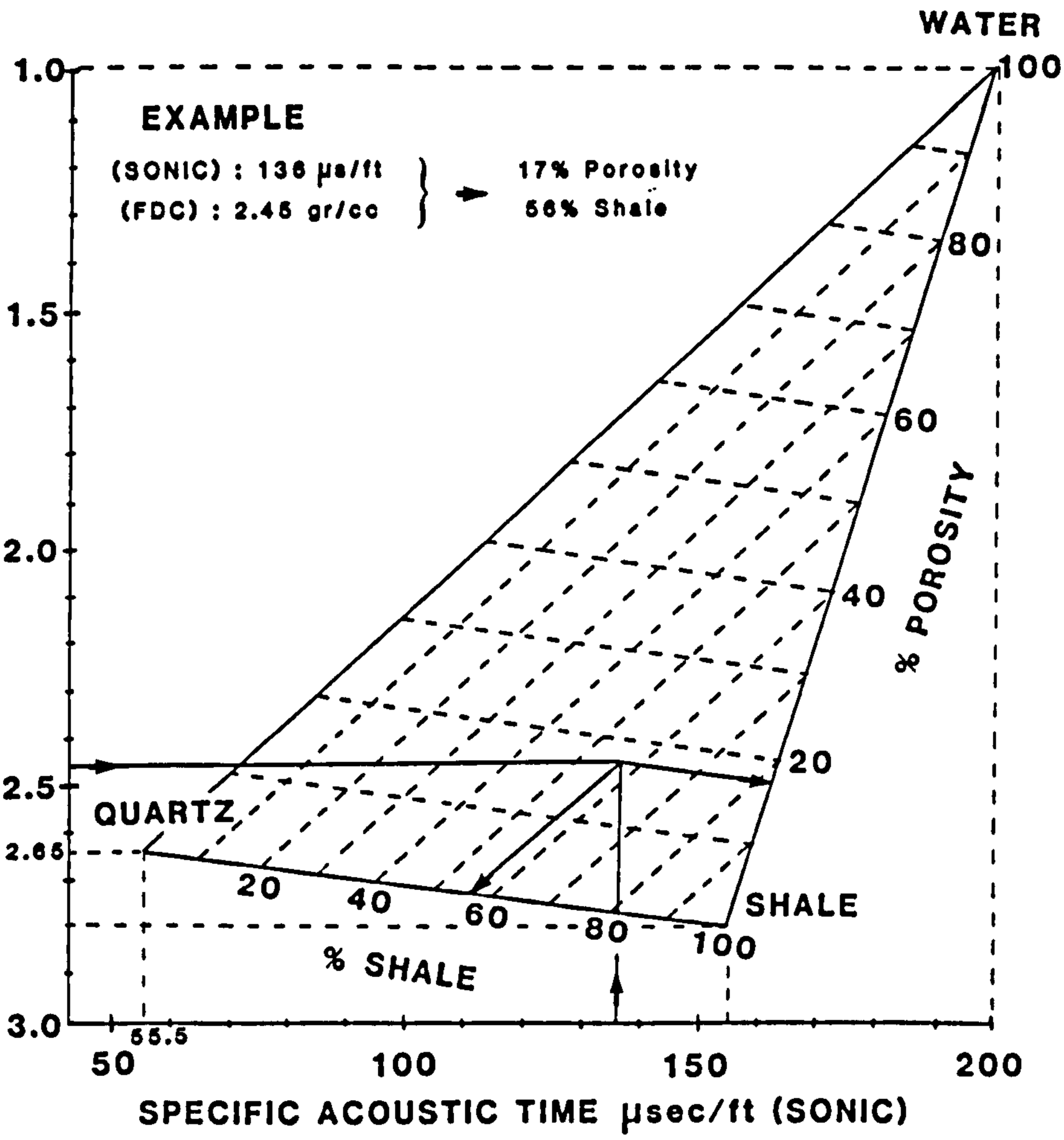

Fig 3.1 Hypothetical Density - Sonic crossplot in order to estimate shale, shaley sand and sandstone porosity in "clean" formations.

3.3.2 Porosity–depth relationship

Porosity depth relationships have been published by various authors, notably Athy (1930), Hedberg (1926, 1936), Dickinson (1953), Heling (1967), Skempton (1968), Rhodehamel (1977), Sclater and Christie (1980). These data reveal that there is no unique porosity-depth relationship. As a result in order to study compaction quantitatively in a given area, it is necessary to produce the porosity-depth curve for the particular sediment in the specific area.

"Normally" pressured stratigraphic sections from 28 wells shown in Fig. 3.2 and in Table 3.1 were used to construct three separate porosity-depth curves shown in Fig. 3.3, 3.4 and 3.5 for the three dominant lithologies of the northern North Sea, shale, shaley sand and sandstone, following the methods described so far. The porosity values were calculated every 100ft corresponding to the interval at which both logs (Sonic-FDC) were digitized. The same wells were used to plot the density values versus depth for "normal" shales shown in Fig. 3.6.

For "normal" pressure sections where the pore pressure is hydrostatic, it seems that for the dominant lithologies in the northern North Sea, the porosity-depth relation can be fitted to a simple exponential relation:

$$f = f_o \, e^{-cz}$$

where f_o is the surface porosity value and z is the depth. This can easily be seen by plotting porosity against depth in a logarithmic-arithmetic scale respectively where their relationship follows roughly a straight line constrained to pass through the surface porosity values of Pryor (1973), Fig. 3.3, 3.4 and 3.5.

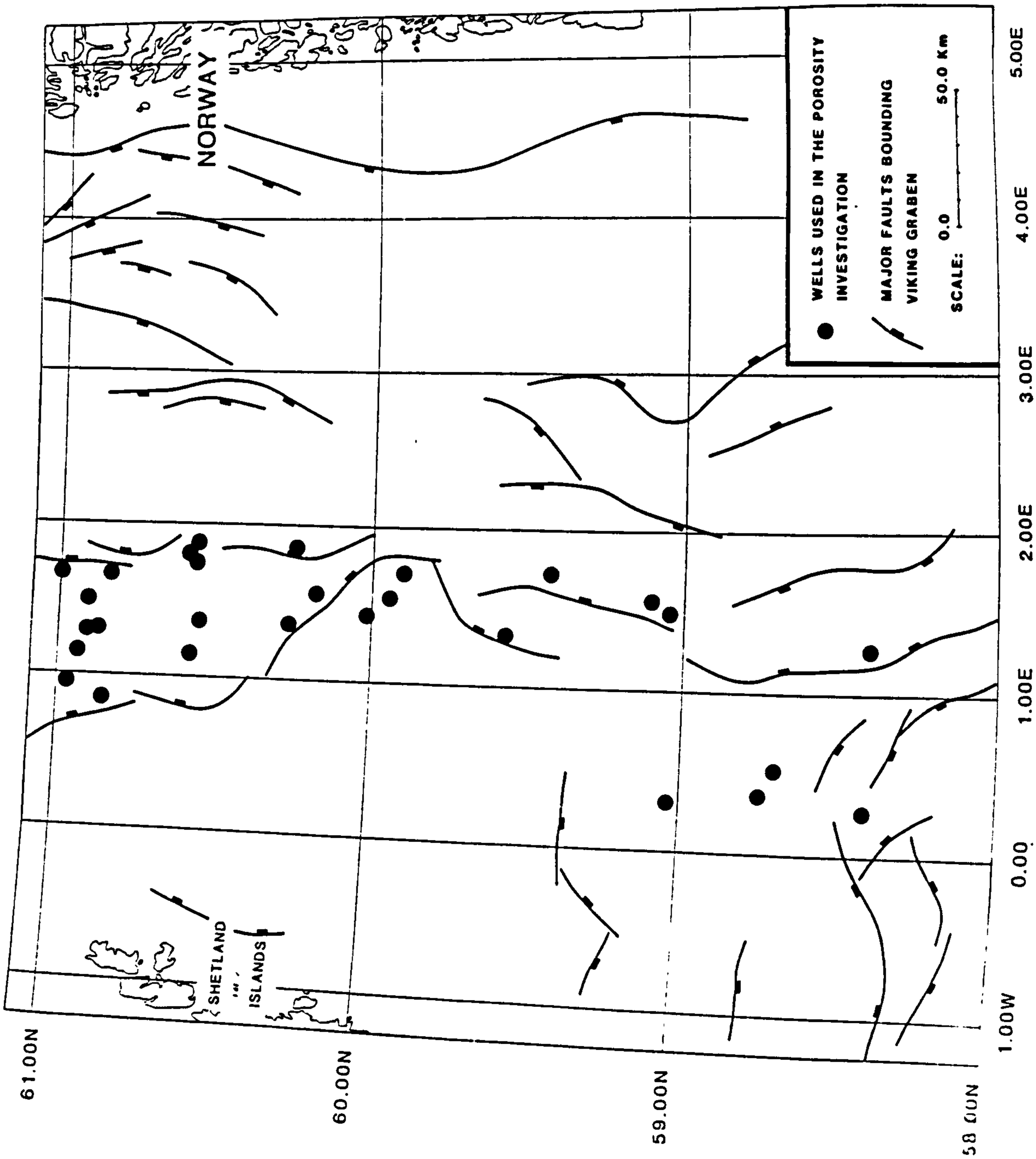

Fig. 3.2 Wells used to estimate porosity - depth reltionship shown in Fig 3.3, 3.4, 3.5 and shale density-depth relationship shown in Fig 3.6.

The scattering of points can be due to:

1. Changes in the lithology not recorded in the composite log.
2. Changes in the mineralogy of individual rock types.
3. Inaccurate pickings from log tools.
4. Limitations of the method itself used for calculating porosity values.
5. Incorporating slightly abnormal values as "normal".
6. Porosity-depth relation cannot be fitted to a simple exponential relation. Such a consistent departure from the straight line can be seen in shales and siltstones porosity values between 1000m and surface (Fig. 3.3 and 3.4).

Table 3.1

Wells used to construct the porosity-depth relationships of Fig 3.3, 3.4, 3.5 and the shale density-depth relationship of Fig 3.6. Their position is shown in Fig. 3.2.

UNION	2/5-1	BALL & COL.	3/23-1
UNION	2/5-10	TOTAL	3/25A-2
MOBIL	3/1-1	SIEBENS	3/28-1
CONOCO	3/2-1	SHELL	8/27-1A
CONOCO	3/2-4	AMOCO	9/3-1
BURMAH	3/3-3	AMOCO	9/4-1
TEXACO	3/4-1	UNION	9/12-1
TEXACO	3/4-7	CONOCO	9/19-2
AMOCO	3/11-1	HAMILTON	9/28-1A
SHELL/ESSO	3/12-1	HAMILTON	9/28-6
TOTAL	3/14A-2B	TEXACO	15/7-1
TOTAL	3/14A-3	TRANSOCEAN	15/8-1
TOTAL	3/15-3	OCCIDENTAL	15/17-7
PHILLIPS	3/22-1	PHILLIPS	16/17-6

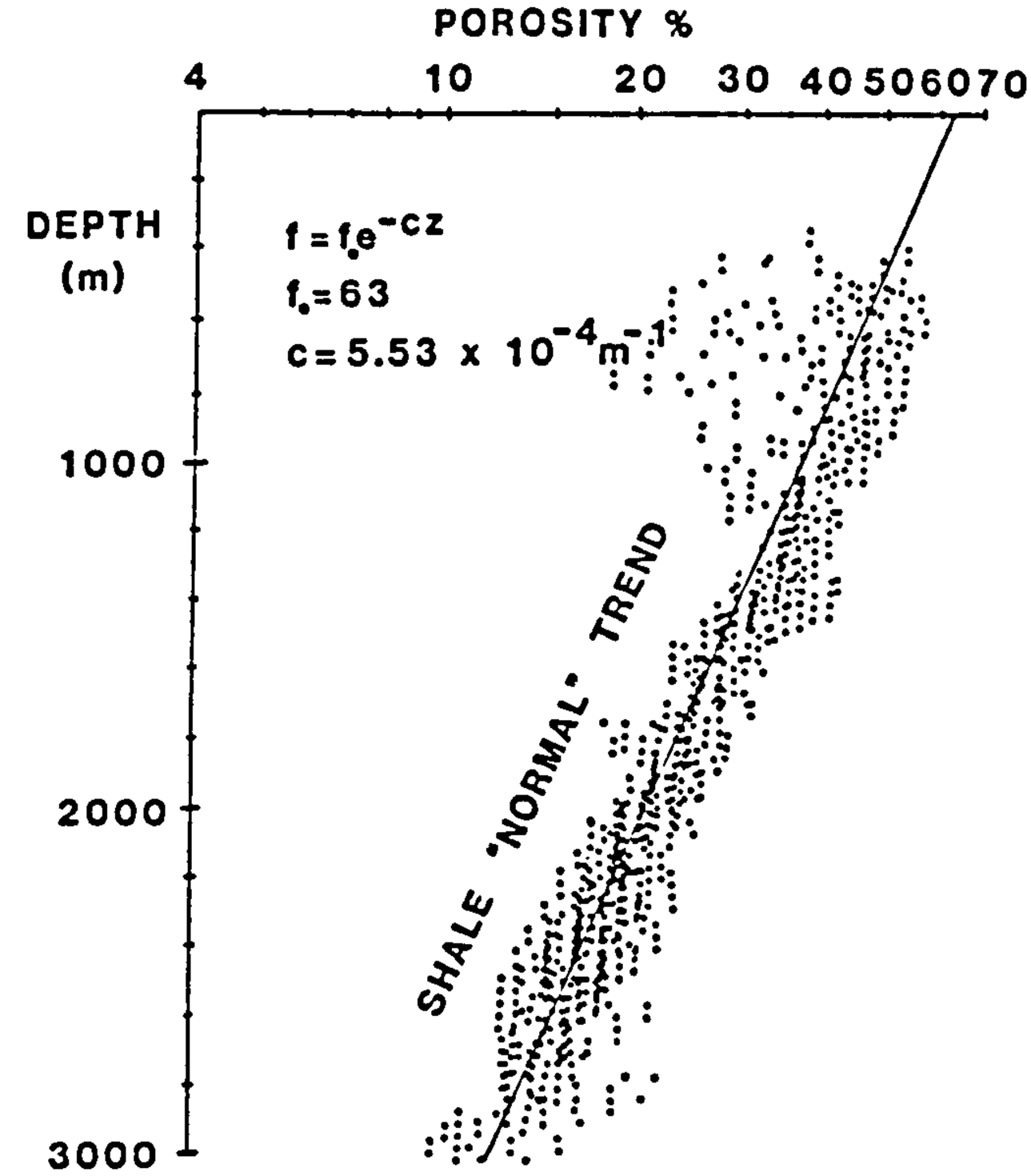

Fig 3.3 *Shale porosity-depth relationship.*

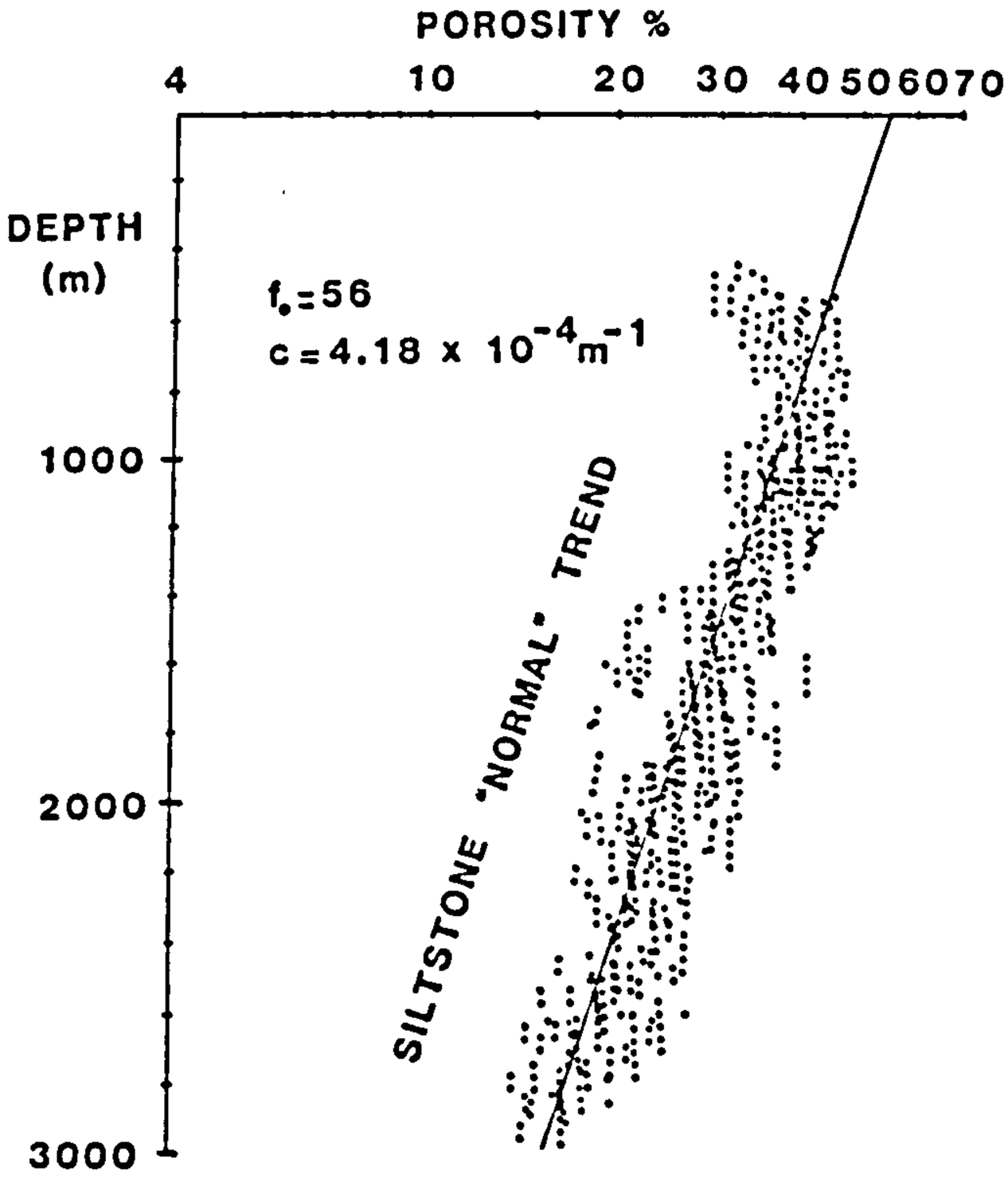

Fig 3.4 *Shaley-sand (siltstone) porosity-depth relationship.*

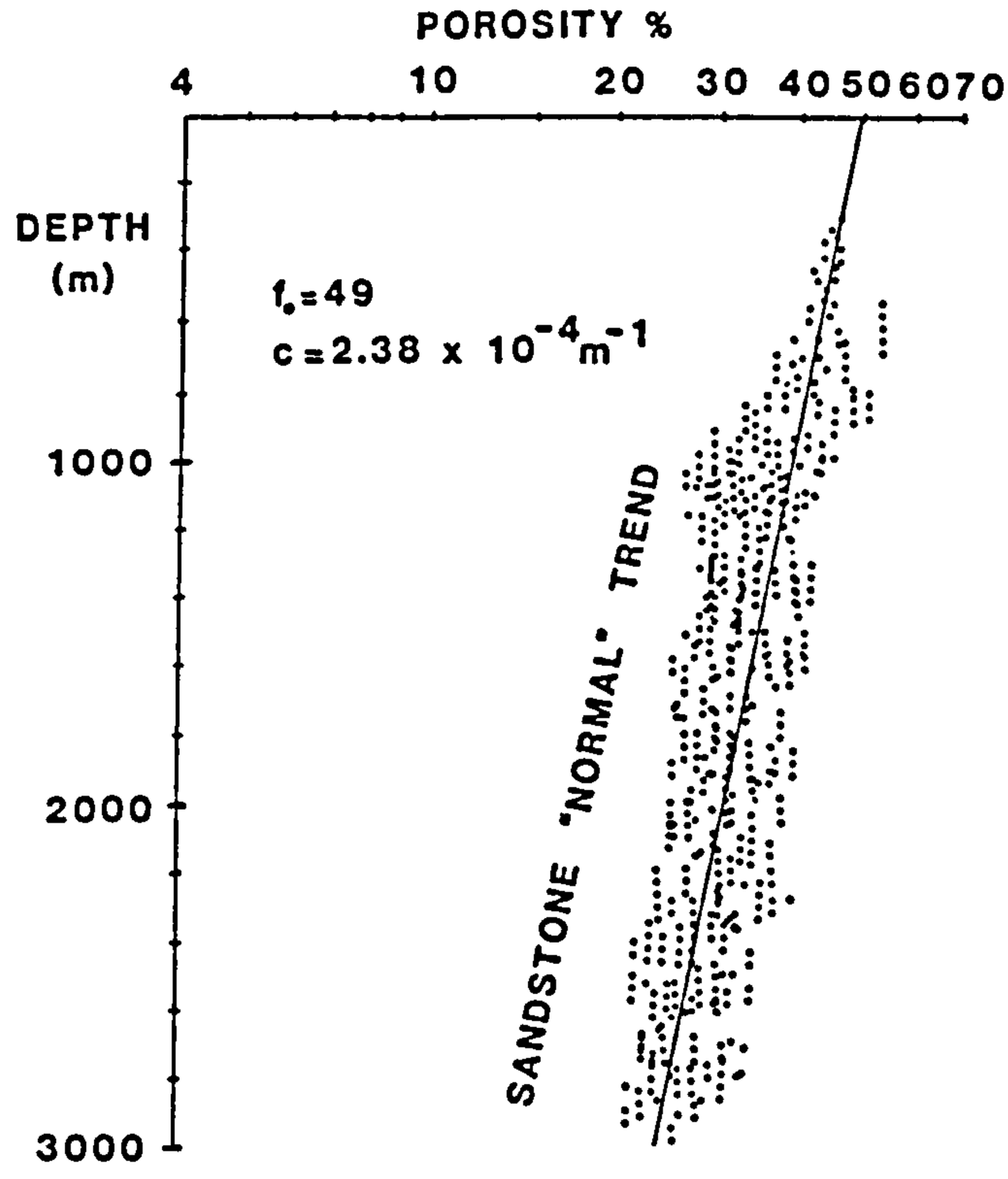

Fig 3.5 *Sandstone porosity-depth relationship.*

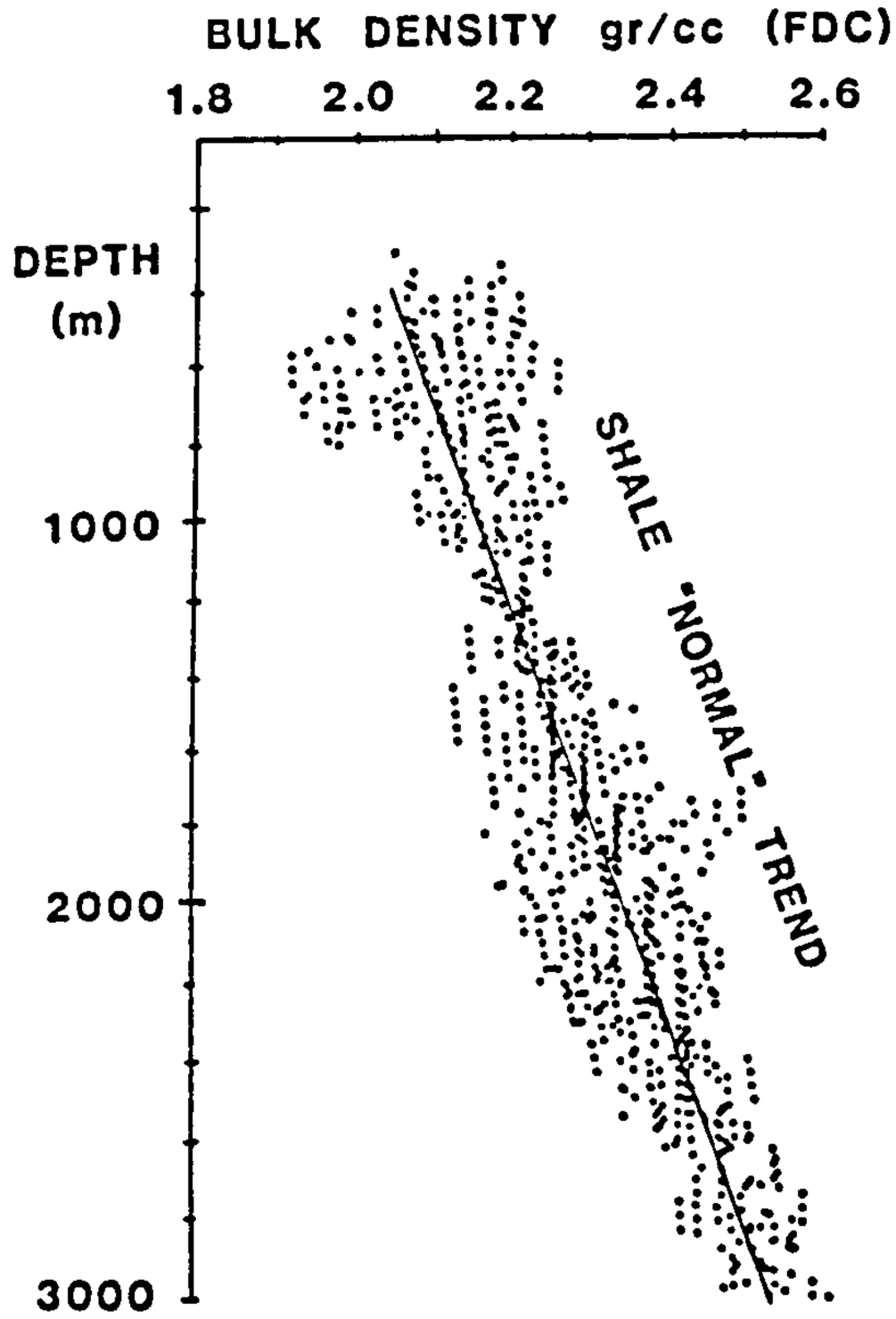

Fig 3.6 *Shale density-depth relationship.*

Sclater and Christie (1980) have calculated similar normal porosity curves from six wells in the central North Sea. They have consistently overestimated the porosity values probably by including slightly undercompacted stratigraphic sections in their study of normal porosity-depth relation.

According to current experience normal or abnormally high porosities are associated with normal or high pore pressure respectively, so by studying porosities conclusions can be drawn about pressures and vice versa.

3.4 Some Remarks on Pressures

Units of pressure and pressure gradient

Most countries in the world have now adopted the SI system, however, the former Imperial system will survive for a long time. Here a few of the most commonly used values are singled out and quoted in commonly used units.

Ever since Dickinson (1953) published his classic paper it has become customary to adopt a value of 2.3g/cc for the average density of sedimentary rocks for the purpose of general discussions. The popularity of this value is easily understood when one considers the resulting total overburden pressure gradient:

$S_z = \rho g z \rightarrow dS_z/dz = \rho g = 1.0$psi/ft for $\rho = 2.3$g/cc, where S_z is the total overburden stress, ρ is the bulk density of the water saturated rock, g is the gravitational acceleration, and z is the depth below the surface. In the SI system the unit of pressure is the Pascal, where $1Pa = 1N/m^2$. This is a very small unit and it is customary to use either KiloPascals (KPa) or MegaPascals (MPa). So the above total overburden pressure gradient converts as follows:

$$1\text{psi/ft} \approx 0.0225\text{MPa/m} = 22.5\text{KPa/m}.$$

Definitions

In any porous system an applied load will be carried jointly by the matrix framework and the pressure of the pore fluid. Skempton (1968) formulated the concept of effective stress as follows:

$$S = \sigma + p$$

where S is the total stress, σ is the matrix or effective stress and ρ is the pore fluid or simply pore pressure.

The FORMATION FLUID PRESSURE (pore pressure) under normal conditions corresponds to the weight of the overlying fluid column. The fresh water pressure gradient is 0.433psi/ft. However, rocks at a depth below a few hundred feet generally contain brines of various concentrations. For a brine with 150 000ppm total solids the gradient is 0.48psi/ft.

In our case we accept the formation fluid pressure (pore pressure) gradient under NORMAL conditions (hydrostatic) in the northern North Sea as:

$$0.45\text{psi/ft} \approx 0.01\text{MPa/m} = 10\text{KPa/m}.$$

3.5 Abnormal Formation Fluid Pressures

There are numerous factors that can cause abnormal formation pressures, such as overpressures and underpressures (abnormal compaction). Frequently, a combination of several superimposed causes prevails in a given basin and as such is related to the stratigraphic, tectonic, and geochemical history of the area.

3.5.1 Subnormal formation fluid pressures

Worldwide experience indicates that subnormal formation pressures occur less frequently than abnormally high ones. Nevertheless, subpressures have been encountered in many areas while drilling for oil and gas, including the Texas and Oklahoma Panhandle area, parts of the Colorado Plateau, the Appalachian region, etc., all in the United States; the Lower Cretaceous Viking Formation in Central Alberta, Canada; Middle Miocene formations in the Chokrak and Karagan areas in the USSR; arid areas in Iran; and elsewhere.

Subnormal formation pressures may also occur artificially by producing oil, gas, and/or water from permeable subsurface formations (reservoirs). Production of large amounts of reservoir fluids can drastically reduce formation pressure (Krynine and Judd, 1957; Marsden and Davis, 1967). Basically, fluid withdrawal such as production, causes a decline in pore fluid pressure if no strong water drive tends to compensate for it; frequently, as a result of this, the production layers compact producing subsequent surface subsidence, Allen (1972).

3.5.2 Abnormally high formation fluid pressures

Observations of higher than normal fluid pressures have been made in almost all parts in the world. Early measurements were reported by Dickinson (1953). Later various authors noted such pressures from the US Gulf Coast, Pakistan, Iran, France, Roumania and Burma. Most recently Fertl (1976) added to the list various places in Europe, the USSR, Africa, Australia and many more. There can be no doubt today that the phenomenon of abnormal fluid pressures is a global one.

3.5.3 Overpressure in the North Sea

In the North Sea area high pressure environments are encountered offshore of Holland, Germany, the United Kingdom, Denmark and Norway. The magnitude of these pressures varies widely over the

entire area in both Tertiary and Mesozoic formations. However, only limited pressure data have been released, including acknowledged overpressures and resulting well-control problems in gas-bearing Triassic sandstones, Upper Permian evaporites, etc. Furthermore, drilling offshore of Norway has encountered overpressured Tertiary and Mesozoic oil and gas sands, but at the present time, the most prolific reservoir rocks are overpressured, chalky, often highly fractured limestones of Upper Cretaceous age in the oil- and gas-bearing structures offshore of Denmark. The same horizon is productive offshore of Norway with the more important zone in the overlying Danian chalk (Ekofisk field). Sidewall cores taken in the overlying Tertiary shales suggest that the Tertiary overpressured shales are the source rock for the oil at Ekofisk. Such a situation suggests that the overpressured shales are preventing vertical migration of hydrocarbons out of the Danian reservoir and providing an effective trapping mechanism. Since these overlying shales are believed to be the source of oil, and since they have a higher fluid pressure than the accumulation, fluid flow should be from the shales into the underlying chalk, Byrd (1975).

3.5.4 Pressure seals

In order for the rock unit to exhibit a fluid pressure regime that deviates from the normal condition the fluid flow to or from such a rock unit must be restricted. This is a basic requirement, regardless of the mechanism called upon to create the abnormal condition. Theoretically, such a seal could be any material or combination of materials in the earth's crust, restrictive or preventive to movement and passage of substantial volumes of fluids. The origin of the pressure seal is physical, chemical, or may be a result of the combination of the two (Louden, 1972). Since modes and origins of such seals can be manifold, the possible types are listed in Table 3.2.

Generally, a pressure seal formation will depend on many factors, including the highly complex phenomena of deformational response of clay minerals to applied physical loads (such as over-burden); behaviour of clays and shales as semi-permeable membranes; the type and quantities of clay minerals present; extremely low shale permeabilities; precipitation of dissolved solids (eg. calcite, silica, feldspar, pyrite, siderite, etc.); composition and possible mixing of brines; sharp subsurface pressure and temperature changes. Then, as fluids and gases can no longer move through this seal in large quantities, further precipitation and cementation by calcite, silica, etc., will be slowed until essentially halted.

Table 3.2

Suggested types of formation pressure seals (after Fertl and Timko, 1972).

Type of seal	Nature of trap	Examples
Vertical	massive shales and siltstones	Gulf Coast, USA
	massive salts	Zechstein, N.Germany
	anhydrite	North Sea, Middle East
	gypsum	USA, USSR
	limestone	
	dolomite	
Transverse	faults	worldwide
	salt and	
	shale diapirs	
Combination of vertical and transverse		worldwide

3.6 Abnormal Formation Fluid Pressures: Suggested Mechanisms

In the following a number of processes leading to higher (and lower) than normal pore pressures will be discussed and their merits and implications assessed.

This evaluation centres on regional conditions. Therefore the well known excess pressures associated with hydrocarbon reservoirs will not be considered. This excess pressure is due to the difference in density between the formation brines and the hydrocarbons. In the case of large gas reservoir with a thick gas column such excess pressures may reach a value of 1000psi (7MPa) or more (Gretener, 1969a, p.266). However, this maximum excess pressure is limited to the crest of the reservoir and declines to zero at the hydrocarbon water interface. It therefore constitutes a purely local phenomenon.

3.6.1 Rapid loading

This process was brought to geologists' attention by Dickinson (1953) and later and possibly more forcefully by Hubbert and Rubey (1959), Rochow (1967), Bredehoeft and Hanshaw (1968), Magara (1971), Fertl and Timko (1972), Smith (1973) and others. It is based on the concept that the rapid application of an external load onto a porous system results in an increase of the pore fluid pressure which may be temporary or permanent in nature (Terzaghi, 1950). The effect is caused by the inability of the fluid to leave the pores which tend to become squeezed under the added load. In a sequence which is encased by salt and therefore essentially hermetically sealed (isolated), even a very slow rate of loading may produce excess pore pressure. On the other hand it has been suggested that during landsliding, which is a form of impact loading, even coarse river gravels may at least temporarily develop high fluid pressures (Pavoni, 1968). It is clear, however, that in general high pore pressures tend to be associated with low permeability rocks such as shales and evaporites.

3.6.2 Phase changes

The main phase change leading to a considerable excess of fluid pressure can be considered the montmorillonite to illite transformation. Such a hypothesis has been investigated by Powers (1967) and more recently re-evaluated by Magara (1975a). According to Burst (1969), such a transformation depends mainly on subsurface temperature, with the averge dehydration temperature being 105°C. As subsurface temperature tends to increase with depth, it eventually must exceed dehydration temperature. The depth at which this critical subsurface temperature is reached will vary with differences in geothermal gradient, both within a sedimentary basin and between one basin and another. That is, there must be local and regional variation in the depth of dehydration. In the Viking Graben area this temperature (105°C) is reached at about 3000m depth close to the Jurassic-Cretaceous boundary (Cimmerian unconformities) according to Carstens and Finstad (1981). Within the Jurassic they observed distinctive rapid temperature rises (up to 70°C/km) increasing sharply the chances of further transformation of montmorillonite to illite.

An important factor controlling the geothermal gradient is the amount of water in the rocks. Because the heat conductivity of water is much less than that of rock matrix, when rocks contain large quantities of water (high porosity), the geothermal gradient becomes greater (Lewis and Rose, 1970; Reynolds 1970). As already mentioned, shale porosity in abnormal-pressure zones is abnormally high; consequently the geothermal gradient also is abnormally high. Where there are abnormal pressures, then, a high subsurface temperature is reached at relatively shallow depths. These conditions will in turn increase the chances for montmorillonite in the abnormal pressure zone to release its interlayer water and be transformed to illite increasing further the pore water pressure.

3.6.3 Aquathermal pressuring

This process has been proposed by Barker (1972) and discussed subsequently in greater detail by Magara (1975b). Barker based his theory on data provided by Kennedy and Holser (1966) which indicate that the pressure of water heated in a closed vessel will rise about 125psi per degree Fahrenheit. The rise depends to a minor degree on the composition of the water, i.e. the amount of solids dissolved. Thus a formation that is isolated and contains brine in the pore space is expected to develop an excess pore pressure which for the temperature increase of 8°F could reach 1000psi. All the formations discussed here are undercompacted. Among undercompacted formations, any that are relatively more compacted tend to retain more abnormal pressures generated mainly by aquathermal effect.

3.6.4 Osmosis

Clays and shales are known to act as semi-permeable membranes that will permit osmotic and electro-osmotic pressures to develop wherever there is a marked contrast in the concentration of the dissolved salts on either side of the clay or shale. Such a mechanism creates small pressure differences of a few hundred psi only.

3.6.5 Tectonics

Lateral tectonic compression is sometimes used as an explanation for abnormal pressures in areas close to tectonically complicated areas. Such a process in fact reduces porosity.

3.7 Data Presentation and Overpressure Detection

Estimation of the "clean" rock porosity (or water content) as a function of depth will reflect the degree of compaction. A section which is undercompacted with regard to its burial depth will be a section whose fluid pressure is abnormally high. An inference of the degree of compaction can be derived from log data (FDC, Sonic).

Thus a practical method for estimating overpressured (undercompacted) formations has been achieved.

Use of the Sonic or FDC logs to detect variations in shale porosity has been applied with good results in the northern North Sea area. For that purpose 14 wells shown in Fig. 3.7 were used, and their results plotted in Fig 3.9.

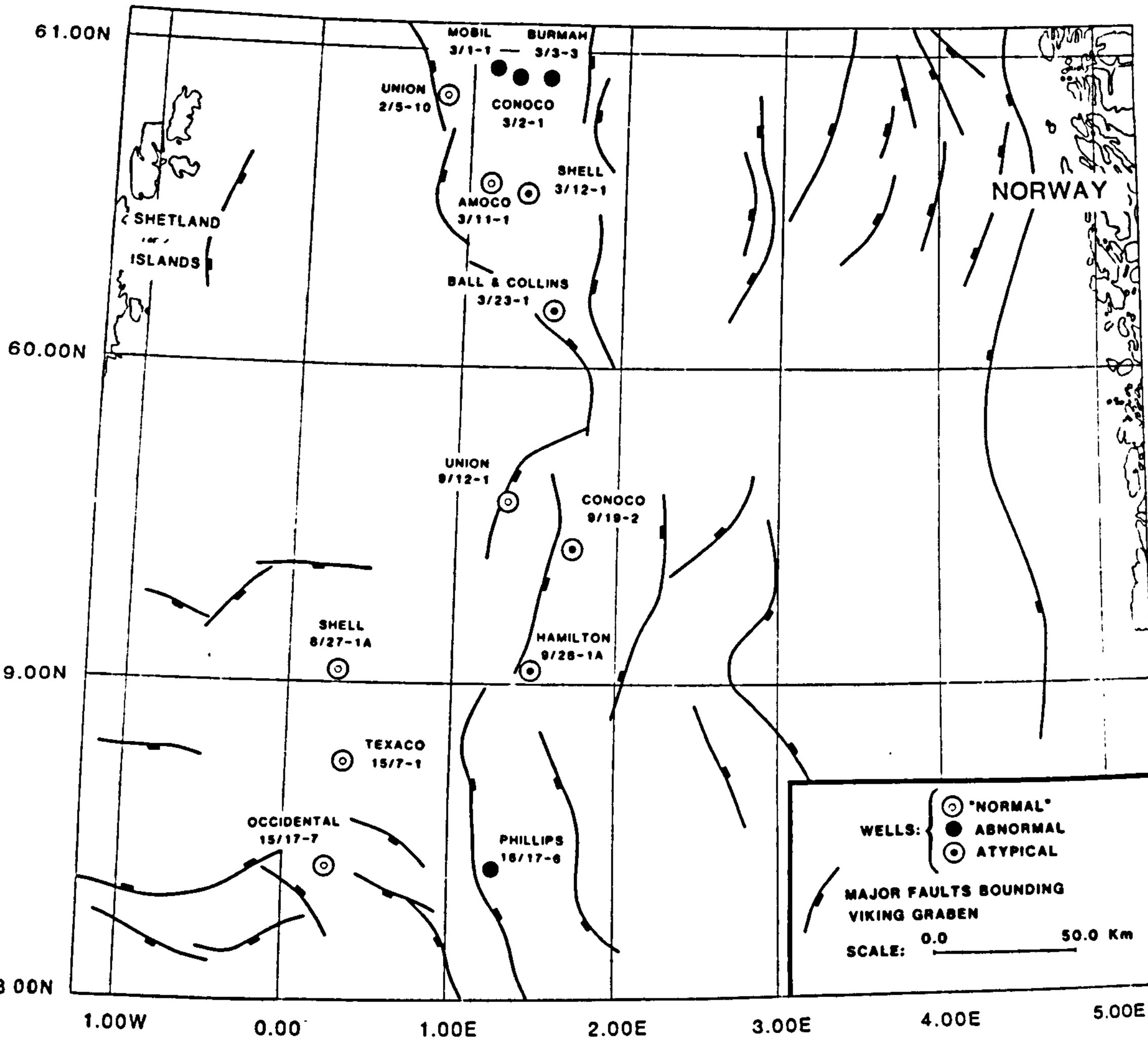

Fig 3.7 Wells used in the porosity study of Fig 3.9.

The interval transit time recorded by the Sonic log may be thought of as a function of lithology and porosity. Since the porosity or water content of the shales decreases with compaction, Δt (shale) should decrease with depth. The undercompaction detection is more pronounced if the interval transit time is displayed on a logarithmic scale versus depth, displayed on a linear scale, (Fig 3.9).

The FDC log is being run more often along with the Sonic log for seismic interpretation purposes. Therefore, the bulk density measurements is frequently available to improve overpressure detection where the lithology and clay content of the shales is variable. Bulk density has been used by itself in a manner similar to that described for the Sonic log, with similar limitations (see Limitations of Sonic and FDC Logs outlined in sections 3.2.1 and 3.2.2 respectively). In this case the density versus depth was plotted on a linear-linear scale (Fig 3.9) (a logarithmic density scale can also be used).

However since both the Sonic log and FDC log respond both to lithology and porosity, the FDC-Sonic crossplot was used (see section 3.3.1) to evaluate porosity or water content, (Fig 3.9). In all the studied wells it can be seen that the porosity is a mirror image of density (as expected).

Most of the typical wells follow the "normal" shale trends in all the three plots, indicating "normally" compacted wells. However, some distinctive abnormally high shale porosity values were observed which require explanation. Rapid shale sedimentation was first examined as the main cause of undercompaction in the northern North Sea, being one of the main reported causes worldwide. Therefore by backstripping and decompacting the wells, sedimentation rates were calculated using all the age information available in the Composite log according to the method described in detail in section 4.2.

3.8 Data Interpretation

In order to study the cause of the abnormally high shale porosity values observed in the northern North Sea, data from 14 wells were used. Two of those wells (CONOCO 9/19-2 and HAMILTON 9/28-1A) have been drilled in commercial oil-gas fields. The presence of hydrocarbons affected significantly the reading of both FDC and Sonic logs and no comparison could be made with readings from "clean" formations observed in other wells, (Fig 3.9). Therefore, it was decided that no porosity estimation would be calculated. In another two wells (SHELL 3/12-1 and BALL & COLLINS 3/23-1) the Sonic or FDC log readings have shown very sharp variations in interval transit time or bulk density without any trend, preventing any reliable porosity estimation. The above four wells are considered ATYPICAL, and they are not included in the porosity study. Six other wells have shown no significant departure from "normal" trends in shale formations and they were considered to be "NORMAL", (Fig 3.9). Finally, only four wells have given indications that can be considered as ABNORMAL. Three of these wells (MOBIL 3/1-1, CONOCO 3/2-1, BURMAH 3/3-3) are located close to each other (average distance 15km) at the far north of the survey area and the fourth (PHILLIPS 16/17-6) at the far south, all of them deep wells (>3000m) located within the main Viking Graben system, (Fig 3.7 and 3.9).

The three wells show similarities in the following:

1. Lithology
2. Geological history
3. Overpressure is indicated by all three methods
4. Shale is the overpressure formation
5. The top overpressure is encountered between 2750m and 3000m depth, in the Turonian (88.5-91my), Upper Cretaceous.
6. The maximum overpressure is located in the Upper Jurassic just below the Cimmerian unconformity at approximately 200m below the top overpressure.

7. At maximum overpressure the Sonic log deviates from the "normal" trend approximately 20-30μs/ft.

8. At maximum overpressure the FDC log deviates from the "normal" trend approximately 0.20-0.25g/cc.

9. At maximum overpressure the estimated porosity is double the expected "normal" porosity.

10. The overpressure horizon is 400-600m thick and mainly Jurassic.

11. The pressure seal seems to be the massive shales (more than 1000m thick) deposited on top of the overpressure horizon.

12. No correlation exists between sedimentation rates and overpressure.

The recorded temperature 116°C at 3300m depth in one of these three wells (CONOCO 3/2-1) is higher than 105°C, the temperature where the maximum expulsion of water takes place due to montmorillonite to illite transformation. At a gradient of 30°C/km, 105°C would occur at about 3000m. This is approximately the depth where overpressure was encountered from the well data, therefore it can be suggested that one of the main causes of overpressure was the phase change from montmorillonite to illite. Unfortunately no temperature information was available in the other two wells.

High sedimentation rate is the most likely other cause able to create substantial undercompaction assuming that the special condition for developing aquathermal pressuring or osmosis effects are not significant. In fact osmosis counts for small magnitude effects and there is no evidence of conditions (eg. close presence of salt dome) leading to sharp temperature increase and the development of the aquathermal effect. From Fig 3.9, though it can be seen that the undercompacted formation is not associated with rapid loading. Therefore it can be proposed that the only main cause of overpressuring at the above three wells is montmorillonite to illite transformation.

Era	Sub-era Period Sub-period		Epoch		Age	Ma age
Cenozoic	Quaternary or Pleistogene		Holocene			0·01
			Pleistocene			2·0
	Tertiary	Neogene Ng	Pliocene	2	Piacenzian	
				1	Zanclian	5·1
			Miocene	3	Messinian	
					Tortonian	
				2	Serravallian	
					Langhian-Late	14·4
					Langhian-Early	
				1	Burdigalian	
					Aquitanian	24·6
		Paleogene Pg	Oligocene	2	Chattian	32·8
				1	Rupelian	38·0
			Eocene	3	Priabonian	42·0
				2	Bartonian	
					Lutetian	50·5
				1	Ypresian	54·9
			Paleocene	2	Thanetian	60·2
				1	Danian	65
Mesozoic	Cretaceous K		K_2	Seno-nian	Maastrichtian	73
					Campanian	83
					Santonian	87·5
					Coniacian	88·5
					Turonian	91
					Cenomanian	97·5
			K_1		Albian	113
					Aptian	119
					Barremian	125
				Neoc-omian	Hauterivian	131
					Valanginian	138
					Berriasian	144
	Jurassic J		Malm J_3		Tithonian	150
					Kimmeridgian	156
					Oxfordian	163
			Dogger J_2		Callovian	169
					Bathonian	175
					Bajocian	181
					Aalenian	188
			Lias J_1		Toarcian	194
					Pliensbachian	200
					Sinemurian	206
					Hettangian	213
	Triassic Tr		Tr_3		Rhaetian	219
					Norian	225
					Carnian	231
			Tr_2		Ladinian	238
					Anisian	243
			Scythian Tr_1		Spathian	
					Smithian	
					Dienerian	
Mz					Griesbachian	248
	Permian P		P_2		Tatarian	253
					Kazanian	
					Ufimian	258
			P_1		Kungurian	263
					Artinskian	268
					Sakmarian	
					Asselian	286

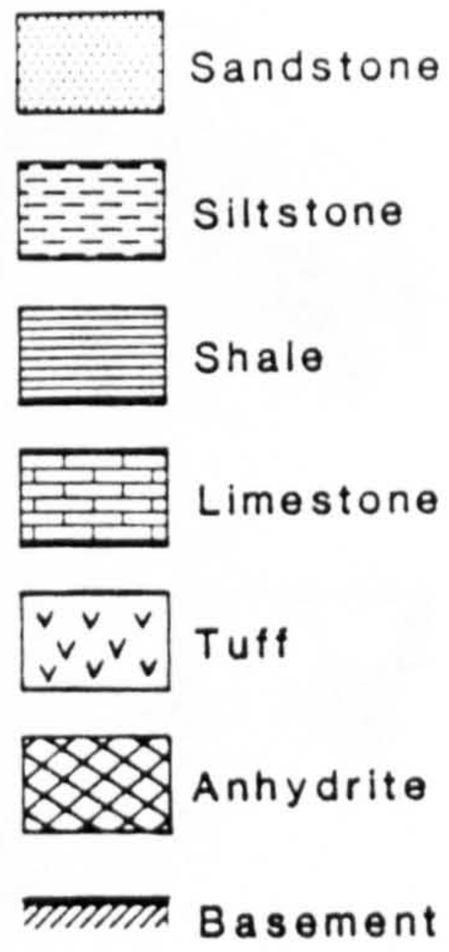

Fig 3.8 *Key used for Fig 3.9. Ages after Harland et al 1982, (p.4).*

Fig 3.9 *(The following 14 pages). Porosity-depth study for wells shown on Fig 3.7. The first indication of undercompacted formations (overpressured) can be detected from FDC or Sonic logs. The sedimentation rates derived from the Composite log (backstripping and allowing for decompaction) were used to find the type of correlation between undercompaction and rapid loading. "Normal" shale Sonic trend after Schlumberger (1969) (page 165). "Normal" shale FDC trend taken from Fig 3.6. For Key see Fig 3.8.*

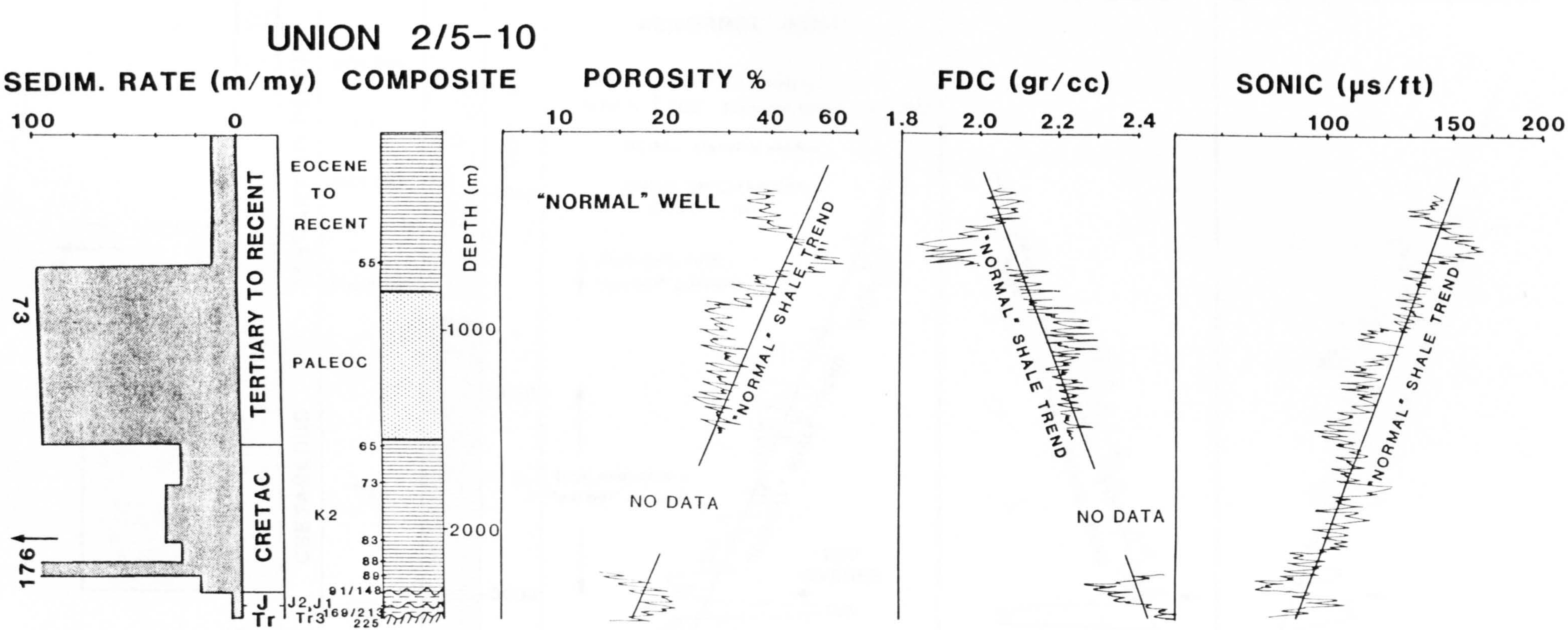
UNION 2/5-10
SEDIM. RATE (m/my)
100
0
73
176
TERTIARY TO RECENT
CRETAC
Tr
EOCENE TO RECENT
PALEOC
K2
J2,J1
Tr3
55
65
73
83
88
89
91/148
169/213
225
DEPTH (m)
1000
2000
COMPOSITE
POROSITY %
10
20
40
60
"NORMAL" WELL
"NORMAL" SHALE TREND
NO DATA
FDC (gr/cc)
1.8
2.0
2.2
2.4
"NORMAL" SHALE TREND
NO DATA
SONIC (µs/ft)
100
150
200
"NORMAL" SHALE TREND

Fig 3.9 (cont.)

MOBIL 3/1-1

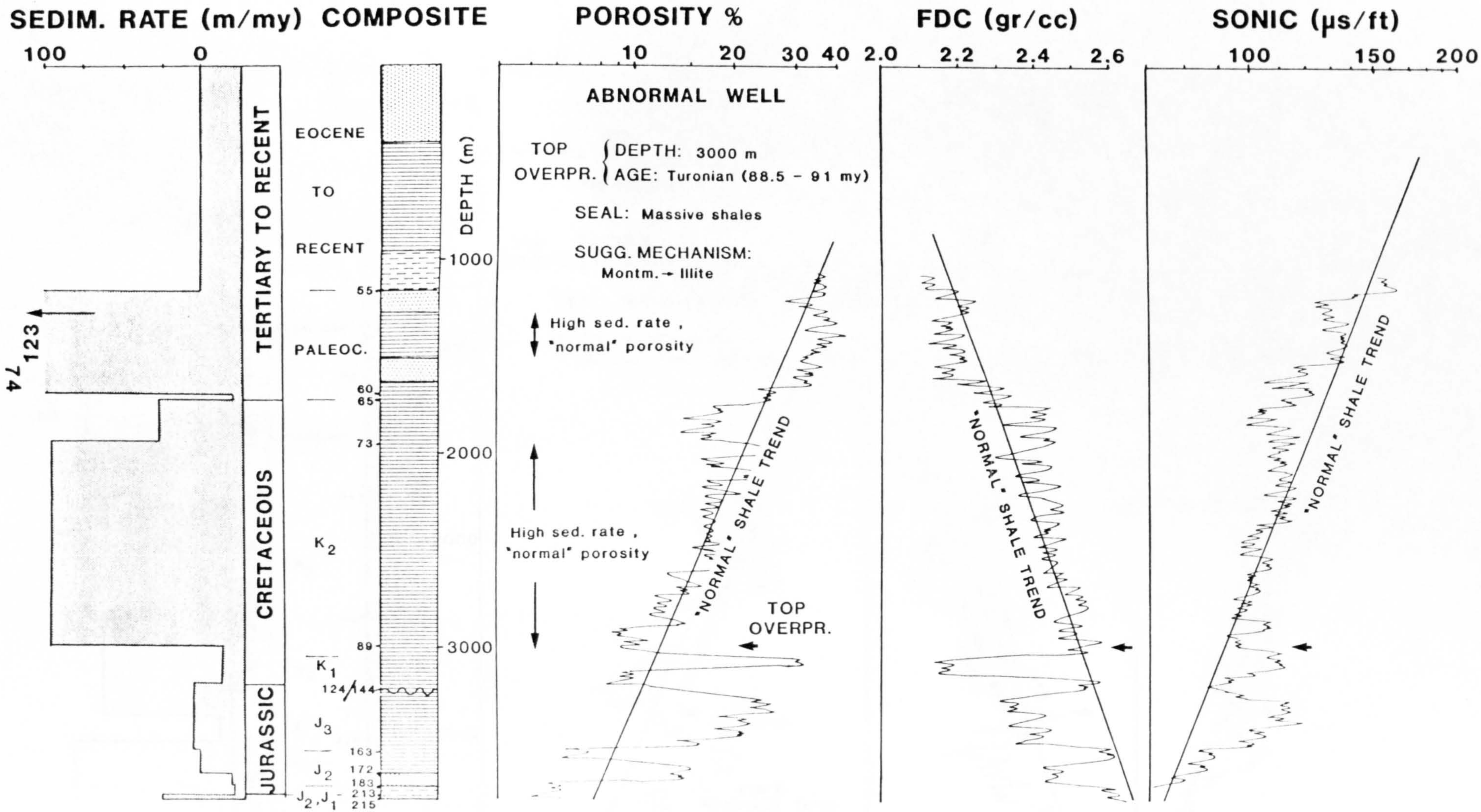

Fig 3.9 (cont.)

CONOCO 3/2-1

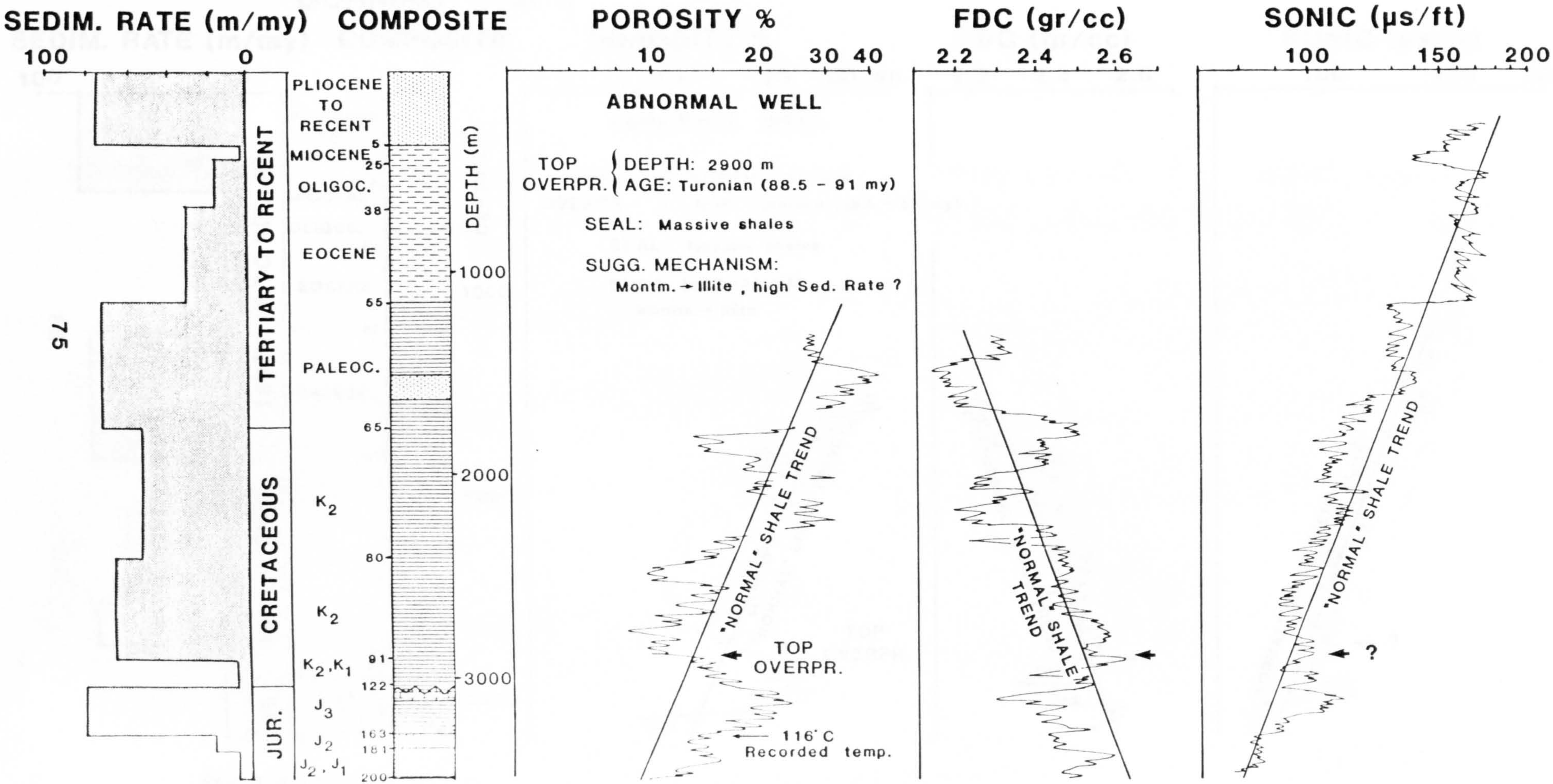

Fig 3.9 (cont.)

BURMAH 3/3-3

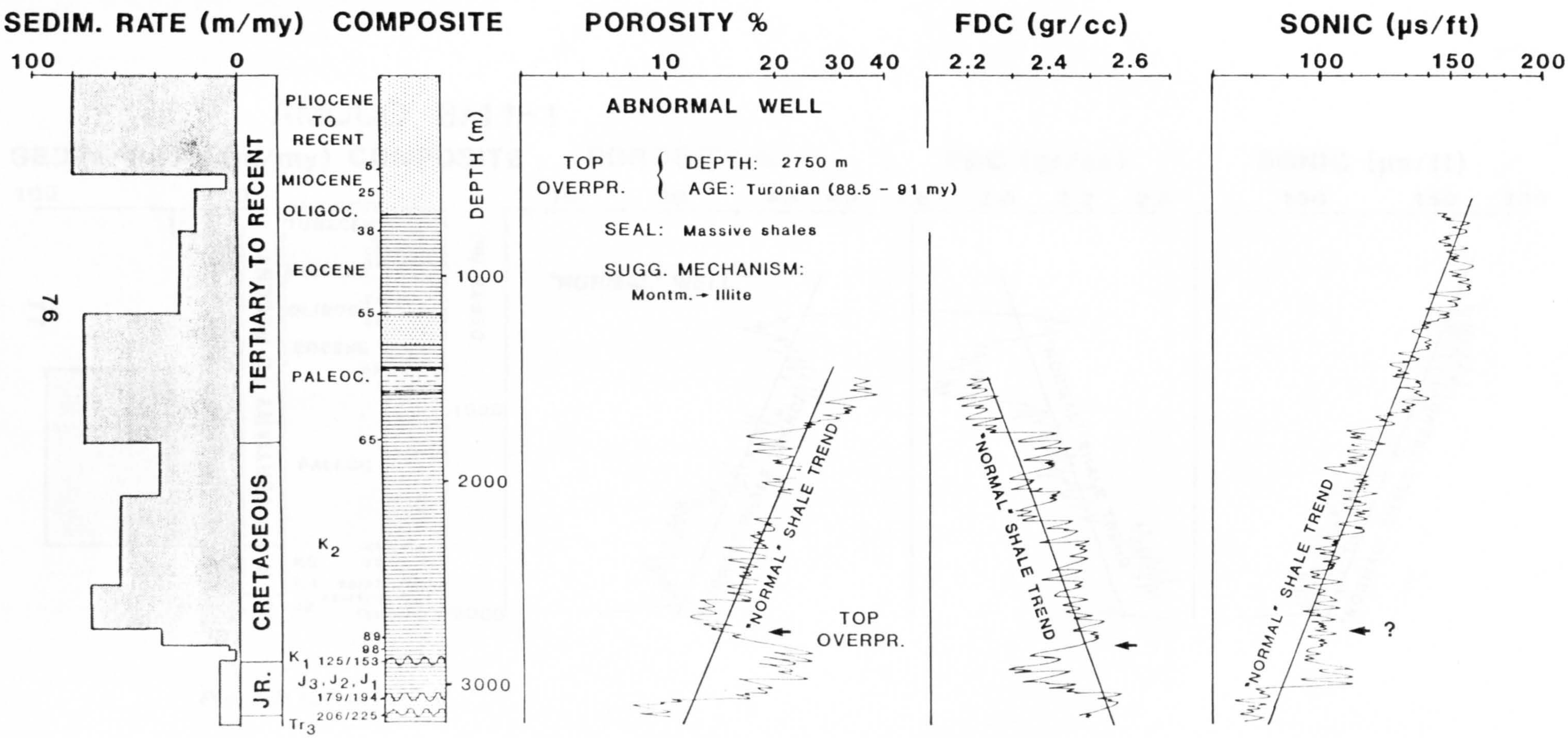

Fig 3.9 (cont.)

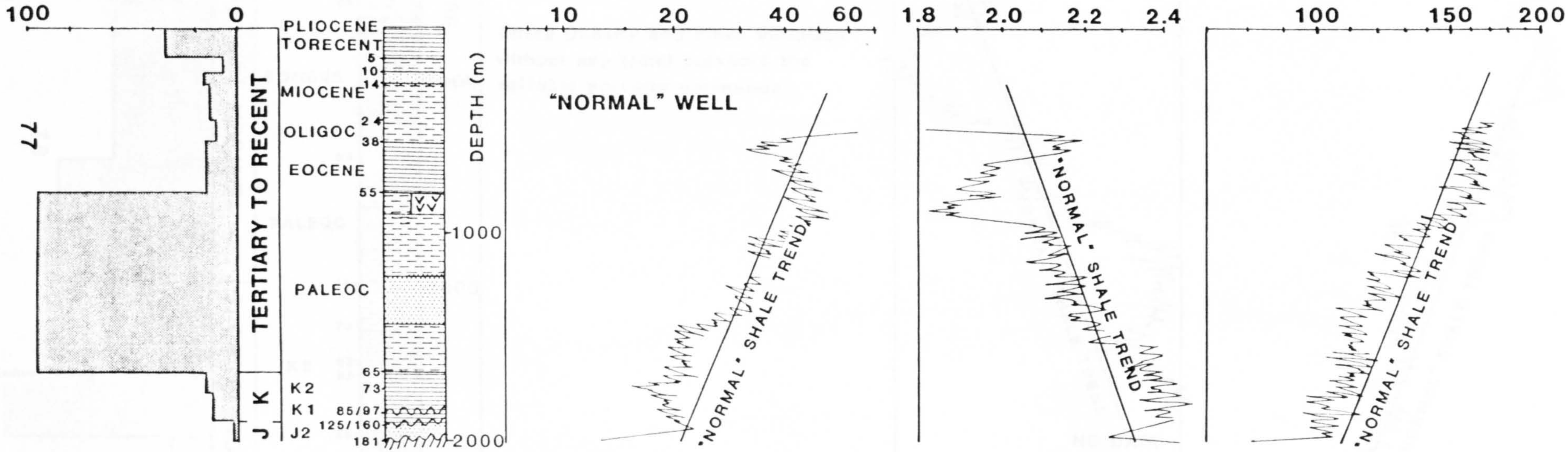
AMOCO 3/11-1
SEDIM. RATE (m/my) COMPOSITE
100
0
PLIOCENE
TOERECENT
MIOCENE
OLIGOC
EOCENE
PALEOC
TERTIARY TO RECENT
J
K
K2
K1
J2
5
10
14
24
38
55
65
73
85/97
125/160
181
DEPTH (m)
1000
2000
POROSITY %
10
20
40
60
"NORMAL" WELL
•NORMAL• SHALE TREND
FDC (gr/cc)
1.8
2.0
2.2
2.4
•NORMAL• SHALE TREND
SONIC (µs/ft)
100
150
200
•NORMAL• SHALE TREND

Fig 3.9 (cont.)

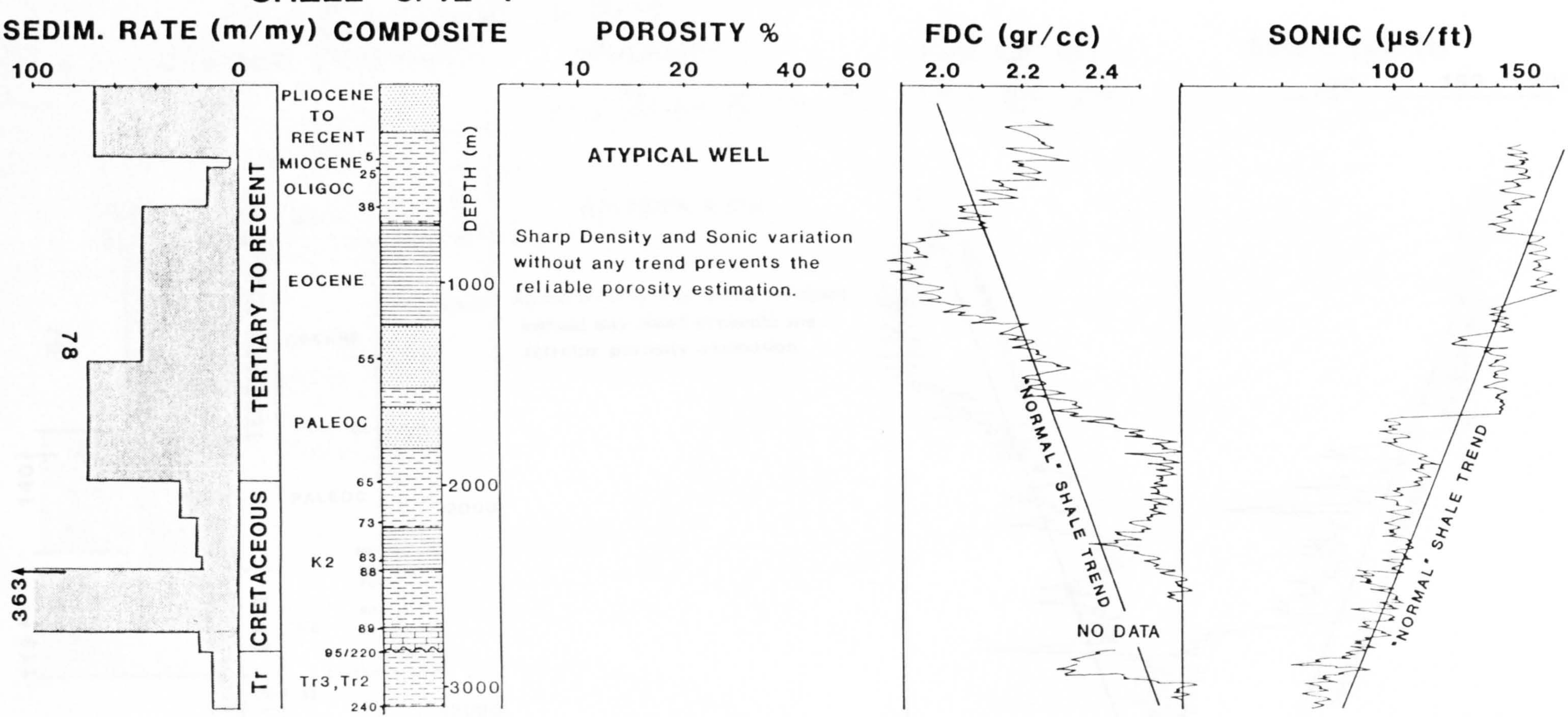
SHELL 3/12-1
SEDIM. RATE (m/my) COMPOSITE
100
0
PLIOCENE TO RECENT
MIOCENE
OLIGOC
EOCENE
PALEOC
K2
Tr3,Tr2
TERTIARY
CRETACEOUS
Tr
78
363
5
25
38
55
65
73
83
88
89
95/220
240
DEPTH (m)
1000
2000
3000
POROSITY %
10
20
40
60
ATYPICAL WELL
Sharp Density and Sonic variation without any trend prevents the reliable porosity estimation.
FDC (gr/cc)
2.0
2.2
2.4
NORMAL SHALE TREND
NO DATA
SONIC (µs/ft)
100
150
NORMAL SHALE TREND

Fig 3.9 (cont.)

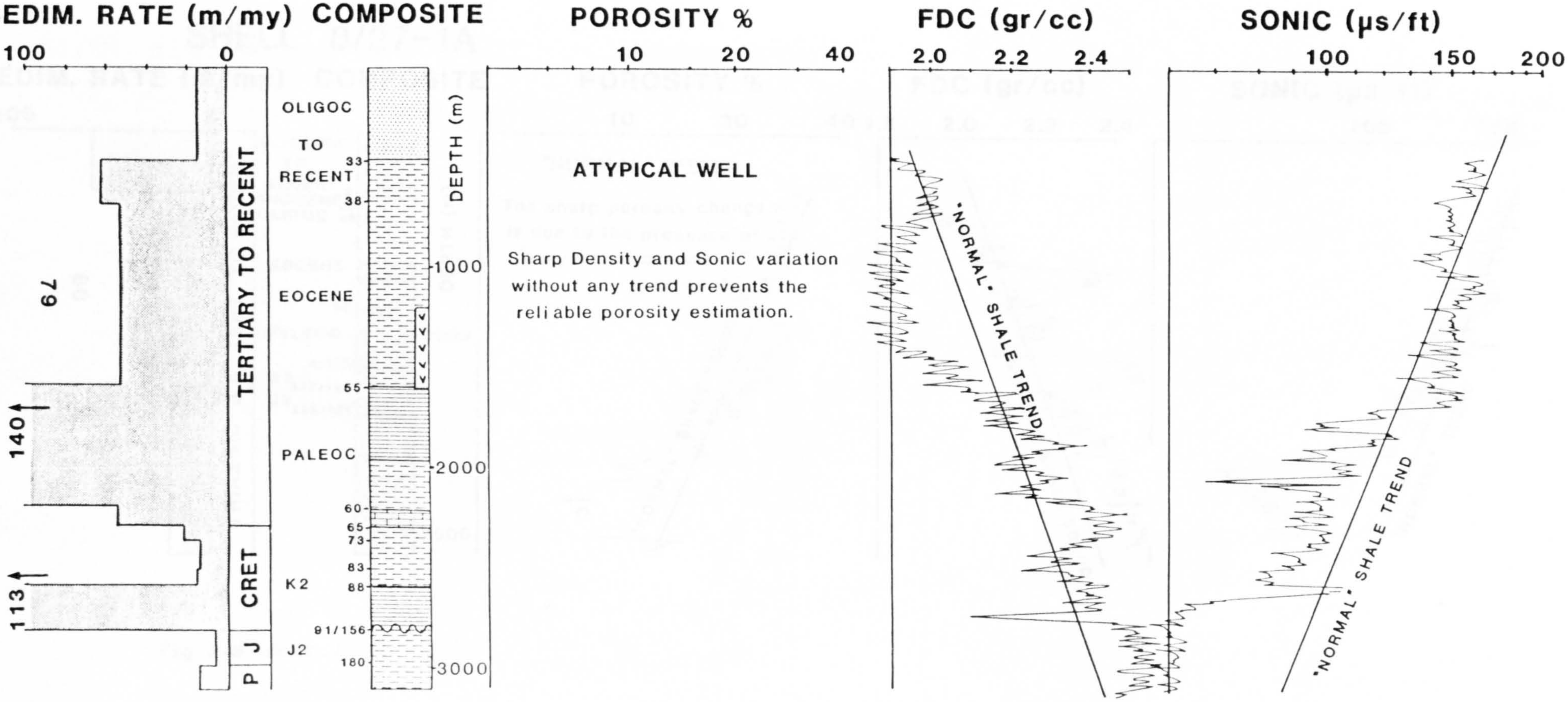
BALL & COLLINS 3/23-1
SEDIM. RATE (m/my) COMPOSITE
100
0
79
140
113
TERTIARY TO RECENT
CRET
J
P
OLIGOC
TO
RECENT
EOCENE
PALEOC
K2
J2
33
38
55
60
65
73
83
88
91/156
180
DEPTH (m)
1000
2000
3000
POROSITY %
10
20
40
ATYPICAL WELL
Sharp Density and Sonic variation without any trend prevents the reliable porosity estimation.
FDC (gr/cc)
2.0
2.2
2.4
"NORMAL" SHALE TREND
SONIC (μs/ft)
100
150
200
"NORMAL" SHALE TREND

Fig 3.9 (cont.)

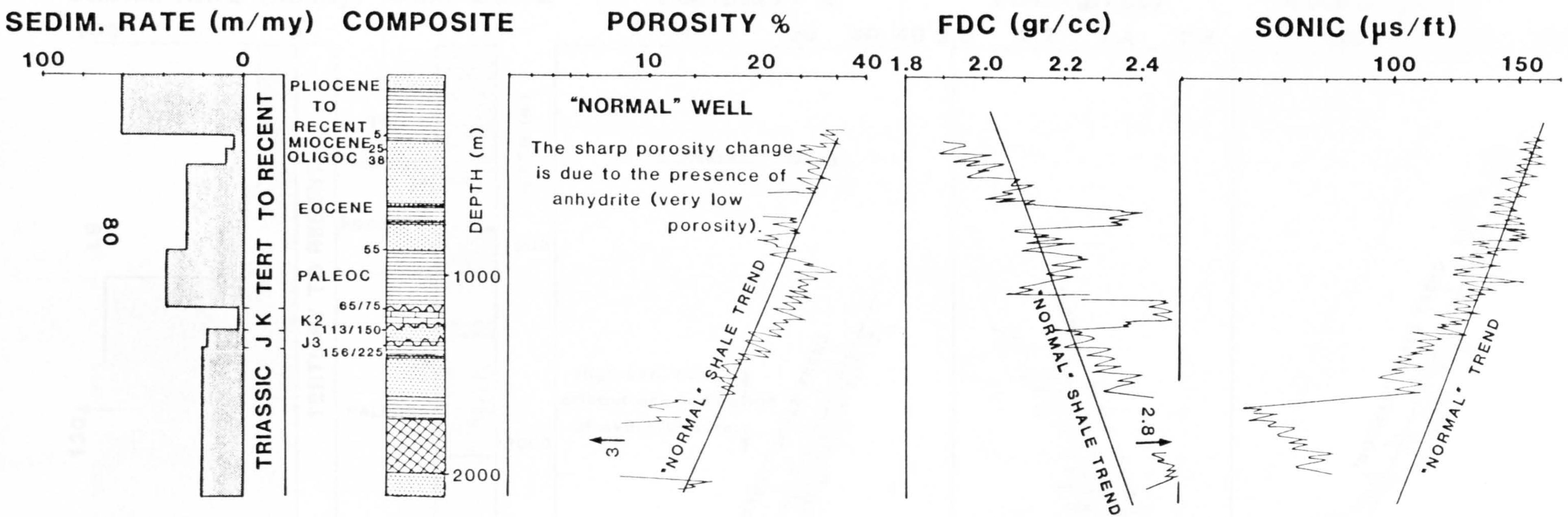
SHELL 8/27-1A
SEDIM. RATE (m/my)
100
0
08
TRIASSIC J K TERT TO RECENT
PLIOCENE TO RECENT
MIOCENE
OLIGOC
EOCENE
PALEOC
K2
J3
5
25
38
55
65/75
113/150
156/225
DEPTH (m)
1000
2000
COMPOSITE
POROSITY %
10
20
40
"NORMAL" WELL
The sharp porosity change is due to the presence of anhydrite (very low porosity).
"NORMAL" SHALE TREND
3
FDC (gr/cc)
1.8
2.0
2.2
2.4
"NORMAL" SHALE TREND
2.8
SONIC (µs/ft)
100
150
"NORMAL" TREND

Fig 3.9 (cont.)

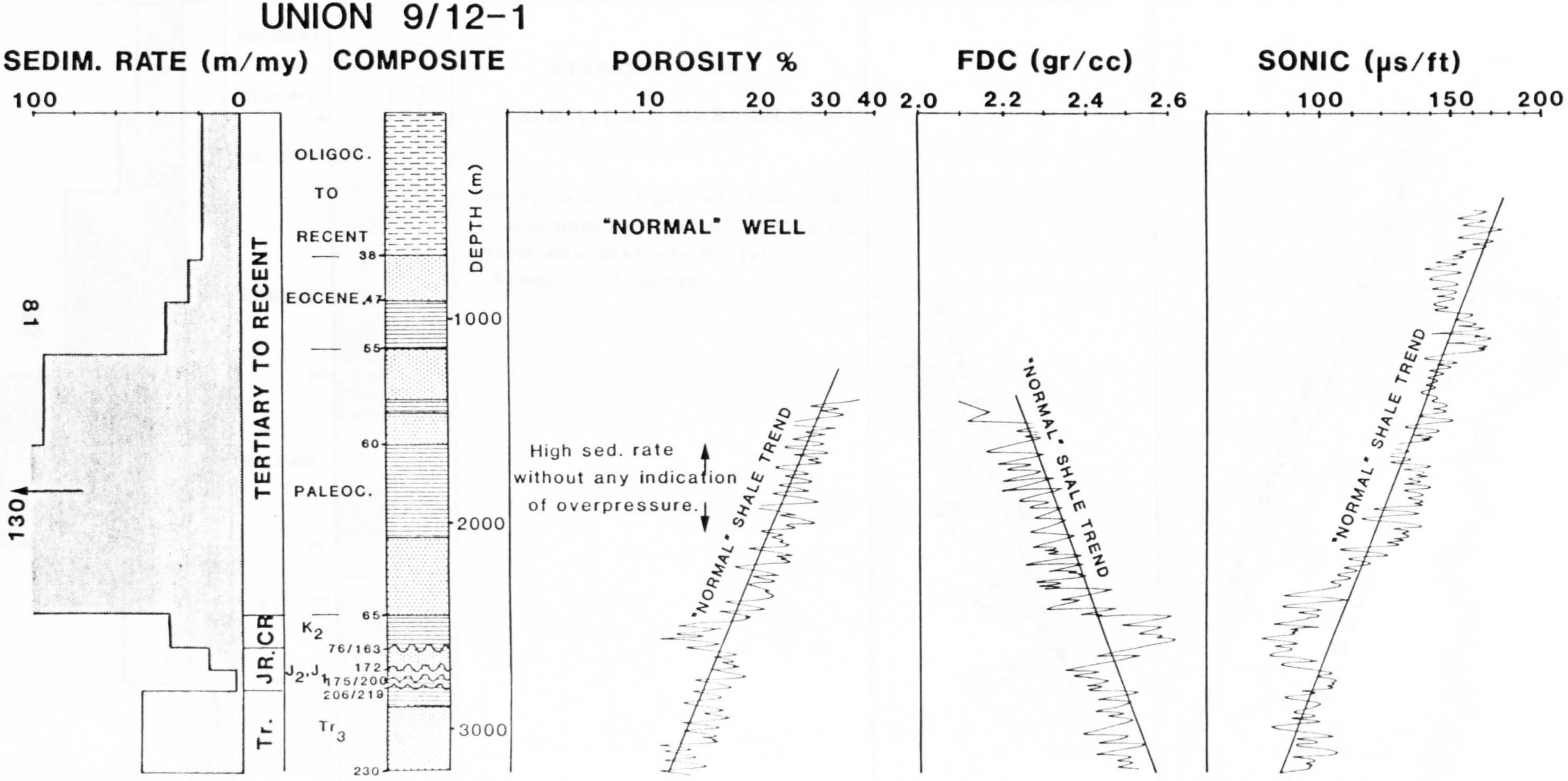
UNION 9/12-1
SEDIM. RATE (m/my) COMPOSITE
100
0
POROSITY %
10
20
30
40
FDC (gr/cc)
2.0
2.2
2.4
2.6
SONIC (µs/ft)
100
150
200
DEPTH (m)
1000
2000
3000
OLIGOC.
TO
RECENT
38
EOCENE
47
55
60
PALEOC.
65
K2
76/163
172
175/200
206/219
J2,J1
Tr3
230
TERTIARY TO RECENT
JR.CR
Tr.
81
130
"NORMAL" WELL
High sed. rate
without any indication
of overpressure.
"NORMAL" SHALE TREND
"NORMAL" SHALE TREND
"NORMAL" SHALE TREND

Fig 3.9 (cont.)

CONOCO 9/19-2

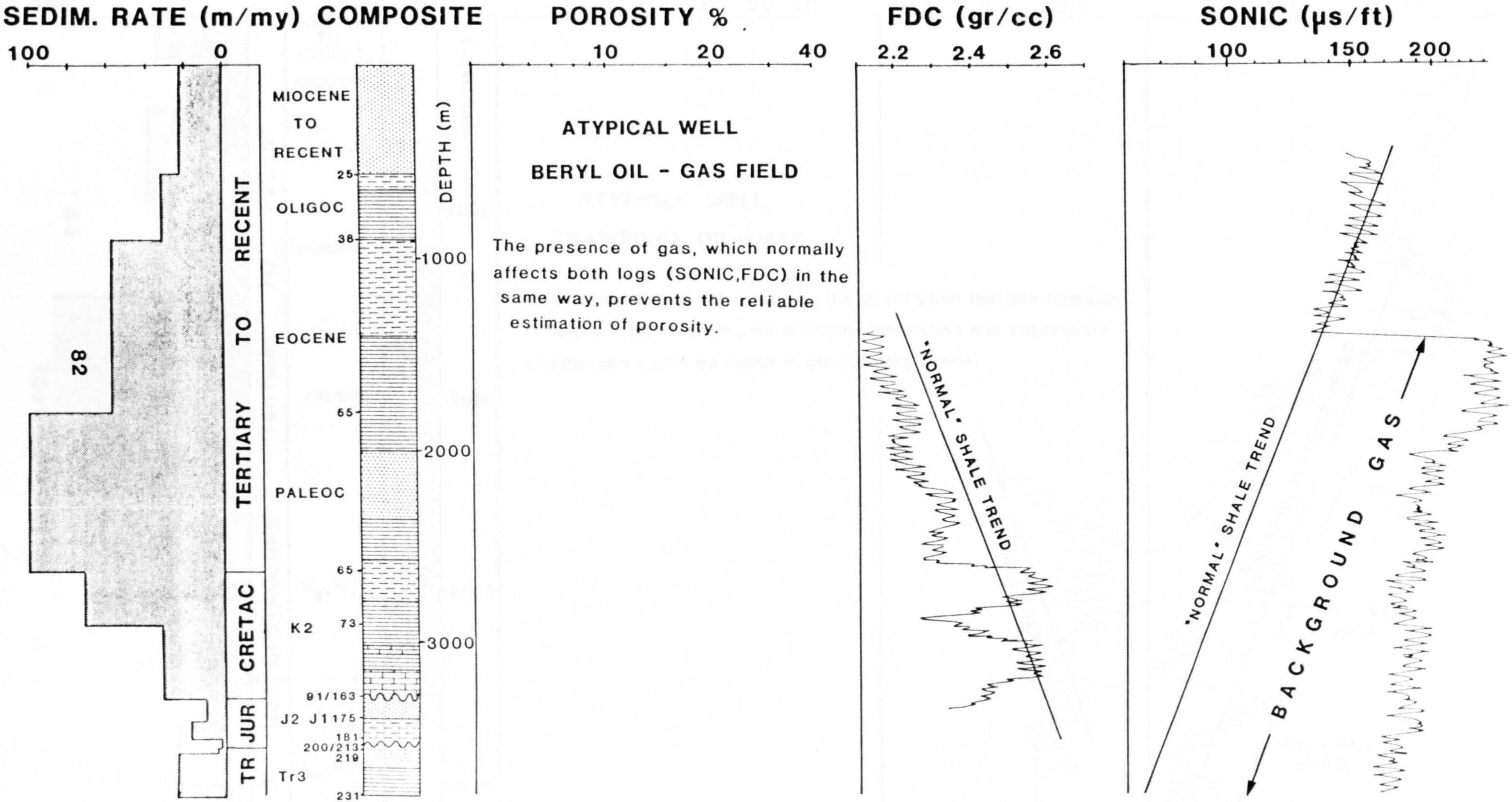

Fig 3.9 (cont.)

HAMILTON 9/28-1A

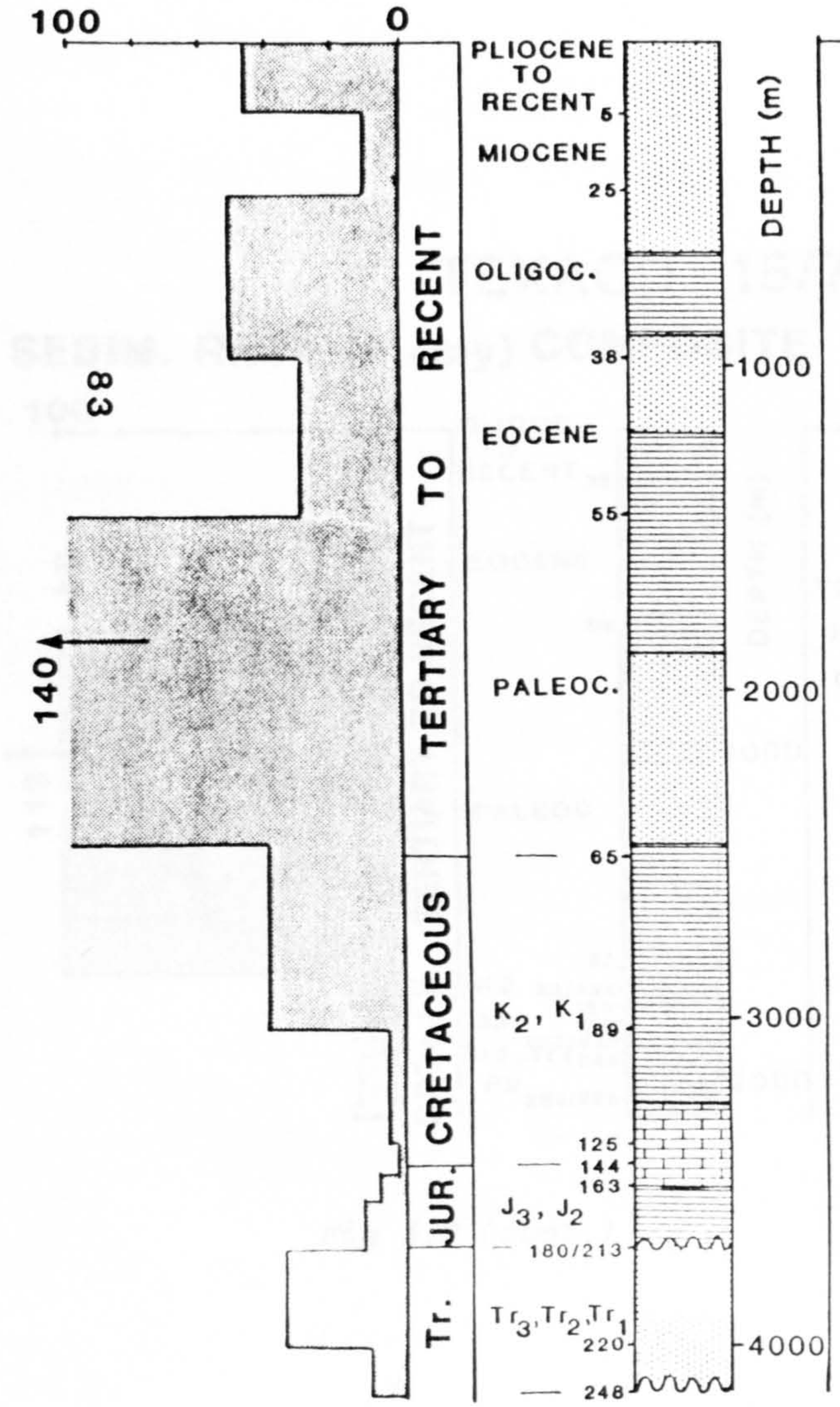

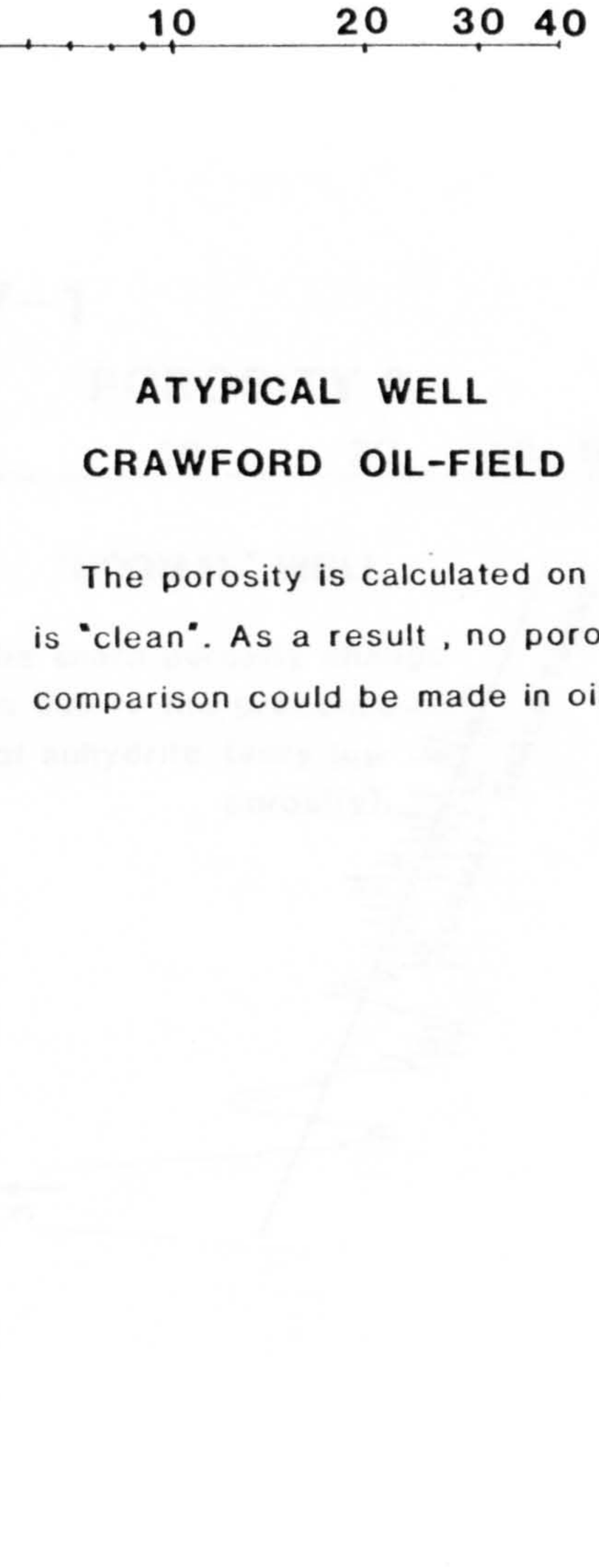

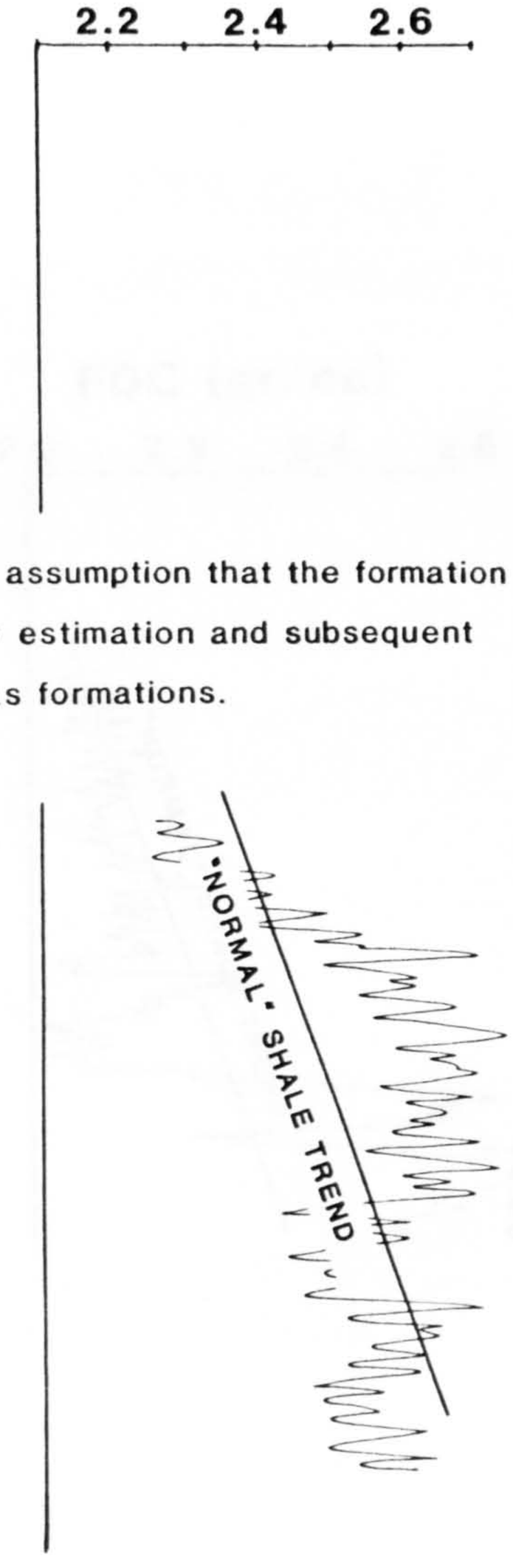

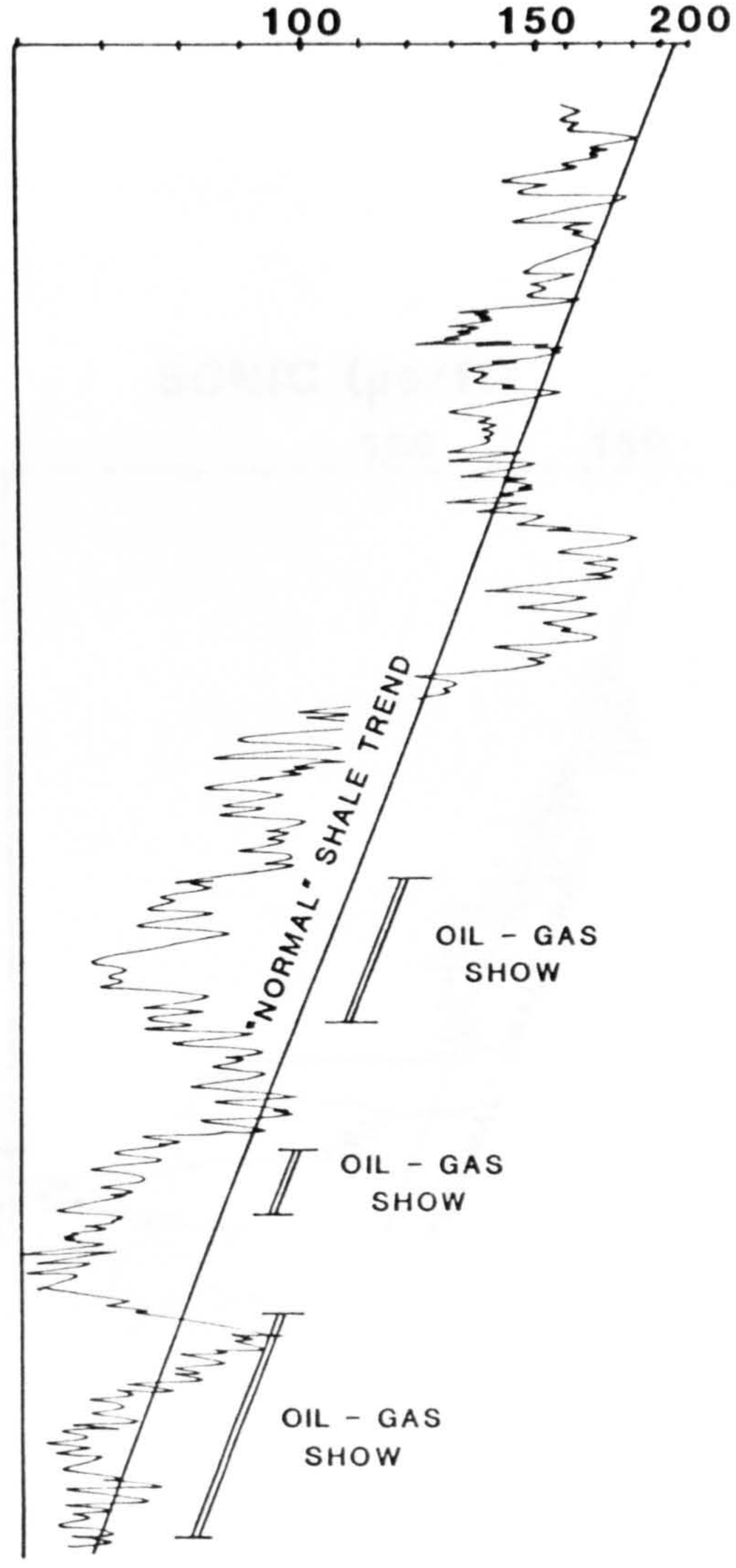

ATYPICAL WELL

CRAWFORD OIL-FIELD

The porosity is calculated on the assumption that the formation is "clean". As a result , no porosity estimation and subsequent comparison could be made in oil-gas formations.

Fig 3.9 (cont.)

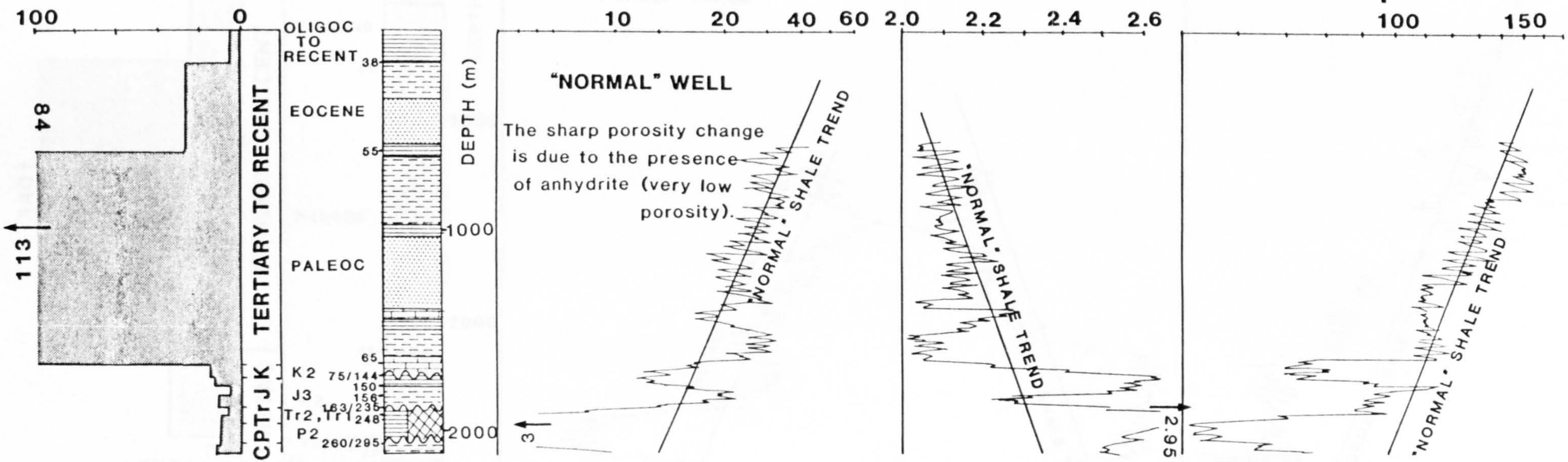
TEXACO 15/7-1
SEDIM. RATE (m/my) COMPOSITE
100
0
OLIGOC TO RECENT
38
EOCENE
55
PALEOC
65
K2 75/144
J3 150
156
Tr2,Tr1 163/235
248
P2 260/295
CPTrJK TERTIARY TO RECENT
84
113
DEPTH (m)
1000
2000
POROSITY %
10
20
40
60
"NORMAL" WELL
The sharp porosity change is due to the presence of anhydrite (very low porosity).
NORMAL SHALE TREND
3
FDC (gr/cc)
2.0
2.2
2.4
2.6
NORMAL SHALE TREND
2.95
SONIC (μs/ft)
100
150
NORMAL SHALE TREND

Fig 3.9 (cont.)

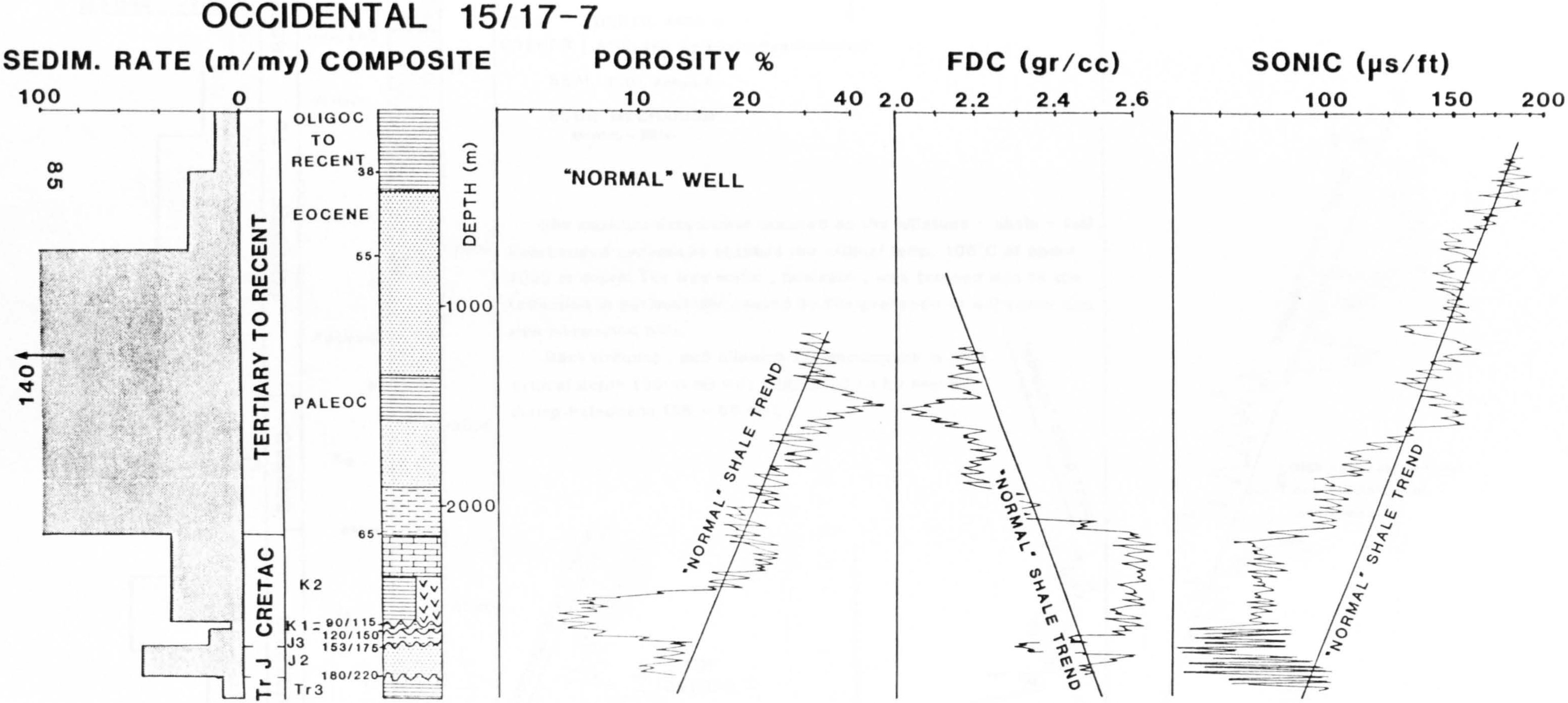
OCCIDENTAL 15/17-7
SEDIM. RATE (m/my) COMPOSITE
100
0
85
140
TERTIARY TO RECENT
Tr J CRETAC
OLIGOC TO RECENT
38
EOCENE
55
PALEOC
65
K2
K1
J3
J2
Tr3
90/115
120/150
153/175
180/220
DEPTH (m)
1000
2000
POROSITY %
10
20
40
"NORMAL" WELL
'NORMAL' SHALE TREND
FDC (gr/cc)
2.0
2.2
2.4
2.6
'NORMAL' SHALE TREND
SONIC (µs/ft)
100
150
200
'NORMAL' SHALE TREND

Fig 3.9 (cont.)

SEDIM. RATE (m/my) COMPOSITE

100 0

135

98

180

TERTIARY TO RECENT

JURASSIC CRETAC. Tr.

PLIOCENE TO RECENT

5

MIOCENE

25

OLIGOC.

38

EOCENE

55

PALEOC.

65

K_2

89/144

J_3

163

J_2

180/231

Tr_2 , Tr_1

1000

2000

3000

4000

5000

POROSITY %

10 20 30 40

FDC (gr/cc)

2.0 2.2 2.4 2.6

SONIC (μs/ft)

100 150

PHILLIPS 16/17-6

ABNORMAL WELL

TOP OVERPR. { DEPTH: 4400 m
AGE: 163 my (Oxfordian/Callovian)

SEAL: Tuff , Anhydrite

SUGG. MECHANISM:
Montm.→ Illite

The maximum dehydration occured as the siltstone – shale – tuff interbedded sequences reached the critical temp. 105°C at about 3000 m depth. The free water , however , was trapped due to the reduction in permeability caused by the presence of anhydrite and well compacted tuffs.

Backstripping , and allowing for decompaction , the critical depth (3000 m) was calculated to be reached during Paleocene (55 – 65 my).

"NORMAL" SHALE TREND

TOP OVERPR.

ANHYDRITE

"NORMAL" SHALE TREND

?

"NORMAL" SHALE TREND

High sed. rate without any indication of overpressure

Fig 3.9 (cont.)

The fourth abnormal well (PHILLIPS 16/17-6) has completely different geological history and structure from the wells studied above, (Fig 3.9). This time the undercompaction (five times the expected porosity) was detected at a depth of 4400m (Oxfordian/Callovian), and again, phase change seems to be the main mechanism of overpressure creation.

In all the above cases of undercompaction there is no high sedimentation rate observed. In other cases high sedimentation rate (>100m/my, MOBIL 3/1-1, UNION 9/12-1) is associated with normally compacted shale formations. Therefore it can be suggested that rapid loading has not significantly affected porosities in the northern North Sea area.

3.9 Pressure Estimation

A direct application of the porosity investigation of this study is the calculation of the pressure gradient or equivalent mud weight used during drilling in overpressured formations. This calculation requires the application of the empirical method of Fig 3.10.

A maximum value (mean in all three northern abnormal wells) of measured t(sh) - t(sh)"normal" ≈ 25 μs/ft gives 0.62psi/ft pressure gradient. A maximum value of f(sh)/f(sh)"normal" ≈ 1.8 gives 0.74psi/ft pressure gradient. Therefore a value of about 0.68psi/ft pressure gradient can be expected when drilling this particular horizon instead of 0.45psi/ft "normal" pressure northern North Sea gradient.

The specific acoustic time difference in the ovepressured horizon of the fourth abnormal well (PHILLIPS 16/17-6) is approximately 25μs/ft which gives 0.62psi/ft pressure gradient. No pressure gradient can be calculated using porosity information for this particular horizon because the porosity values are out of scale.

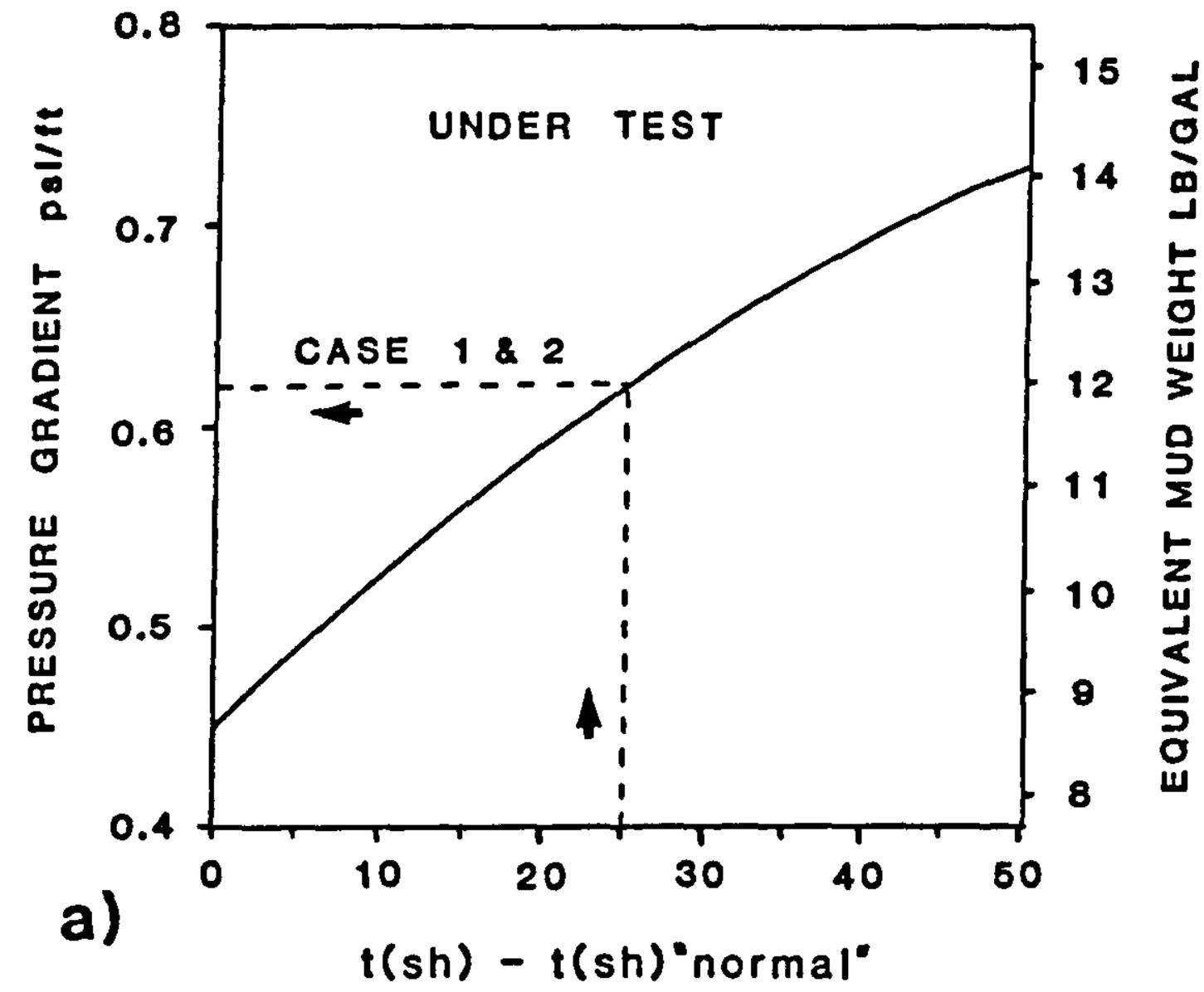

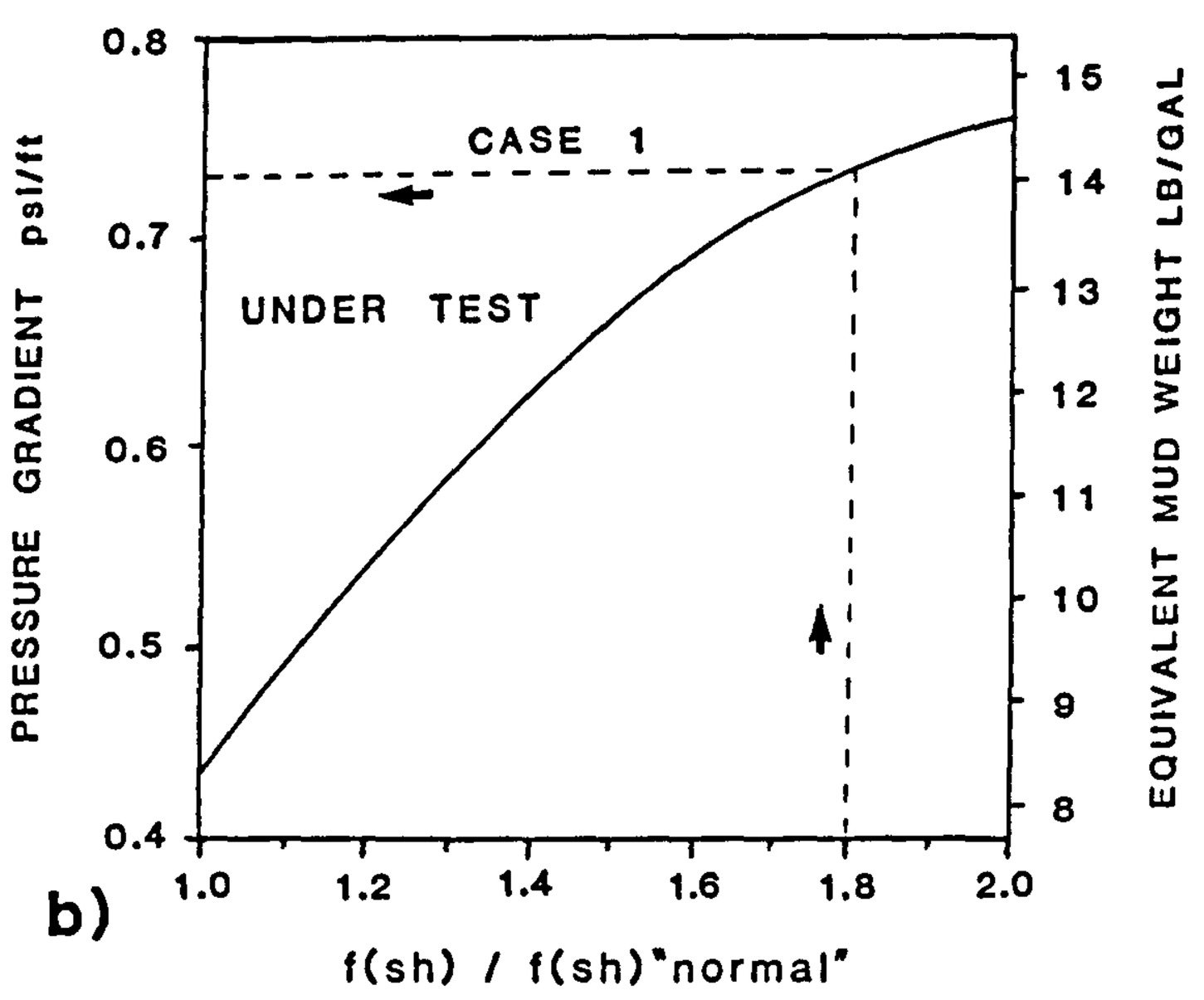

Fig 3.10 a) Pressure gradient-travel time in the southern area of the northern North Sea basin. b) Tentative correlation between f(sh)/f(sh)"normal", (after Schlumberger, (1974) p.166 and 168 respectively).

The pressure correlation with travel time and porosity in the northern North Sea of Fig 3.10 is still under test, therefore, the above porosity gradients are under speculation.

3.10 Conclusions

The use of the sonic and FDC logs to determine "normal" porosity gradient and detect undercompacted formation gives very good results in the northern North Sea. The calculated total porosities is estimated to be within 5% of the actual value.

Even though high sedimentation is suggested to be the main cause of overpressure in many areas of the world eg. Louisiana Gulf Coast, Harkins and Baugher (1969), where the sedimentation rate is approximately 120m/my, it does not seem to be the case in the northern North Sea. Here the main cause seems to be phase change. In fact variation in sedimentation rates does not seem to have any effect on the compaction of the sediment.

Using reliable pressure gradient-travel time or porosity relationships, drilling pressures can be predicted in wells that have the same structure and the same geological history.

The possibility of encountering overpressured horizons at different depths than those observed, created by different causes than that proposed cannot be ruled out in the northern North Sea area. No regional conclusions can be reached due to the limited number of publications (no more than half a dozen) about the subject in the above area. To give specific answers to the origin and distribution of overpressures in the northern North Sea it seems that a very large number of deep wells, possibly more than 200, is required. In addition to that, it would be necessary to analyse the mineralogy of core samples obtained from a few typical wells, a task outside of the objectives of this study.

The main intention of this study was to present and use available data as a basis for a discussion of the factors which control porosity gradients and hopefully to provide a point of departure for more sophisticated studies.

CHAPTER 4

SUBSIDENCE CALCULATIONS

Introduction

In order to determine the subsidence history of a sedimentary basin from well log information the effects of sedimentary loading and changes in water depth must be taken into account. The method of backstripping developed by Steckler and Watts (1978) involves removing successive time slices and reconstructing the sedimentary section at different times in the past, so that the depth to the basement can be corrected for the sediment load present at that time. The depth to basement relative to sea level, calculated at different times, can then be compared with the subsidence paths predicted by theoretical models of basin formation.

This chapter deals with the method of obtaining basement subsidence paths from well data. Having established the porosity-depth relationship of the sediments (section 3.3.2) the effects of correcting for compaction when backstripping were studied. All the units below the basement level were assumed to have been fully compacted prior to the basin initiation, so that all the sediments above this were decompacted during the backstripping process. As the sedimentary basin evolves, the basement is subjected to loads, due to variations in the depth of deposition and due to the sediment infill. The above effects of loading were accounted for assuming a plate with no lateral strength (local loading), and the basement level filled with water only, relative to present day sea level, was obtained.

4.1 Data

The data set consists of detailed chronostratigraphic description of 25 commercial released wells situated along 6 seismic profiles across the Viking Graben. The same data set was earlier used in the gravity investigation to determine the deep crustal structure (Fig. 2.5). The position of the wells and the seismic profiles is shown in Fig. 4.1. No wells have been drilled on the East Shetland Platform and Stord Basin. Wells that penetrated the base Triassic were selected where possible, and those that did not, were extrapolated to this horizon using the appropriate seismic profile. The depths of deposition were taken from released micropaleontological and lithological information available in well reports.

The detailed description of the data used will be given in individual sections.

4.2 Decompaction

To correct for sedimentary loading effects in the basement it is necessary to know the original sediment thickness, the mean sedimentary density for the total sediment column at each time during the development of the basin and the water depth. As the sediments are progressively buried the pore fluids are expelled and the sediment thickness decreases. The mean density of the sediment pile will also change as a consequence of this compaction, since as the fluid is expelled the mean density of the sediment approaches the sediment grain density.

The model of decompaction used was developed by Sclater and Christie (1980) based on the simple porosity - depth relationship of Rubey and Hubbert (1960),

$$f = f_o e^{-cz}$$

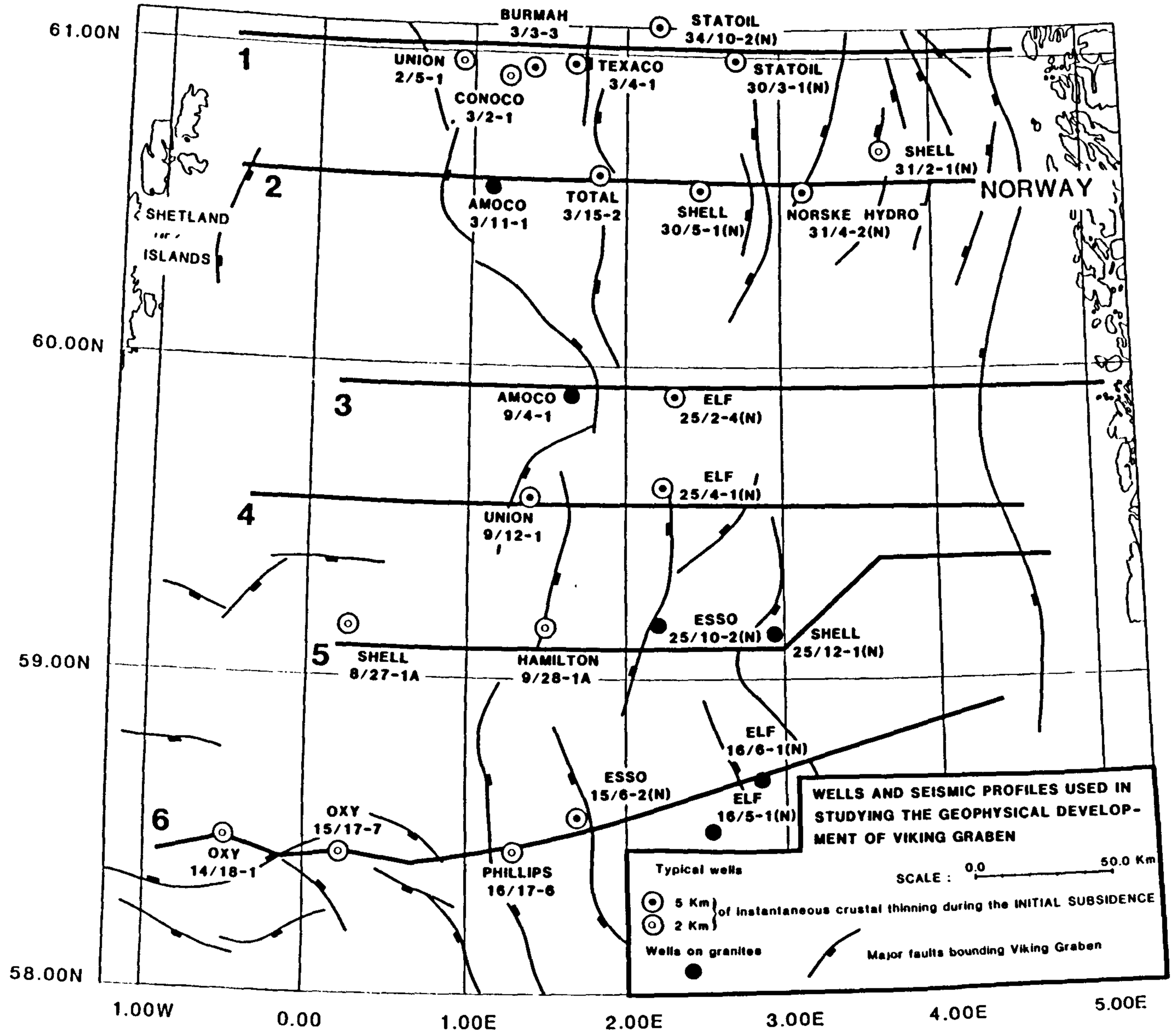

Fig 4.1 Summary diagram of wells and seismic profiles used in the study of basement subsidence from well log data.

where f is the porosity, f_o the surface porosity, z is the depth below the surface in metres and c is a constant determined by the lithology.

Not all sediments compact in exactly the same way, so that the variation of different lithologies needs to be taken into account. The parameters of the exponential relation between porosity and depth for the three dominent lithologies of the northern North Sea (sandstone, siltstone and shale) were determined in section 3.3.2. Parameters for the limited limestone sedimentary sections observed in few wells were taken from Sclater and Christie (1980). A summary of the porosity parameters for the four generalized lithologies used above is given in Table 4.1.

The sediments are assumed to lie on a completely compacted basement surface, so that only the units above this are decompacted during backstripping. In the wells studied all the units below Late Permian are assumed to have been completely lithified by Triassic times.

Table 4.1

Porosity parameters and density of grains used in the decompaction and sediment unloading respectively for different lithologies. Sandstone ρ_{sg} after Schlumberger (1974), shale ρ_{sg} after Magara (1976a), limestone ρ_{sg} after Scholle (1977), ρ_{sg} for shale/sand (silt) equals 2.68 g/cc and ρ_w equals 1.03 g/cc.

	fo	c,x10^{-4}	ρ_{sg},g/cc
sandstone	49	2.38	2.65
siltstone	56	4.18	2.68
shale	63	5.53	2.72
limestone	70	7.10	2.71

As a layer is removed during backstripping the top of the next unit is brought to the surface and the sediment column below is decompacted to its original thickness at that time, allowing for differences in lithology within the section. As each lithology unit is moved up and decompacted the new base level for this unit becomes the top of the next unit.

Since the sediment is expanded by decompaction the result of correcting for compaction is to increase the depth to basement at each time. The effect of decompaction using well data is shown in Fig 4.2 following the method described by Sclater and Christie (1980) p. 3734-3735.

The effect of correcting for compaction is to lower the observed subsidence curve and therefore reduce the rapid subsidence seen in the Tertiary, hence the "decompacted subsidence" path is "close" to linear.

All the well sections are assumed to be normally pressured. If a section is overpressured this means that the pore fluid supports some of the weight of the overburden instead of this being supported on the grain to grain contact. In an overpressured section the original thickness of the unit will have been overestimated by assuming a normal pressure gradient.

In the porosity study of Chapter 3 (section 3.8) three wells (BURMAH 3/3-3, CONOCO 3/2-1, PHILLIPS 16/17-6) were found to contain overpressured horizons with thickness less than 10% of the total depth drilled. The assumption that the porosity is normal was found not to appreciably affect the results, therefore, no overpressure correction was applied.

All the wells were taken down to the base Triassic, apart from 6 wells drilled on granitic basement, Fig. 4.1 and 2.5, lying beneath Jurassic or Cretaceous sediments.

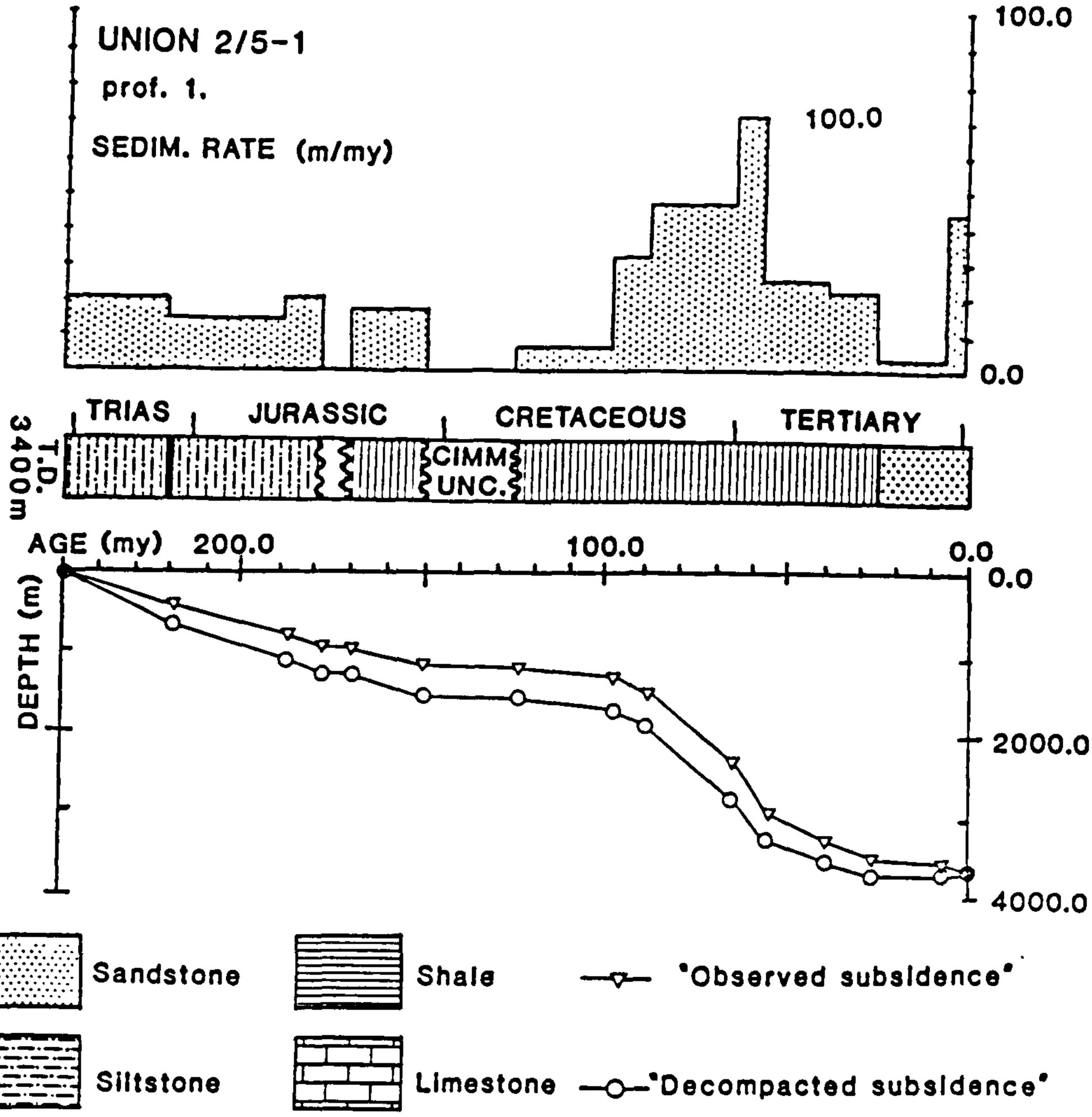

Fig 4.2 *The effect of decompacting the sediments using well data. The generalized chronostratigraphy was derived from the Composite logs. Heavy line in the chronostratigraphic column indicates the total depth drilled (T.D.) with the rest of the section extrapolated from the corresponding seismic profile. Question marks in some horizons indicate age uncertainties. Ages after Harland et al. (1982), see Fig. 3.8. Sedimentation rates were calculated from thicknesses of decompacted sections. "Observed subsidence" indicates the sediment thickness at each time as seen in the present day well section. "Decompacted subsidence" shows the original sediment thickness. Unconformities are treated as times of zero sedimentation and hence plotted as a horizontal line.*

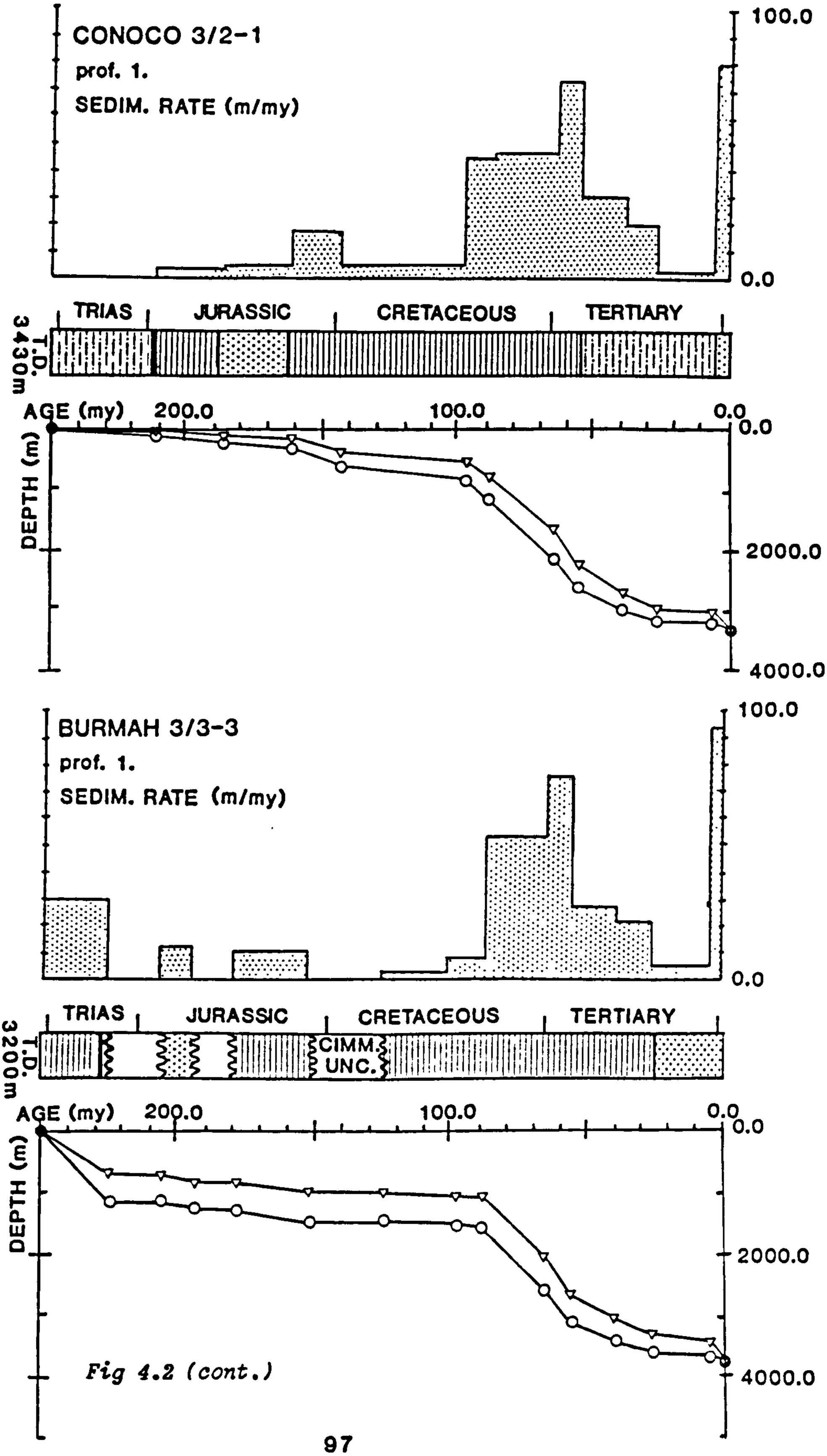
CONOCO 3/2-1
prof. 1.
SEDIM. RATE (m/my)
100.0
0.0
TRIAS
JURASSIC
CRETACEOUS
TERTIARY
T.D. 3430m
AGE (my)
200.0
100.0
0.0
DEPTH (m)
0.0
2000.0
4000.0
BURMAH 3/3-3
prof. 1.
SEDIM. RATE (m/my)
100.0
0.0
TRIAS
JURASSIC
CRETACEOUS
TERTIARY
CIMM. UNC.
T.D. 3200m
AGE (my)
200.0
100.0
0.0
DEPTH (m)
0.0
2000.0
4000.0

Fig 4.2 (cont.)

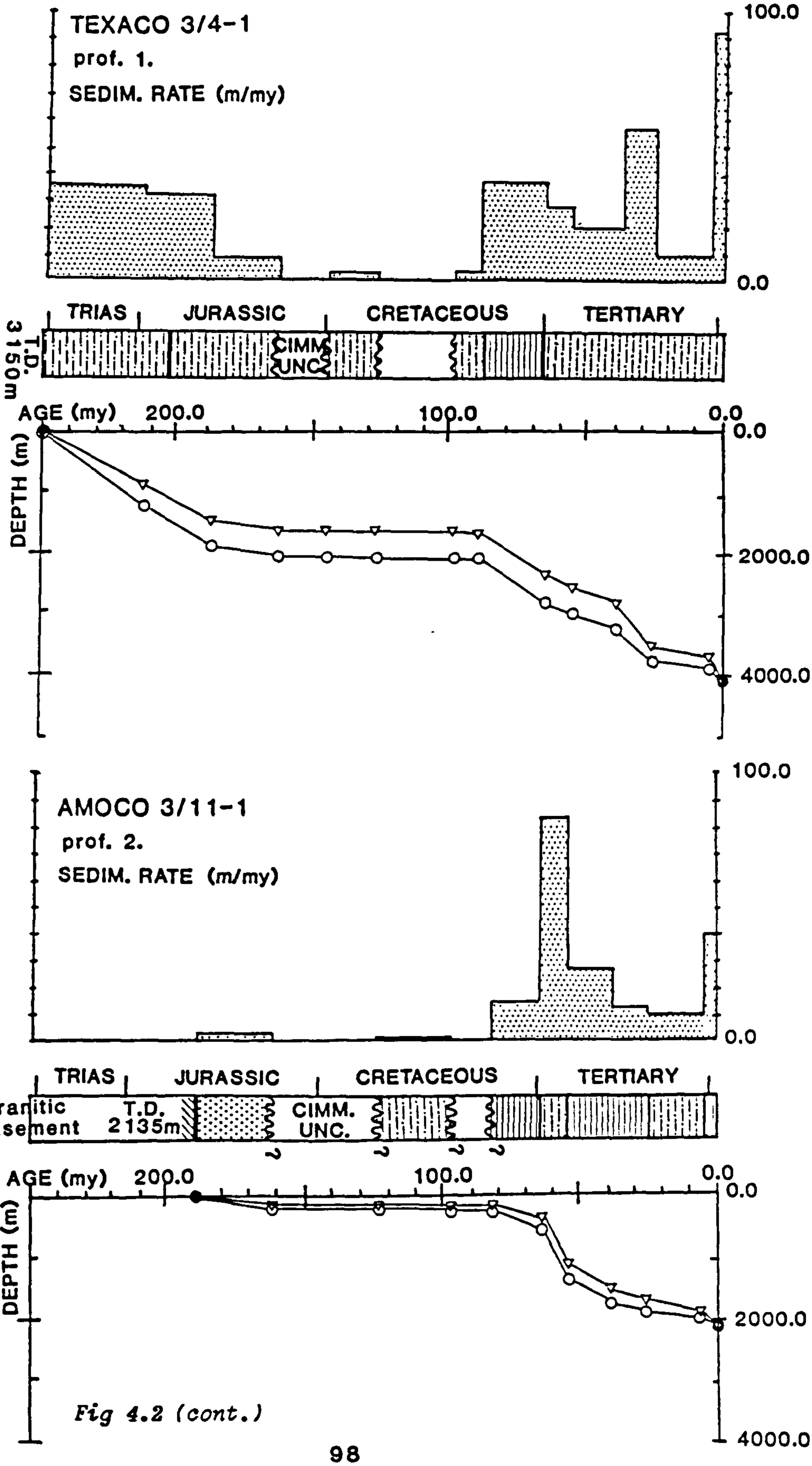
TEXACO 3/4-1
prof. 1.
SEDIM. RATE (m/my)
100.0
0.0
TRIAS
JURASSIC
CRETACEOUS
TERTIARY
T.D. 3150m
CIMM. UNC.
AGE (my)
200.0
100.0
0.0
DEPTH (m)
0.0
2000.0
4000.0
AMOCO 3/11-1
prof. 2.
SEDIM. RATE (m/my)
100.0
0.0
TRIAS
JURASSIC
CRETACEOUS
TERTIARY
Granitic Basement
T.D. 2135m
CIMM. UNC.
AGE (my)
200.0
100.0
0.0
DEPTH (m)
0.0
2000.0
4000.0

Fig 4.2 (cont.)

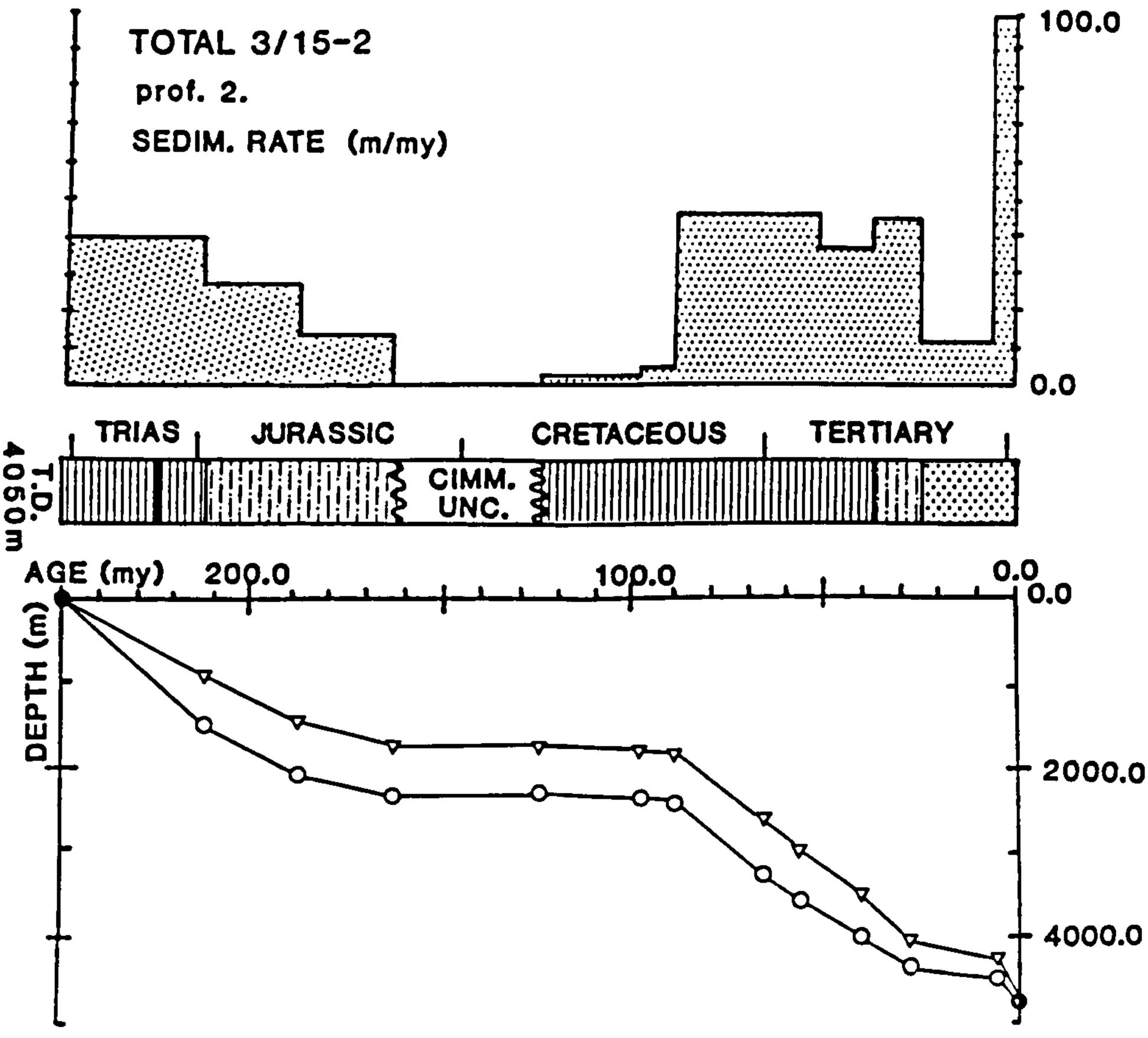
TOTAL 3/15-2
prof. 2.
SEDIM. RATE (m/my)
100.0
0.0
TRIAS
JURASSIC
CRETACEOUS
TERTIARY
T.D. 4060m
CIMM. UNC.
AGE (my)
200.0
100.0
0.0
DEPTH (m)
0.0
2000.0
4000.0

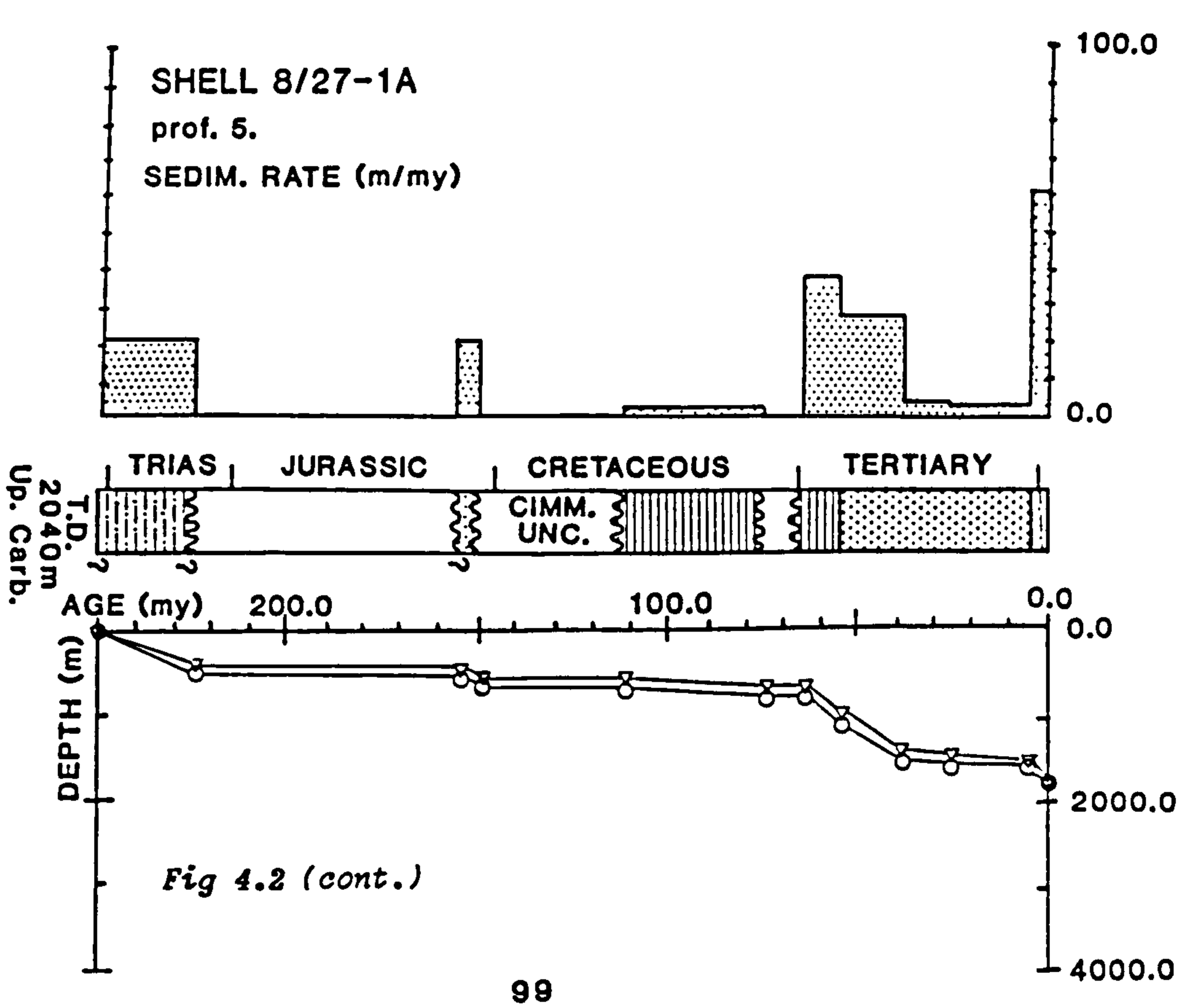
SHELL 8/27-1A
prof. 5.
SEDIM. RATE (m/my)
100.0
0.0
TRIAS
JURASSIC
CRETACEOUS
TERTIARY
T.D. 2040m Up. Carb.
CIMM. UNC.
AGE (my)
200.0
100.0
0.0
DEPTH (m)
0.0
2000.0
4000.0

Fig 4.2 (cont.)

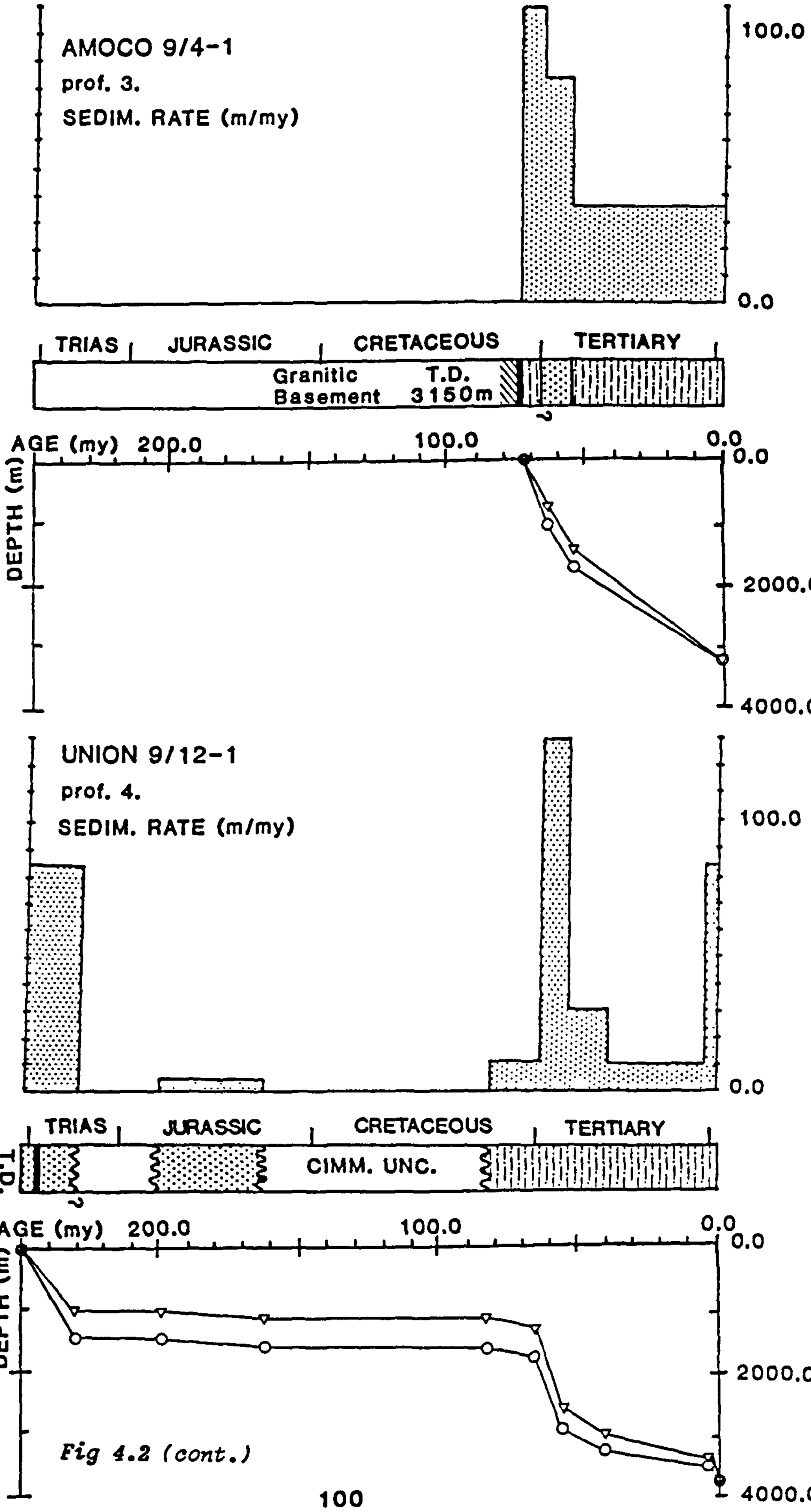
AMOCO 9/4-1
prof. 3.
SEDIM. RATE (m/my)
100.0
0.0
TRIAS
JURASSIC
CRETACEOUS
TERTIARY
Granitic Basement
T.D. 3150m
AGE (my) 200.0
100.0
0.0
DEPTH (m)
0.0
2000.0
4000.0
UNION 9/12-1
prof. 4.
SEDIM. RATE (m/my)
100.0
0.0
TRIAS
JURASSIC
CRETACEOUS
TERTIARY
CIMM. UNC.
T.D. 3150m
AGE (my) 200.0
100.0
0.0
DEPTH (m)
0.0
2000.0
4000.0

Fig 4.2 (cont.)

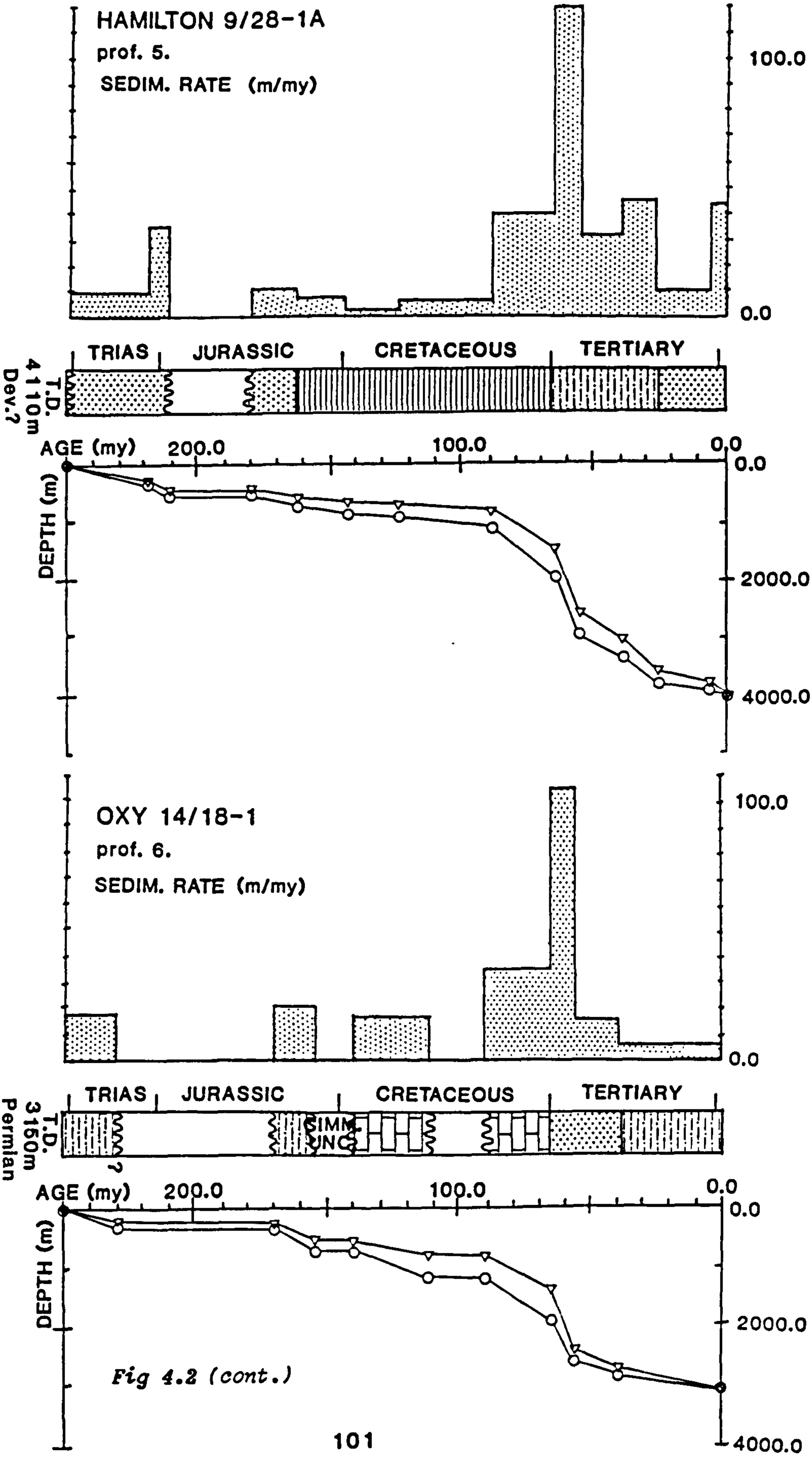
HAMILTON 9/28-1A
prof. 5.
SEDIM. RATE (m/my)
100.0
0.0
TRIAS
JURASSIC
CRETACEOUS
TERTIARY
T.D. 4110m
Dev.?
AGE (my)
200.0
100.0
0.0
DEPTH (m)
0.0
2000.0
4000.0
OXY 14/18-1
prof. 6.
SEDIM. RATE (m/my)
100.0
0.0
TRIAS
JURASSIC
CRETACEOUS
TERTIARY
T.D. 3150m
Permian
?
SIMM-
UNG
AGE (my)
200.0
100.0
0.0
DEPTH (m)
0.0
2000.0
4000.0

Fig 4.2 (cont.)

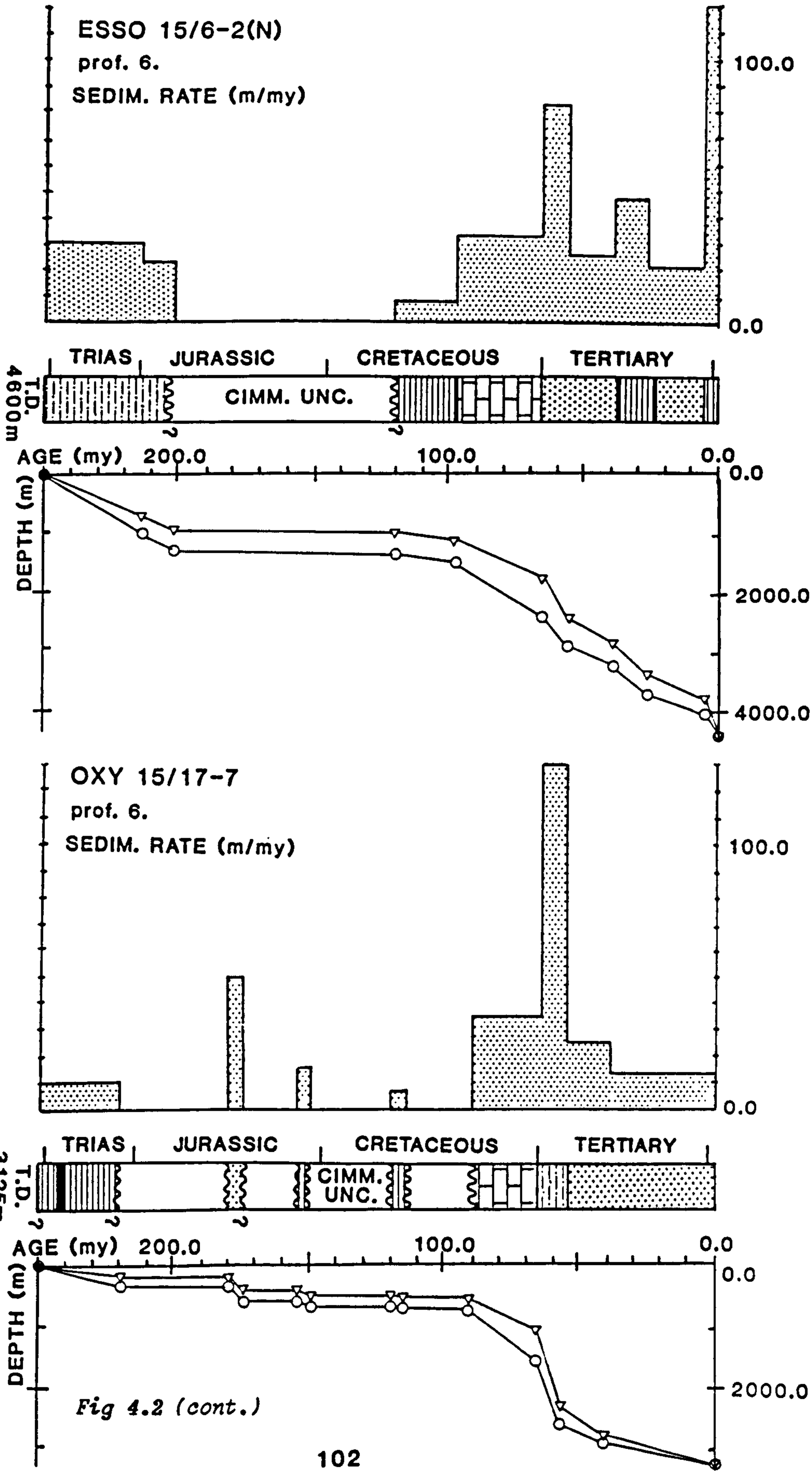
ESSO 15/6-2(N)
prof. 6.
SEDIM. RATE (m/my)
100.0
0.0
TRIAS
JURASSIC
CRETACEOUS
TERTIARY
T.D. 4800m
CIMM. UNC.
AGE (my) 200.0
100.0
0.0
DEPTH (m)
0.0
2000.0
4000.0
OXY 15/17-7
prof. 6.
SEDIM. RATE (m/my)
100.0
0.0
TRIAS
JURASSIC
CRETACEOUS
TERTIARY
T.D. 3125m
CIMM. UNC.
AGE (my) 200.0
100.0
0.0
DEPTH (m)
0.0
2000.0

Fig 4.2 (cont.)

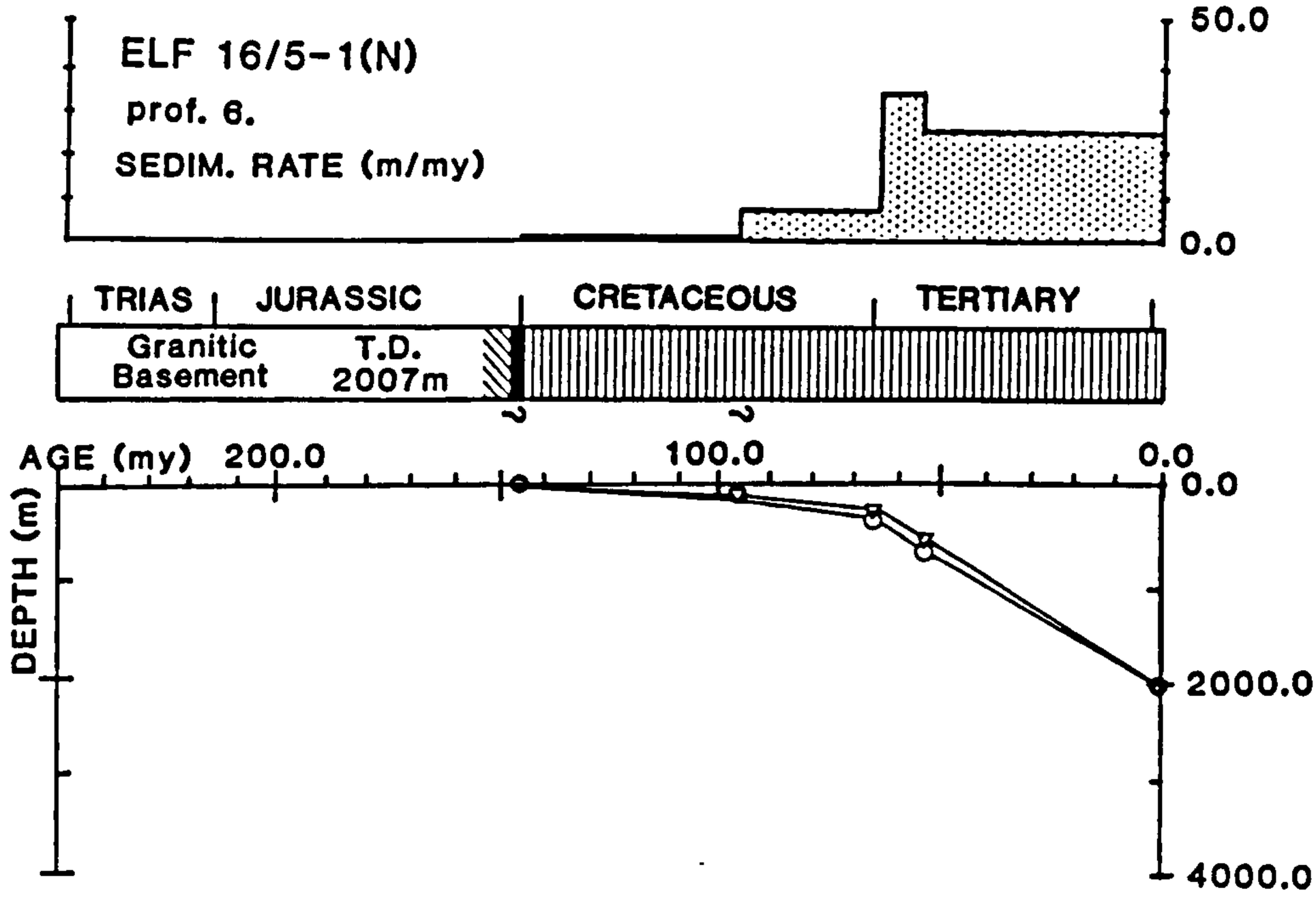
ELF 16/5-1(N)
prof. 6.
SEDIM. RATE (m/my)
50.0
0.0
TRIAS
JURASSIC
CRETACEOUS
TERTIARY
Granitic Basement
T.D. 2007m
AGE (my) 200.0
100.0
0.0
DEPTH (m)
0.0
2000.0
4000.0
ELF 16/6-1(N)
prof. 6.
SEDIM. RATE (m/my)
50.0
0.0
TRIAS
JURASSIC
CRETACEOUS
TERTIARY
Granitic Basement
T.D. 1930m
AGE (my) 200.0
100.0
0.0
DEPTH (m)
0.0
2000.0
4000.0

Fig 4.2 (cont.)

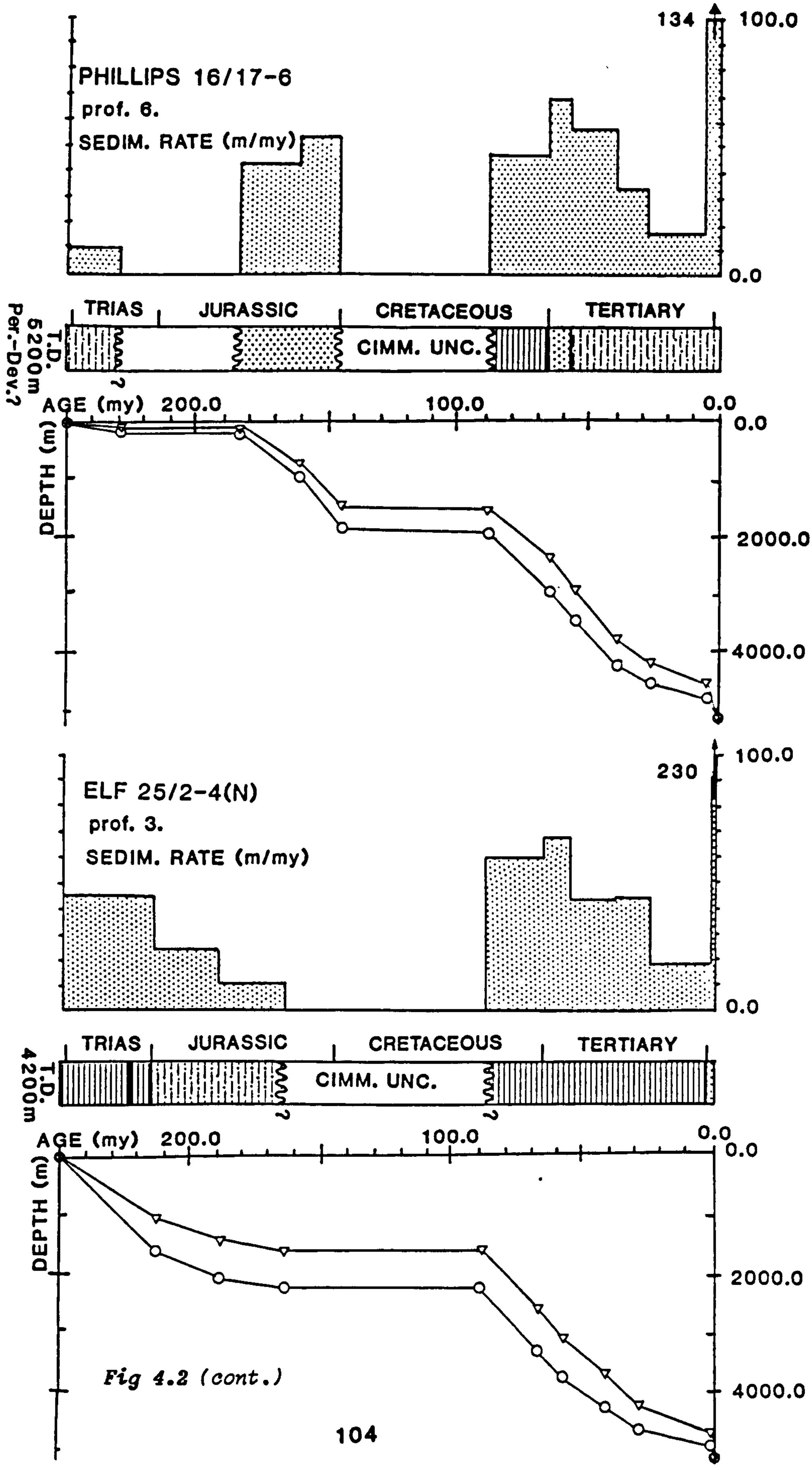
PHILLIPS 16/17-6
prof. 6.
SEDIM. RATE (m/my)
134
100.0
0.0
TRIAS
JURASSIC
CRETACEOUS
TERTIARY
T.D. 5200m Per.-Dev.?
CIMM. UNC.
AGE (my) 200.0
100.0
0.0
DEPTH (m)
0.0
2000.0
4000.0
ELF 25/2-4(N)
prof. 3.
SEDIM. RATE (m/my)
230
100.0
0.0
TRIAS
JURASSIC
CRETACEOUS
TERTIARY
T.D. 4200m
CIMM. UNC.
AGE (my) 200.0
100.0
0.0
DEPTH (m)
0.0
2000.0
4000.0

Fig 4.2 (cont.)

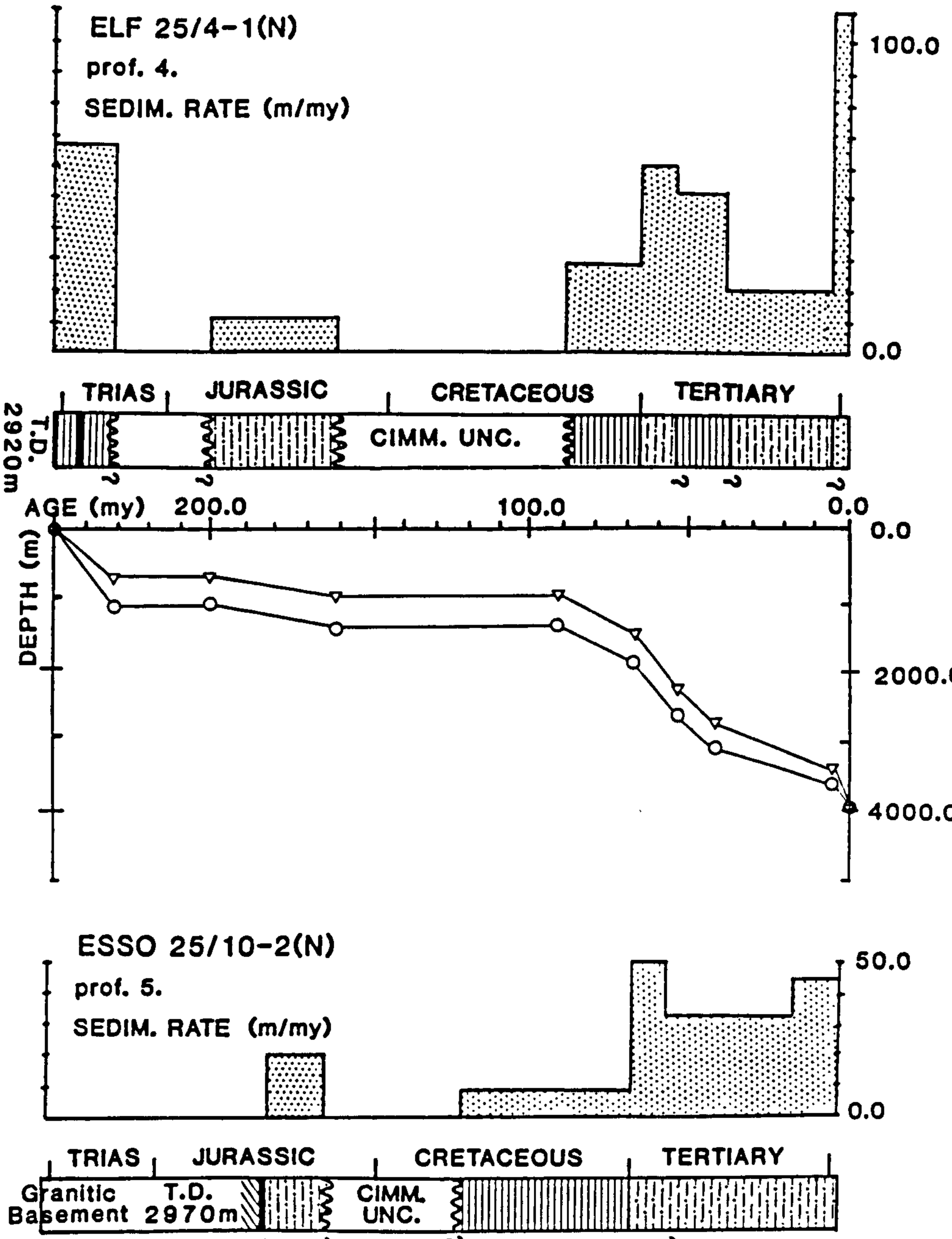
ELF 25/4-1(N)
prof. 4.
SEDIM. RATE (m/my)
100.0
0.0
TRIAS
JURASSIC
CRETACEOUS
TERTIARY
T.D. 2920m
CIMM. UNC.
AGE (my)
200.0
100.0
0.0
DEPTH (m)
0.0
2000.0
4000.0
ESSO 25/10-2(N)
prof. 5.
SEDIM. RATE (m/my)
50.0
0.0
TRIAS
JURASSIC
CRETACEOUS
TERTIARY
Granitic Basement
T.D. 2970m
CIMM. UNC.
AGE (my)
200.0
100.0
0.0
DEPTH (m)
0.0
2000.0
4000.0

Fig 4.2 (cont.)

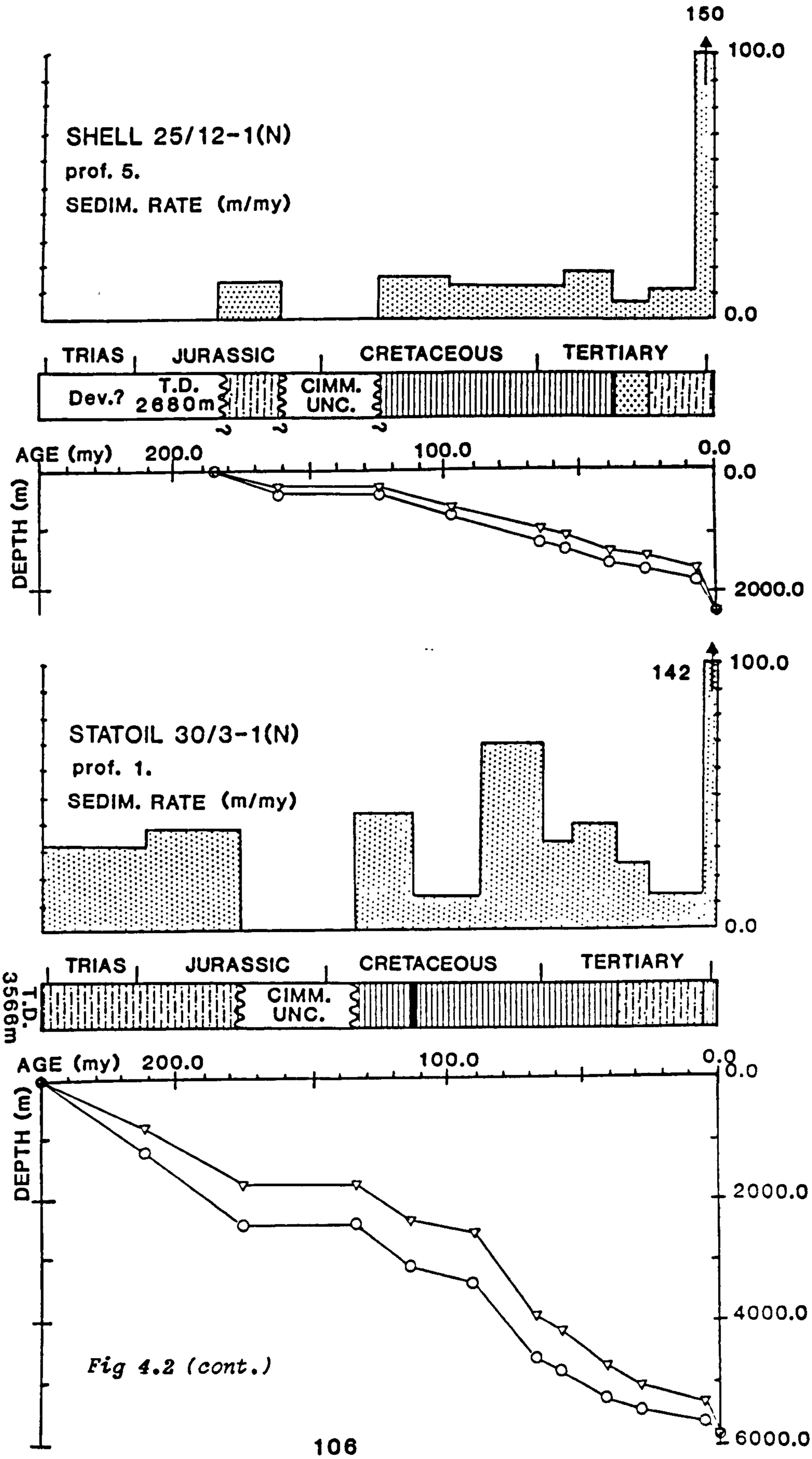
150
100.0
SHELL 25/12-1(N)
prof. 5.
SEDIM. RATE (m/my)
0.0
TRIAS
JURASSIC
CRETACEOUS
TERTIARY
Dev.?
T.D. 2680m
CIMM. UNC.
AGE (my)
200.0
100.0
0.0
0.0
DEPTH (m)
2000.0
142
100.0
STATOIL 30/3-1(N)
prof. 1.
SEDIM. RATE (m/my)
0.0
TRIAS
JURASSIC
CRETACEOUS
TERTIARY
T.D. 3568m
CIMM. UNC.
AGE (my)
200.0
100.0
0.0
0.0
DEPTH (m)
2000.0
4000.0
6000.0

Fig 4.2 (cont.)

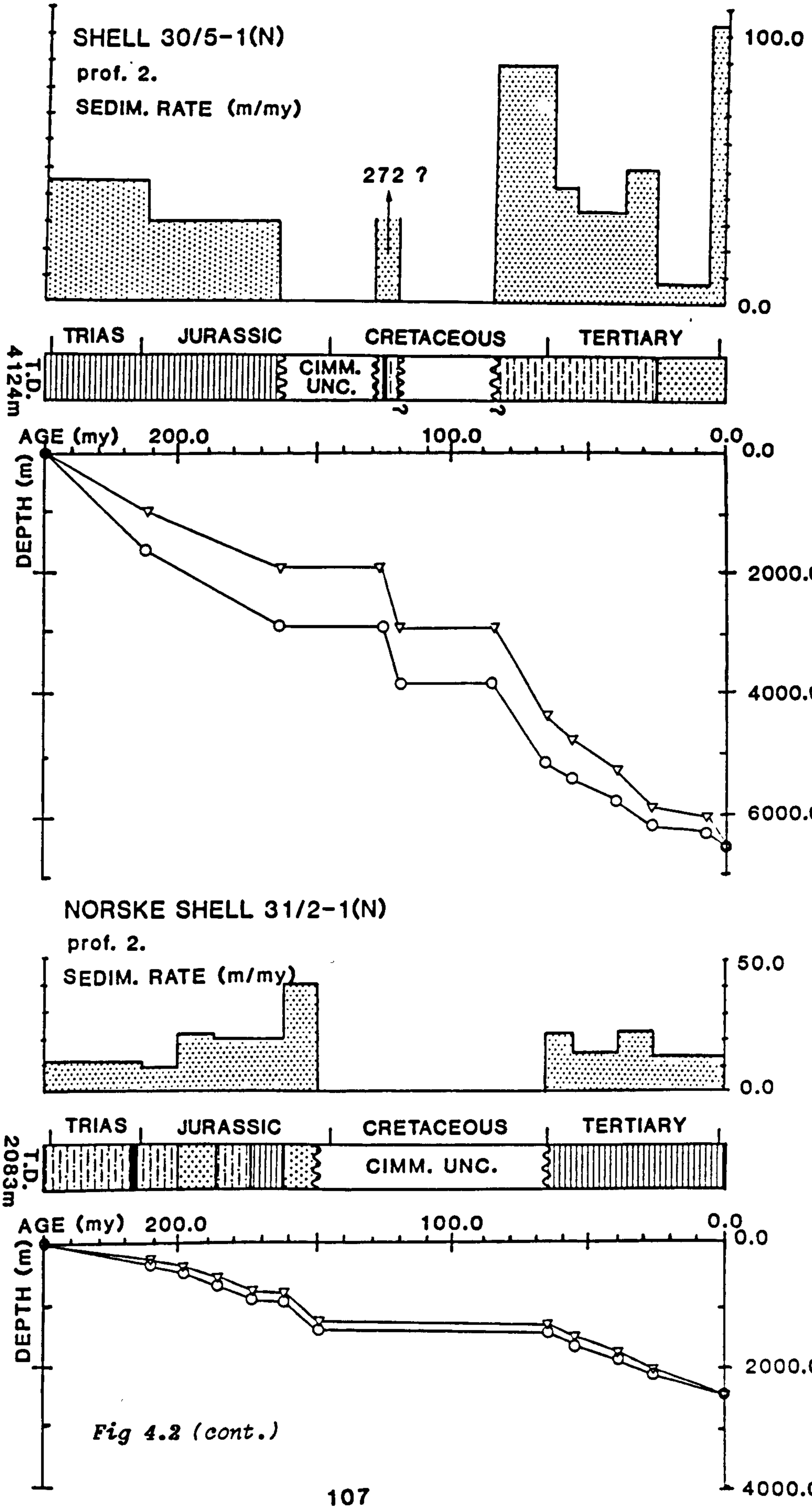
SHELL 30/5-1(N)
prof. 2.
SEDIM. RATE (m/my)
100.0
0.0
272 ?
TRIAS
JURASSIC
CRETACEOUS
TERTIARY
T.D. 4124m
CIMM. UNC.
AGE (my)
200.0
100.0
0.0
DEPTH (m)
0.0
2000.0
4000.0
6000.0
NORSKE SHELL 31/2-1(N)
prof. 2.
SEDIM. RATE (m/my)
50.0
0.0
TRIAS
JURASSIC
CRETACEOUS
TERTIARY
T.D. 2083m
CIMM. UNC.
AGE (my)
200.0
100.0
0.0
DEPTH (m)
0.0
2000.0
4000.0

Fig 4.2 (cont.)

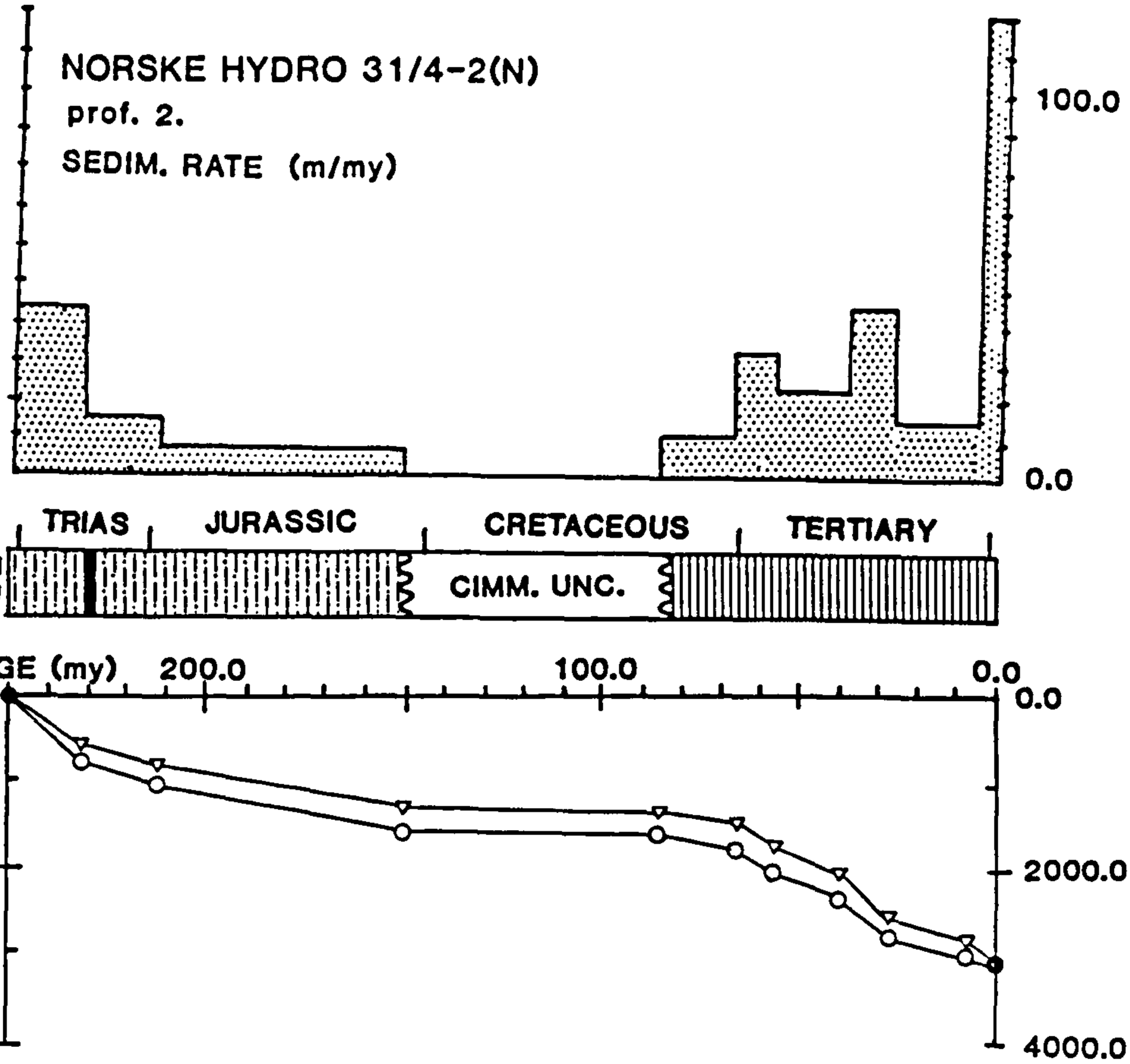
NORSKE HYDRO 31/4-2(N)
prof. 2.
SEDIM. RATE (m/my)
100.0
0.0
TRIAS
JURASSIC
CRETACEOUS
TERTIARY
T.D. 2580m
CIMM. UNC.
AGE (my)
200.0
100.0
0.0
DEPTH (m)
0.0
2000.0
4000.0

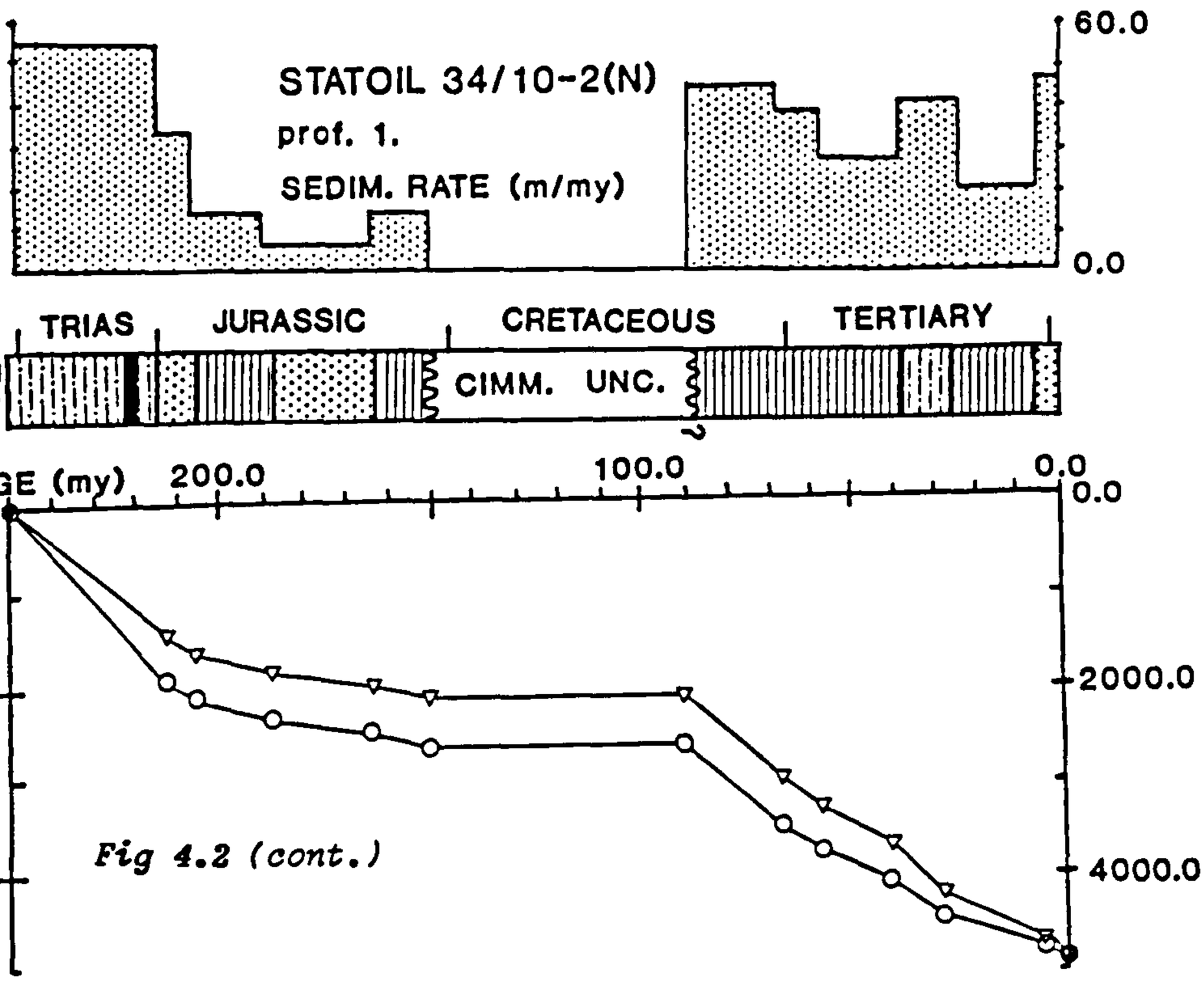
STATOIL 34/10-2(N)
prof. 1.
SEDIM. RATE (m/my)
60.0
0.0
TRIAS
JURASSIC
CRETACEOUS
TERTIARY
T.D. 3410m
CIMM. UNC.
AGE (my)
200.0
100.0
0.0
DEPTH (m)
0.0
2000.0
4000.0

Fig 4.2 (cont.)

4.3 Sedimentation Rates

The "decompacted subsidence" curve of the basement is a direct measurement of sediment accumulation, since changes in the sedimentation rates produce changes in gradient of the curve. In Figure 4.2 rapid sedimentation rate is shown by a steep gradient on the graphs, while very slow sedimentation is indicated by shallow gradient. The top of the diagram shows the same results plotted as a block diagram of sediment accumulation rate ("sedim. rate") for each time interval of individual wells.

Studying the regional presentation of the sedimentation rates (Fig. 4.3) several trends are observed, despite problems with the chronostratigraphy in some wells and can be summarized as follows:

No deposition or low sedimentation rate is observed during Triassic to Mid-Jurassic in wells on the flanks of the basin, eg. CONOCO 3/2-1. Wells in the centre of the basin however, eg. ESSO 15/6-2(N), indicate average sedimentation rate in the Triassic with a progressive decrease towards the Mid-Jurassic, (see also Fig. 4.1). This is due to the initial tectonic activity (Permo-Triassic event, Ziegler (1981)) and subsequent sediment supply, which were both concentrated mainly in the middle of the basin, (see also section 5.6).

Most wells reveal that the Mid-Jurassic to Mid-Cretaceous period was dominated by unconformities (see also section 5.4.5) or very slow sedimentation with a progressive increase towards Tertiary times.

The Paleocene displays a very distinctive peak in the sedimentation rate in the west side of the graben exceeding by two to three times the sedimentation rate in the east side. The above observation is associated with the East Shetland Platform uplift, (see also section 5.4.8).

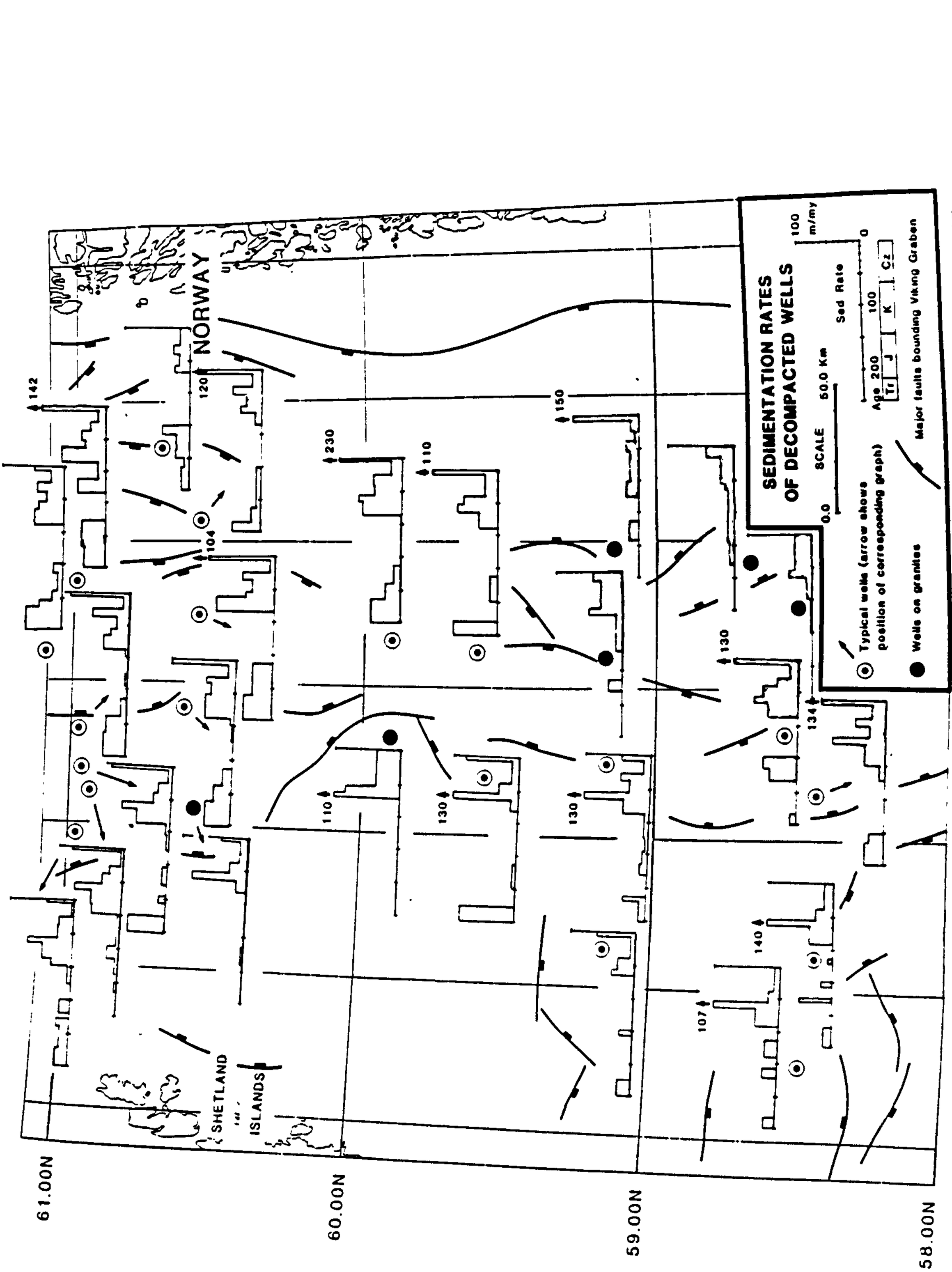

Fig 4.3 A regional presentation of the sedimentation rates in the northern North Sea since Triassic times .

A progressive decrease in the sediment supply results in very low sedimentation rates during Miocene times, but during Pliocene-Pleistocene times the highest rates of sedimentation are observed in the whole basin since Triassic. The sediment supply in the east side of the basin seems to be two to five times higher than in the west side. This event is associated with the Pliocene-Pleistocene glaciation period and subsequent erosion of Scandinavia which has mainly affected the east side of the basin, Cameron et al (1986).

Wells on granitic basement (see also Fig. 4.1), when the relevant information is available, display both the Paleocene and Pleiocene-Pleistocene distinctive peaks, but no deposition or low sedimentation rate since Mid-Jurassic approximately. None of them exhibit any deposition of sediments earlier than Mid-Jurassic. This is due to the buoyant effect of the granites (see also section 5.7).

4.4 Loading Correction

The accumulation of sediments in a basin constitutes a load on the lithosphere. The load is made up of the sediment load and water load. The sediment load results from the sediments deposited in the northern North Sea since Top Permian times, while the water load results from changes in the depth of deposition within the basin.

Assuming that the lithosphere has lateral strength it will respond not only to the load above but also to the surrounding load. The flexural rigidity of the lithosphere is governed by the elastic thickness (T_e) of the plate. If the lithosphere has no lateral strength and a zero elastic thickness it will only respond to the load immediately above it, achieving equilibrium by the displacement of a weak fluid asthenosphere. This is known as Airy or local compensation.

The isostasy curves of Fig. 2.5 suggest that basement subsidence and sediment loading have been largely accommodated by local Airy type isostatic equilibration (section 2.10). Barton and Wood (1984) came to the same conclusion studying the subsidence of the Central Graben. Therefore, the effect of loading within the continental lithosphere is examined assuming local loading only. In order to calculate this effect it is necessary to know (a) the water depth at the time of deposition (Paleobathymetry) and (b) the densities of individual sedimentary layers.

4.4.1 Paleobathymetry

The water depth at the time of deposition was taken from the Completion Reports for individual UK wells. This information is derived from paleontological and lithological core studies. Such information was not available for Norwegian wells. In this case, the Viking Graben was considered to be a 2-D symmetrical structure along its N-S axis (deepest part) and all the paleobathymetry information from the UK sector was extrapolated to the Norwegian sector. Barton and Wood (1984) have also extrapolated the paleobathymetry of the Viking Graben from the study of 19 wells in the Central and Witchground Grabens. My results were combined with those of Barton and Wood (1984) and the paleogeographic maps of Ziegler (1981) to produce the paleobathymetry at given times shown in Fig. 4.4 plotted against the chronostratigraphic column for each well. According to this figure the following generalisations can be made regarding the paleobathymetry of individual periods.

Triassic

The sediments appear to have been deposited under shallow water conditions, average depth inner - middle neritic (0-100m). The absence of marine organisms suggests a fluvio-lacustrine environment. A sedimentary model outlined by Clemmensen et al (1980) is compatible with these observations. They suggest marginal alluvial fans, feeding through branded streams and

stabilised distributary channels into a central, northwards draining elongated basin or coalescing series of basins, which would have included lacustrine and sabkha environments.

Jurassic

Lower and Middle Jurassic predominently consists of strata deposited in middle to outer neritic (30-200m) environments. Their boundary is variable, commonly an unconformity but of different magnitude in different parts of the northern North Sea. Upper Jurassic strata are marine throughout deposited in outer neritic to mid-upper bathyal (100-400m) environment.

Cretaceous

The Jurassic-Cretaceous boundary is an unconformity (late Cimmerian) throughout the basin, and is examined in detail in section 5.4.5. Early Cretaceous is characterised by tectonically controlled sedimentation with extensive areas of land. Late Cretaceous, on the contrary, is dominated by a regional subsidence centred over the axial graben system and much quieter fully marine conditions of average depth 200-600m (upper bathyal).

Tertiary

The paleobathymetry of Early Tertiary continues the pattern observed in Late Cretaceous (upper bathyal). Towards recent times the water depth decreases progressively to outer neritic (100-200m) which is approximately the depth of deposition observed today.

4.4.2 Density of a sedimentary layer

The compaction model assumes that the sediments are made up of a matrix of grains, with a density ρ_{sg} peculiar to each lithology (see Table 4.1), with the interconnected pore spaces filled with water of density ρ_w. Therefore, following Sclater and Christie (1980) the sediment density of a layer ρ_s, can be related to the mean porosity of a layer f by

$$\rho_s = f\rho_w + (1-f)\rho_{sg}$$

Therefore, the mean sediment density of the total column $\bar{\rho}_s$ is given by

$$\bar{\rho}_s = \frac{\Sigma_i[\bar{f}_i\rho_w + (1 + \bar{f}_i)\rho_{sgi}]z_i}{S}$$

where $\bar{f}_i$ is the mean porosity of the ith layer, ρ_{sgi} the sediment grain density of the same layer, z_i the individual layer thickness, and S the total thickness of the column corrected for compaction. The loading effect of the sedimentary column for each time interval can then be calculated using ρ_s and S. This procedure is discussed in the next section.

4.4.3 Local loading estimation

The load on the plate is treated as a series of point loads each compensated independently from the others. Isostatic equilibrium is maintained so that an increase in sediment load is compensated by displacement of mantle material.

According to Steckler and Watts (1978) the depression of the basement Y caused by the sediment and water load is

$$Y = S\frac{(\rho_m - \rho_s)}{(\rho_m - \rho_w)} + WD$$

where Y is the actual depth of the basement, S the decompacted thickness of sediment, ρ_s the mean sediment density, ρ_m the density of mantle (3.33 g/cc), ρ_w the density of water and WD the water depth during the time of burial.

Using the paleobathymetric, lithologic and stratigraphic information obtained from the wells, the sediments were backstripped and unloaded to find the water filled basement level (Y) relative to the present day sea level assuming Airy-local compensation, see Fig. 4.4.

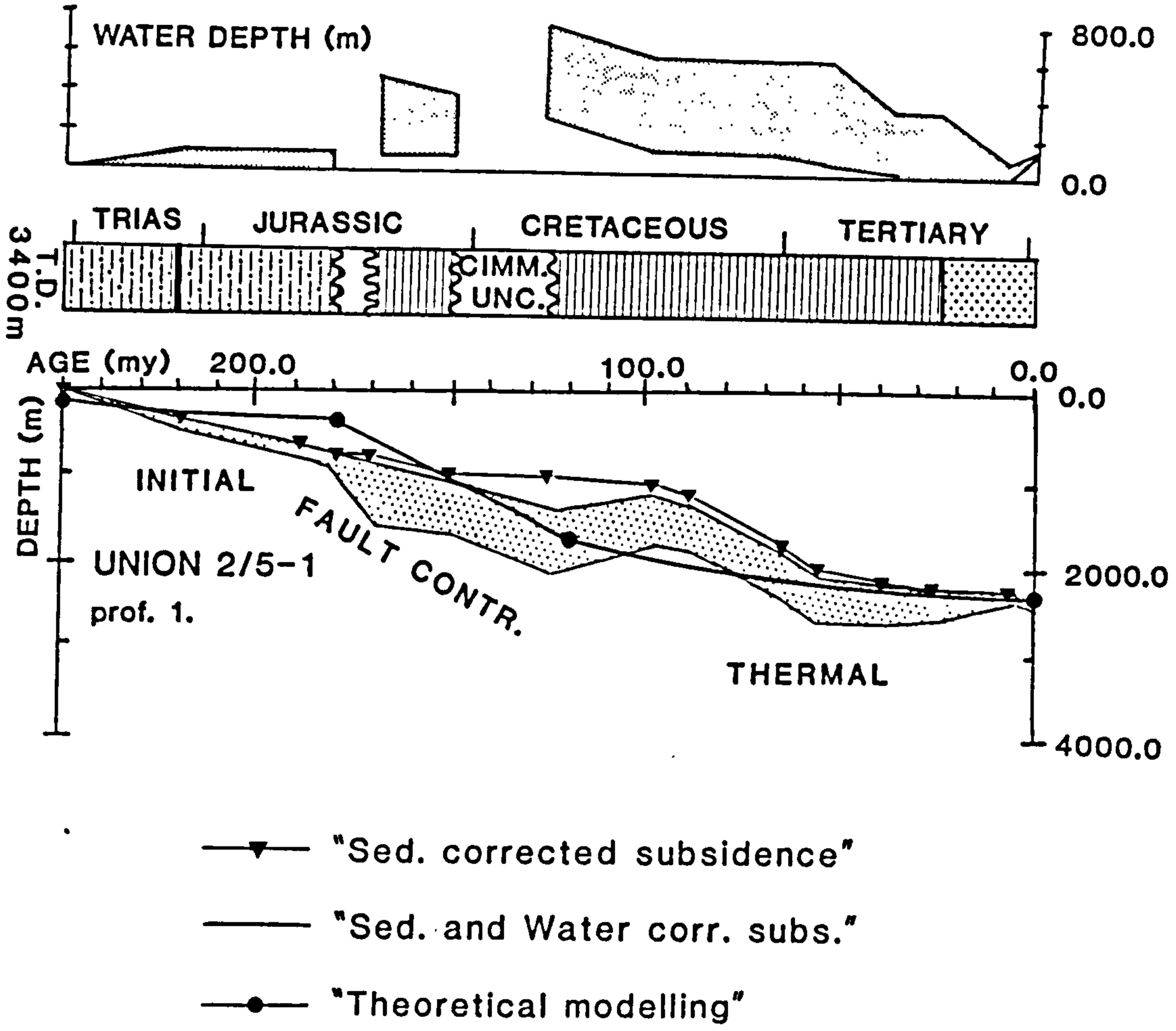

Fig 4.4 The effect of unloading the basement using well data. "Water depth" refers to the depth of deposition (paleobathymetry). "Sed. corrected subsidence" indicates subsidence corrected for compaction and sediment load only. "Sed. and Water corr. subs." represents the totally corrected subsidence taking into account the depth of deposition. The shaded area exhibits the uncertainties in the totally corrected subsidence due to ambiguities in paleobathymetry. "Theoretical modelling" represents the predicted subsidence (see section 5.2). Chronostratigraphy, ages, total depth (T.D.) as in Fig. 4.2.

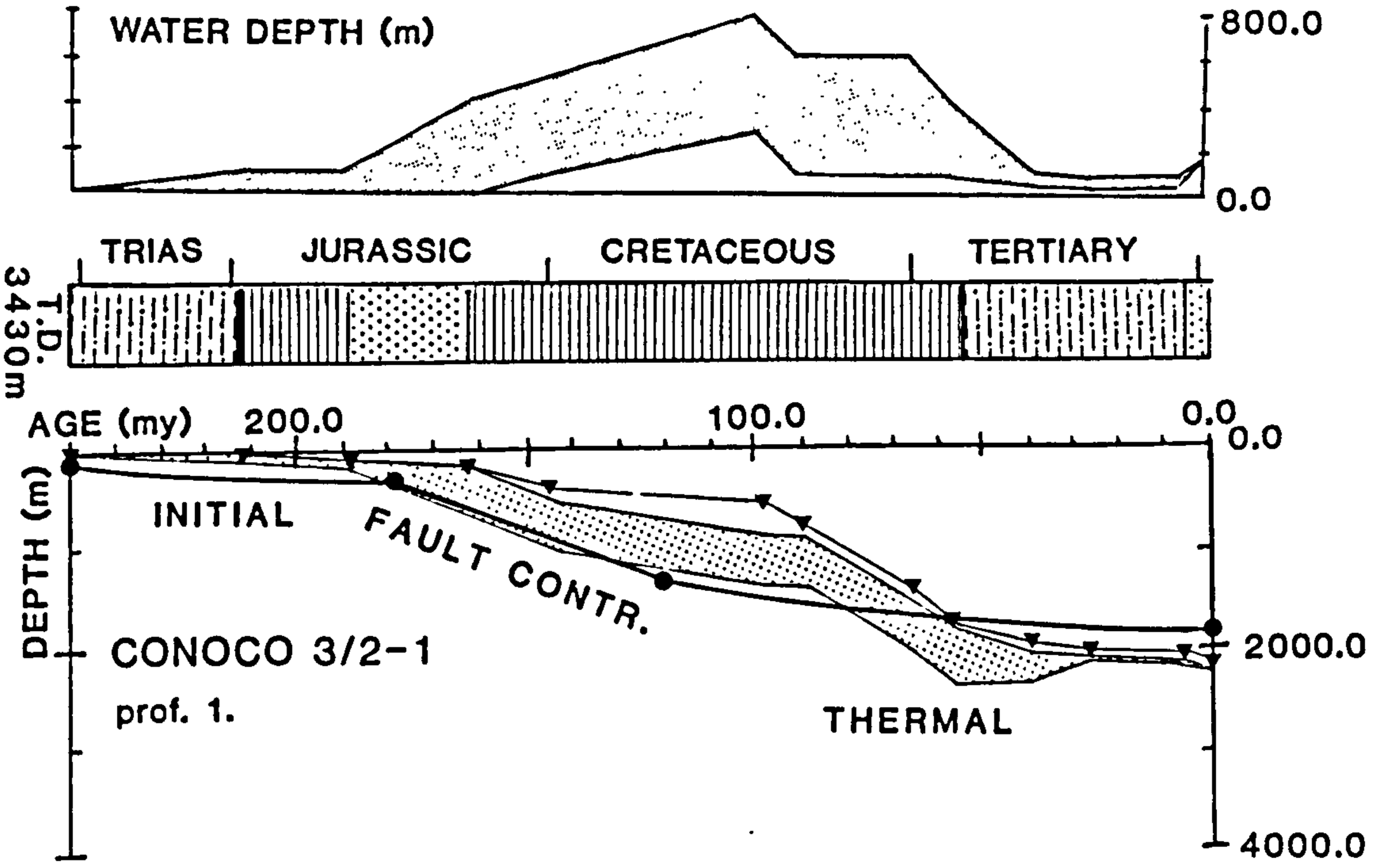
WATER DEPTH (m)
800.0
0.0
TRIAS
JURASSIC
CRETACEOUS
TERTIARY
T.D.
3430 m
AGE (my)
200.0
100.0
0.0
0.0
DEPTH (m)
INITIAL
FAULT CONTR.
CONOCO 3/2-1
prof. 1.
THERMAL
2000.0
4000.0

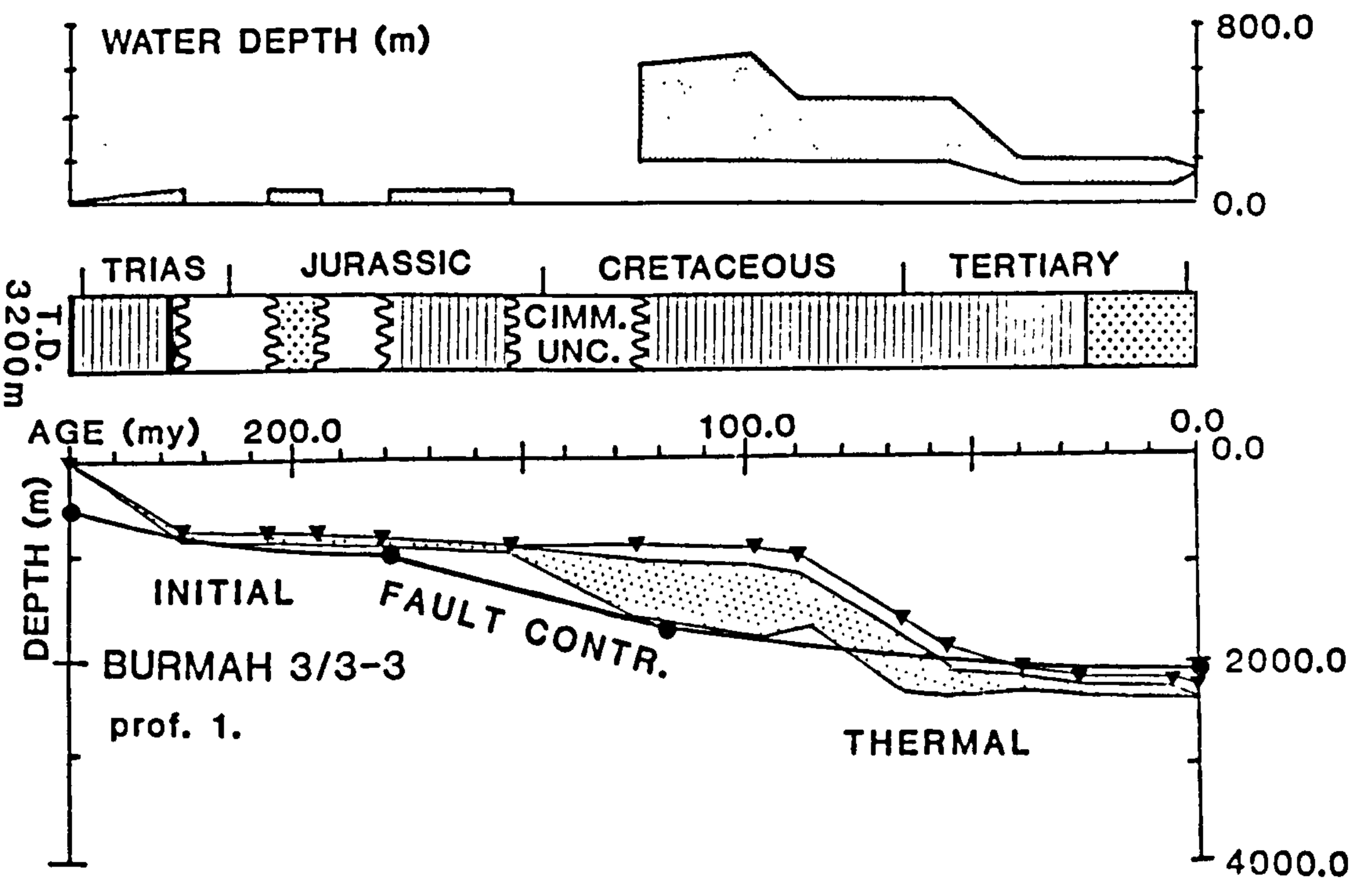
WATER DEPTH (m)
800.0
0.0
TRIAS
JURASSIC
CRETACEOUS
TERTIARY
CIMM.
UNC.
T.D.
3200 m
AGE (my)
200.0
100.0
0.0
0.0
DEPTH (m)
INITIAL
FAULT CONTR.
BURMAH 3/3-3
prof. 1.
THERMAL
2000.0
4000.0

Fig 4.4 (cont.)

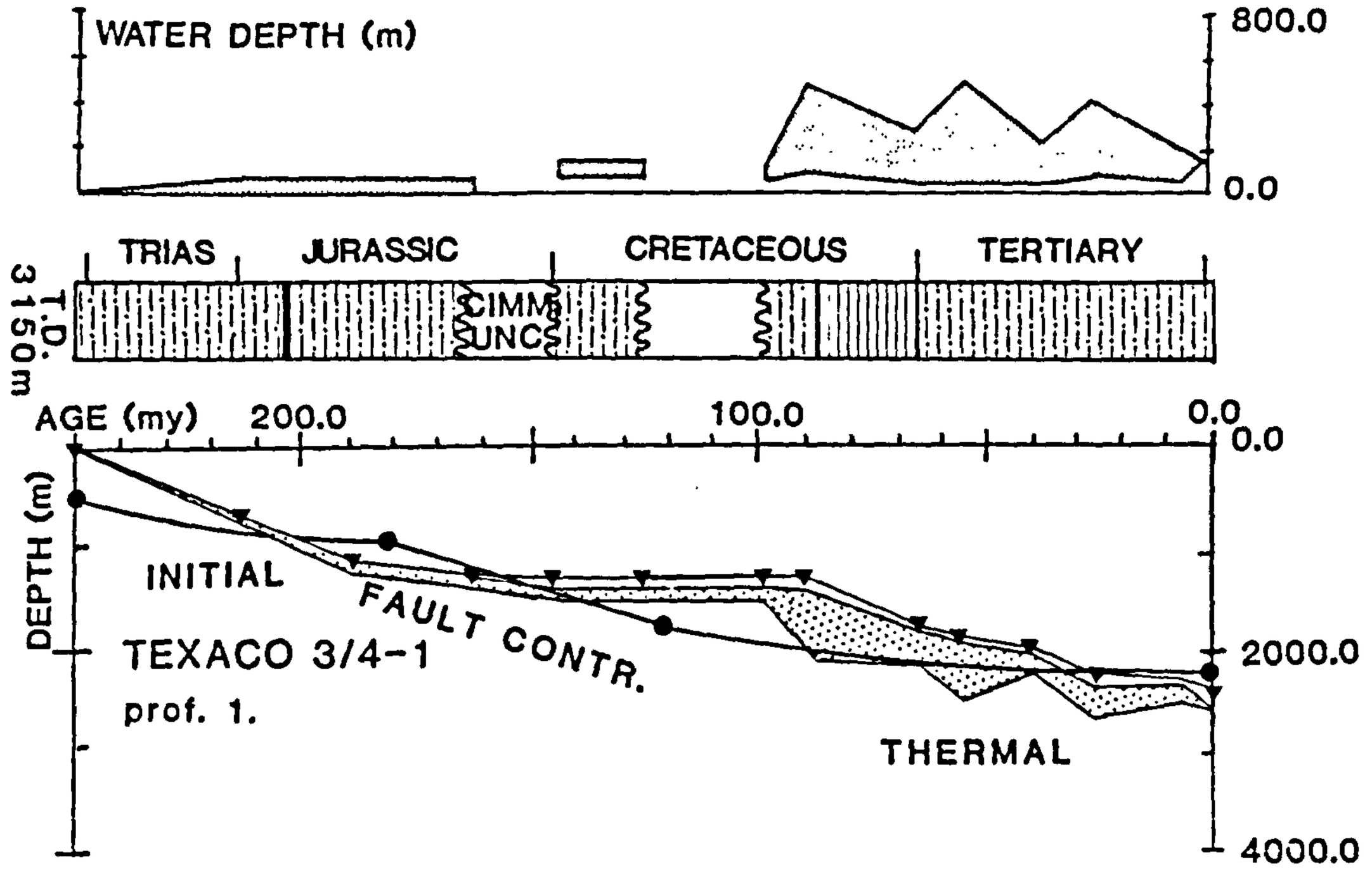
WATER DEPTH (m)
800.0
0.0
TRIAS
JURASSIC
CRETACEOUS
TERTIARY
T.D.
3150m
CIMM.
UNC.
AGE (my)
200.0
100.0
0.0
DEPTH (m)
INITIAL
FAULT CONTR.
TEXACO 3/4-1
prof. 1.
THERMAL
2000.0
4000.0

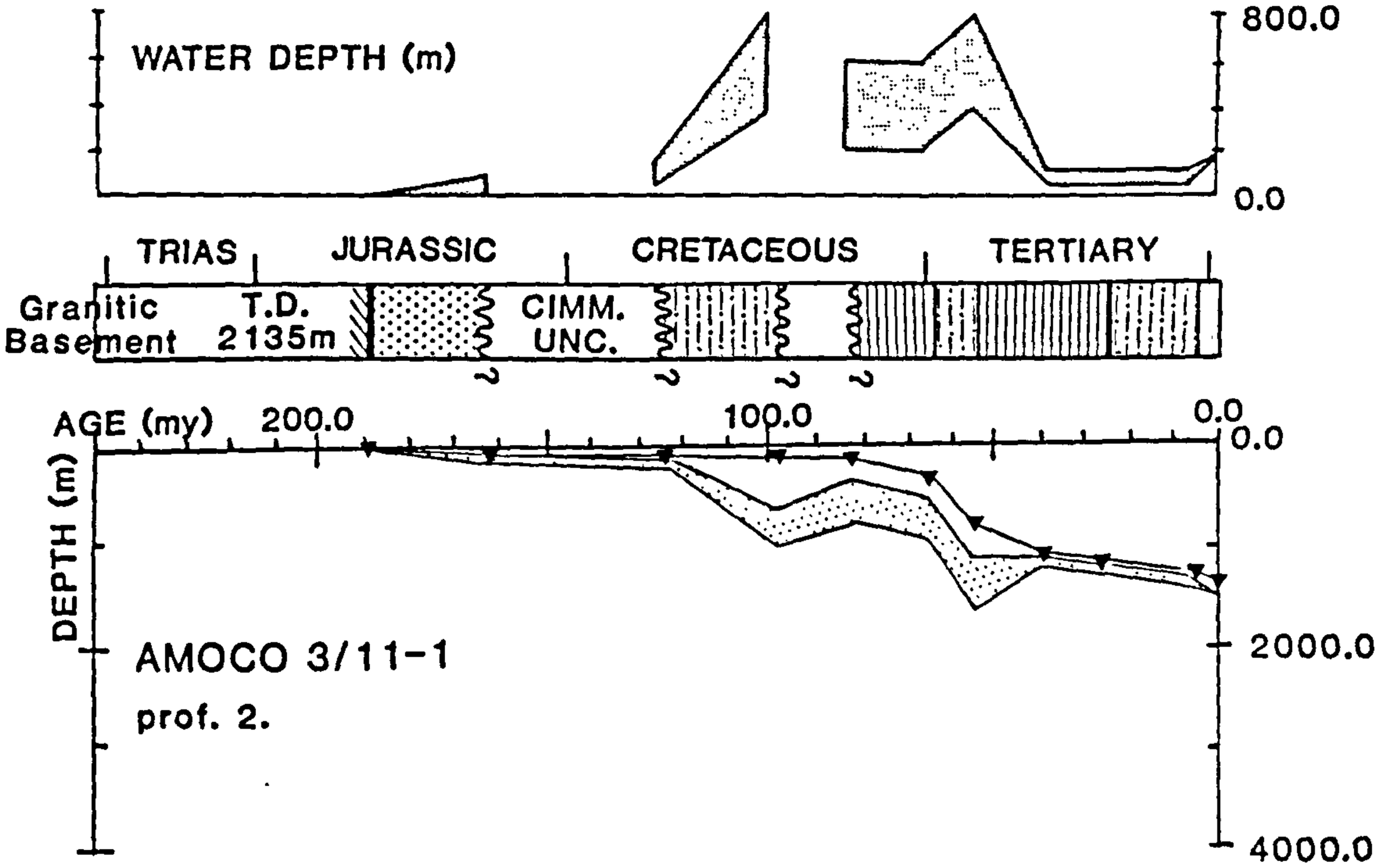
WATER DEPTH (m)
800.0
0.0
TRIAS
JURASSIC
CRETACEOUS
TERTIARY
Granitic
Basement
T.D.
2135m
CIMM.
UNC.
AGE (my)
200.0
100.0
0.0
DEPTH (m)
AMOCO 3/11-1
prof. 2.
2000.0
4000.0

Fig 4.4 (cont.)

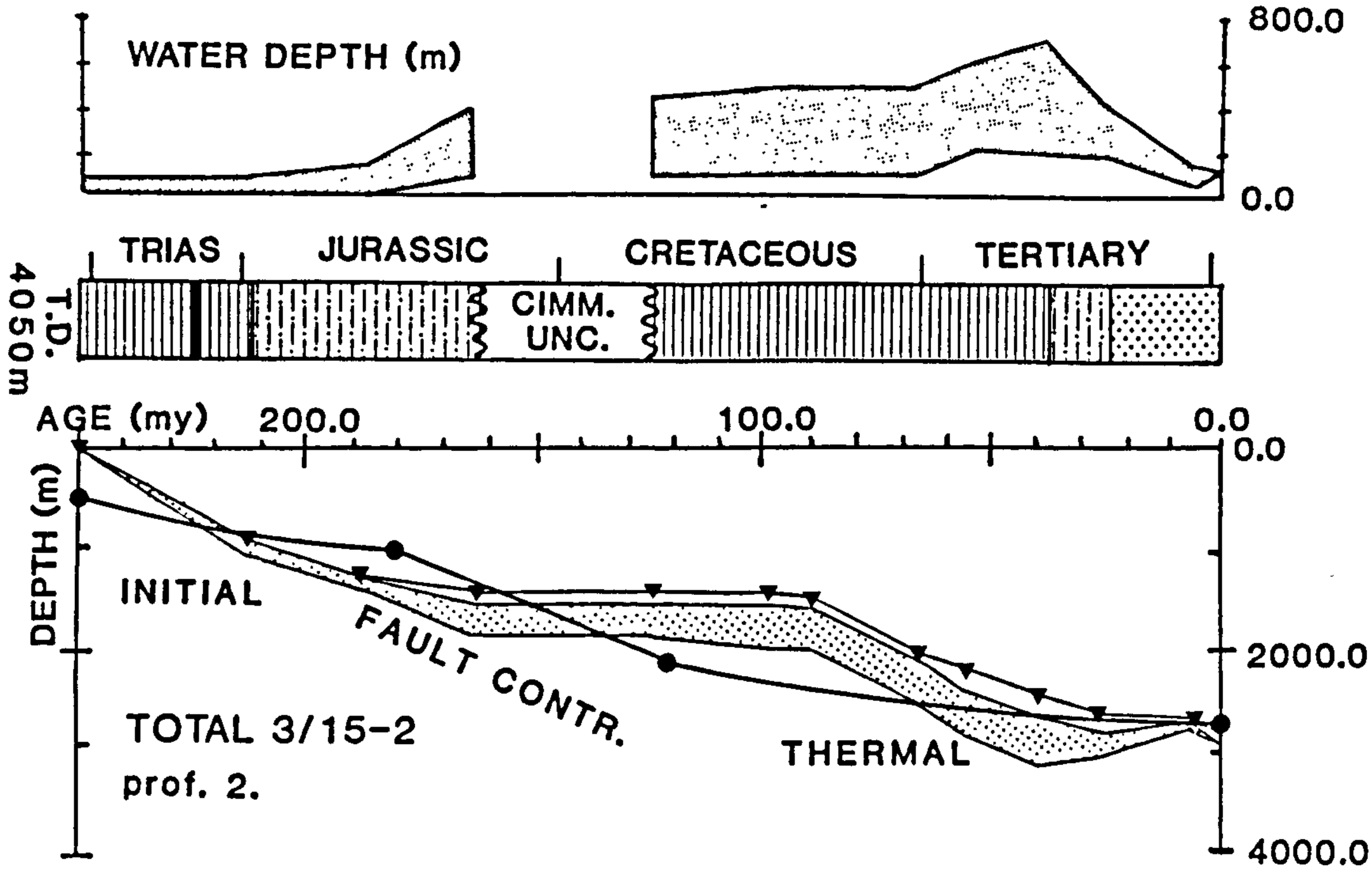
WATER DEPTH (m)
800.0
0.0
TRIAS
JURASSIC
CRETACEOUS
TERTIARY
T.D. 4050 m
CIMM. UNC.
AGE (my)
200.0
100.0
0.0
DEPTH (m)
INITIAL
FAULT CONTR.
THERMAL
TOTAL 3/15-2
prof. 2.
2000.0
4000.0

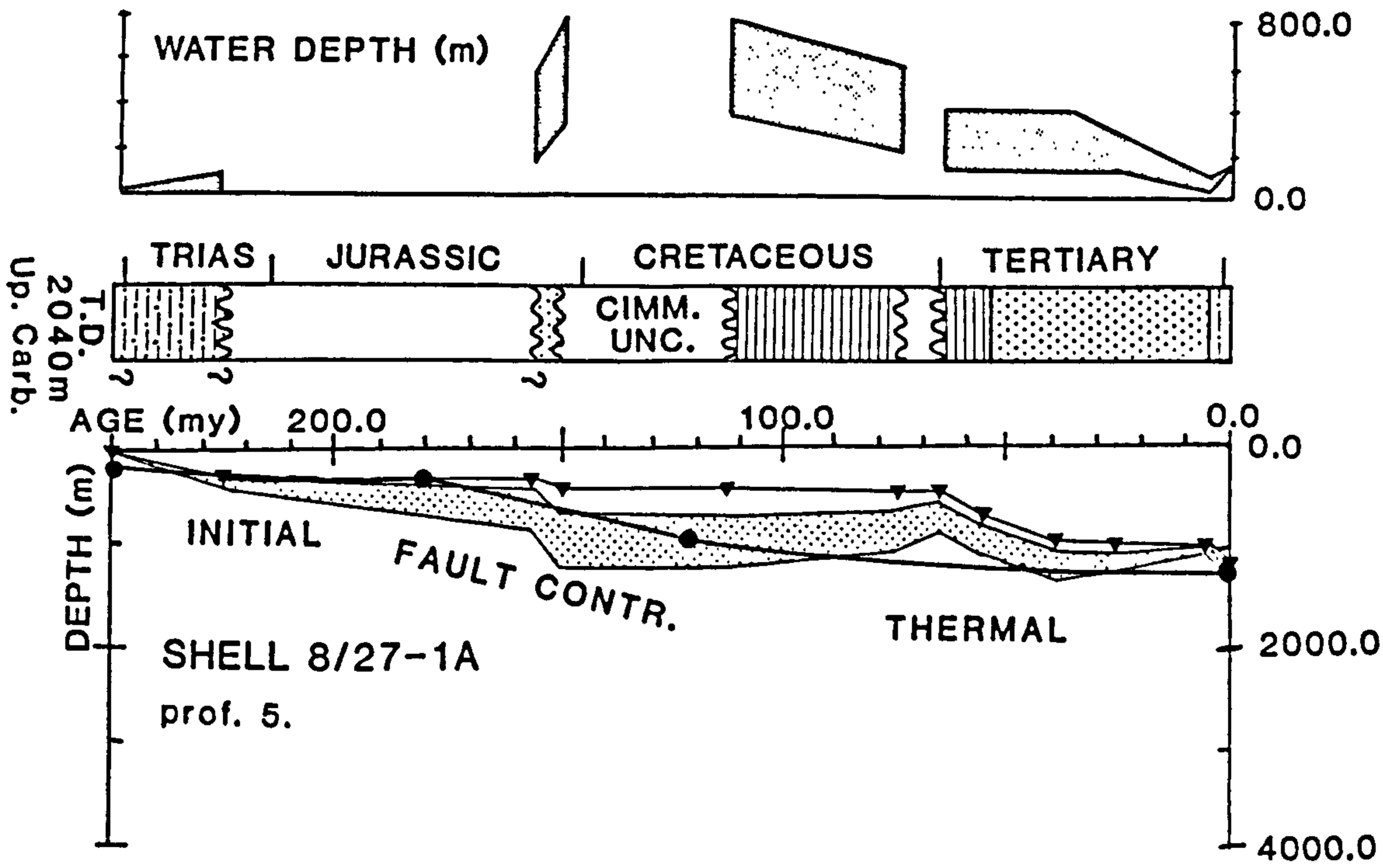
WATER DEPTH (m)
800.0
0.0
TRIAS
JURASSIC
CRETACEOUS
TERTIARY
T.D. 2040m Up. Carb.
CIMM. UNC.
AGE (my)
200.0
100.0
0.0
DEPTH (m)
INITIAL
FAULT CONTR.
THERMAL
SHELL 8/27-1A
prof. 5.
2000.0
4000.0

Fig 4.4 (cont.)

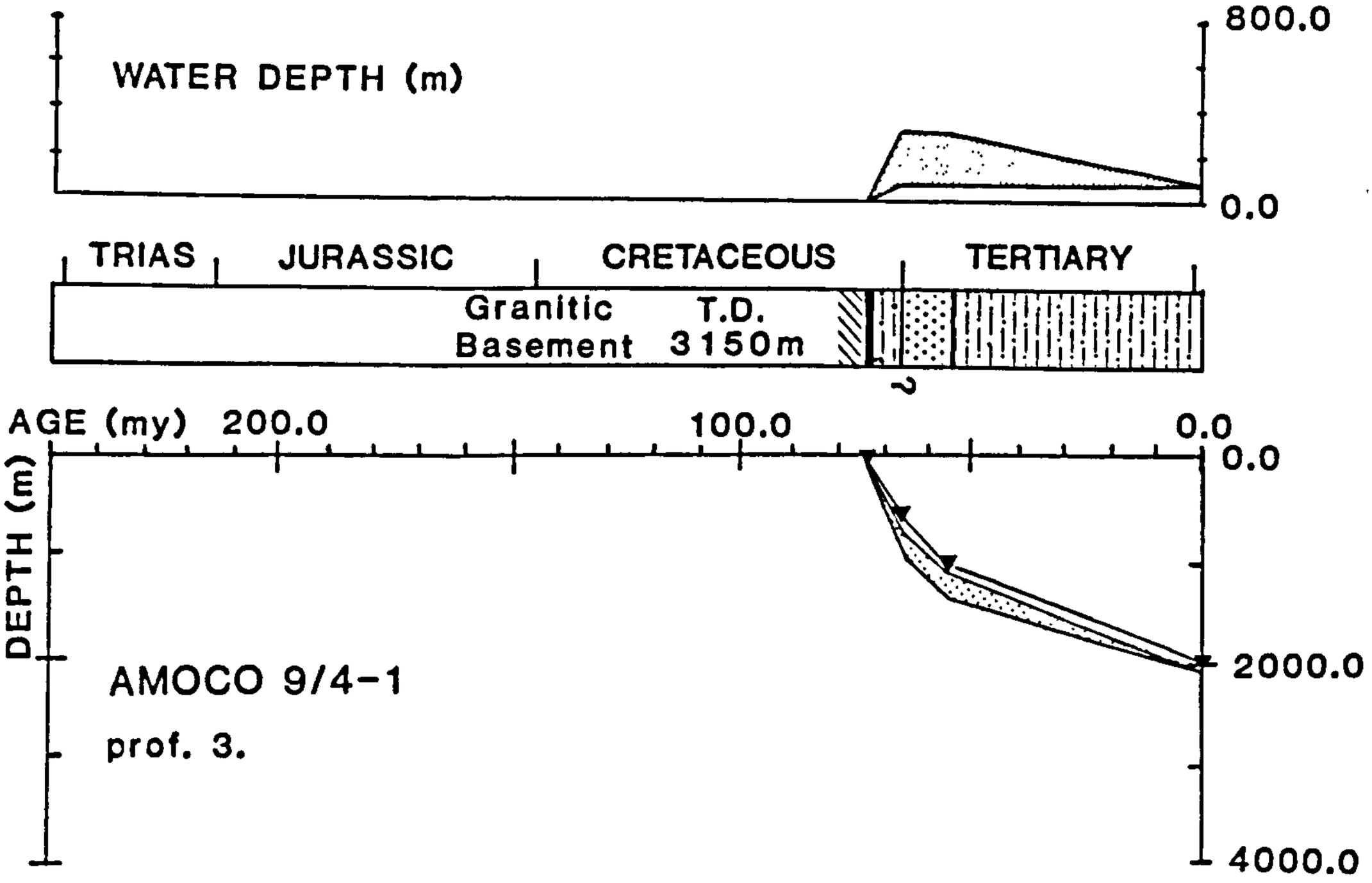
WATER DEPTH (m)
800.0
0.0
TRIAS
JURASSIC
CRETACEOUS
TERTIARY
Granitic Basement
T.D. 3150m
?
AGE (my) 200.0
100.0
0.0
DEPTH (m)
0.0
2000.0
4000.0
AMOCO 9/4-1
prof. 3.

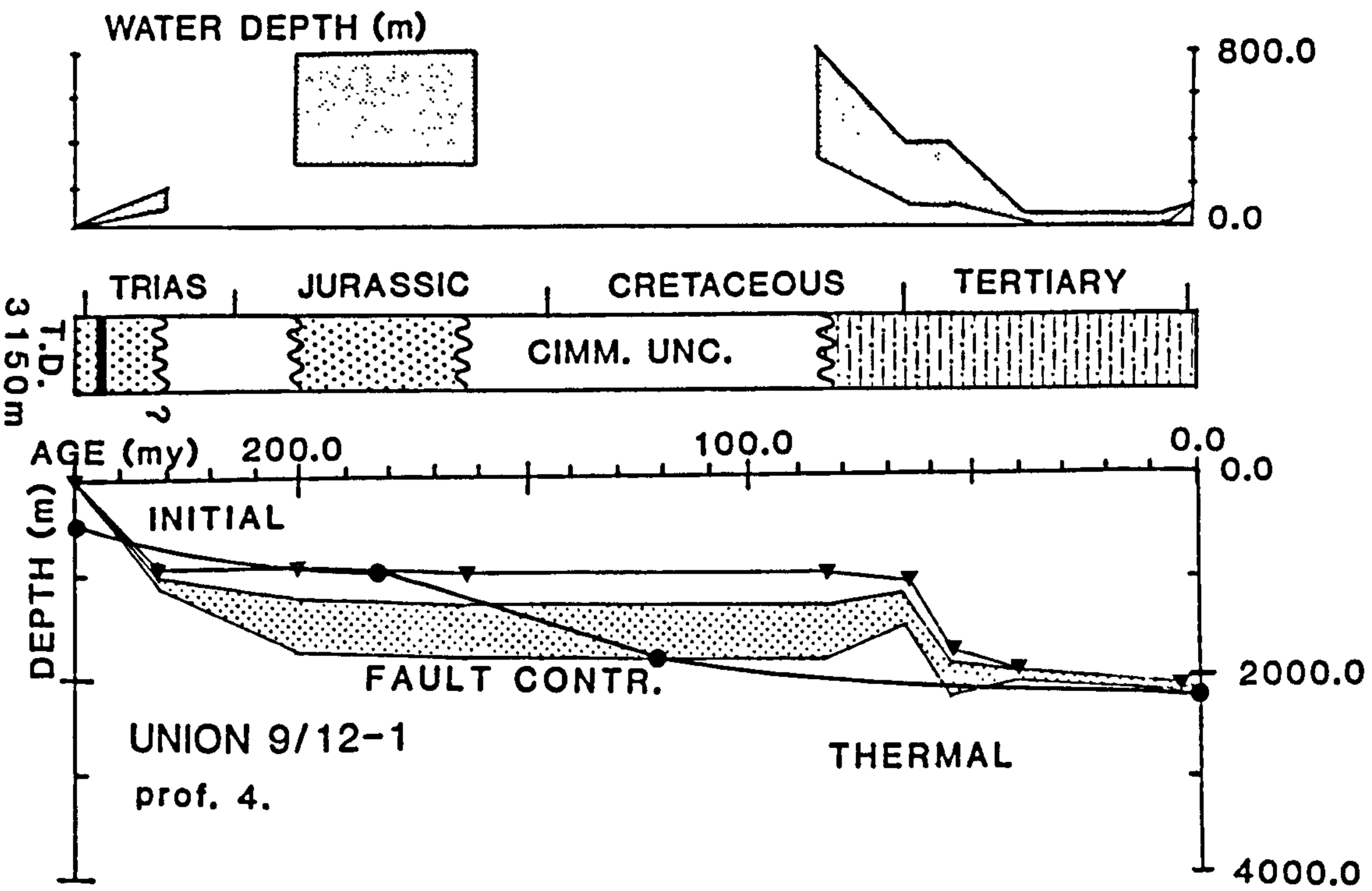
WATER DEPTH (m)
800.0
0.0
TRIAS
JURASSIC
CRETACEOUS
TERTIARY
T.D. 3150m
?
CIMM. UNC.
AGE (my) 200.0
100.0
0.0
DEPTH (m)
0.0
INITIAL
FAULT CONTR.
THERMAL
2000.0
4000.0
UNION 9/12-1
prof. 4.

Fig 4.4 (cont.)

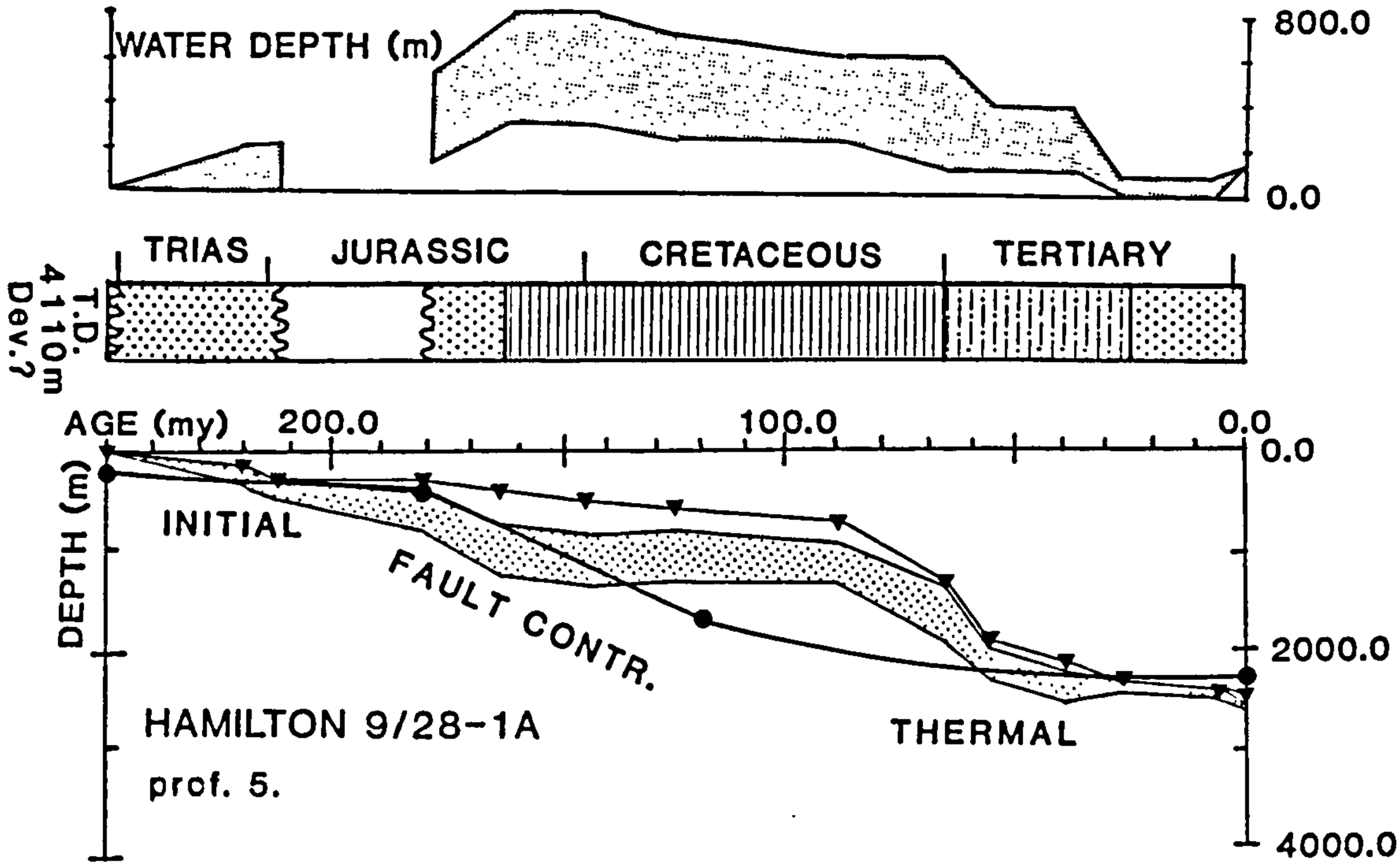
WATER DEPTH (m)
800.0
0.0
TRIAS
JURASSIC
CRETACEOUS
TERTIARY
T.D.
4110m
Dev.?
AGE (my)
200.0
100.0
0.0
DEPTH (m)
INITIAL
FAULT CONTR.
THERMAL
2000.0
4000.0
HAMILTON 9/28-1A
prof. 5.

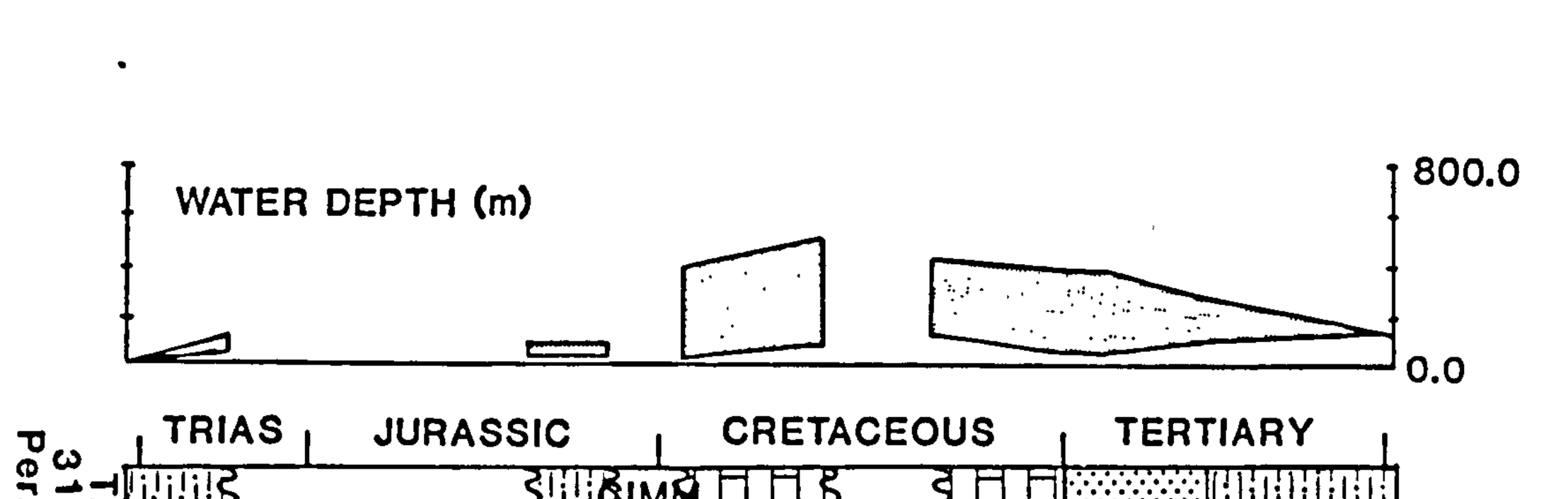
WATER DEPTH (m)
800.0
0.0
TRIAS
JURASSIC
CRETACEOUS
TERTIARY
T.D.
3150m
Permian ?
AGE (my)
200.0
100.0
0.0
DEPTH (m)
INITIAL
FAULT CONTR.
THERMAL
2000.0
4000.0
OXY 14/18-1
prof. 6.

Fig 4.4 (cont.)

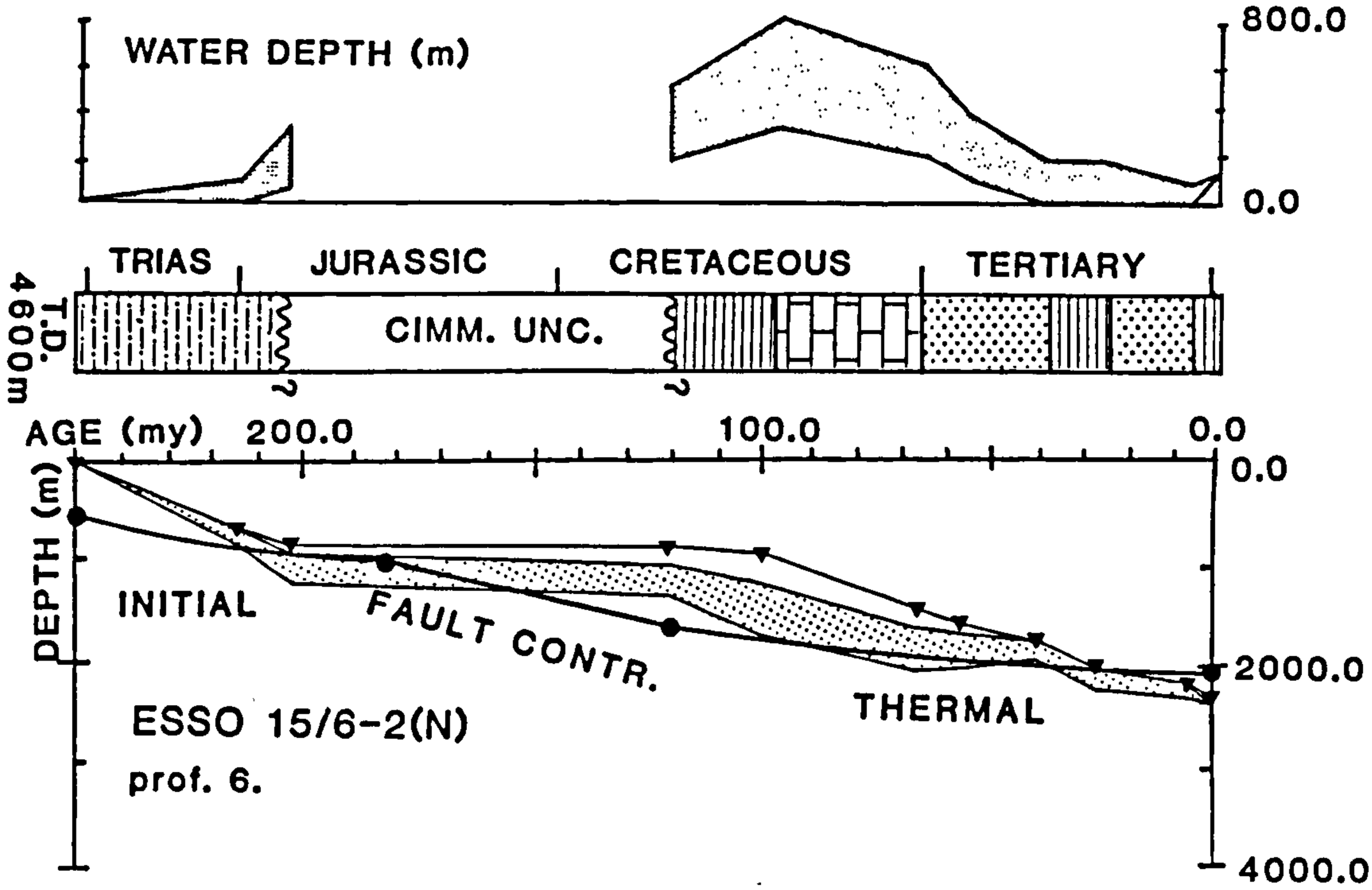
WATER DEPTH (m)
800.0
0.0
TRIAS
JURASSIC
CRETACEOUS
TERTIARY
T.D. 4800m
CIMM. UNC.
AGE (my)
200.0
100.0
0.0
DEPTH (m)
INITIAL
FAULT CONTR.
THERMAL
2000.0
4000.0
ESSO 15/6-2(N)
prof. 6.

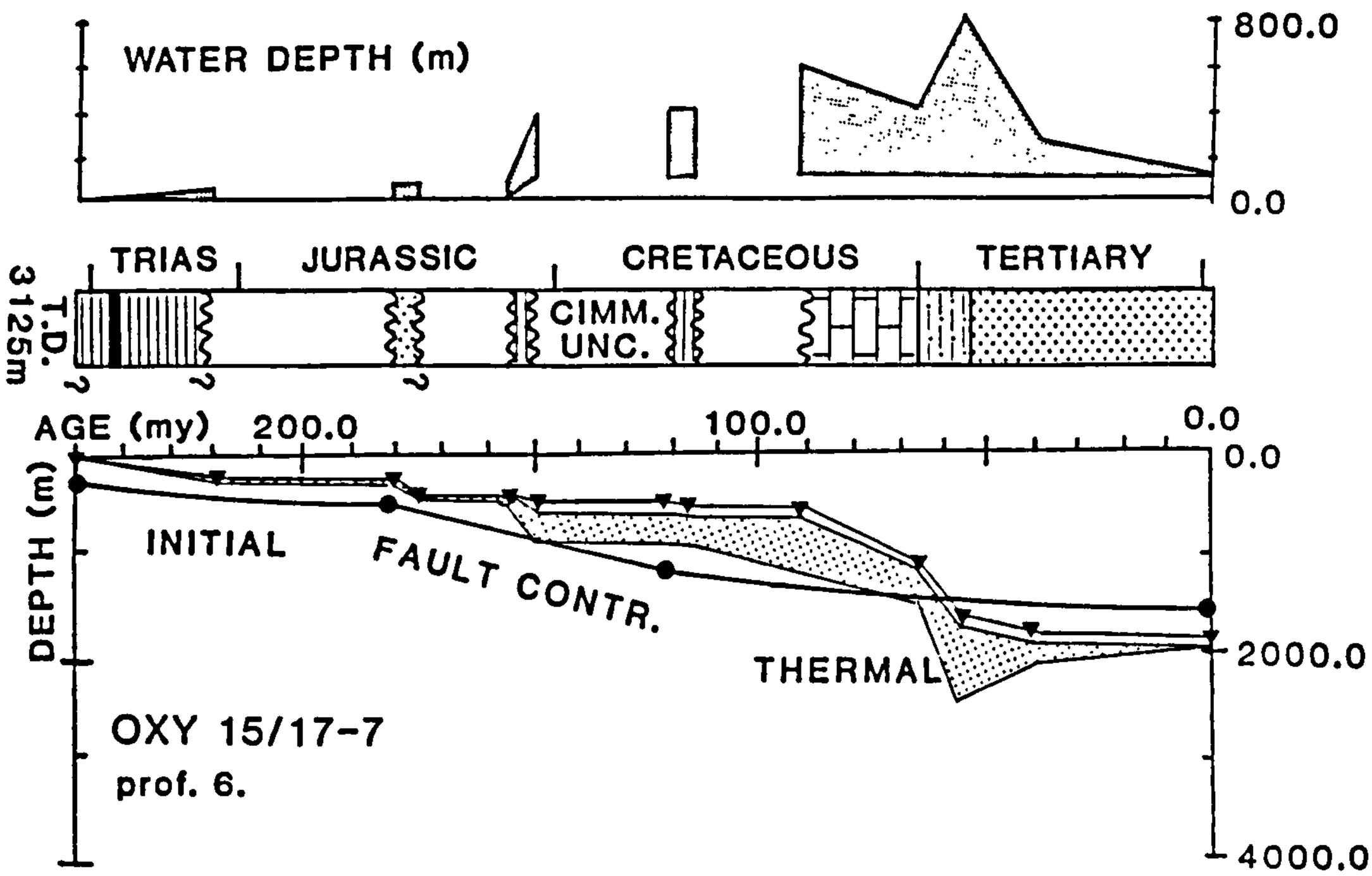
WATER DEPTH (m)
800.0
0.0
TRIAS
JURASSIC
CRETACEOUS
TERTIARY
T.D. 3125m
CIMM. UNC.
AGE (my)
200.0
100.0
0.0
DEPTH (m)
INITIAL
FAULT CONTR.
THERMAL
2000.0
4000.0
OXY 15/17-7
prof. 6.

Fig 4.4 (cont.)

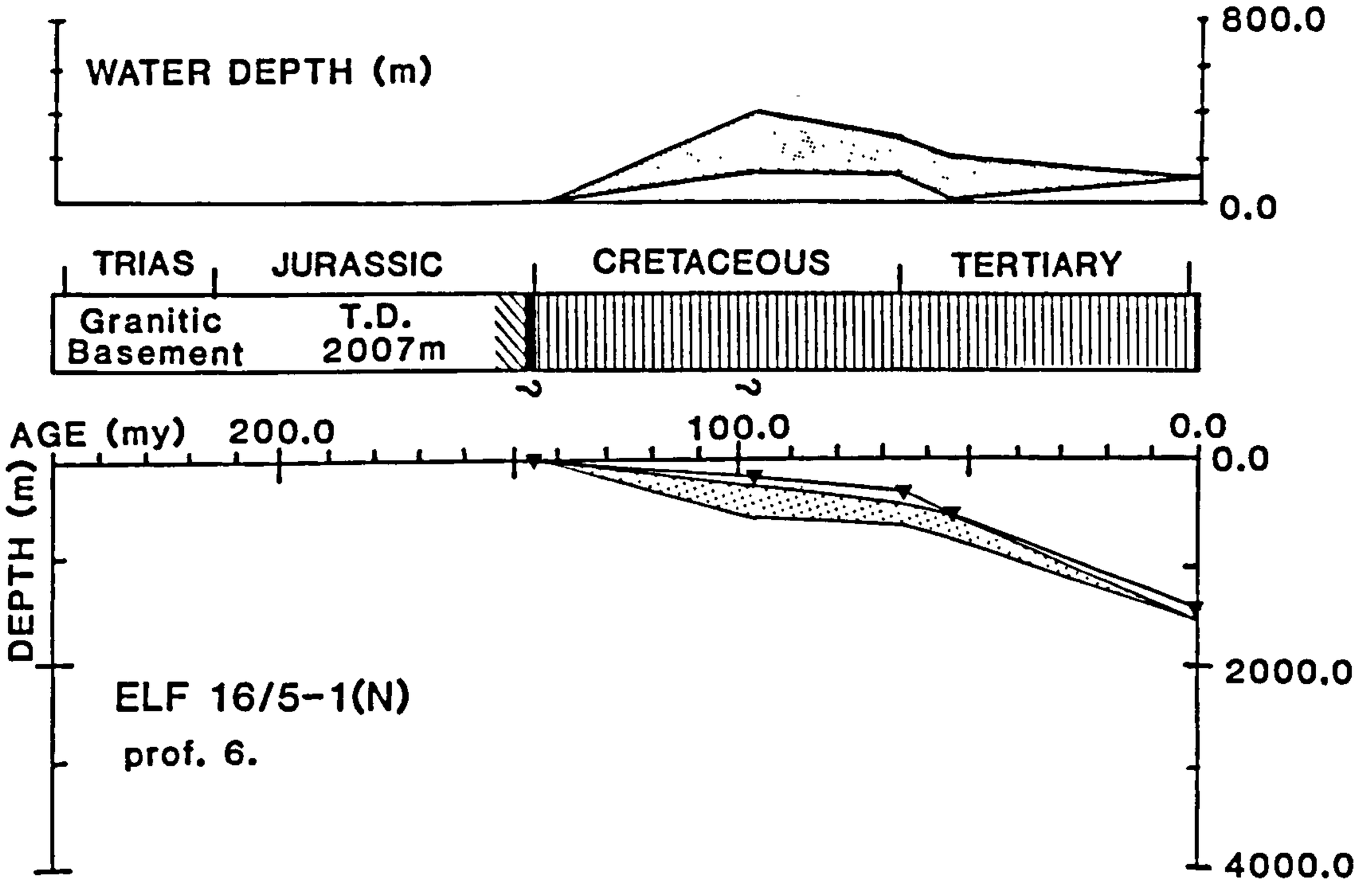
WATER DEPTH (m)
800.0
0.0
TRIAS
JURASSIC
CRETACEOUS
TERTIARY
Granitic Basement
T.D. 2007m
AGE (my)
200.0
100.0
0.0
DEPTH (m)
0.0
2000.0
4000.0
ELF 16/5-1(N)
prof. 6.

WATER DEPTH (m)
800.0
0.0
TRIAS
JURASSIC
CRETACEOUS
TERTIARY
Granitic Basement
T.D. 1930m
AGE (my)
200.0
100.0
0.0
DEPTH (m)
0.0
2000.0
4000.0
ELF 16/6-1(N)
prof. 6.

Fig 4.4 (cont.)

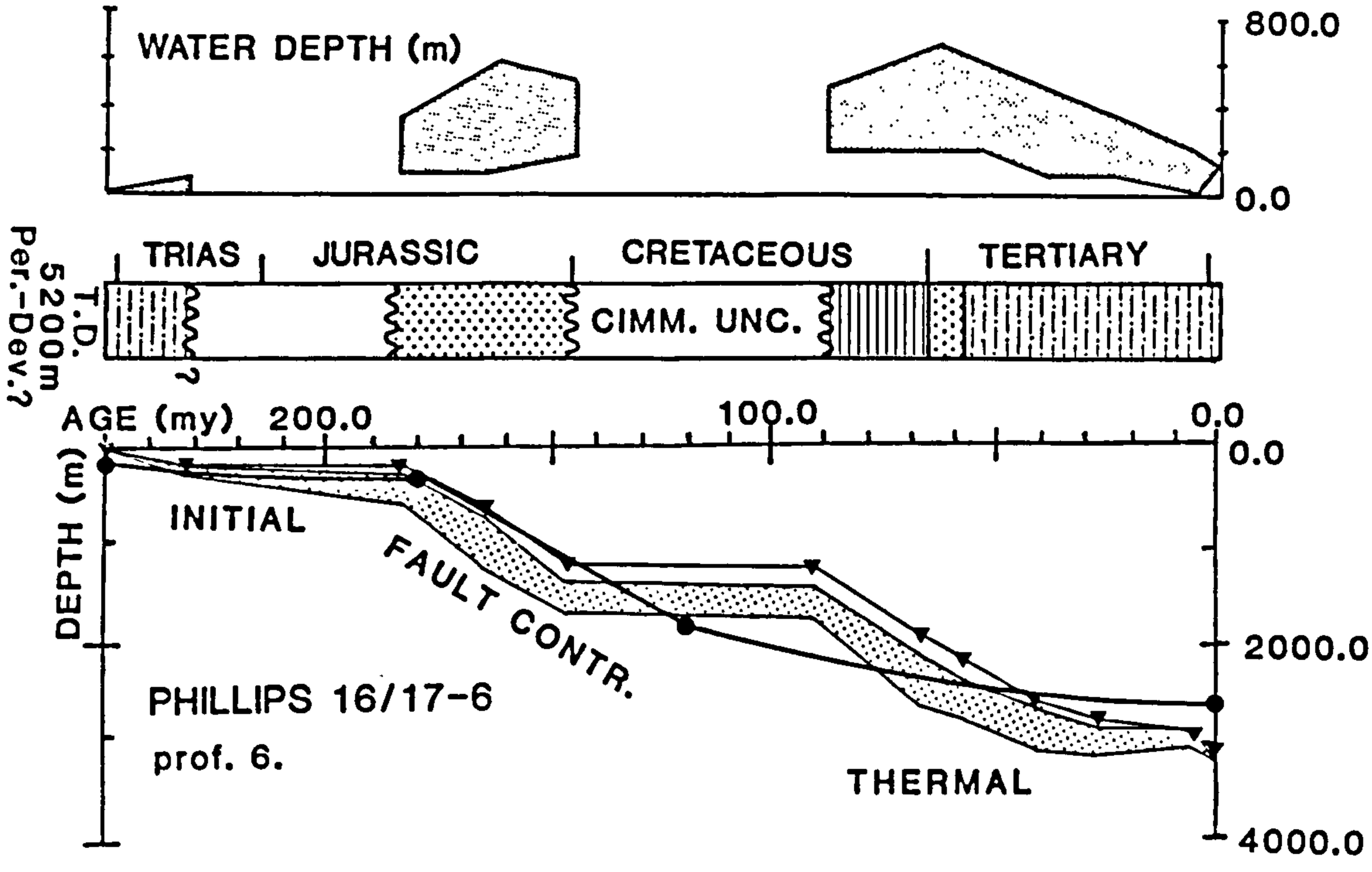
WATER DEPTH (m)
800.0
0.0
TRIAS
JURASSIC
CRETACEOUS
TERTIARY
T.D. 5200m Per.-Dev.?
?
CIMM. UNC.
AGE (my) 200.0
100.0
0.0
DEPTH (m)
0.0
INITIAL
FAULT CONTR.
2000.0
PHILLIPS 16/17-6
prof. 6.
THERMAL
4000.0

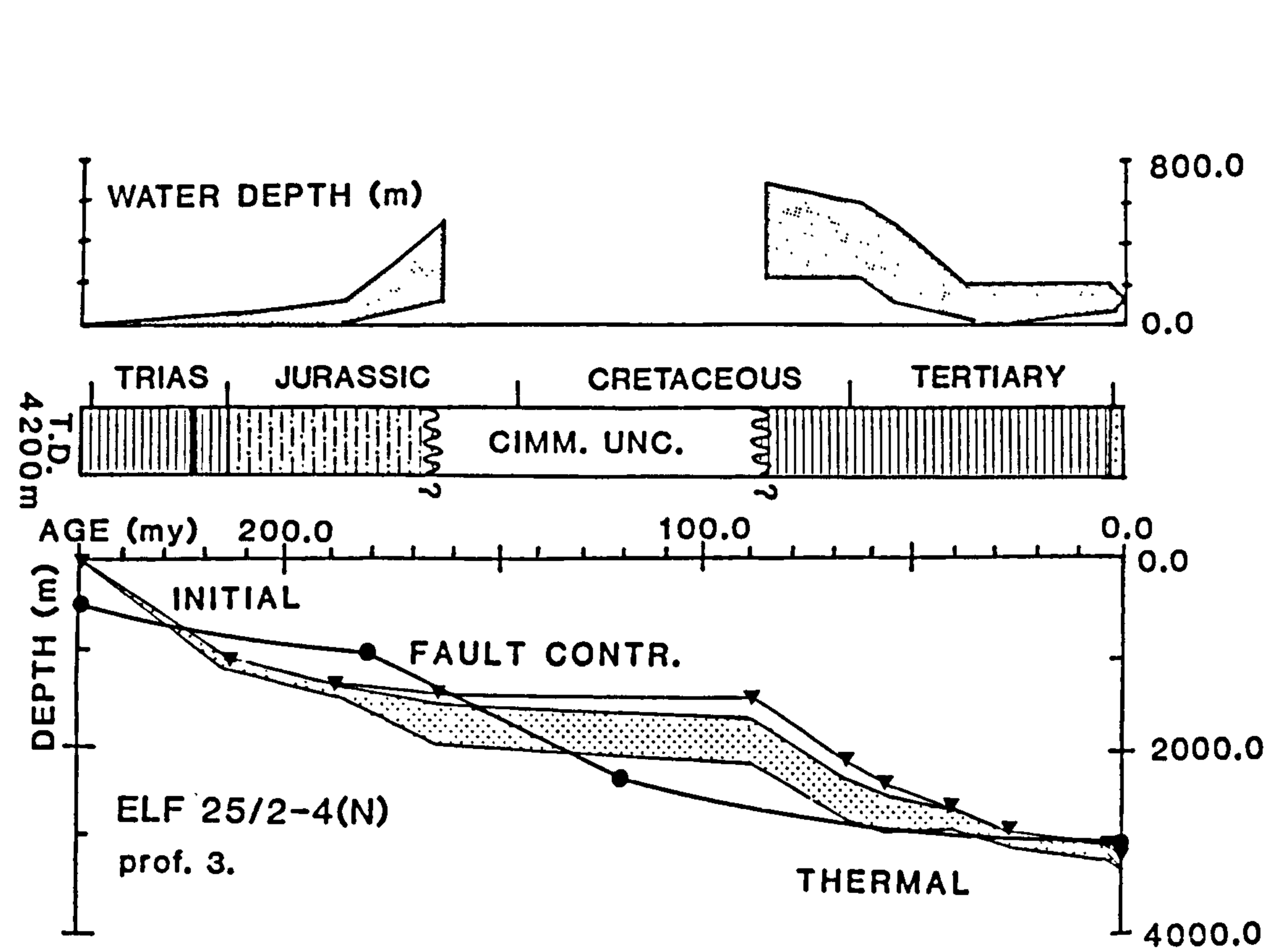
WATER DEPTH (m)
800.0
0.0
TRIAS
JURASSIC
CRETACEOUS
TERTIARY
T.D. 4200m
?
CIMM. UNC.
?
AGE (my) 200.0
100.0
0.0
DEPTH (m)
0.0
INITIAL
FAULT CONTR.
2000.0
ELF 25/2-4(N)
prof. 3.
THERMAL
4000.0

Fig 4.4 (cont.)

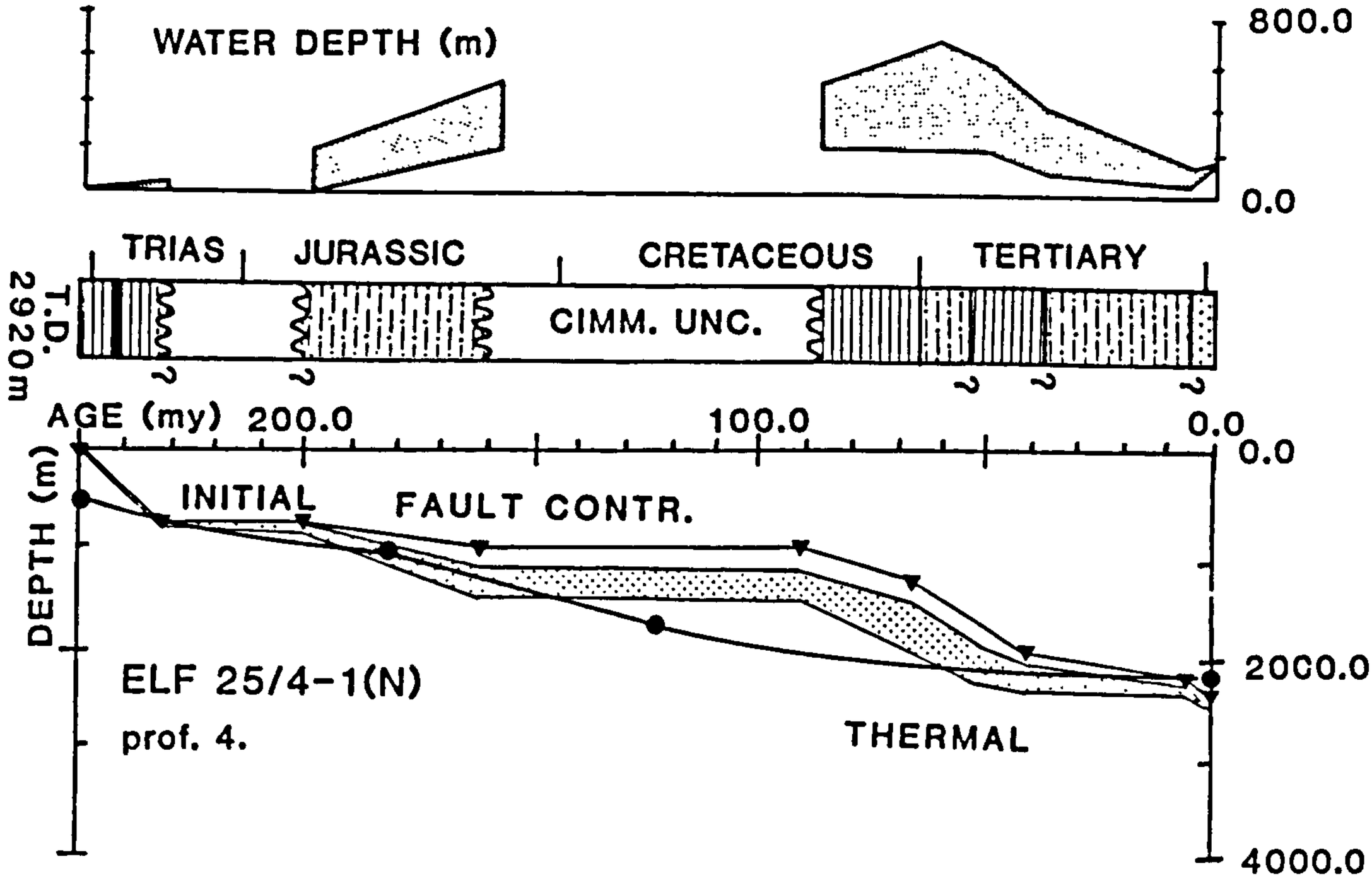
WATER DEPTH (m)
800.0
0.0
TRIAS
JURASSIC
CRETACEOUS
TERTIARY
T.D.
2920m
CIMM. UNC.
AGE (my)
200.0
100.0
0.0
DEPTH (m)
INITIAL
FAULT CONTR.
THERMAL
2000.0
4000.0
ELF 25/4-1(N)
prof. 4.

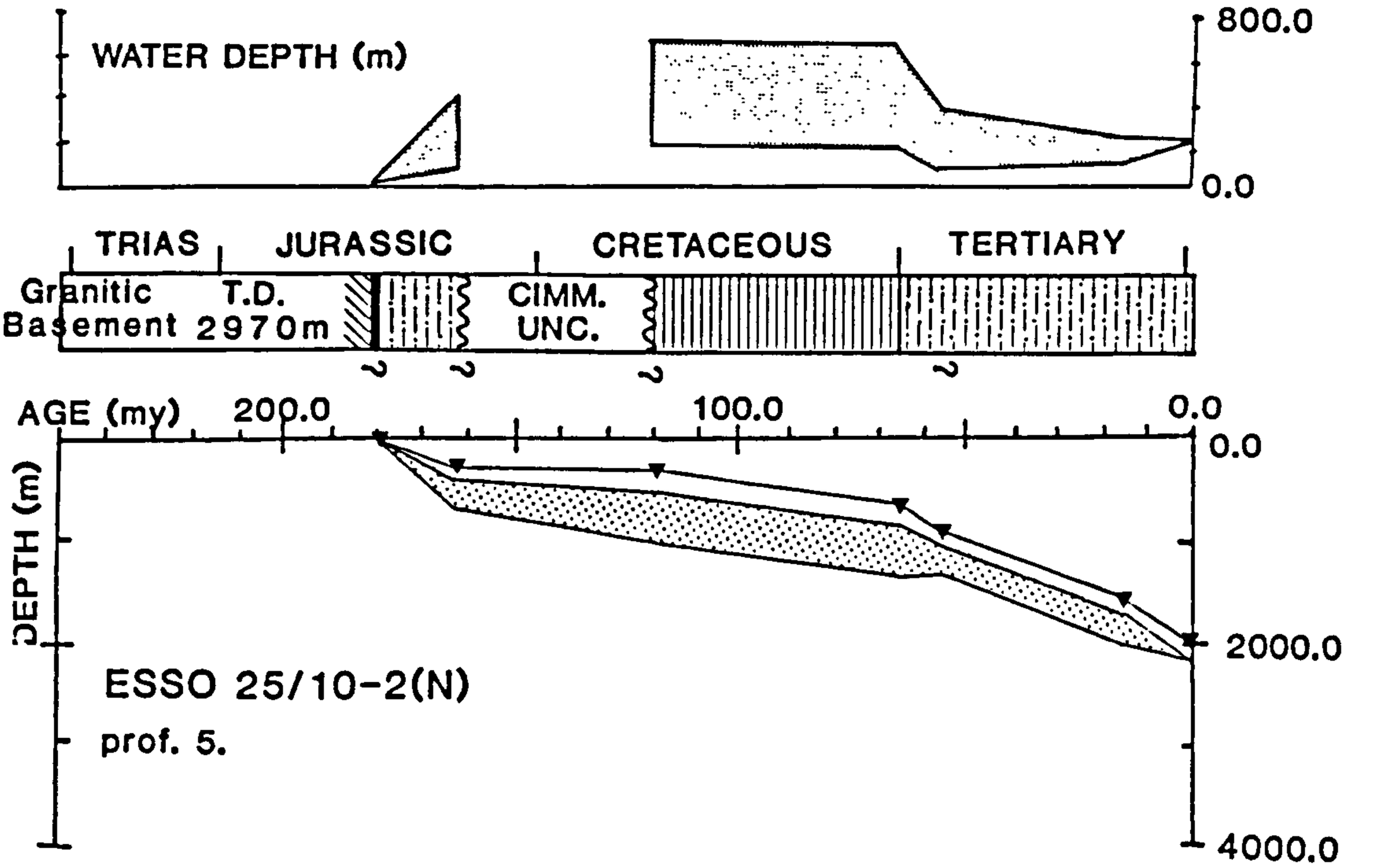
WATER DEPTH (m)
800.0
0.0
TRIAS
JURASSIC
CRETACEOUS
TERTIARY
Granitic
Basement
T.D.
2970m
CIMM.
UNC.
AGE (my)
200.0
100.0
0.0
DEPTH (m)
2000.0
4000.0
ESSO 25/10-2(N)
prof. 5.

Fig 4.4 (cont.)

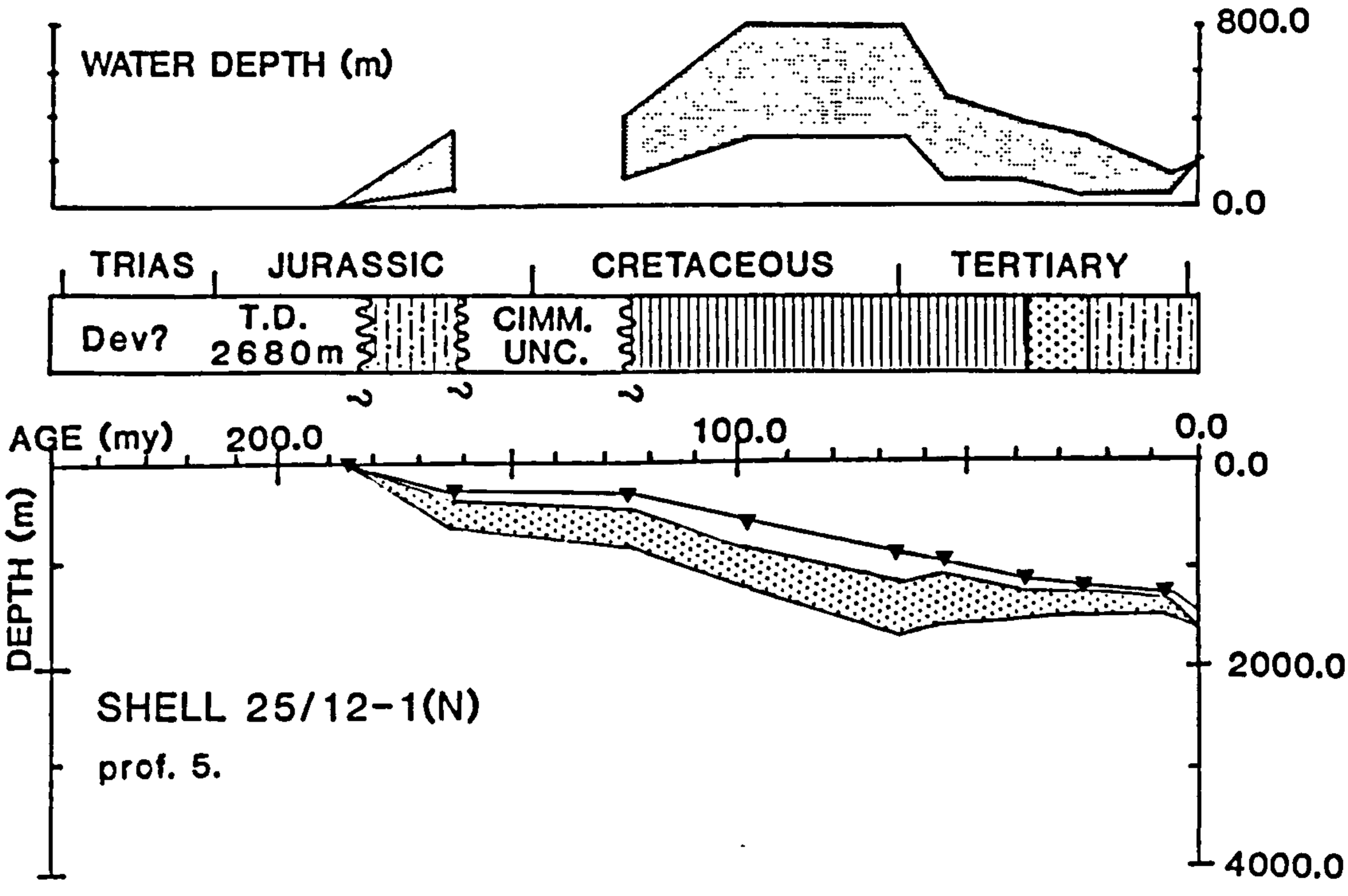
WATER DEPTH (m)
800.0
0.0
TRIAS
JURASSIC
CRETACEOUS
TERTIARY
Dev?
T.D.
2680m
CIMM.
UNC.
AGE (my)
200.0
100.0
0.0
DEPTH (m)
0.0
2000.0
4000.0
SHELL 25/12-1(N)
prof. 5.

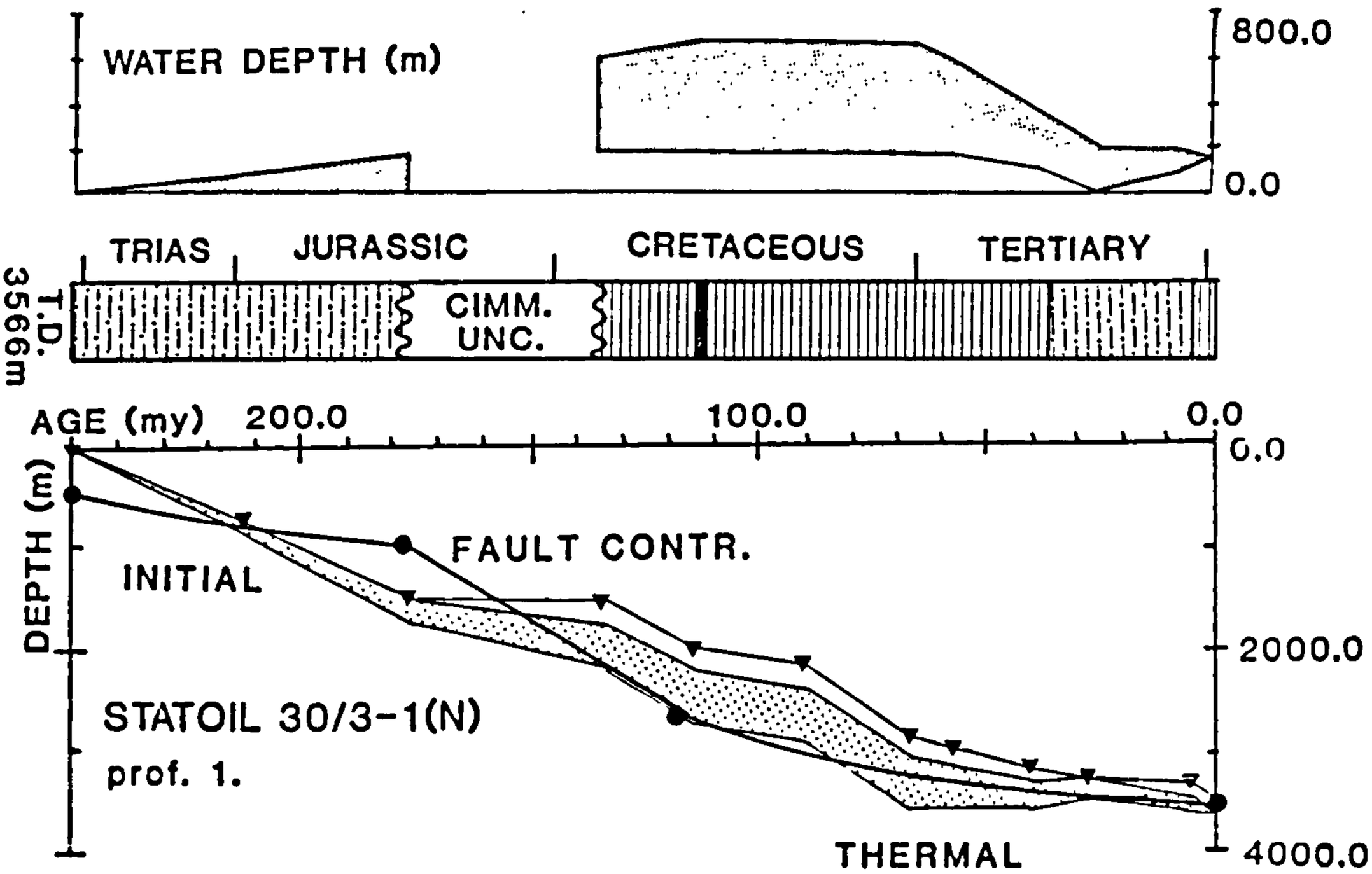
WATER DEPTH (m)
800.0
0.0
TRIAS
JURASSIC
CRETACEOUS
TERTIARY
T.D.
3566m
CIMM.
UNC.
AGE (my)
200.0
100.0
0.0
DEPTH (m)
0.0
2000.0
4000.0
INITIAL
FAULT CONTR.
THERMAL
STATOIL 30/3-1(N)
prof. 1.

Fig 4.4 (cont.)

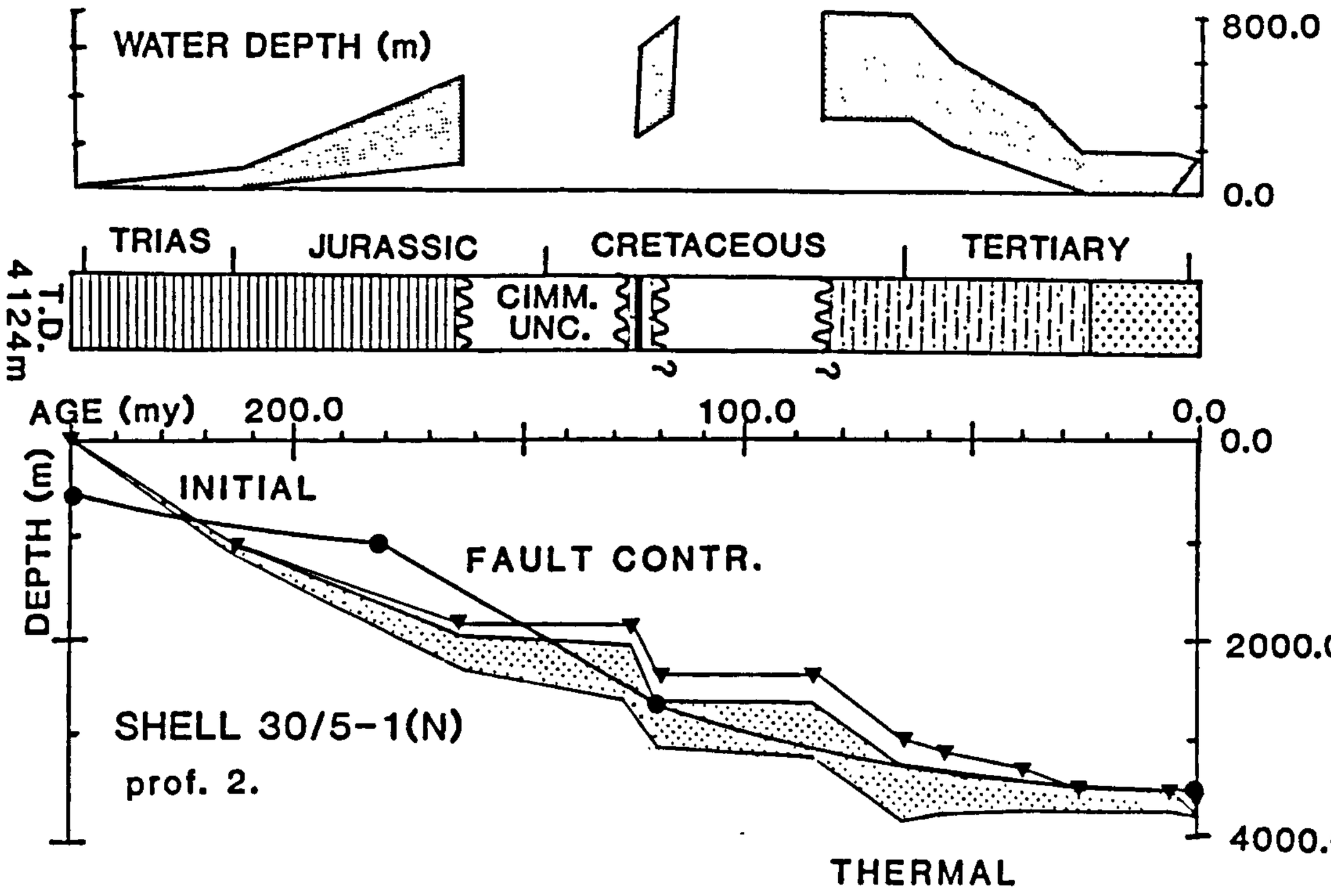
WATER DEPTH (m)
800.0
0.0
TRIAS
JURASSIC
CRETACEOUS
TERTIARY
T.D.
4124m
CIMM.
UNC.
AGE (my)
200.0
100.0
0.0
DEPTH (m)
INITIAL
FAULT CONTR.
SHELL 30/5-1(N)
prof. 2.
THERMAL
2000.0
4000.0

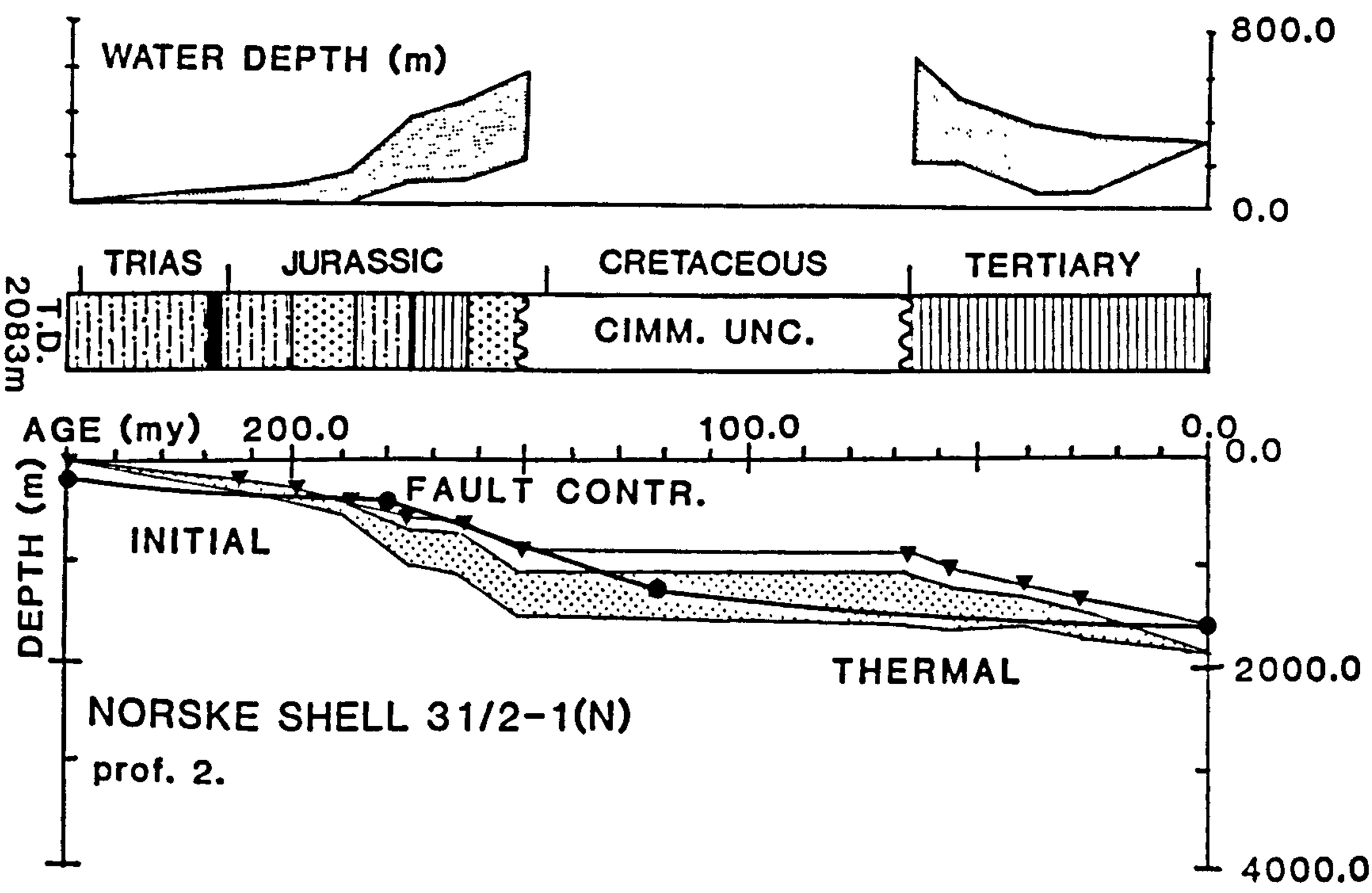
WATER DEPTH (m)
800.0
0.0
TRIAS
JURASSIC
CRETACEOUS
TERTIARY
T.D.
2083m
CIMM. UNC.
AGE (my)
200.0
100.0
0.0
DEPTH (m)
FAULT CONTR.
INITIAL
THERMAL
2000.0
4000.0
NORSKE SHELL 31/2-1(N)
prof. 2.

Fig 4.4 (cont.)

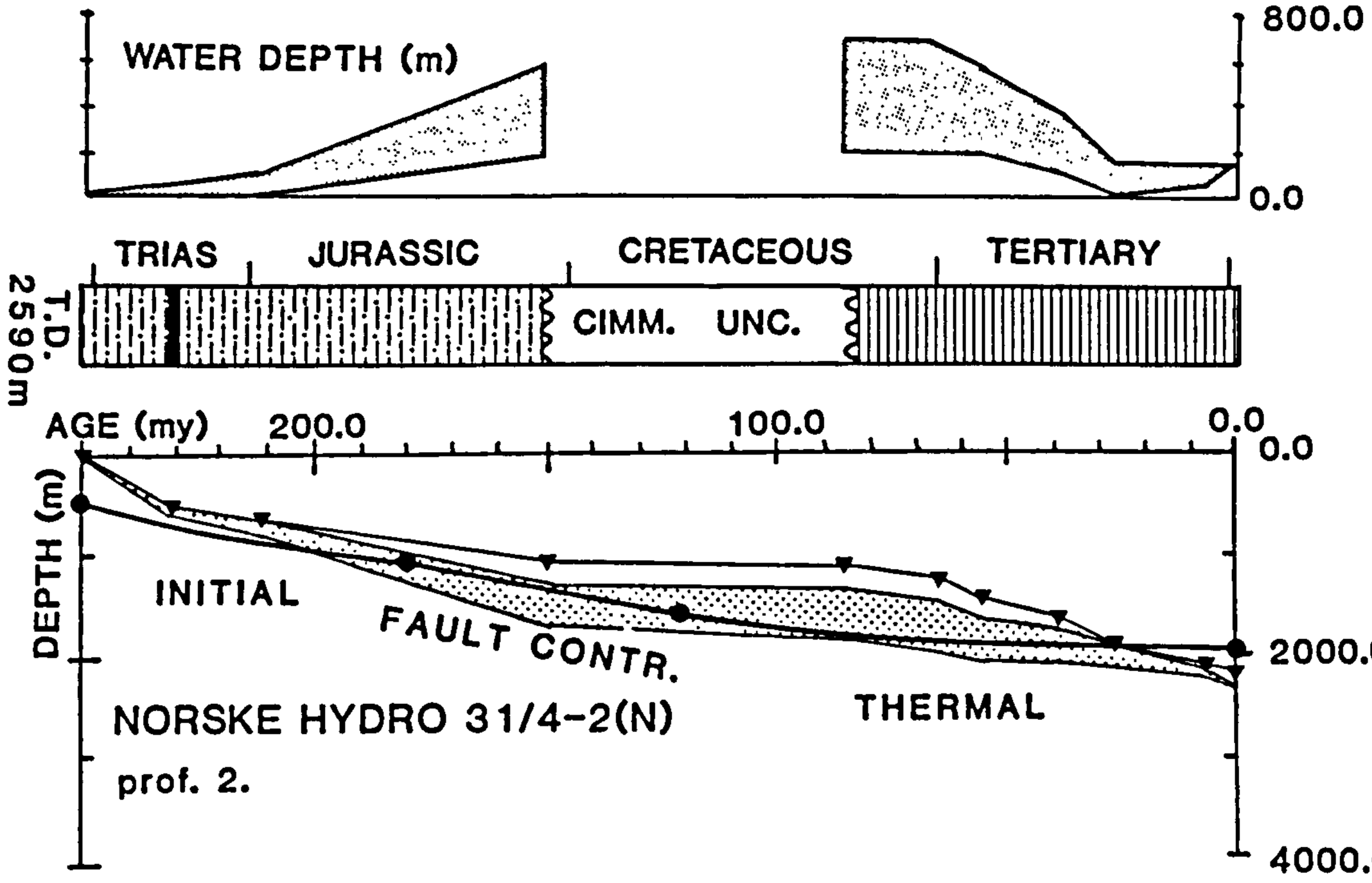
WATER DEPTH (m)
800.0
0.0
TRIAS
JURASSIC
CRETACEOUS
TERTIARY
T.D. 2590 m
CIMM. UNC.
AGE (my)
200.0
100.0
0.0
DEPTH (m)
INITIAL
FAULT CONTR.
THERMAL
2000.0
4000.0
NORSKE HYDRO 31/4-2(N)
prof. 2.

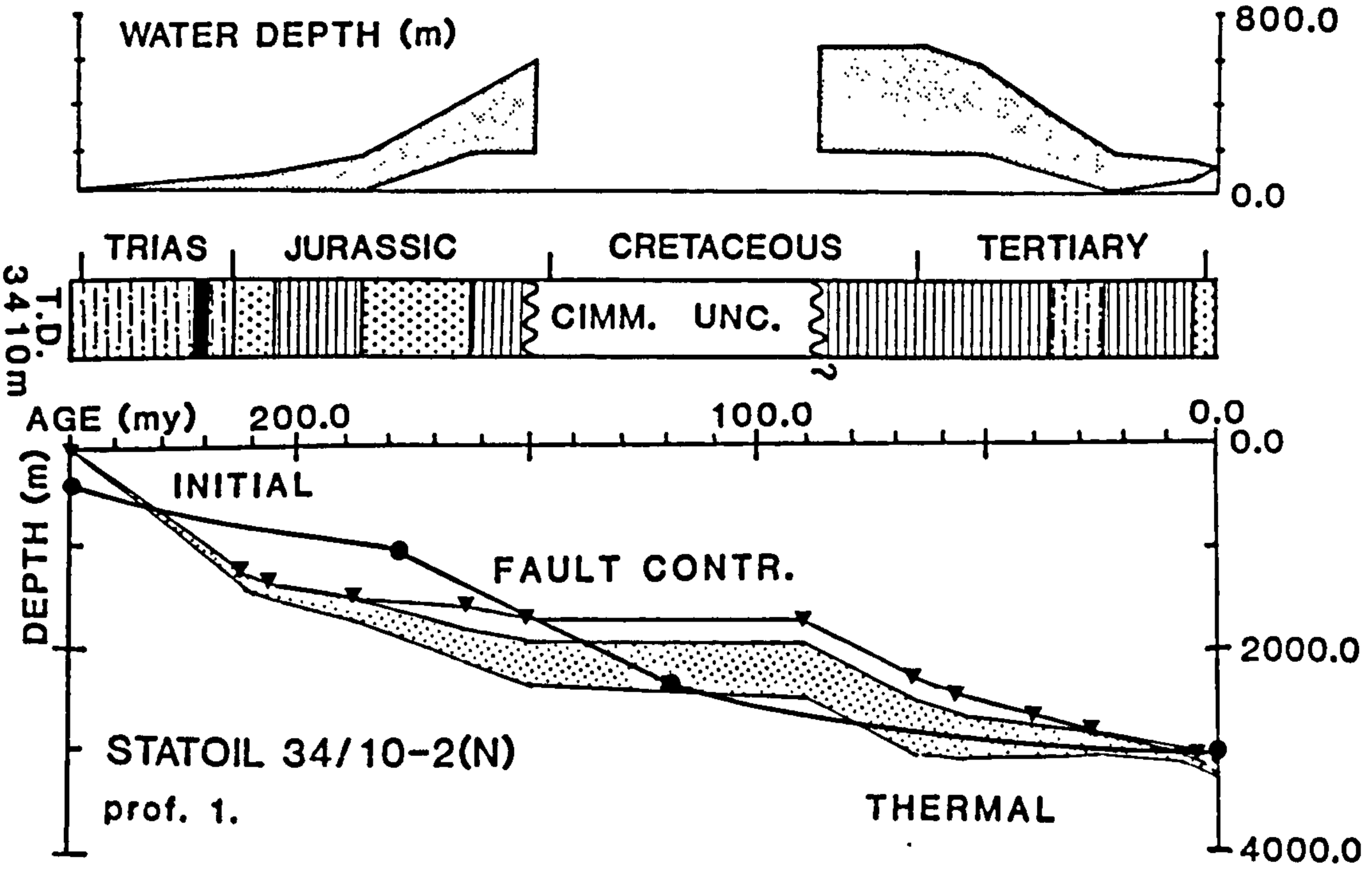
WATER DEPTH (m)
800.0
0.0
TRIAS
JURASSIC
CRETACEOUS
TERTIARY
T.D. 3410 m
CIMM. UNC.
AGE (my)
200.0
100.0
0.0
DEPTH (m)
INITIAL
FAULT CONTR.
THERMAL
2000.0
4000.0
STATOIL 34/10-2(N)
prof. 1.

Fig 4.4 (cont.)

The basement value of the Top Permian (250my) was set to zero, since deposition at this time was at or close to sea level, and all other basement values are plotted relative to this point. In the case of the wells drilled over granites, the oldest penetrated age above the granitic basement was set to zero (sea-level).

A general view of the subsidence can be seen from the curve corrected for compaction and sediment load only ("Sed. corrected subsidence"), Fig. 4.4. Because of the uncertainties in the water depth determinations, once the basement has been corrected for the total load ("Sed. and Water corr. subs."), there is a range of possible values for (Y) constrained by the maximum and minimum water depths at that time. The uncertainties in paleobathymetry and totally corrected subsidence are shown by shaded areas in the above diagram.

It can be seen that, once the wells have been corrected for loading, the variation in basement depth with age becomes linear or concave upwards, and the apparent increase in subsidence seen in the Plio-Pleistocene is greatly reduced. The pattern of subsidence is similar in all wells except the six wells situated on top of granites (Atypical wells). These wells subsided much later than the rest of them due to the buoyancy effect of the granites, (see section 5.7). Slower subsidence rates and less total subsidence is seen in the more marginal wells, than in those situated in the centre of the basin, as observed by Barton and Wood (1984) in the central North Sea.

4.4.4 Sea level variations

All basement subsidence paths so far mentioned in this study have been derived assuming that sea level has remained constant. However, sea level is believed to have varied during Mesozoic and Cenozoic, although there are problems in determining the magnitude of these eustatic changes. The excess water associated with a high stand in sea level acts as a load on the basement and depresses it.

Therefore, the actual depth of the basement (see section 4.4.3) according to Steckler and Watts (1978) taking into account eustatic sea level (SL) changes becomes:

$$Y = S\,\frac{(\rho_m - \rho_s)}{(\rho_m - \rho_w)} + WD - SL\,\frac{(\rho_m)}{(\rho_m - \rho_w)}$$

However, the magnitude of the long-term sea level changes through time is a subject of controversy at the present time. Pitman (1978) estimated that sea level has fallen by about 300m since the Late Cretaceous using changes in the volume of mid-ocean ridge crests through time. This estimate appears to agree with that of Sleep (1976), based on the present elevation of Cretaceous sediments in a tectonically undisturbed region of the continental interior. Watts and Steckler (1979) estimated that sea level has fallen by less than about 200m since the Late Cretaceous using well data off eastern North America. Their values yield a minimum estimate, but are in better agreement with the magnitudes estimated from continental flooding (Wise, 1974; Bond, 1978).

Vail et al (1977) have proposed that superimposed on the long term changes in sea level are short term changes. Based on the recognition of sedimentary sequences on seismic reflection profiles they have recognized slow rises in sea level followed by abrupt falls. The major periods of sea level rise were grouped by Vail et al (1977) into supercycles, which range from about 5 to 100my in duration. There is considerable debate at present, however, whether supercycles identified by Vail et al (1977) represent sea level changes or whether they represent tectonic changes (for example, Bally 1980).

Pitman (1978) remarked that changes in the time scale would drastically alter the spreading rates and hence the sea level curve based on the volume of mid-ocean ridges. His estimates of the

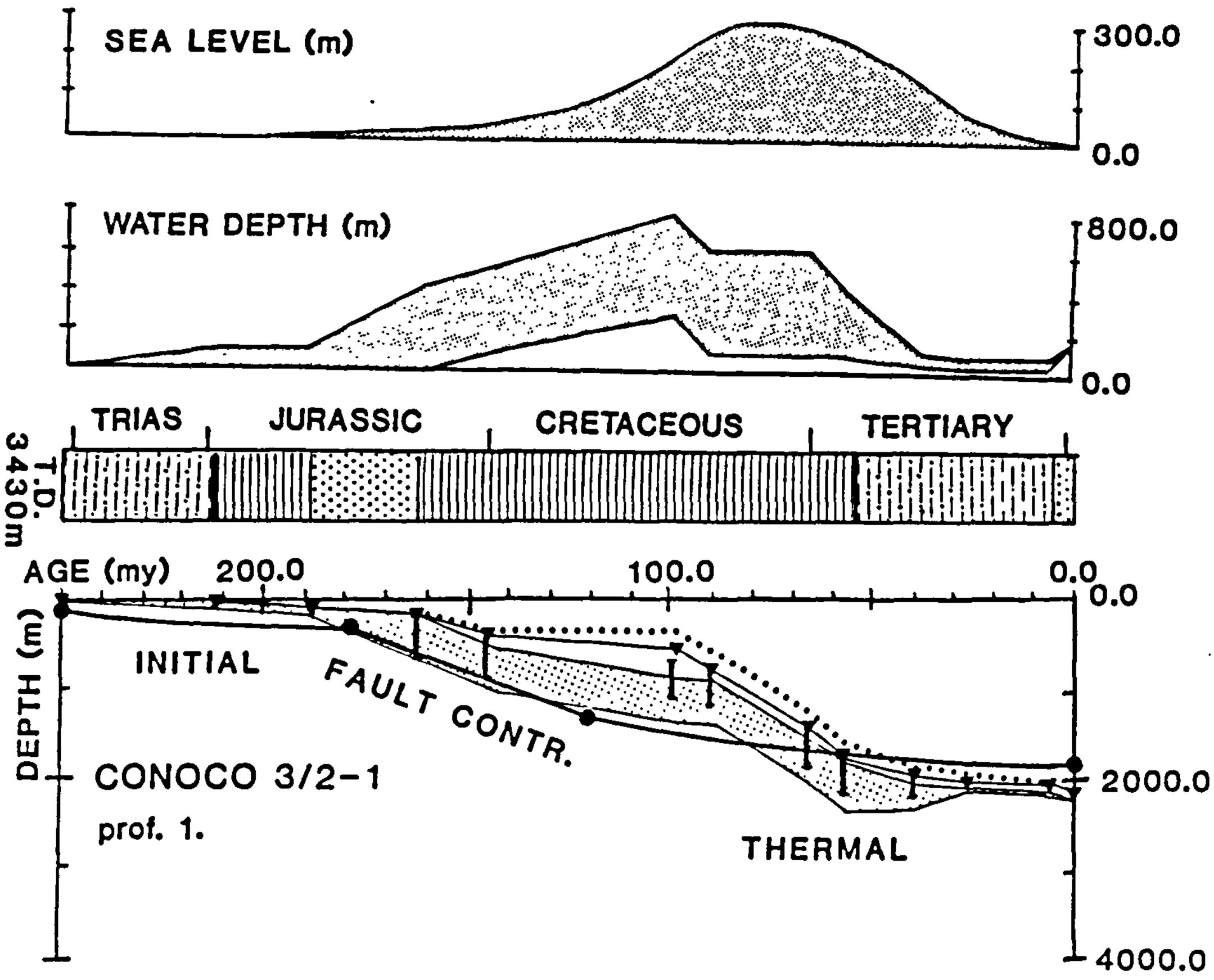

Fig 4.5 The effect of eustatic sea level variations on the unloaded basement. subsidence. Sea level curve after Pitman (1978). Dotted line denotes the basement subsidence path corrected for sediment load and sea level variations. The error bars indicate the uncertainty in the above curve including the depth of deposition (paleobathymetry) corrections. For Key and further explanations refer to Fig. 4.4.

volume of the mid ocean ridges were calculated using the Phanerozoic time scale modified by Berggren (1969).

In order to get the maximum effect on the subsidence of the basement from sea level variation Pitman's (1978) curve was applied because it is higher than any other curve by a magnitude of two to three. Therefore, the effect of any other curve will be lower by a factor of two to three. The above curve was replotted using the time scale of Harland et al (1982) and applied on the subsidence of the basement, (Fig. 4.5). Because of the predicted rise in sea level during the Late Cretaceous the effect is to pull up the subsidence of the basement and decrease the subsidence rate during the same time, although without significantly affecting the results.

By recalculating the volume of mid ocean ridges following Pitman's (1978) method and applying the new time scale (Harland et al 1982), the spreading rates will be reduced, lowering substantially the Late Cretaceous high stand seen in Pitman's sea level curve.

By applying the recalculated Pitman's curve the effect will be even smaller than the one observed in Fig. 4.5 and the effect of applying any other curve was found to be minimal. Because of the unrealiable nature of the predictions and the small significance of their effect, sea level was assumed to have remained at its present level.

4.5 Observed Subsidence Review

Combining the calculated sedimentation rates (Fig. 4.2), the paleobathymetry information (Fig. 4.4) and Pitman's sea level variations (Fig. 4.5), the following generalisation can be made regarding the subsidence history of the basin, assuming that the deposition of sediment was at sea level at Top Permian times (250my).

The Top Permian to Mid-Jurassic subsidence and sedimentation rates were very low and average, for wells situated in the flanks and the middle of the basin respectively. In both cases the sediments were deposited in shallow marine environment and the sedimentation rates kept pace with the subsidence. Correcting for sea level rise, deep water conditions were established by Mid-Cretaceous, progressively since Late Jurassic, indicating that during this period the basement subsidence exceeded by far the moderate sediment supply observed. In the Late Cretaceous sedimentation rates somewhat exceeded subsidence rates, and eustatic sea level rises. However, the shallow water conditions were not yet established in the basin. During Paleocene and Eocene the high sedimentation rates, apparently exceeding the subsidence rates and the fall in the sea level, caused the shallowing of the basin. During Oligocene and Miocene though, the subsidence and sedimentation rates were more or less in balance and the drop in sea level resulted in further shallowing of the basin. Finally, during the Pliocene - Pleistocene both subsidence and sedimentation were very high. The latest observation correlates with the last glaciation period and subsequent erosion of neighbouring land mass.

CHAPTER 5

SUBSIDENCE MODELLING

Introduction

In this chapter the results of the totally unloaded basement subsidence are compared with patterns predicted by theoretical models of basin formation and a model is proposed to account for the development of the northern North Sea. Part of the subsidence is modelled assuming instantaneous stretching during a rifting phase (McKenzie, 1978) and the rest of it assuming extension over a period of time during rifting (Jarvis and McKenzie, 1980). The various limitations involved in the different stages of the above study are examined.

The present day crustal thickness estimations calculated by the subsidence modelling were compared with values derived from the detail gravity investigation of Chapter 2. Finally the amount of crustal stretching during the rifting phases is approximately estimated and the influence of granites during the various stages of development of the northern North Sea is discussed.

5.1 Theoretical Models

5.1.1 Instantaneous extension

McKenzie (1978) proposed a simple model for the evolution of sedimentary basins as a result of work in the Aegean region (1978b). A basin is produced by sudden stretching of the crust and lithosphere followed by a slow cooling. The subsidence and heat flow can be predicted as a function of the extension factor β, where β is the increase in surface area.

Extension occurs instantaneously resulting in the development of grabens due to brittle failure of the crust, and ductile flow in

the subcrustal lithosphere. These processes allow hot asthenospheric material to rise beneath the thinned portion of the crust. Since isostatic compensation is preserved throughout, a fault controlled initial subsidence results due to the replacement of the crust by the more dense asthenosphere. Condition for the subsidence is initial crustal thickness (Tc) > 20km.

A thermal anomaly is produced by the passive upwelling of the hot asthenosphere. As this thermal anomaly decays the lithosphere thickens and subsides following a similar path to the ocean floor as it moves away from the mid ocean ridge, as observed by Sleep (1971) and quantified by Parsons and Sclater (1977).

The total subsidence is the sum of the initial instantaneous fault controlled subsidence and thermal one and is shown in Fig. 5.1 as a function of the extension factor β.

5.1.2 Finite period extension

The assumption of instantaneous stretching will not lead to significant error in the North Sea ($\beta < 1.7$) if the duration of the stretching is less than 20my (Jarvis and McKenzie, 1980). The main extensional event in the North Sea, however, lasted from Middle Jurassic to Aptian times, approximately 60my. A model to account for this extension (60my) has been developed by Jarvis and McKenzie (1980).

This model has been successfully employed to relate the amount of crustal thinning to the heat flow and subsidence histories of basins on the eastern margin of North America, Watts and Steckler (1979), Keen (1979), Royden and Keen (1980), Royden et al (1980), Keen et al (1981a, b), Beaumont et al (1982), of the North Sea, Christie and Sclater (1980), Sclater and Christie (1980), Wood and Barton (1983) and of the intra-Carpathian basins in central Hungary, Sclater et al (1980).

Fig. 5.2 gives the total subsidence predicted by the above model. The subsidence is seen to increase rapidly during stretching followed by a slower exponentially decreasing subsidence during cooling. Since the total subsidence depends only on β when all

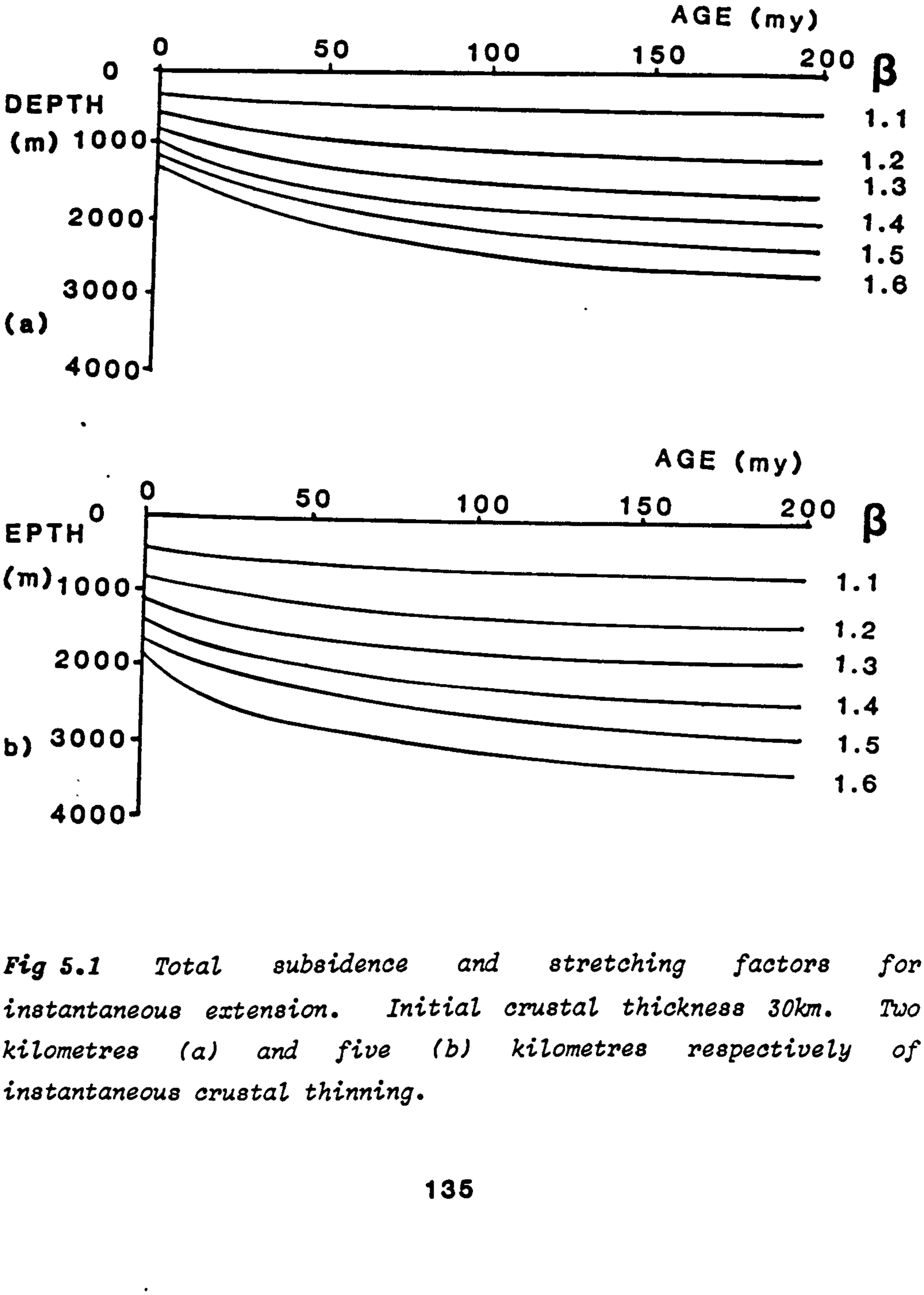

Fig 5.1 Total subsidence and stretching factors for instantaneous extension. Initial crustal thickness 30km. Two kilometres (a) and five (b) kilometres respectively of instantaneous crustal thinning.

other parameters are constant the total subsidence is the same for both the instantaneous and the finite duration of stretching at infinite time after the extensional event. However, when stretching occurs over a finite period of time, heat is lost during stretching, hence a reduced thermal anomaly is produced.

The lithospheric parameters used in applying the instantaneous and finite period extension models were taken from Cochran (1982) unless otherwise stated.

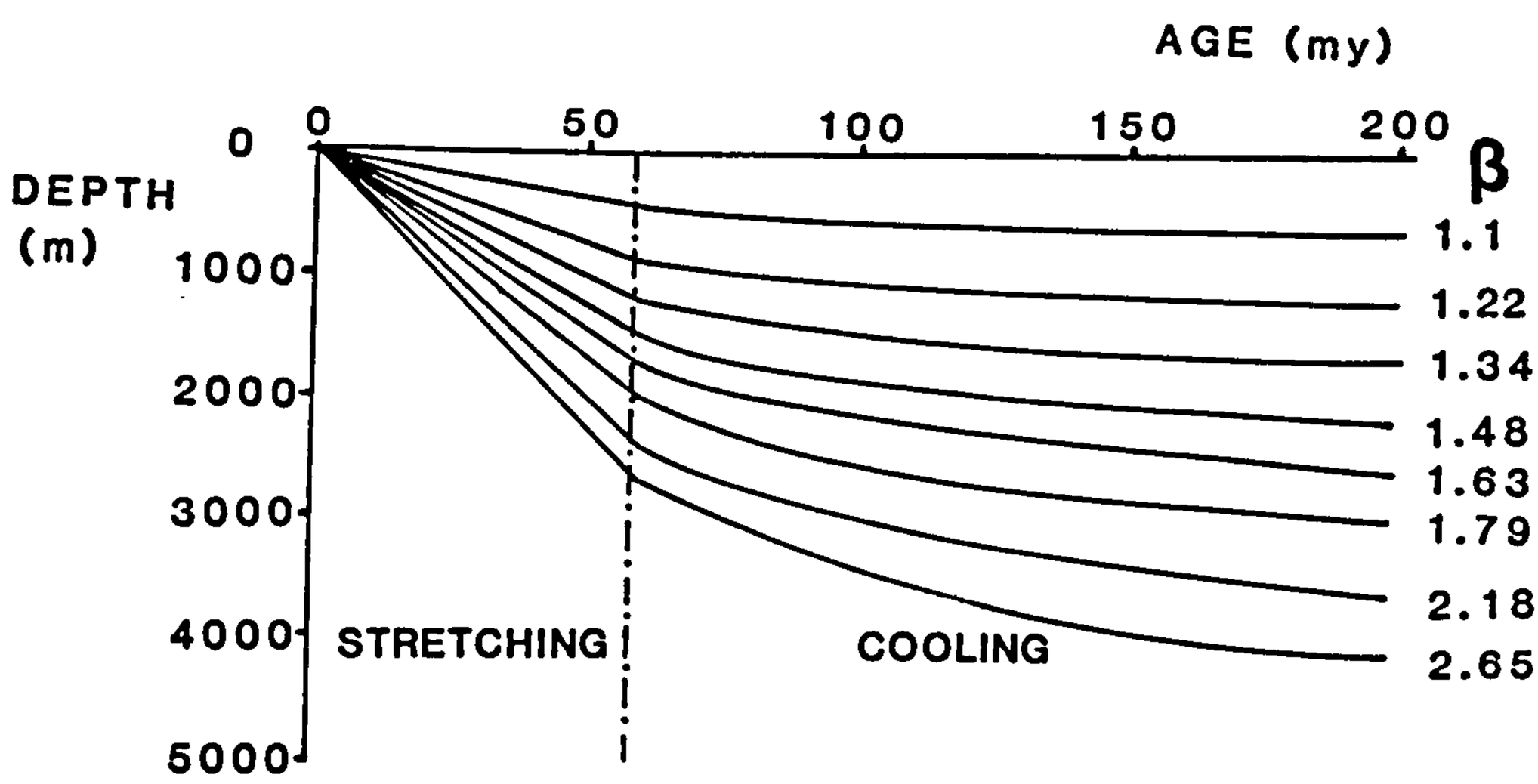

Fig 5.2 Total subsidence and stretching factors for finite period (60my) extension. Initial crustal thickness 30km.

5.2 Application of Models

The above subsidence paths predicted by the theory give the depth to basement when filled with water to mean sea level, enabling direct comparison with the basement subsidence (Y), obtained from the well data. An INITIAL subsidence phase is assumed to have started in the Top Permian (250my) and ended in the Mid-Jurassic. Any detailed modelling for the above period would be unrealistic because the majority of the typical wells do not penetrate the base Jurassic and their chronostratigraphic column, lithology and paleobathymetry have been extrapolated according to the known geology of the area. Therefore, the simple instantaneous stretching model of McKenzie (1978) was applied (see Fig. 4.4). The instantaneous stretching was assumed to have occurred 250my ago and accounts for the Permo-Triassic stretching event observed in the basin, Ziegler (1981). After stretching, lithospheric cooling took place to account for the observed subsidence during Triassic and Mid-Jurassic (250-180my).

In all the calculations crustal density and initial crustal thickness of 2.8g/cc and 30km respectively were assumed, according to the results derived from the crustal investigation of Chapter 2.

Five and two kilometres of instantaneous crustal thinning (corresponding to β values of 1.2 and 1.07) were assumed for wells situated in the centre and the flanks of the basin respectively (see also Fig. 4.1 and Table 5.1).

The main faulting event of the North Sea basin lasted approximately 60my from Mid-Jurassic to late Lower Cretaceous (180-120my), Ziegler (1981), Threlfall (1981), Deegan and Brown (1981), Barton and Wood (1984). Therefore the finite period extension model of Jarvis and McKenzie (1980) was applied for 60my of extension (180-120my, FAULT CONTR. subsidence) followed by passive subsidence until the present day (THERMAL subsidence), (Fig. 4.4). In this,

Table 5.1

Crustal thicknesses and β factors derived from well modelling, see Fig. 4.4. Wells situated on granitic basement were considered Atypical and they were not modelled.

Wells on the flanks	a	b	c	d	e	f	Wells in the centre	a	b	c	d	e	f
UNION							BURMAH						
2/5-1			19		1.48	1.6	3/3-3			19		1.30	1.6
CONOCO							TEXACO						
3/2-1			21		1.34	1.4	3/4-1			19		1.34	1.6
SHELL							TOTAL						
8/27-1A			23		1.22	1.3	3/15-2			17		1.48	1.8
HAMILTON							UNION						
9/28-1A			19		1.48	1.6	9/12-1			19		1.34	1.6
OXY							ESSO						
14/18-1	30	28	23	1.07	1.22	1.3	15/6-2(N)			19		1.30	1.6
OXY							ELF						
15/17-7			23		1.22	1.3	25/2-4(N)	30	25	16	1.20	1.55	1.9
PHILLIPS							ELF						
16/17-6			18		1.55	1.7	25/4-1(N)			19		1.34	1.6
SHELL							STATOIL						
31/2-1(N)			22		1.30	1.4	30/3-1(N)			14		1.79	2.1
							SHELL						
							30/5-1(N)			14		1.79	2.1
							N. HYDRO						
							31/4-2(N)			20		1.22	1.5
							STATOIL						
							34/10-2(N)			16		1.55	1.9
AVERAGE	30	28	21	1.07	1.35	1.4	**AVERAGE**	30	25	17	1.20	1.45	1.8

(a) initial crustal thickness (km)

(b) crustal thickness after the Permo-Triassic stretching event (km)

(c) present day crustal thickness (km)

(d) β factors for the instantaneous crustal extension

(e) β factors for the finite period crustal extension

(f) β factors for the total extension

case it was assumed that the initial crustal thickness was either 28 or 25km depending on the position of the well.

The theoretical curves were chosen to give the closest fit to the total part of the subsidence, while not exceeding the initial subsidence apparent in the well, (see also Table 5.1). The theoretical curves are not constrained to pass through the present day basement value, because this point is considered to be unrepresentative of the overall subsidence pattern because of the sea level and loading fluctuations resulting from the last glaciation period.

5.3 Discrepancies of Models

Although there is good agreement between observed subsidence and model predictions there are some systematic discrepancies as well. The predicted paths for the Permo-Triassic event show better agreement in wells on the flanks than those in the centre of the basin (eg. CONOCO 3/2-1, ESSO 15/6-2(N) respectively). Although on the flanks the theoretical model does not show any trends towards over or under estimation, in the centre the model clearly underestimates the subsidence by approximately 500m.

The majority of the wells show slow subsidence during the Mid-Jurassic to Early-Cretaceous faulting event. In contrast the model predicts FAULT CONTR. subsidence of much higher slope, overestimating the subsidence, especially in the wells in the centre of the basin.

The same pattern of slow subsidence continues through most of the Cretaceous until the Late-Cretaceous (80my approximately). Very rapid subsidence continues afterwards until Early Eocene times (50my approximately) followed by a very slow one, up to recent times. The above observed subsidence variations were modelled by a

very slow subsidence (THERMAL) which overestimates the above observed patterns heavily in the Late-Cretaceous and follows them quite accurately in the Mid-Late-Tertiary.

5.4 Reasons for Discrepancies

The reasons for the discrepancies described above, between the observed subsidence paths and the theoretical predictions can be summarised as follows:

5.4.1 Paleobathymetry

The estimate of water depth variation that occurred during the evolution of the basin is obtained from micropaleontological and relevant geological information. Such an estimate is not highly reliable. In addition to this, the paleobathymetry of the Norwegian sector was based on information mainly available from the UK sector of the basin. Therefore, inaccuracies in water depth estimation can be expected, mainly in the Norwegian sector of the northern North Sea.

5.4.2 Decompaction

The sediments were decompacted along "normal" porosity curves of four generalized lithologies (see section 4.2). The scattering of porosity values for the same lithologic type (Fig. 3.3, 3.4, 3.5) suggests that different wells can have a porosity variation at certain depths without being considered overpressured. This porosity variation for individual wells and compensation for overpressured horizons was not taken into account. However, overpressured horizons were encountered in a few wells mainly in the Jurassic, in the porosity study of Chapter 3 (see Fig. 3.9) and there are some indications of Tertiary overpressure sediments in the central North Sea (Sclater and Christie, 1980).

5.4.3 Stratigraphy

All the chronostratigraphic well columns were simplified into four lithologies based on Composite logs. Most of the wells did not penetrate the base Triassic and were extrapolated by the nearby seismic profile and by any relevant geological information. Therefore, the lithology simplification, the Triassic extrapolation and the age uncertainties (question marks on the chronostratigraphic column, Fig 4.2, 4.4) introduce inaccuracies which are greater in the deepest (central) part of the graben.

5.4.4 Position of wells

Most of the wells have been drilled on top of rotated listric fault blocks (structural highs) for hydrocarbon exploration purposes, therefore, non-typical positions for studying the basement subsidence history.

5.4.5 Unconformities

The most common unconformities present in the northern North Sea basin occurred during the Mid-Jurassic to Mid-Cretaceous period. A general reference for them is Cimmerian unconformities (Fig. 4.2, 4.4). Vail and Todd (1981) and Rawson and Riley (1982) attribute many of the unconformities observed in the above period to sea level changes. Fyfe et al (1981) give evidence of fault block tilting and local uplift in addition to eustatic changes as causes for the Cimmerian unconformities. Further confusion can arise from the misinterpretation of a condensed sedimentary sequence as an unconformity. Therefore, due to a lack of any reliable information to assess the amount of section missing and hence the amount of subsidence or uplift during that time a decision was made to treat unconformities as time of zero sedimentation, and hence to plot them as horizontal lines (Fig. 4.2).

5.4.6 Sea level

The effect of any sea level curve in the calculation of the basement subsidence is not significant as described in section 4.4.4. However, the application of eustatic changes increases the discrepancy between observations and theoretical predictions especially in the Upper Cretaceous when the maximum sea level rise is believed to have occurred.

5.4.7 Modelling parameters and assumptions

The lithospheric parameters used when modelling sedimentary basin subsidence were chosen to give an internally consistent isostatically balanced system (Cochran, 1982). However, small variations in the densities and thicknesses of the crust or the lithosphere cannot be ruled out and can result in large differences in the amount of subsidence without significantly affecting the balance of the system. For example, 0.1g/cc increase in the crustal density in the instantaneous model of $\beta = 1.6$ can result in 600m overestimation of the subsidence.

The instantaneous extension model gives results which differ little from the finite period extension model provided that the time taken to extend by a factor β is less than $60/\beta^2_{my}$(Jarvis and McKenzie, 1980). Therefore, the predicted model does not significantly differ from the observations if it is assumed that the Permo-Triassic event in the North Sea of β factor 1.07 and 1.2, lasted less than 40my approximately.

In applying the finite period extension model it is assumed: (1) that horizontal extension in the brittle upper crust occurs by fracturing and rotation of crustal blocks along listric faults; (2) that the thermal effects of the Permo-Triassic stretching event had decayed by Mid-Jurassic times and (3) that the crust has the same thermal properties as the mantle when calculating the

subsidence due to the thermal contraction. This last assumption results in errors of 1.3% in the estimate of the total post-extensional subsidence (Jarvis and McKenzie, 1980).

From the uncertainties described so far (1 to 7) none can drastically alter the shape of the observed or predicted subsidence.

5.4.8 Paleocene uplift

It is now generally accepted that Greenland separated from Northwest Europe at some time in the late Paleocene or Early Eocene, Lovell (1984). Uplift is normally associated with the early breakup of a continental plate. Such an uplift of northwest Britain (Bott, 1975), including shelf areas northeastward to Shetland, produced tensional forces in the North Sea hinterland. These forces induced renewed rotational movements along pre-existing Jurassic grabenal faults, Rochow (1981). The regional uplift in the East Shetland Platform is estimated to be approximately 200m or more (comment by Knox in Rochow (1981)). However, in our study no reactiviation of any tectonism was taken into account during the above period. Thermal subsidence was assumed instead throughout Tertiary. It seems that the above tectonic activity caused the major discrepancy between observations and predictions during Late Cretaceous to Mid-Tertiary times.

5.4.9 Flexure

The elastic model predicts progressive overstepping of younger strata onto basement due to the increase in elastic thickness (Te) with age since basin initiation. Sediments that infill the basin, soon after formation, load a relatively weak plate, whereas sediments that infill the basin later in its evolution, load a relatively strong plate, see also section 4.4.

To date, most workers have discounted flexure as an important contribution to the development of models in the North Sea because its evolution can apparently be explained without it (Sclater and Christie, 1980; Christie and Sclater, 1980; Barton and Wood, 1984).

The North Sea basin, however, contains on the west side Late Cretaceous to Recent sediments progressively onlapping onto the basement, according to the predictions of the elastic model, Fig. 1.2.

The main difference with the model is that on the eastern margin of the basin, sediments decrease in age progressively towards the basin centre, typical of visco-elastic basin development (Beaumont, 1978). The eastern margin appears, however, to have been truncated by Late Pleistocene uplift and erosion after ice loading of the Fennoscandian shield, so that subsequent sedimentary processes have modified the stratigraphy of the east edge of the northern North Sea basin. Therefore, any visco-elastic hypothesis is not substantiated.

There are a number of other examples in the geological record of basins that show onlap at their edges; the western margin of the West Siberia basin (Zhabrev et al 1975), the coastal plain of northwest Africa (Vail et al 1977), Gippsland Basin in southeast Australia (Hocking, 1976) and others. Each example shows a progressive widening of the basin with time after its initiation.

The modelling of the North Sea basin assuming Airy isostasy only, causes the under-estimation of β factors in the graben area and over-estimation in the adjacent unstretched regions, provided that the crust is deformed by flexure (as the stratigraphy of the recent sediments indicate). The under-estimation in the graben is due to the basement not subsiding as far as it would with Airy isostasy and the over-estimation on the margins is caused by the fact that subsidence has occurred in the absence of thinning.

As discussed above, flexure may well be important in this basin, thus questioning the applicability of McKenzie (1978), Jarvis and

McKenzie (1980) models and the backstripping, both of which assume Airy isostasy. Clearly, additional data, such as seismic reflection and refraction coupled with gravity, are required to better constrain stretching estimates that are based only on well data.

5.4.10 Lateral heat flow

This study was based on models that considered only the vertical cooling of the lithosphere during basin formation. In fact, the heat within the stretched lithosphere will flow laterally as well as vertically, cooling the centre of the basin but heating the unstretched lithosphere of the basin flanks. Lateral heat flow can have a significant effect on the subsidence history, the distribution of sediments and the thermal history of the basin.

Such a model taking into account both lateral and vertical heat flow was developed by Cochran (1983). In particular, the post-rift subsidence is decreased by more than 25% for a 20my rifting event and by more than 10-15% for a rifting event as short as 10my.

Furthermore, unlike the models applied in this study, the shape of the basin available for sediments does not remain constant during basin evolution. While the fault controlled subsidence is identical, at later times heat flows laterally out of the basin, producing a thermal bulge in flanking regions. The maximum uplift exceeds 250m and occurs early in the thermal subsidence of the basin. As time progresses, the uplift decreases but also broadens as the heat diffuses outwards. The uplift in the flanks of the basin is accompanied by rapid subsidence on the basin side of the hinge zone. This region loses heat and therefore subsides more rapidly than the centre of the basin. As heat diffuses laterally, the basin flattens out but the level of the basement remains a few hundred metres deeper than in the simple model, even after 100my.

Therefore, the lateral heat flow will significantly decrease the subsidence rates in the post-rift stage and this implies that

inferences concerning the structure, development, and thermal history of the basin derived from using "β curves" to interpret backstripped subsidence can be greatly in error.

Probably the best and simplest way to test Cochran's (1983) model, apart from "β curves" comparison, is to attempt to identify in the sediment stratigraphy the thermal bulges of about 250m at the edges of the basin, occurring in the early stages of the thermal subsidence.

The first thermal event in the North Sea, which took place during Triassic and part of the Jurassic (250-180my), was followed by the main extension and faulting episode of Mid-Jurassic to late Early Cretaceous (180-120my). Consequently, no sediment disturbances of such a small scale are expected to be seen in the Triassic sediments since the quality of the seismic sections is not good enough due to the great depth of burial (about 5km).

The second thermal event took place in the Upper Cretaceous to Recent times and most of the sediments remain undisturbed. Hence, some sort of uplift is expected to be seen during Early Tertiary in the flanking regions of the basin. Unfortunately though such evidence, if it ever existed, has vanished due to: first the Paleocene uplift and subsequent erosion of the East Shetland Platform in the west margin of the basin, and secondly due to the Late Pleistocene uplift and severe erosion after the ice loading of the Fennoscandian shield in the east margin of it.

The only way to test the applicability of the simple stretching models used in this study, considering the uncertainties and assumptions described so far, is to compare the stretching factors and thinning of the crust with results derived from another independent method. This comparison is described in the following section.

5.5 Gravity Evidence

Independent evidence of the stretching factors can be obtained using the variation in the crustal thickness (β=orig.th./pres.th.) across the basin derived from the de-tailed gravity investigation of Chapter 2, Fig. 2.5. The results of the above study and the well modelling predictions are shown in Fig 5.3 and Table 5.2. Their comparison indicates the following:

There is a very good agreement among the values of the present day crustal thickness calculated by the two independent methods with the maximum discrepancy not greater than 2km. Ten wells have under-estimated, seven have over-estimated and two have accurately predicted the crustal thickness.

Therefore, apart from the close agreement of the results there is not even a tendency for under or over estimation. As a result the stretching factors obtained from the wells have been successfully modelled assuming an extensional origin for the North Sea with the first stretching event being instantaneous in the Base Triassic and the second of 60my duration taking place from Mid-Jurassic to Late Cretaceous.

However, no geological situation is expected to fit a theoretical model exactly due to the uncertainties described so far, but the reasonable approximation between the predicted and observed subsidence curves suggests that the North Sea basin development can be explained assuming local isostasy only, without taking into account lateral heat flow.

5.6 Crustal stretching

According to both well and gravity modelling the initial crustal thickness beneath the basin was assumed to be approximately 30km (see sections 5.2 and 2.7). However, in the North Sea area, basin

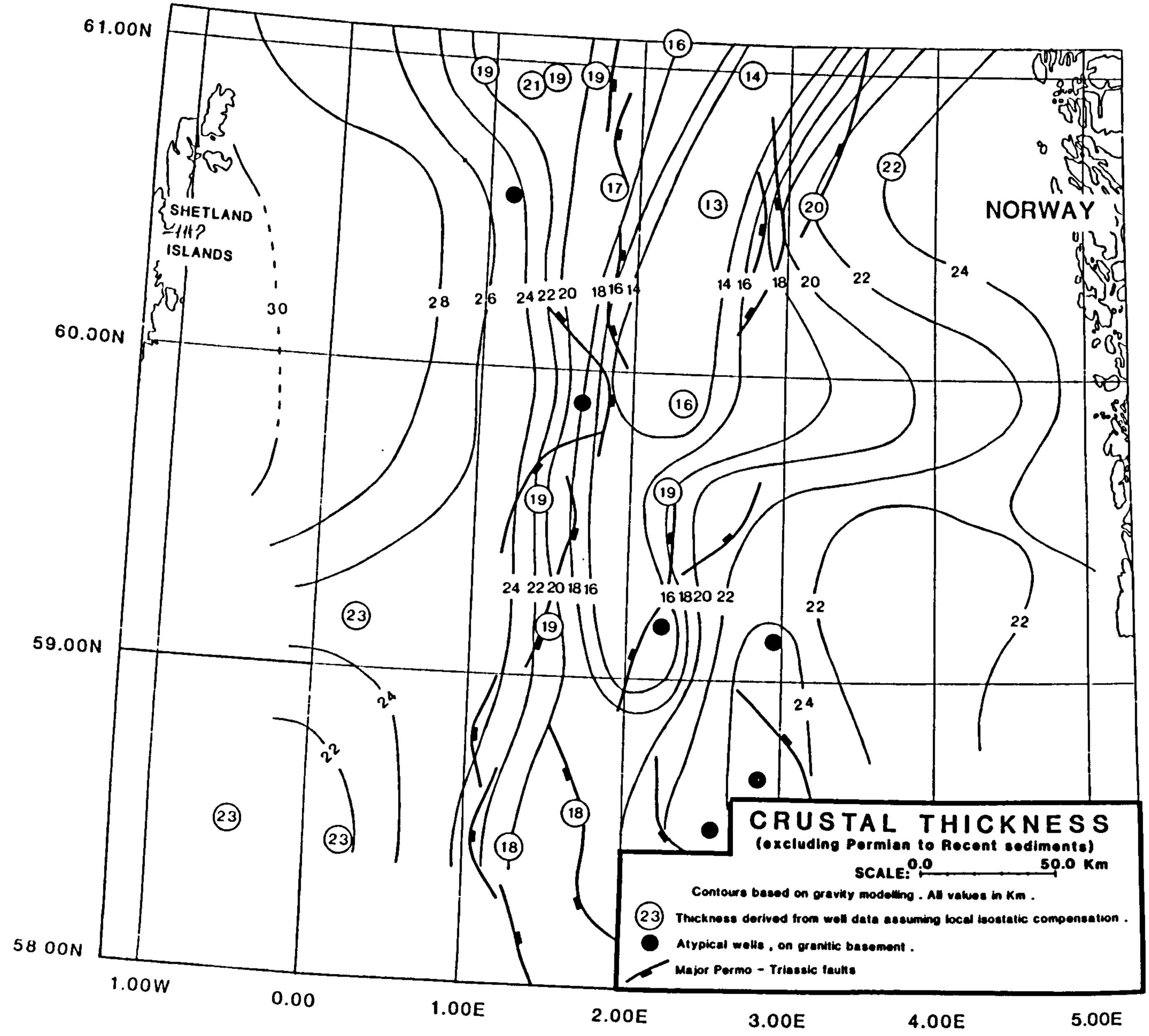

Fig 5.3 *The contours of crustal thickness are based on the gravity investigation of Fig. 2.5. The spotted values represent the predicted crustal thicknesses derived from well modelling, see Table 5.1.*

Table 5.2

Present day crustal thicknesses and stretching factors derived from well predictions and gravity calculations.

Position (flanks)	T_w	T_G	β_w	β_G	Position (centre)	T_w	T_G	β_w	β_G
UNION					BURMAH				
2/5-1	19	21	1.6	1.4	3/3-3	19	20	1.6	1.5
CONOCO					TEXACO				
3/2-1	21	21	1.4	1.4	3/4-1	19	20	1.6	1.5
SHELL					TOTAL				
8/27-1A	23	23	1.3	1.3	3/15-2	17	19	1.8	1.6
HAMILTON					UNION				
9/28-1A	19	21	1.6	1.4	9/12-1	19	21	1.6	1.4
OXY					ESSO				
14/18-1	23	21	1.3	1.4	15/6-2(N)	19	18	1.6	1.7
OXY					ELF				
15/17-7	23	21	1.3	1.4	25/2-4(N)	16	14	1.9	2.1
PHILLIPS					ELF				
16/17-6	18	20	1.7	1.5	25/4-1(N)	19	17	1.6	1.8
SHELL					STATOIL				
31/2-1(N)	22	24	1.4	1.3	30/3-1(N)	14	12	2.1	2.5
					SHELL				
					30/5-1(N)	14	13	2.1	2.3
					N. HYDRO				
					31/4-2(N)	20	21	1.5	1.4
					STATOIL				
					34/10-2(N)	16	18	1.9	1.7
AVERAGE	**21**	**22**	**1.4**	**1.4**	**AVERAGE**	**17**	**18**	**1.8**	**1.7**

T_w, β_w crustal thicknesses (km) and stretching factors respectively, predicted by the theoretical modelling of wells.

T_G, β_G crustal thicknesses (km) and stretching factors respectively, calculated by gravity modelling.

formation was preceded by a major orogeny (Caldeonian), and it is difficult to envisage a pre-stretching crust uniform across the width of the basin, Smythe et al (1980).

At the beginning of the Triassic the well modelling predicts that the crust had already undergone the first stretching event which resulted in the thinning of the crust by approximately 2km at the flanks and 5km in the centre of the basin, β = 1.07 and 1.2 respectively, thus allowing the hotter asthenosphere to ascend beneath the thinned lithosphere. As the anomaly produced by the hot asthenosphere decayed, the basin underwent a regional subsidence which lasted from the Base Triassic to Mid-Jurassic.

The total water filled subsidence due to the above events is shown in Fig. 5.4a, where the main subsidence (> 0.5km) which can be attributed to the rifting stage, extends over an area of approximately 100km. Therefore an average extension of 15km (β=1.15) accounts for the first rifting event.

The second extensional event, which was the main rifting phase of the North Sea, began in the Middle Jurassic and continued through the Early Cretaceous. As a result the crust underwent substantial thinning and at the end of rifting the crustal thickness was similar to the present day observed crustal thickness, which is approximately 22km at the flanks and not less than 14km in the centre of the graben. The water filled subsidence due to the main rifting phase described above is shown in Fig. 5.4b and extends over an area of approximately 200km. However, taking into account the results of Table 5.2 an average extension of 75km (β = 1.6) accounts for the second rifting event. Therefore, the total crustal extension in the northern North Sea calculated by well modelling was found to be approximately 90km.

Using the variation of crustal thickness across the basin, derived from the detailed gravity modelling of Chapter 2, six total stretching factors were derived to account for the six profiles

shown in Fig. 2.5. These factors are 1.40, 1.28, 1.44, 1.29, 1.41 and 1.38 calculated from the profiles one to six respectively by picking crustal thicknesses every 20km across the basin. Therefore, an average extension of more than 85km (β = 1.4) is estimated by the gravity modelling over 300km, which is in very good agreement with the total value given by the well modelling (90km).

The estimates of crustal stretching and extension are compatible with the results of Barton and Wood (1984) in the Central Graben indicating that the width of the basin appears to have increased by about 70km reaching a maximum β value of about 1.6 beneath the centre of the graben during the main rifting phase. Their results from the crustal thickness and subsidence studies show that the Mid-Jurassic stretching event occurred on crust already slightly thinned beneath the Central Graben. Therefore, by reconstructing the Pre-Permian crustal profile they suggested that residual variation in the crustal thickness may have been inherited from the Caledonian orogeny, and that over 100km of extension may have occurred since the Paleozoic.

Stretching factors across the basin can also be estimated using the geometry of the faulting observed on seismic reflection profiles, eg. Le Pichon and Sibuet (1981). The problems concerning this method are discussed by Foucher et al (1982). They emphasize the fact that the extension estimates are dependent on the velocities used when converting seismic sections into depth sections, since the dip of both the faults and the bedding planes is controlled by the velocities. In addition, current theories of fault evolution (Proffett, 1977; Jackson and McKenzie, 1983) suggest that visible high-angle faults may represent only the most recent generation of faulting in a region; older faults have rotated to near horizontal and are difficult to detect. Furthermore, internal deformation of the fault blocks such as faults and joints will not be visible on the seismics, therefore β will be under-estimated.

However, the continual improvement in the resolution of the basement imaging derived from the seismic reflection method and hence a constant increase in the number of faults detected, lead Barton and Wood (1983) to the conclusion that the estimation of stretching factors from fault geometry can give very similar results to the ones estimated by the two independent methods described in this study.

5.7 Acidic Intrusions and Subsidence

The development of the sediment unloaded basement subsidence during the three main phases of the evolution of the basin is demonstrated in Fig. 5.4. It can be seen that the INITIAL subsidence (Fig. 5.4a) was restricted to the main graben where the basement subsided 1 to 1.5km approximately, avoiding the areas occupied by the two major granites, see section 2.4.1, where no subsidence is observed.

The FAULT CONTROLLED subsidence (Fig. 5.4b) which followed, resulted in further deepening the main graben area by approximately 0.5 to 1.5km. Thus the development of the Stord Basin in the east, the East Shetland Basin in the north west, and the Witch Ground Graben in the south west of the Viking Graben was initiated. The basement subsidence in all of them was slightly greater than 0.5km. The areas occupied by granites still do not give any evidence of subsidence.

The striking difference between the subsidence patterns observed so far and the THERMAL subsidence (Fig. 5.4c) which followed, is that the latter is no longer limited to the graben and surrounding basins but extends over the whole width of the basin. The granites during this period did not exhibit any control and subsided by approximately 1km.

Therefore, the tectonic influence of the granites was effective during the periods of taphrogenic subsidence when faulting

permitted the bouyant forces of the low density intrusions to be accommodated. However, the granites were unable to exhibit any form of control during the thermal subsidence which affected the whole crustal region. Accordingly subsidence of granites should be expected during the thermal phase of the initial subsidence (Fig. 5.4a) but such subsidence was minimal due to the very small scale taphrogenic episode which resulted only to 2-5km of crustal thinning.

There are numerous similar examples of the control which granites may exhibit during the development of sedimentary basins, i.le. deviation of the faulted margin around the granite block, giving rise to the fault pattern observed today. These include the Northern Pennines (Bott, 1967) and the Market Weighton region (Bott et al 1978).

If the granites observed in this study do date from the Caledonian period (see section 2.4.1) then they may have influenced the area before the main North Sea Graben system developed. Insufficient knowledge of the distribution of the later Paleozoic sediments, however, makes any earlier influence impossible to determine.

Fig. 5.4 *(Following three pages).Extent of basement subsidence during the three main phases of the northern North Sea basin evolution. By unloading the sediments the "true behaviour" of the basement is revealed which is only due to lithospheric stretching or thermal cooling. Contours were derived from well data assuming local isostasy, see Fig. 4.4. Dashed contours were derived from selected hypothectical wells deduced from the six seismic profiles across the basin.*

Fig 5.4a

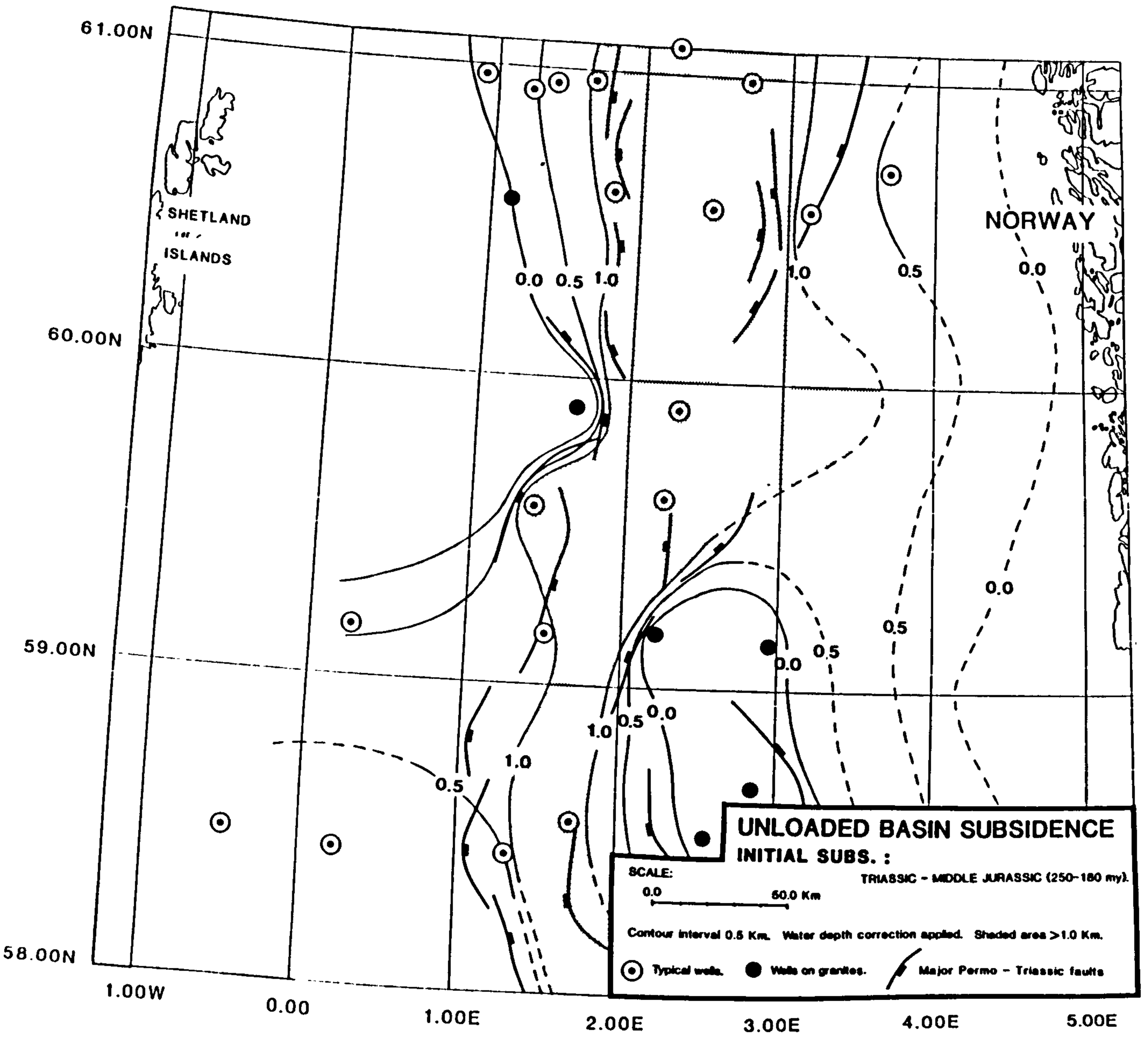
61.00N
60.00N
59.00N
58.00N
1.00W
0.00
1.00E
2.00E
3.00E
4.00E
5.00E
SHETLAND ISLANDS
NORWAY
0.0
0.5
1.0
UNLOADED BASIN SUBSIDENCE
INITIAL SUBS. :
TRIASSIC - MIDDLE JURASSIC (250-180 my).
SCALE:
0.0
50.0 Km
Contour interval 0.5 Km. Water depth correction applied. Shaded area >1.0 Km.
Typical wells.
Wells on granites.
Major Permo - Triassic faults

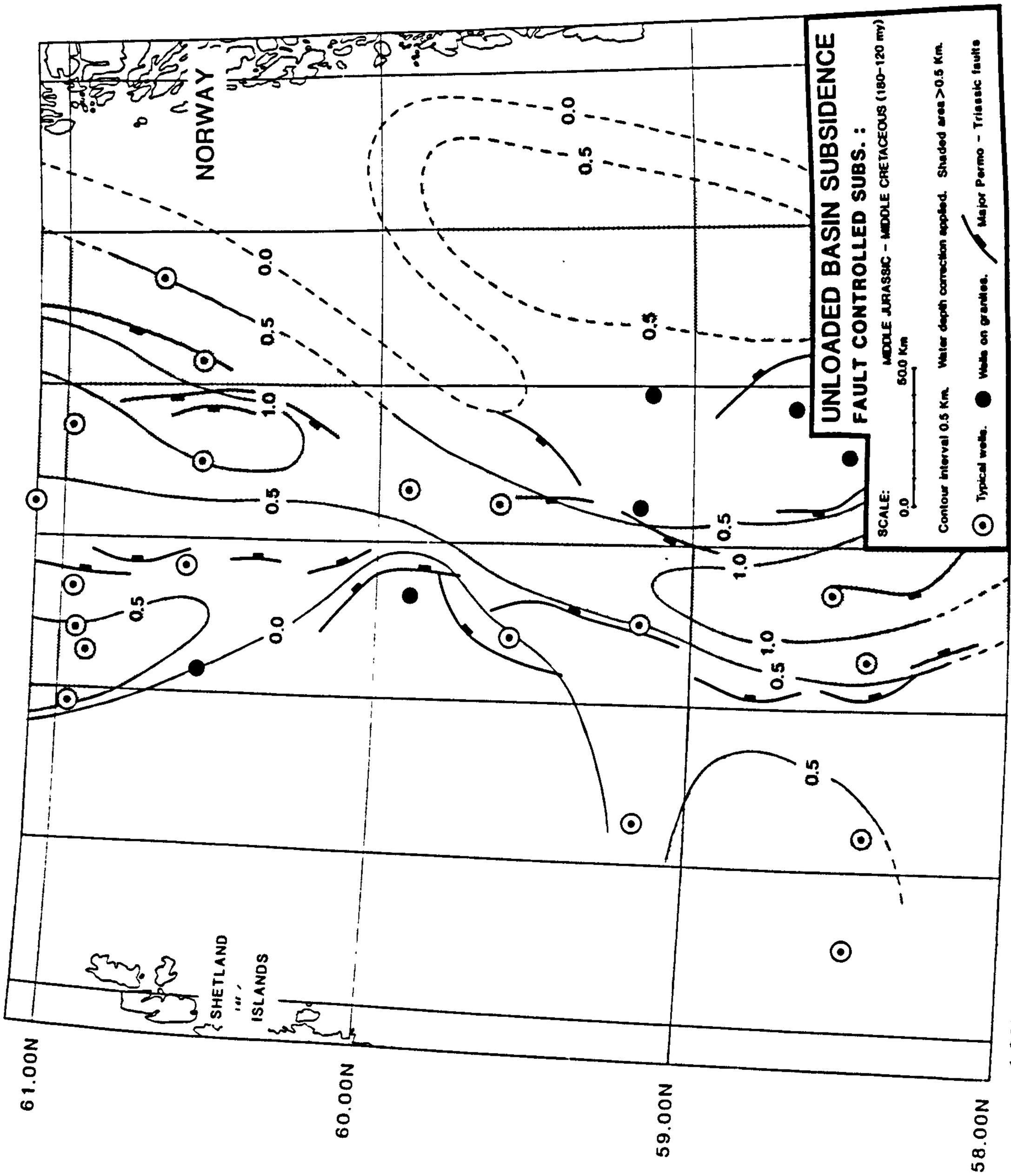
NORWAY
SHETLAND ISLANDS
UNLOADED BASIN SUBSIDENCE
FAULT CONTROLLED SUBS. :
MIDDLE JURASSIC – MIDDLE CRETACEOUS (180–120 my)
SCALE:
50.0 Km
Contour interval 0.5 Km. Water depth correction applied. Shaded area >0.5 Km.
Typical wells. Wells on granites. Major Permo – Triassic faults
0.0
0.5
1.0
61.00N
60.00N
59.00N
58.00N
5.00E
4.00E
3.00E
2.00E
1.00E
0.00
1.00W

Fig 5.4b

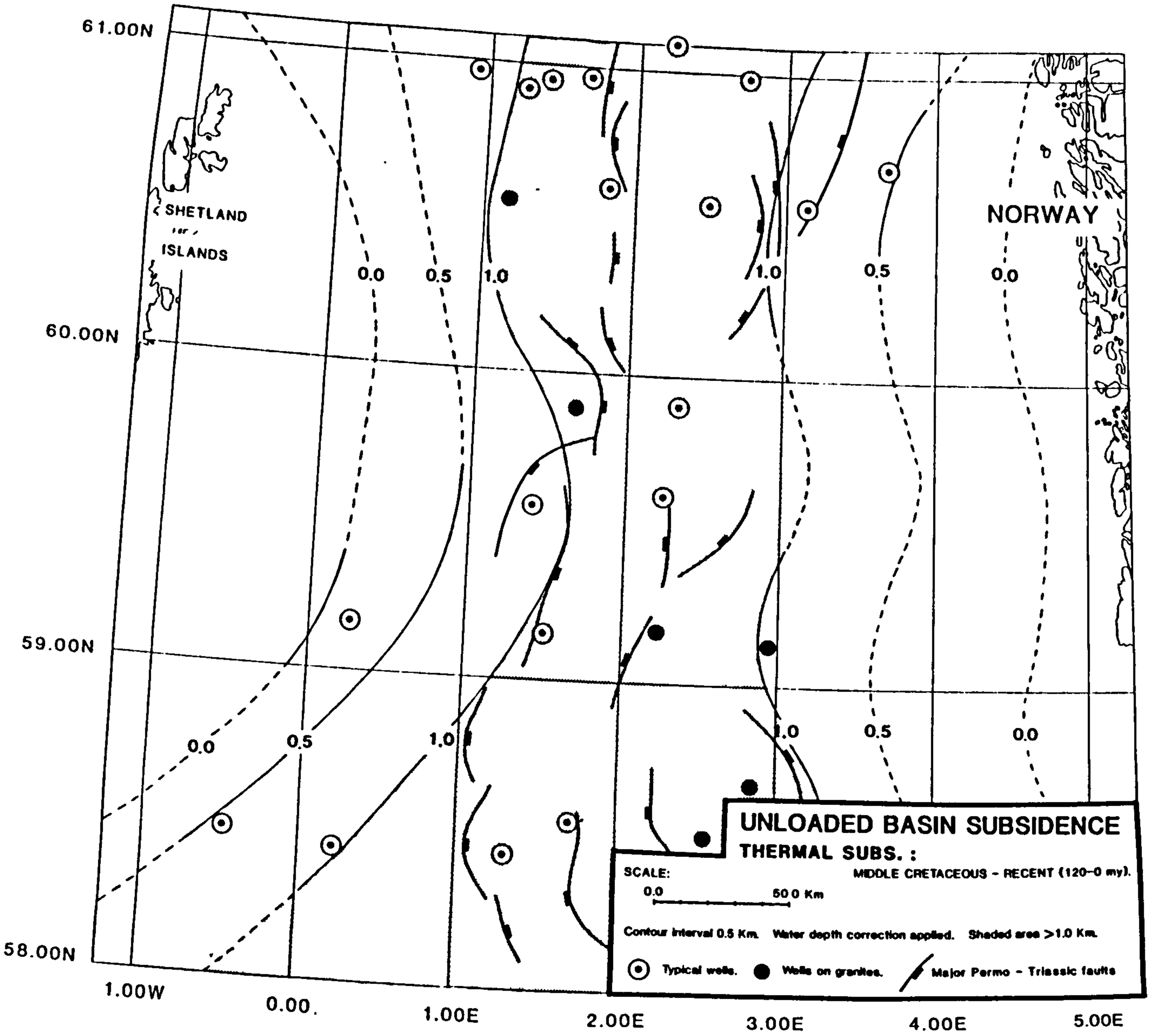
61.00N
60.00N
59.00N
58.00N
1.00W
0.00
1.00E
2.00E
3.00E
4.00E
5.00E
SHETLAND
ISLANDS
NORWAY
0.0
0.5
1.0
UNLOADED BASIN SUBSIDENCE
THERMAL SUBS. :
SCALE:
MIDDLE CRETACEOUS - RECENT (120-0 my).
0.0
500 Km
Contour interval 0.5 Km. Water depth correction applied. Shaded area >1.0 Km.
Typical wells.
Wells on granites.
Major Permo - Triassic faults

Fig. 54c

5.8 Conclusions

The main conclusion that can be drawn from this study is that the post Triassic subsidence pattern observed in the northern North Sea can be accounted for by uniform extension causing thinning of the crust and lithosphere. Simple crustal extension which assumes local isostatic compensation without any lateral heat flow can explain the major features of the North Sea, without appealing to non-uniform extension, phase changes or any other ad hoc mechanism of basin formation. By combining the results from over 100 commercial wells, 6 seismic profiles, 2 refraction profiles and detailed gravity data from the whole area of interest, both the crustal thinning and the subsidence can be accounted for.

R E F E R E N C E S

ALLEN, D.R. 1972. Environmental aspects of oil-producing operations - Long Beach, California. J. Pet. Technol., 24, 125-131.

ARTEMJEV, M.E. & ARTYUSHKOV, E.V. 1971. Structure and isostasy of the Baikal rift and the mechanism of rifting. J. Geophys. Res., 76, 1197-1211.

ARTYUSHKOV, E.V., SHLESINGER, A.E. & YAUSHIN, A.L. 1980. The origin of vertical crustal movements within lithospheric plates. In: Dynamics of plate interiors, Geodynamics series volume 1, 37-51. Edited by A.W. Bally, P.L. Bender, T.R. McGetchin and R.I. Walcott, Amer Geoph. Union.

ATHY, L.F. 1930. Density, porosity and compaction of sedimentary rocks. Amer. Assoc. Petrol. Geol. Bull., 14, 1-24.

BALLY, A.W. 1980. Basins and subsidence - A summary. In: Dynamics of plate interiors, Geodynamics Series Volume 1, 5-25. Edited by A.W. Bally, P.L. Bender, T.R. McGetchin and R.I. Walcott, Amer. Geoph. Union.

BAMFORD, D., NUNN, K., PRODEHL, C. & JACOB, B. 1978. LISPB - IV. Crustal structure of Northern Britain. Geophys. J.R. astr. Soc., 54, 43-60.

BARKER, C. 1972. Aquathermal Pressuring-Role of Temperature in Development of Abnormal-Pressure Zones. Amer. Assoc. Petrol. Geol. Bull., 56/10, 2068-2071.

BARTON, P. & WOOD, R. 1983. Crustal thinning and subsidence in the North Sea; reply to matters arising by P.A. Ziegler. Nature, 304, 561.

BARTON, P., MATTHEWS, D., HALL, J. & WARNER, M. 1984. Moho beneath the North Sea compared on normal incidence and wide-angle seismic records. Nature, 308, 55-56.

BARTON, P.J. & MATTHEWS, D.H. 1984. Deep structure and geology of the North Sea region interpreted from a seismic refraction profile. Annales Geophysicae, 2, 6, 663-668.

BARTON, P.J. & WOOD, R.J. 1984. Tectonic evolution of the North Sea basin. Geophys. J. Roy. astr. Soc., 79, 987-1022.

BEAUMONT, C. 1978. The evolution of sedimentary basins on a viscoelastic lithosphere: theory and examples. Geophys. J.R. Astron. Soc., 55, 471-497.

BEAUMONT, C. 1979. On rheological zonation of the lithosphere during flexure. Tectonophysics, 59, 347-365.

BEAUMONT, C., KEEN, C.E. & BOUTILIER, R. 1982. On the evolution of rifted continental margins: comparison of models and observations for the Nova Scotian margin. Geophys. J. R. Astron. Soc. 70, 667-715.

BERGGREN, W.A. 1969. Cenozoic chronostratigraphy, planktonic foraminiferal zonation and the radiometric time scale. Nature, 224, 1073 .

BLUNDELL, D.J. 1978. A gravity survey across the Garder Igneous Province, SW Greenland. J. Geol. Soc. London, 135, 545-554.

BOND, G. 1978. Speculations on real sea level changes and vertical motions of continents at selected times in the Cretaceous and Tertiary periods. Geology, 6, 247-250.

BOTT, M.H.P. 1967. Geophysical investigations of the northern Pennine Basement rocks. Proc. Yorks. geol. Soc., 36, 139-168.

BOTT, M.H.P. & WATTS, A.B. 1970. Deep sedimentary basins proved in the Shetland-Hebridean continental shelf and margin. Nature, 225, 265-268.

BOTT, M.H.P. 1971. Evolution of young continental margins and formation of shelf basins. Tectonophysics, 11, 319-327.

BOTT, M.H.P. & DEAN, D.S. 1972. Stress systems at young continental margins. Nature, 235, London, 23-25.

BOTT, M.H.P. 1973. Shelf subsidence in relation to the evolution of young continental margins. In: D.H. TARLING and S.K. RUNCORN, (eds.). Implication of continental drift to the earth sciences, 2, Academic Press, London and New York, 675-683.

BOTT, M.H.P. 1975. The structure and evolution of the North Sea Basin, the Faeroe Block and the intervening region. In: WOODLAND, A.W. (ed), q.v. 105-116.

BOTT, M.H.P., ROBINSON, J. & KOHNSTAMM, M.M. 1978. Granite beneath Market Weighton, East Yorkshire. J. geol. Soc. London, 135, 535-543.

BOTT, M.H.P. 1980. Mechanisms of subsidence at passive continental margins. In: Dynamics of Plate Interiors, Geodynamics Series volume 1, 27-35.

BREDEHOEFT, J.B. & HANSHAW, B.B. 1968. On the maintenance of anomalous fluid pressures, I. Thick sedimentary sequences. Geol. Soc. Amer. Bull., 79: 1097-1106.

BREWER, J., MATTHEWS, D., WARNER, M., HALL, J., SMYTHE, D. & WHITTINGTON, R. 1983. BIRPS seismic reflection studies of the British Caledonides. Nature, 305, 206-210.

BREWER, J.A. & SMYTHE, D.K. 1984. MOIST and the continuity of crustal reflector geometry along the Caledonian-Appalachian orogen. J. Geol. Soc. London, Vol. 141, 105-120.

BULLARD, E.C. & GRIGGS D.T. 1961. The Nature of the Mohorovicic discontinuity. Geophys. J.R.A.S., 6, 118-123.

BURST, J.F. 1969. Diagenesis of Gulf Coast clay sediments and its possible relation to petroleum migration. Amer. Assoc. Petrol. Geol. Bull., 53, no.1, 73-93.

BYRD, W.D. 1975. Geology of the Ekofisk Field, Offshore Norway. In: WOODLAND, A.W. (ed)., q.v. 439-445.

CAMERON, T.D.J., STOKER, M.S. & LONG, D. 1986. The history of Quaternary sedimentation in the UK sector of the North Sea basin. Journ of Geol. Soc., 143, in press.

CARSTENS, H & FINSTAD, K.G. 1981. Geothermal Gradients of the Northern North Sea Basin, 59-62°N. In: ILLING, L.V. and HOBSON, G.D. (eds), q.v. 152-161.

CASSELL, B.R. 1982. A method for calculating synthetic seismograms in laterally varying media. Geophys. J.R. astr. Soc., 69, 339-355.

CASSELL, B.R., MYKKELTVEIT, S., KANESTROM, R. & HUSEBYE, E.S. 1982. North Sea-Southern Norway seismic crustal profile. Geophys. J. R. astr. Soc., 72, 733-753.

CHASE, G.C. & GILMER, T.H. 1973. Precambrian plate tectonics: the midcontinental gravity high. Earth Planet. Sci. Lett., 21, 70-78.

CHRISTIE, P.A.F. 1982. Interpretation of refraction experiments in the North Sea. Phil. Trans. R. Soc. Lond. A 305, 101-112.

CHRISTIE, P.A.F. & SCLATER, J.G. 1980. An extensional origin for the Witchground/Buchan graben in the northern North Sea. Nature, 283, 729-732.

CLARK, R.H. 1973. Cenozoic subsidence in the North Sea. Earth Planet. Sci. Lett., 18, 329-332.

CLEMMENSEN, L., JACOBSEN, V. & STEEL, R. 1980. Some aspects of Triassic sedimentation and basin development, East Greenland, North Sea. N.P.F. The sedimentation of North Sea Reservoir Rocks, Geilo XVII, 1-21.

COCHRAN, J.R. 1982. The magnetic quiet zone in the eastern Gulf of Aden: implications for the early development of the continental margin. Geoph. Journ. R. Astr. Soc., 68, 171-201.

COCHRAN, J.R. 1983. Effects of finite rifting times on the development of sediment basins. Earth and Planetary Science Letters, 66, 289-302.

COLLETTE, B.J. 1968. On the subsidence of the North Sea. In: DONOVAN, D.T. (ed.). Geology of the shelf seas. Oliver and Boyd, London, 15-30.

COLLETTE, B.J., LANAAY, R.A. & RITSENA, A.R. 1965. Depth of the Mohorovicic discontinuity under the North Sea basin. Nature, 203, 688-689.

DAY, G.A., COOPER, B.A., ANDERSEN, C., BURGERS, W., RONNEVIK, H. & SCHONEICH, H. 1981. Regional seismic structure maps of the North Sea. In: ILLING, L.V. & HOBSON, G.D. (eds), q.v. 76-84.

DEEGAN, C.E. & BROWN, S. 1981. Jurassic. In: Introduction to the Petroleum Geology of the North Sea. JAPEC course notes.

DICKINSON, G. 1953. Geological Aspects of Abnormal Reservoir Pressures in Gulf Coast Louisiana. Amer. Assoc. Petrol. Geol. Bull., 37/2, 410-423.

DIETZ, R.S. 1963. Collapsing continental rises: an actualistic concept of geosynclines and mountain buildings. Journal of Geology, 71, 314-333.

DIMITROPOULOS, K. & DONATO, J.A. 1981. The Inner Moray Firth central ridge, a geophysical interpretation. Scott. J. Geol., 17, 27-38.

DIXON, J.E., FITTON, J.G. & FROST, R.T.C. 1981. The tectonic significance of the post-Carboniferous igneous activity in the North Sea basin. In: ILLING, L.V. & HOBSON, G.D. (eds), q.v. 121-137.

DONATO, J.A. & TULLY, M.C. 1981. A regional interpretation of North Sea gravity. In: ILLING, L.V. & HOBSON, G.D. (eds), q.v. 65-75.

DONATO, J.A. & TULLY, M.C. 1982. A proposed granite batholith along the western flank of the North Sea Viking Graben. Geophys. J.R. astr. Soc., 69, 187-195.

DRESSER ATLAS 1974. Log Review 1. Dresser Industries INC.

DRONG, H.J., PLEIN, E., SANNEMANN, D., SCHUEPBACH, M.A. & ZIMDARS, J. 1982. Der Schneverdingen - Sandstein des Rotliegended - eine aölische Sedimenfüllung alter Graben Strukturen. Zeit. deutsch. geol. Ges.,133, 699-725.

FAERSETH, R.B., MACINTYRE, R.M. & NATERSTAD, J. 1976. Mesozoic alkaline dykes in the Sunnhordland region, western Norway: ages, geochemistry and regional significance. Lithos, 9, 331-345.

FALVEY, D.A. 1974. The development of continental margins in plate tectonic theory. J. Australian Petrol. Explor. Assoc., 14, 95-106.

FERTL, W.H. & TIMKO, D.J. 1972. How downhole temperatures, pressures affect drilling, 1. Origin of abnormal Formation pressures. World Oil, 174 (7), 67-71.

FERTL, W.H. 1976. Abnormal Formation Pressures. Elsevier N.Y., 382 pp (with contributions by G.V. Chilingarian and H.H. Rieke, III).

FLINN, D. 1961. Continuation of the Great Glen Fault beyond the Moray Firth. Nature, 191, 589-591.

FOUCHER, J.P., LE PICHON, X. & SIBUET, J.C. 1982. The ocean continent transition in the uniform lithospheric stretching model: role of partial melting in the mantle. Phil. Trans. R. Soc. London, 305, 27-43.

FROST, R.T.C., FITCH, F.J. & MILLER, J.A. 1981. The age and nature of the crystalline basement of the North Sea basin. In: ILLING, L.V. & HOBSON,G.D. (eds), q.v. 43-57.

FYFE, J.A., ABBOTTS, I. & CROSBY, A. 1981. The subcrop of the mid Mesozoic unconformity in the UK area. In: ILLING, L.V. & HOBSON, G.D. (eds), q.v. 236-244.

GLENNIE, K.W. & BOEGNER, P. 1981. Solt Pit inversion tectonics. In: ILLING, L.V. and HOBSON, G.D. (ed.), q.v. 110-120.

GLENNIE, K.W. 1984. The structural framework and the pre-Permian history of the North Sea Area. In: GLENNIE, K.W. (ed), q.v. 17-39.

GLENNIE, K.W. (ed). 1984. Introduction to the Petroleum Geology of the North Sea. JAPEC (UK). Blackwell Scientific Publications, 236 pp.

GOFF, J.C. 1983. Hydrocarbon generation and migration from Jurassic source rocks in the E Shetland Basin and Viking .Graben of the northern North Sea. Journ. Geol. Soc. Lond., 140, 445-474.

GRETENER, P.E. 1969 . Fluid Pressure in Porous Media - Its importance in Geology: A Review; Can. Soc. Petr. Geol., 17/3, 255-295.

HALL, J., BREWER, J., MATTHEWS, D. & WARNER, M. 1984. Crustal structure across the Caledonides from the 'WINCH' seismic reflection profile: influences on the evolution of the Midland Valley of Scotland. Trans. of the Royal Soc. of Edinburgh: Earth Sciences, 75, 97-109.

HAMAR, G.P. 1979. Tectonic map of the North Sea, scale 1:1 000 000. Statoil, Stavanger.

HAMAR, G.P., JAKOBSSON, J., KOBSSON, K.H., ORMAASEN, D.E. & SHARPNES, O. 1980. The tectonic development of the North Sea north of Central Highs. In: The sedimentation of the North Sea reservoir rocks. Norwegian Petroleum Society, Oslo, part III, 1-23.

HARKINS, K.L. & BAUGHER, J.W. 1969. Geological significance of abnormal formation pressures. Journ. Petrol. Technol., 21, 961-966.

HARDMAN, R. (ed). 1980. The sedimentation of North Sea Reservoir Rocks. Norwegian Petroleum Society, Oslo, 389pp.

HARLAND, W.B., COX, A.V., LLEWELLYN, P.G., PICTON, C.A.G., SMITH, A.G. & WALTERS, R. (assisted by K E Fancett) 1982. A geologic time scale. Cambridge Un. press, Cambridge, 131pp.

HAXBY, W.F., TURCOTTE, D.L. & BIRD, J.M. 1976. Thermal and mechanical evolution of the Michigan Basin. Tectonophysics, 36, 57-75.

HEDBERG, H.D. 1926. The effect of gravitational compaction on the structure of sedimentary rocks. Amer. Assoc. Petrol. Geol. Bull., 10, part 2, 1035-1072.

HEDBERG, H.D. 1936. Gravitational compaction of clays and shales. Am. Jour. Sci., 5th Series, 31, no. 184, 241-287.

HELING, D. 1967. Die Porositaten toniger Keuper-und Jura-Sedimente Sudwest-deutschlands. Contr. Mineral. und Petrol., 15, 224-232.

HOCKING, J.B. 1976. In: DOUGLAS, J.G. and FERGUSON, J.A. (eds). Geology of Victoria. Geol. Soc. Aust. spec. Bull., 5.

HOSPERS, J. & FINNSTROM, E.G. 1984. The gravity field of the Norwegian sector of the North Sea. Norges geol. unders. Bull., 396, 25-34.

HOSPERS, J. & RATHORE, J.R. 1984. Interpretation of aeromagnetic data from the Norwegian sector of the North Sea. Geophysical Prospecting, 32, 929-942.

HOWITT, F., ASTON, E.R. & JACQUE, M. 1975. The occurrence of Jurassic volcanics in the North Sea. In: WOODLAND, A.W. (ed),q.v. 379-387.

HSÜ, K.J. 1965. Isostasy, crustal thinning, mantle changes, and the disappearance of ancient land masses. Am. J. Sci., 263, 97-109.

HUBBERT, M.K. & RUBEY, W.W. 1959. Role of Fluid Pressure in Mechanics of Overthrust Faulting, I Mechanics of Fluid-Filled Porous Solids and its Application to Overthrust Faulting. Boul. Geol. Soc. Amer., 70/2, 115-166.

ILLING, L.V. & HOBSON, G.D. (eds) 1981. Petroleum geology of the Continental Shelf of north-west Europe. Heyden and Son, London, 521 pp.

JACKSON, J. & MCKENZIE, D. 1983. The geometrical evolution of normal fault systems. Journ. struct. Geol., 5(5), 471-482.

JARVIS, .T. & McKENZIE, D. 1980. Sedimentary basin formation with finite extention rates. Earth Planet. Sci. Lett., 48, 42-52.

KEEN, C.E. 1975. Review of North Sea Basin Development. Journal of Geol. Soc. London, 131, 435-468.

KEEN, C.E. 1979. Thermal history and subsidence of rifted continental margins - evidence from wells on the Nova Scotian and Labradoe Shelves. Can. J. Earth Sci., 16, 505-522.

KEEN, C.E., BEAUMONT, C. & BOUTILIER, R. 1981a. Preliminary results from a thermo-mechanical model for the evolution of Atlantic type continental margins. Oceanol. Acta, Proc. 26th Int. Geological Congress, Geology of Cont. Margins Symposium, Paris, July 7-17, 1980, 123-128.

KEEN, C.E., BEAUMONT, C. & BOUTILIER, R. 1981b. A summary of thermo-mechanical model results for the evolution of continental margins based on three rifting processes. Hedberg Research Conference of the AAPG, Galveston, Texas.

KENNEDY, G.C. & HOLSER, W.T. 1966. Pressure-Volume-Temperature and Phase Relations of Water and Carbon Dioxide. Geol. Soc. Amer., Mem.#97, 371-384.

KENT, P.E. 1975. Review of North Sea Basin Development. Journal of Geol.Soc. London, 131, 435-468.

KRYNINE, D.P. & JUDD, W.R. 1957. Principles of Engineering Geology and Geotechnics. McGraw-Hill, New York, N.Y., 730 pp.

KUSZNIR, N.J. & BOTT, M.H.P. 1977. Stress concentration in the upper lithosphere caused by underlying visco-elastic creep. Tectonophysics, 43, 247-256.

LE PICHON, X. & SIBUET, J.C. 1981. Passive margins: a model of formation. Journ. Geoph. Res., 86 (B5), 3708-3720.

LECKIE, G.G. 1982. Lithology and Subsidence in the North Sea. Phil. Trans. R. Soc. Lond., A 305, 85-99.

LEWIS, C.R. & ROSE, S.C. 1970. A theory relating high temperatures and overpressures. Jour. Petr. Techn., 22, no.1, 11-16.

LOUDEN, L.R. 1972. Origin and maintenance of abnormal pressures. SPE 3843, 3rd Symp. on Abnormal Subsurface Pore Pressure, Louisiana State.

LOVELL, J.P.B. 1984. Cenozoic. In: GLENNIE, K.W., q.v. 151-169.

LOWELL, J.D., GENIK, G.J., NELSON, T.H. & TUCKER, P.M. 1975. Petroleum and plate tectonics of the southern Red Sea, In: Petroleum and Global Tectonics, ed. by A G Fischer and S Judson, Princeton U. Press. Princeton, N.J.

LUDWIG, J.W., NAFE, J.E. & DRAKE, C.L. 1970. Ch. 2, Seismic Refractions. In: Maxwell A.E. (ed) The Sea: Vol 4, John Wiley, New York, 53-84.

MAGARA, K. 1971. Permeability considerations in generation of abnormal pressures. Soc. Petrol. Eng. Journ., 11: 236-242.

MAGARA, K. 1975a. Re-evaluation Pressure and Hydrocarbon Migration. Amer. Assoc. Petrol. Geol. Bull., 5 9/2, 292-302.

MAGARA, K. 1975b. Importance of Aquathermal Pressuring Effect in Gulf Coast. Amer. Assoc. Petrol. Geol. Bull, 59/10, 2037-2045.

MAGARA, K. 1976a. Thickness of removed sedimentary rocks, Paleopore pressure and paleotempertures, southwestern part of western Canada Basin. Amer. Ass. Petrol. Geol., 60, 554-565.

MARESCHAL, J.C., GANGI, A.F. & LAMPING, N.L. 1982. The Moho as a phase change: a test of hypothesis. J. Geophys. Res. 87 (B6), 4723-4730.

MARSDEN, S.S. & DAVIS, S.N. 1967. Geological subsidence. Sci. Am., 216, 93-100.

McKENZIE, D. 1978. Some remarks on the development of sedimentary basins. Earth Planet. Sci. Letts., 40, 25-32.

McKENZIE, D. 1978b. Active tectonics of the Alpine-Himalayan belt: the Aegean Sea and surrounding regions. Geoph. Journ. R. Astr. Soc, 55, 217-254.

McQUILLIN, R. & BROOKS, M. 1967. Geophysical surveys in the Shetland Islands. Geophysical Paper No. 2, NERC, IGS, London. HMSO.

MIDDLETON, M.F. 1980. A model of intercretonic basin formation entailing deep crustal metamorphism. Geophys. J. R. Astron. Soc., 62, 1-14.

MORTON, W.H. & BLACK, R. 1974. Crustal attenuation in Afaz. In: Proceedings of an International Symposium on the Afaz Region and Related Rift Problems, edited by A Pilger and A Rosler. E Schwiezerbart'she Verlagsbuchhandlung, Stuttgart, West Germany.

NEUGEBAUER, H.J. & SPOHN, T. 1978. Late stage development of mature Atlantic-type continental margins. Tectonophysics, 50, 275-305.

OCOLA, L.C. & MEYER, R.P. 1973. Central North American Rift System 1: Structure of the axial zone from seismic and gravimetric data. J. Geophys. Res., 78, 5173-5194.

O'CONNELL, P.J. & WASSERBERG, G.J. 1967. Dynamics of the motion of plate boundary to change in pressure. Rev. Geophys., 5, 329-338.

PARASNIS, D.S. 1979. Principles of Applied Geophysics. A Halsted Press Book, John Wiley & Sons, third edition, New York.

PARSONS, B. & SCLATER, J.G. 1977. An analysis of the variation of ocean floor bathymetry and heat flow with age. Journ. Geoph. Res., 82, 803-827

PAVONI, N. 1968. Uber die Entstehung der Kiesmassen im Bergsturzgebiet von Bonaduz-Reichenau (Graubünden). Ecl. geol. helv., 61/2, 494-500.

PITCHER, W.A. 1969. Northeast-trending faults of Scotland and Ireland. In KAY, M. (ed) North Atlantic Geology and Continental Drift. Mem. Am. Assoc. Pet. Geol. No. 12, 724-733.

PITMAN, W.C. 1978. The relationship between eustacy and stratigraphic sequences of passive margins. Bull. Geol. Soc. Am., 89, 1389-1403.

PLAUMANN, S. 1979. Eine Schwerekarte der Nordsee fur den Bereich ostlich der Shetland Inseln. Geol. Jb., 14, 11-23.

POWERS, M.C. 1967. Fluid-Release Mechanisms in Compacting Marine Mud Rocks and their Importance in Oil Exploration. Amer. Assoc. Petrol. Geol, Bull., 51/7, 1240-1254.

PROFFETT, J.M. 1977. Cenozoic geology of the Yerrington district, Nevada and implications for the nature and origin of Basin and Range faulting. Geol. Soc. Amer. Bull., 88, 247-266.

PRYOR, W.A. 1973. Permeability-porosity patterns and variations in some Holocene sand bodies. Amer. Assoc. Petrol. Geol. Bull., 57, 162-189.

RAMBERG, I.B. 1972. Crustal structure across the Permian Oslo Graben from gravity measurements. Nature, 240, 149-153.

RAMBERG, I.B., GABRIELSEN, R.H., LARSEN, B.T. & SOLLI, A. 1977. Analysis of fracture patterns in southern Norway. J. of the R. Geol. and Min. Soc. of the Netherlands, 56, 295-311.

RAWSON, P.F. & RILEY, L.A. 1982. Latest Jurassic-early Cretaceous events and the 'Late Cimmerian Unconformity' in the North Sea area. Bull. Am. Ass. Petrol. Geol., 66, 2628-2648.

REYNOLDS, E.B. 1970. Predicting overpressured zones with seismic data. World Oil, 171, no.5, 78-82.

RHODEHAMEL, E.C. 1977. Sandstone porosities, Geological Studies on the Cost B-2 Well, US Mid-Atlantic Outer Continental Shelf Area. U.S. Geol. Surv. Circ., 750, 23.

RINGWOOD, A.E. & GREEN, D.H. 1966. An experimental investigation of the gabbro-eclogite transformation and some geophysical implications. Tectonophysics, 3, 383-421.

ROCHOW, R.W. 1967. Relationship of mineral composition of shales to density. Trans. Gulf Coast Assoc. Geol. Soc., 17: 135-142.

ROCHOW, K.A. 1981. Seismic Stratigraphy of the North Sea "Palaeocene" Deposits. In: ILLING, L.V. & HOBSON, G.D. (eds), q.v. 255-266.

ROYDEN, L. & KEEN, C.E. 1980. Rifting process and thermal evolution of the continental margin of eastern Canada, determined from subsidence curves. Earth Plan. Sci. Lett., 51, 343-361.

ROYDEN, L., SCLATER, J.C. & VON HERTZEN, R.P. 1980. Continental margin subsidence and heat flow: important parameters in formation of petroleum hydrocarbons. Am. Assoc. Petrol. Geol. Bull., 64, 173-187.

RUBEY, W.W. & HUBBERT, M.K. 1960. Role of fluid pressure in mechanics overthrust faulting II, Overthrust belt in geosynclinal area of western Wyoming in light of fluid pressure hypothesis. Geol. Soc. Amer. Bull., 60, 167-205.

SCHLUMBERGER 1969. Log Interpretation Principles. Schlumberger, New York, 110pp.

SCHLUMBERGER, 1974. Well Evaluation Conference North Sea. Schlumberger, 171pp. Schlumberger.

SCHOLLE, R.A. 1977. Chalk diagenesis and its relation to petroleum Exploration: Oil from chalks, a modern miracle. Amer. Ass. Petrol. Geol. Bull., 61, 982-1009.

SCLATER, J. & CHRISTIE, P. 1980. Continental stretching: an explanation of the post-mid-Cretaceous subsidence of the central North Sea Basin. Jr.Geoph. Res., 85, No. B7, 3711-3739.

SCLATER, J. ROYDEN, L., HORVATH, F., BIRCHFIELD, B., SEMKEN, S. & STEGENE, L. 1980. The formation of the intra-Carpathian basins as determined from subsidence data. Earth Planet. Sci. Lett., 51, 139-162.

SELLEY, R.C. 1976. The Habitat of North Sea Oil. Proc. Geol. Assoc London, 87, 359-388.

SELLEY, R.C. 1978. Porosity gradients in North Sea oil-bearing sandstones. Journ. Geol. Soc. Lond., 135, 119-132.

SKEMPTON, A.W. 1968. The consolidation of clays by gravitational compaction. Proc. Geol. Soc. London, no. 1648, 75-80.

SLEEP, N.H. 1971. Thermal effects of the formation of Atlantic continental margins by continental breakup. Geophys. J.R. Astr. Soc., 24, 325-350.

SLEEP, N.H. 1973. Crustal thinning on Atlantic continental margins: evidence from older margins. In: D.H. TARLING and S.K. RUNCORN, (eds.). Implications of Continental drift to the earth sciences, 2, Academic Press, London and New York, 685-692.

SLEEP, N.H. 1976. Platform subsidence mechanisms and "eustatic" sea level changes. Tectonophysics, 36, 45-56.

SLEEP, N.H., NUMM, J.A. & LEI CHON. 1980. Platform basins. Ann. Rev .Earth and Planet. Sci., 8, 624pp.

SMITH, J.E. 1973. Shale compaction. Soc. Petrol. Eng. Journ., 12, 12-22.

SMYTHE, D.K., SKUCE, A.G. & DONATO, J.A. 1980. Geological objections to an extensional origin for the Buchan and Witchground Graben in the North Sea. Nature, 287, 467.

SOLLI, M. 1976. En seismisk skorpeundersokelse Norge-Shetland. Thesis, Univ. of Bergen, 155pp.

STECKLER, M.S. & WATTS, A.B. 1978. Subsidence of the Atlantic type continental margin off New York. Earth and Planet. Sci. Lett., 41, 1-13.

TERZAGHI, K. 1950. Mechanics of Landslides. Geol. Soc. Amer. Berkey Volume, 83-123.

THRELFALL, W.F. 1981. Structural framework of the central and northern North Sea. In: ILLING, L.V. & HOBSON, G.D. (eds), q.v. 98-103.

TULLY, M.C. & DONATO, J.A. 1985. 1:100 000 northern North Sea Bouguer anomaly gravity map. Rep. Br. Geol. Surv. Vol. 16, No. 6.

TURCOTTE, D.L. 1980. Models for the evolution of sedimentary basins. In: Dynamics of plate interiors, American Geophysical Union, Geodynamics Series V1, 21-26.

VAIL, P.R. & TODD, R.G. 1981. Northern North Sea Jurassic unconformities, chronostratigraphy and sea level changes from seismic stratigraphy. In: ILLING, L.V. & HOBSON, G.D. (eds), q.v. 216-235.

VAIL, P.R., MITCHUM, R.M. & THOMSON, S. 1977. Seismic stratigraphy and global changes of sea level, stratigraphic interpretation of seismic data. Mem. Am. Ass. Petrol. Geol., 26, 83-97.

VETTER, U.R. & MEISSNER, R.O. 1979. Rheologic properties of the lithosphere and applications to continental margins. Tectonophysics, 59, 367-380.

VOIGHT, B. 1974. Thin-skinned graben, plastic wedges and deformable plate tectonics. In: Approaches to Taphrogenesis, edited by J Illies and K Fuchs, Schweizerbeck, Stuttgart, West Germany.

WALCOTT, R.I. 1972. Gravity, flexure and the growth of sedimentary basins at continental edge. Bull. Geol. Soc. Am., 83, 1845-1848.

WATSON, J.M. & SWANSON, C.A. 1975. North Sea - Major Petroleum Province. Bull. Amer. Assoc. Petrol. Geol., 59, 1098-1112.

WATTS, A.B. & RYAN, W.B.F. 1976. Flexure of the lithosphere and continental margin basins. Tectonophysics, 36, 25-44.

WATTS, A.B. & STECKLER, M.S. 1979. Subsidence and eustasy at the continental margin of eastern North America. Maurice Ewing Symposium, Series 3, Amer. Geophys. Union, 218-234.

WATTS, A.B. & STECKLER, M.S. 1981. Subsidence and tectononics of Atlantic-type continental margins, Oceanologica Acta, Geology of Continental margins Symp., Proceeding of 26th Intern. Congr., Paris, 4, 143-153.

WISE, D.V. 1974. Continental margins, freeboard and the volumes of continents and oceans through time. In: Burke, C.A. and Ozake, C.L. (Eds).. The geology of continental margins 45-58.

WOOD, R. & BARTON, P. 1983. Crustal thinning and subsidence in the North Sea. Nature, 302, 134-136.

WOODHALL, D. & KNOX, R.W. O'B. 1979. Mesozoic volcanism in the northern North Sea and adjacent areas. Bull. geol. Surv. G.B., 70, 34-56.

WOODLAND, A.W. (ed) 1975. Petroleum and the Continental Shelf of North-West Europe, Vol. 1: Geology, Applied Science Publ., London, 501pp.

ZHABREV, I.P., ZUBOV, I.P., KRYLOV, N.A. & SEMENOVICH, V.V. 1975. In: Proceeding of the Ninth World Petroleum Congress, vol. 2 (Geology), 83-91.

ZIEGLER, P.A. 1975a. Geologic evolution of the North Sea and its tectonic framework. Bull. Amer. Assoc. Petrol. Geol., 59, 1073-1097.

ZIEGLER, P.A. 1975b. North Sea Basin History in the Tectonic Framework of North-Western Europe. In: WOODLAND, A.W. (ed.), q.v. 131-150.

ZIEGLER, P.A. 1977. Geology and hydrocarbon provinces of the North Sea. Geol. Journal, 1, 7-32.

ZIEGLER, P.A. 1978. North-western Europe: tectonics and basin development. Geol. Mijnbouw, 53, 43-50.

ZIEGLER, P.A. 1981. Evolution of sedimentary basins in north-west Europe. In: ILLING, L.V. & HOBSON, G.D. (eds), q.v. 3-39.

ZIEGLER, P.A. 1982. Geological Atlas of Western and Central Europe. Elsevier, Amsterdam, 130 pp.

ZIEGLER, W.H. 1975. Outline of the geological history of the North Sea. In: WOODLAND, A.W. (ed.). q.v. 165-190.